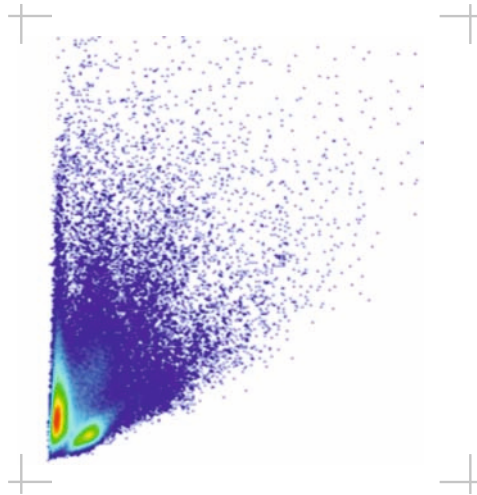


# B7-H1 as a new molecular target for the treatment of pancreatic adenocarcinoma

---

Katharina von Ahn



Inaugural-Dissertation zur Erlangung des Grades eines  
**Dr. med. vet.**  
beim Fachbereich Veterinärmedizin der Justus-Liebig-Universität Gießen



*édition scientifique*  
**VVB LAUFERSWEILER VERLAG**

**Das Werk ist in allen seinen Teilen urheberrechtlich geschützt.**

**Die rechtliche Verantwortung für den gesamten Inhalt dieses Buches liegt ausschließlich bei den Autoren dieses Werkes.**

Jede Verwertung ist ohne schriftliche Zustimmung der Autoren oder des Verlages unzulässig. Das gilt insbesondere für Vervielfältigungen, Übersetzungen, Mikroverfilmungen und die Einspeicherung in und Verarbeitung durch elektronische Systeme.

1. Auflage 2015

All rights reserved. No part of this publication may be reproduced, stored in a retrieval system, or transmitted, in any form or by any means, electronic, mechanical, photocopying, recording, or otherwise, without the prior written permission of the Authors or the Publisher.

1<sup>st</sup> Edition 2015

© 2015 by VVB LAUFERSWEILER VERLAG, Giessen  
Printed in Germany



*édition scientifique*  
**VVB LAUFERSWEILER VERLAG**

STAUFENBERGRING 15, D-35396 GIESSEN  
Tel: 0641-5599888 Fax: 0641-5599890  
email: [redaktion@doktorverlag.de](mailto:redaktion@doktorverlag.de)

[www.doktorverlag.de](http://www.doktorverlag.de)

Aus dem Klinikum Veterinärmedizin,  
Klinik für Kleintiere  
der Justus – Liebig – Universität Gießen

Betreuer: Prof. Dr. Reto Neiger

und

der Chirurgischen Klinik  
der Ruprecht-Karls-Universität Heidelberg

Betreuer: Prof. Dr. Alexandr V. Bazhin

Dr. Svetlana Karakhanova

---

**B7-H1 as a new molecular target for the  
treatment of pancreatic adenocarcinoma**

**Inaugural-Dissertation**

zur Erlangung des Grades eines  
Dr. med. vet.  
beim Fachbereich Veterinärmedizin  
der Justus – Liebig – Universität Gießen

eingereicht von

**Katharina von Ahn**

Tierärztin aus Ottersberg

**Gießen 2015**

Mit Genehmigung des Fachbereichs Veterinärmedizin  
der Justus-Liebig-Universität Gießen

Dekan: Prof. Dr. Dr. h.c. Martin Kramer

Gutachter: Prof. Dr. med. vet. Reto Neiger  
Prof. Dr. Alexandr V. Bazhin

Tag der Disputation: 06.07.2015

### **Eidesstattliche Erklärung**

Ich erkläre: „Ich habe die vorgelegte Dissertation selbständig und ohne unerlaubte fremde Hilfe und nur mit den Hilfen angefertigt, die ich in der Dissertation angegeben habe. Alle Textstellen, die wörtlich oder sinngemäß aus veröffentlichten oder nicht veröffentlichten Schriften entnommen sind, und alle Angaben, die auf mündlichen Auskünften beruhen, sind als solche kenntlich gemacht. Bei den von mir durchgeführten und in der Dissertation erwähnten Untersuchungen habe ich die Grundsätze guter wissenschaftlicher Praxis, wie sie in der „Satzung der Justus-Liebig-Universität Gießen zur Sicherung guter wissenschaftlicher Praxis“ niedergelegt sind, eingehalten.“

## **Meinen Eltern**



## **I. Table of contents**

I. Table of contents.....	6
II. List of Abbreviations .....	10
1. Introduction .....	15
1.1 The anatomy and physiology of the pancreas .....	15
1.2 Tumors of the pancreas .....	16
1.3 Etiology and progression of PDAC .....	16
1.4 Symptoms of PDAC .....	17
1.5 Diagnosis of PDAC .....	18
1.6 Therapy of PDAC .....	19
1.6.1 Surgical therapy of pancreas cancer .....	20
1.6.2 Radiotherapy of PDAC.....	21
1.6.3 Chemotherapy of PDAC.....	21
1.6.4 Immune therapy .....	23
1.7 The immune system.....	24
1.8 Cells of the immune system .....	25
1.8.1 Lymphocytes.....	25
1.8.2 Dendritic cells (DC) .....	27
1.8.3. Natural killer cells.....	28
1.8.4. Immune regulation .....	28
1.8.4.1 Regulatory T cells (Treg) .....	28
1.8.4.2 Myeloid derived suppressor cells (MDSC) .....	29
1.8.4.3 The B7-H1 molecule .....	31
1.9. The goal of this thesis .....	32
2. Material and Methods .....	33
2.1 Material .....	33
2.1.1 Mice .....	33

## Table of contents

---

2.1.2 Pancreas carcinoma cells .....	33
2.1.3 Pharmaceutical products.....	33
2.1.4 Anti-mouse Antibodies for the flow cytometry.....	34
2.1.5 Laboratory Equipment.....	35
2.1.6 Laboratory consumables .....	36
2.1.7 Laboratory solutions.....	37
2.1.8 Media and Buffers.....	37
2.1.8.1 Buffers for the flow cytometry.....	37
2.1.8.2 Medium, buffer and solutions for the cell culture .....	38
2.1.8.3 Buffer for MACS.....	39
2.1.9 Software .....	39
2.2 Methods .....	39
2.2.1 Orthotopic mouse model .....	39
2.2.2 Treatment of the mice with IFN $\alpha$ , with 5-FU or with the combination of IFN $\alpha$ +5-FU.....	40
2.2.3 Preparation of tumors and spleens, collecting blood samples .....	40
2.2.4 Preparation of a single-cell suspension.....	41
2.2.5 Flow cytometry.....	42
2.2.5.1 Immunophenotyping .....	42
2.2.5.2 Extracellular staining.....	43
2.2.5.3 Intracellular staining.....	43
2.2.6 Treatment of splenocytes in culture .....	44
2.2.7 Investigation of MDSC suppressive activity.....	44
2.2.7.1 CFSE cell labeling of splenocytes.....	44
2.2.7.2. Digestion of tumors .....	45
2.2.7.3 Magnetic activated cell sorting (MACS) .....	45
2.2.7.4 Coculture .....	46

2.2.8 Luminex (Bioplex) assay .....	47
2.2.9 Statistical analysis.....	47
3. Results .....	49
3.1 Effects of chemo (5-FU) - and immunotherapy (IFN $\alpha$ ) on the constellation of leukocyte subsets and on the expression of B7-H1/B7-DC molecules on splenocytes of healthy WT and B7-H1 KO mice in <i>in vitro</i> cultures .....	49
3.1.1 Analysis of CD4 <sup>+</sup> /CD8 <sup>+</sup> T cells .....	49
3.1.2 Analysis of regulatory T cells (Treg) .....	71
3.1.3 Analysis of dendritic cells (DC).....	74
3.1.4 Analysis of Gr-1 <sup>+</sup> CD11b <sup>+</sup> cells.....	86
3.2 <i>In vivo</i> Effects of chemo (5-FU) - and immunotherapy (IFN $\alpha$ ) on the constellation of leukocyte subsets and the expression of B7-H1/B7-DC molecules in tumor-bearing WT and B7-H1 KO mice .....	90
3.2.1 Analysis of CD4 <sup>+</sup> /CD8 <sup>+</sup> T cells .....	90
3.2.2 Analysis of Myeloid derived suppressor cells (MDSC) .....	112
3.2.3 Analysis of B7-H1/B7-DC expression on MDSC .....	125
3.2.4 Analysis of regulatory T cells (Treg) .....	129
3.2.5 Analysis of dendritic cells (DC).....	134
3.3 Effects of chemo (5-FU) - and immunotherapy (IFN $\alpha$ ) on cytokine concentration in blood serum of tumor-bearing WT and B7-H1 KO mice.....	149
3.4 Role of B7-H1 expression on the functional phenotype of MDSC and on the sensitivity of splenocytes to MDSC mediated suppression.....	155
3.4.1 Effect of B7-H1 expression on the functional phenotype of MDSC .....	155
3.4.2 Effect of B7-H1 expression on the sensitivity of splenocytes to MDSC mediated suppression.....	162
3.5 Effects of B7-H1 presence on cytokines production in <i>in vitro</i> cocultures of WT/ B7-H1 KO splenocytes and WT MDSC .....	169
3.6 Effects of chemo (5-FU) - and immunotherapy (IFN $\alpha$ ) on tumor volume and metastasis rate of WT and B7-H1 KO tumor-bearing mice.....	178

## Table of contents

---

3.7 Effects of chemo (5-FU) - and immunotherapy (IFN $\alpha$ ) on the survival rate of WT and B7-H1 KO tumor-bearing mice .....	184
3.8 Analysis of the correlation between tumor volume and specific immune cell populations .....	188
4. Discussion.....	190
5. Summary.....	205
6. Zusammenfassung.....	206
III. List of Literature .....	207
IV. List of Figures .....	224
V. List of Tables .....	234
VI. Acknowledgement.....	235

## II. List of Abbreviations

%	percentage
°C	degree Celsius
µg	microgram
µl	microliter
µM	micromole
µm	micrometer
5-FU	5-Fluorouracil
ANOVA	Analysis of Variance
APC	antigen-presenting cells
APC-Cy7	Allophycocyanine-cyanine-7
Arg-1	Arginase-1
B cells	B- lymphocytes
B7.1	CD80
B7.2	CD86
B7-DC	programmed death-ligand 2, PD-L2, CD273
B7-H1	programmed death-ligand 1, PD-L1,CD274
Bl6	C57Bl/6 mouse
CD	Cluster of Differentiation
cDC	conventional myeloid dendritic cells
CFSE	Carboxyfluorescein Succinimidyl Ester

## List of Abbreviations

---

co	control
CT	computer tomography
CTLA-4	cytotoxic-T-lymphocyte-associated protein 4
DC	dendritic cells
dim	diminished
DMSO	dimethyl sulfoxide
DNA	deoxyribonucleic acid
EDTA	Ethylenediaminetetraacetate
ESPAC	European Study Group for Pancreatic Cancer
FACS	Fluorescence activated cell sorting
Fig.	Figure
FITC	Fluorescein isothiocyanate
Foxp3	Forkhead-Box-Protein P3
FSC	Forward Scatter
g	gravity (centrifuge)
gMDSC	granulocytic myeloid derived suppressor cells
HCL	hydrochloric acid
HCO <sub>3</sub> <sup>-</sup>	hydrogen carbonate
IFN $\alpha$	Interferon-alpha (Mouse)
IFN $\gamma$	Interferon-gamma
IL	Interleukin
IMC	immature myeloid cells
iNOS	inducible nitric oxide synthase

## List of Abbreviations

---

int	intermediate
iTreg	adaptive or inducible Treg
KO	knockout
MACS	Magnetic activated cell sorting
MDSC	myeloid derived suppressor cells
MFI	mean fluorescence intensity
MHC-II-molecule	Major Histocompatibility Complex-II-molecule
MHC-I-molecule	Major Histocompatibility Complex-I-molecule
min	minutes
ml	milliliter
mM	millimolar
mMDSC	monocytic myeloid derived suppressor cells
n	sample size, number
N/A	not applicable
NaCl	sodium chloride
NaOH	sodium hydroxide
NK cells	natural killer cells
NO	nitric oxide
NOS	nitric oxid synthase
nTreg	naturally occurring Treg
PanIN	pancreatic intraepithelial neoplasia
PBS	phosphate buffer saline
PD-1	programmed cell death protein1

## List of Abbreviations

---

PDAC	Pancreatic ductal adenocarcinoma
pDC	plasmacytoid dendritic cells
PD-L1	programmed death-ligand 1, B7-H1, CD274
PD-L2	programmed death-ligand 2, B7-DC, CD273
PE	phycoerythrin
PE-Cy	phycoerythrin-cyanine
PerCP-Cy5.5	peridinin chlorophyll protein complex- cyanin-5.5
ROS	reactive oxygen species
rpm	rates per minute
SEM	standard error of mean
SPF	specific pathogen-free
SSC	Side Scatter
Tab.	table
Tcm	central memory T cells
Tcon	conventional T cells
Teff	effector T cells
Tem	effector memory T cells
TGF- $\beta$	Transforming growth factor-beta
TH1	Type 1 helper cells
TH2	Type 2 helper cells
Tnaive	naïve T cells
TNF	Tumor necrosis factor
Treg	regulatory T cells

## List of Abbreviations

---

U/ml	units per milliliter
Vol%	volume percent
WT	Wild Type
$\alpha$	alpha
$\beta$	beta
$\gamma$	gamma
$\zeta$	zeta
$\chi^2$ -test	chi-square test

## 1. Introduction

Pancreatic ductal adenocarcinoma (PDAC) continues to be a devastating disease due to its unspecific early symptoms, poor prognosis and low survival rates in patients. Therefore, a timely diagnosis and effective curative therapies for PDAC remain a challenge to this day in the medical field. That is why this type of cancer is extremely interesting for scientists as well as oncologists. However, in order to investigate this disease further, first it is important to be aware of the anatomy and physiology of a healthy pancreas.

### 1.1 The anatomy and physiology of the pancreas

In the human organism, the pancreas is located behind the stomach, reaching from the duodenum to the spleen. Anatomically, this organ can be subdivided into the head, Caput pancreatis, which is located within the duodenal curve on the right side, the body, Corpus pancreatis, and the narrow tail of the pancreas, Cauda pancreatis, which extends to the gastric surface of the spleen [1].

As in humans, in small animals the pancreas can also be divided into three parts. The Corpus pancreatis, which is located next to the pars cranialis duodeni, the Lobus pancreatis sinister, which points towards the spleen, and the Lobus pancreatis dexter, which is positioned in the Mesoduodenum descendens [2].

The pancreas consists of two separate types of glandular tissue with different functions: the exocrine and the endocrine pancreas. The function of the exocrine section is to produce pancreatic juice that flows into the duodenum and neutralizes the HCL from the stomach chymus with the help of production of  $\text{HCO}_3^-$ . This digestive juice also contains the precursors of many enzymes that are necessary for the digestion of proteins, carbohydrates as well as fat. The endocrine pancreas, also known as the islets of Langerhans, produces hormones responsible for the regulation of the blood glucose level [3].

These physiological processes occurring in the pancreas make it an important organ of the human body, but unfortunately, also a target for diseases such as pancreatic cancer.

### **1.2 Tumors of the pancreas**

PDAC is a lethal malignancy with high mortality rates, for example in the USA, PDAC is the fourth most common cause of death related to all cancers deaths. In terms of cancer incidence it is ranked 11<sup>th</sup> [4, 5]. Due to medical progress, death rates for other common tumors such as cancers of the stomach, lungs, colon and prostate have decreased, whereas mortality rates of PDAC have remained the same [4, 5].

As a result of the malignant transformation of pancreas cells, pancreatic cancer can occur in different regions and tissues of this organ. Cancer of the pancreas includes tumors of the endocrine tissue, e.g. islet cell carcinoma, as well as tumors of the exocrine section of the gland, for example the PDAC that constitutes approximately 90% of all pancreatic cancers [6].

Tumors of the exocrine pancreatic tissue are seldom in animals; when they do occur they are most likely found in older cats and dogs. Most of animal tumors are of epithelial origin. Adenocarcinomas are the most common and are characterized by destructive and infiltrative tumor growth as well as an early metastasis rate in the peritoneum, the liver and lymphnodes of the thorax [7, 8]. Below, I will concentrate on the etiology and progression of PDAC.

### **1.3 Etiology and progression of PDAC**

The etiology of PDAC still remains unknown in most aspects. There are different triggers discussed that can increase the risk of this disease.

One of the environmental risk factors that is avoidable is smoking. This can increase the chance of getting PDAC up to 30-50 % [9]. Alcohol abuse is a second factor that can increase the risk of this disease [10]. Chronic pancreatitis is also determined to have a significant influence with a six-fold higher risk [11]. Another discussed cause

for PDAC is diabetes mellitus, however so far the exact mechanisms and the relationship between these diseases has yet to be determined and remains controversial [12]. Several studies also point to a hereditary component. Here, an autosomal dominant transmission is often considered. Patients from families with a history of this cancer have a predisposition to get the disease and may have at least two first-degree relatives that had PDAC. There are estimations that up to 4% of all pancreatic cancers are of hereditary origin [13, 14].

Due to histological and molecular observations, a multistep progression model is suggested for the development of PDAC [15]. The noninvasive precursor lesions in the pancreas, known as pancreatic intraepithelial neoplasia (PanIN) [16], share molecular alterations and mutations, for example in the oncogene KRAS2 or tumor-suppressor genes BRCA2 or the TP53, which are described in invasive PDAC [17, 18]. Telomere shortening has been determined as an important factor in cell immortality and a transformation to cancer as well. This is associated with reactivation of the enzyme telomerase in cells with shortened telomeres [19]. Telomere shortening is nearly universal in all PanINs, and can result in chromosomal instability, one early trigger of carcinogenesis [20].

The development of PDAC is a slow progression, taking approximately 11.7 years from the initiation of tumorigenesis until the first cell of a parental clone is formed, and another 6.8 years from the parental clone to the index metastasis [21]. Unfortunately, in most patients pancreatic cancer is first diagnosed in the last two years of the entire tumorigenic process, partially due to its slow progression, which also results in unspecific symptoms.

### **1.4 Symptoms of PDAC**

Early symptoms of PDAC are disturbed digestion and weight loss. In the advanced stages, lesions sometimes invade retroperitoneal nerves which results in abdominal and back pain. Later symptoms are steatorrhea and diabetes mellitus [22, 23].

Clinical manifestations of the cancer of the pancreas head differ from those located in the tail region. The main difference is the frequency of jaundice occurrence and the

symptom of a palpable gallbladder hydrops [24]. Most of the tumors are located in the head of the pancreas, and therefore cause stricture of the intrapancreatic section of the common bile duct, which leads to jaundice with its typical yellow discoloration of the skin and sclera [23, 25].

Common symptoms of ductal pancreatic adenocarcinoma in small animals are weight loss, poor general conditions as well as anorexia. Less often are increased weakness, ascites, diarrhea or palpable masses in the cranial abdomen. Jaundice can be seen when the cancer induces an obstruction of the extrahepatic bile duct. Another symptom described in dogs is pancreatic insufficiency combined with maldigestion syndrome [8].

Generally, the majority of symptoms become apparent only in advanced stages of tumor progression, making an early diagnosis of this disease difficult.

### **1.5 Diagnosis of PDAC**

Early diagnosis of pancreatic cancer is a decisive factor for the prognosis and the chance of a successful treatment. 74% of all PDAC patients die within the first year, and about 94% within five years after diagnosis. In cases of small tumors that were diagnosed at an earlier tumor stage, these percentages are lower. According to current statistics, PDAC has the lowest relative survival rate of all cancers [4, 5].

Different methods are used in the diagnosis of pancreatic cancer. Nowadays, the most common techniques are ultrasound and computer tomography. Advantages of ultrasound are that it is simple to use, available and affordable. However, CT possesses higher sensitivity compared to ultrasound, and allows a better overview of the size and shape of the tumor as well as other affected organs.

Endoscopic ultrasonography has reported a high sensitivity to also detect tumors the size of 10 mm, and also can be applied for histological examinations using fine needle aspiration [26].

Positron emission tomography with labeled fluorodeoxyglucose is another established noninvasive imaging method with high sensitivity for the early detection

of malignancies such as PDAC. The metabolism of the fluorodeoxyglucose allows an early diagnosis of small-sized tumors and the localization of metastasis [27].

In the endoscopic retrograde cholangiopancreatography, an endoscopy of the oesophagus, the stomach and the duodenum is performed, and both the pancreas and bile ducts can be visualized with the help of a contrast agent. This method has a high sensitivity at approximately 90%, but a notable issue is that smaller-sized tumors may not be identified [23, 28]. Different studies reveal that this method can also be used in dogs, but so far remains an exception in the diagnosis of PDAC [29].

On a molecular level, CA19-9 is a tumor marker that increases and can frequently be detected in PDAC patients. This marker is used to trace the progress and development of the tumor. However, it is not suitable for a general screening of PDAC [24, 30].

### **1.6 Therapy of PDAC**

The therapy of PDAC is successful in few patients due to a late diagnosis of this cancer and its high metastatic rate. Different types of therapy are commonly used for PDAC patients. For the curative treatment of PDAC, surgery is the only known potential cure [31]. After complete removal of recognizable tumors, adjuvant therapy is applied to combat any unverifiable metastasis, and therefore improves the long-term chances of curing tumor patients. Examples for applied adjuvant therapy are chemotherapy, radiotherapy or immune therapy.

Neoadjuvant therapy is defined as the preoperative intervention with the aim to convert unresectable tumors to resectable ones due to a volume reduction, or to increase the probability of complete microscopic tumor resection [32]. Examples for a neoadjuvant therapy are chemotherapy and radiotherapy.

Palliative treatment is another important therapeutic approach and is considered if a cure seems unlikely. Since 80-90% of diagnosed tumors are unresectable due to local invasion or metastasis [33], the therapeutic goal here is to improve the life quality and overall survival of those PDAC patients. Palliative treatment includes the relief of

secondary symptoms caused by gastric obstruction, jaundice and pain, and is therefore essential for tumor patients (reviewed in[34]).

### **1.6.1 Surgical therapy of pancreas cancer**

Surgery represents the only curative therapy for PDAC patients, but because of the late diagnosis, surgery is only an option in about 20% of the diagnosed tumors [35]. The mortality rate of this operation is relatively low at less than 5% [36]. Nevertheless, in patients who have undergone surgery, the median survival rate is still low and considered to be less than two years [35]. Approximately 30% of the patients die within the first year after this medical intervention [37]. Characteristics such as age, tumor size and grade as well as nodal and margin status of the cancer are considered to be prognostic factors for the survival rate of patients after resection [38, 39].

There are different methods for the resection of tumors located in the head of the pancreas. The standard technique is the partial pancreaticoduodenectomy, according to Whipple and Kausch. This resection includes the removal of the head of the pancreas, the distal portion of the stomach, the duodenum, gall bladder and of the intrahepatic portion of the bile duct together with their associated lymph nodes. Other methods are the pylorus-preserving pancreaticoduodenectomy characterized by preservation of the stomach and the sphincter muscle, or a total pancreatectomy, which is done when the corpus of the pancreas is involved in the lesion. However, this method is problematic in the aspect of blood glucose level regulation [23].

In small animals like cats and dogs, a resection is often not to be considered because of already metastasizing tumors due to the late diagnosis [8].

Resection of PDAC can also be combined with adjuvant radiotherapy. The survival rate, depending on the recurrence of the tumor, has been evaluated for such approaches. However, local recurrence of tumors remains high in these patients [40].

### **1.6.2 Radiotherapy of PDAC**

Radiotherapy is applied on PDAC patients whose tumors are locally advanced, unresectable, irregular shaped and large sized. However, the appropriate dose of radiation for this type of tumor is difficult to dispense [41].

The three-dimensional conformal radiotherapy is the most commonly used radiotherapy for the treatment of PDAC. With this technique, the profile of each radiation beam is adjusted to the exact shape of the tumor. The advantage of this method is that the relative toxicity of radiation to the normal surrounding tissue is reduced, since the treatment volume conforms to the shape of the tumor. This in turn allows for the use of a higher radiation dose specifically for the tumor tissue [42].

A second method used is intensity modulated radiation therapy. The distinguishing feature of this method is that high radiation doses can be focused on regions within the tumor so that the surrounding structures, especially the duodenum, receive minimized doses of radiation. Therefore, higher doses can be used with fewer side effects. This method is used for PDAC in an early stage and is locally restricted [43].

Often the combination of radiotherapy and chemotherapy is applied. Studies have revealed an advantage in the survival rate of patients for chemoradiotherapy in comparison to radiotherapy on its own, as well as an survival advantage for using chemoradiotherapy followed by chemotherapy compared to using chemotherapy alone (reviewed in [44]).

### **1.6.3 Chemotherapy of PDAC**

Treatment with chemotherapeutics is of a great importance, even though it cannot lead to a complete cure of patients with pancreatic cancer. Rather it is used to slow down the tumor growth or to relieve pain. Chemotherapeutics can be administered before resection of tumor tissue as a neoadjuvant chemotherapy, or it can be given as adjuvant chemotherapy after surgery to assist the resection and lower the risk of recurrence, or it can be used in a palliative setting.

Often used chemotherapeutics are gemcitabine, a pyrimidine analogue, and 5-fluorouracil (5-FU), which belongs to the group of fluoropyrimidines.

Gemcitabine is the current standard chemotherapeutic used for the treatment of metastatic or unresectable tumors of the pancreas, either as a monotherapy or in combination with other medication [45].

Early studies of gemcitabine treatment in patients with pancreatic cancer showed a relief in symptoms. In 1997, a clinical benefit response in 23.8% of the patients treated with gemcitabine as compared to 4.8% in 5-FU treated patients was described. Moreover, the survival rate of 12 months was only 2% in the group of 5-FU treated patients as compared to 18% in the group of gemcitabine [45].

In 2001, a ESPAC 1-plus study showed that a benefit in the median survival was achieved in patients receiving 5-FU compared to the no chemotherapy group [46].

For the therapy of 5-FU combinations, clinical studies showed a survival benefit in humans with PDAC in comparison with no chemotherapy. However, clinical studies showed no difference in the survival rate between a treatment of 5-FU combination-(5-FU, Adriamycin, Mitomycin) and 5-FU monotherapies [47].

To date, the very promising setting, FOLFIRINOX, is a combination of different chemotherapeutics that has shown to achieve a survival benefit for PDAC patients and is considered to be an option for patients with metastatic pancreatic cancer in relatively good condition. This combination therapy includes the pharmaceuticals oxaliplatin, irinotecan, leucovorin and 5-FU. Clinical studies with FOLFIRINOX compared to patients treated with gemcitabine demonstrated that the median overall survival was 11.1 months in the first group as compared to 6.8 months in the gemcitabine group. Another aspect investigated was the objective response rate, which was higher in the FOLFIRINOX group (31.6%) as compared to the gemcitabine group (9.4%) [48].

The above mentioned therapies provide good treatment options, however many tumor patients develop resistances to chemo- and radiotherapy. Therefore, nowadays it is important to search for advanced treatment approaches.

### 1.6.4 Immune therapy

In addition to chemotherapy or radiotherapy, immune therapy could present another possibility to prolong life and improve the quality of life for pancreatic cancer patients. This is why more than 80 immunotherapeutic trials are currently being performed for PDAC [49].

Immune therapy is intended to modify the performance of the immune system to improve its original ability to recognize and eliminate the body's own cancerous cells. This can be reached for example by recruiting and activating T cells to recognize tumor-specific antigens and therefore achieve a more effective response against PDAC to either defeat the tumor or to slow down tumor growth. Immune therapy includes different approaches in activating treatment with cytokines such as interleukins and interferons (for example interferon alpha (IFN $\alpha$ )), or activating antibodies. Another strategy is the blockade of immunological checkpoints.

Recombinant monoclonal antibodies target tumor-specific antigens and kill the tumor cells through delivery of a conjugated cytotoxic agent or by direct lysis (reviewed in [50]). Many studies have shown that antibodies are clinically quite successful and can be used in diagnosis, as prognostic indicators as well as for the treatment of cancer (reviewed in [50]).

IFN $\alpha$  is one example of immune therapies already being applied in patients suffering from cancers like renal cell carcinoma, malignant melanoma or chronic myeloid leukemia [51, 52]. IFN $\alpha$ , a type I interferon, is produced by various cell types such as monocytes, macrophages, lymphoblastoid cells, fibroblasts and plasmacytoid dendritic cells [53]. IFN $\alpha$  can manifest direct suppressive effect on tumor growth in vitro and in preclinical medical studies [54]. With its considerable radio- and chemo sensitizing effects it is able to improve the impact of other applied therapies like radiotherapy or chemotherapy [55, 56]. One example for such a combined therapy was shown in an orthotopic mouse model of PDAC. The combination of 5-FU and IFN $\alpha$  pointed out an increase in tumor infiltrating NK cells, which also showed enhanced cytotoxicity against Panc02 cancer cells. Furthermore, this therapy enhances the immunogenicity of pancreatic tumors by the higher expression of MHC class 1 molecules [57]. Another study showed a prolonged survival when 5-FU chemotherapy was combined with IFN $\alpha$  [58]. Moreover, IFN $\alpha$  enhances tumor immunogenicity [59].

Importantly, IFN $\alpha$  is considered to increase the immune response by activation of natural killer cells, by augmentation of the differentiation, maturation and function of dendritic cells, by induction of CD8<sup>+</sup> memory cells as well as by an increase of macrophage activity [55, 56, 60, 61]. Although it has been shown that IFN $\alpha$  has activating characteristics, a prolonged survival rate has yet to be achieved.

Moreover, generally the use of immune stimulatory approaches have so far not been as promising as expected [50]. The possible reasons for this are described in detail in 1.8.4. and were previously mentioned as so-called immunological checkpoint molecules.

Immunological checkpoint molecules are inhibitory pathways that fulfill two main purposes: they help generate and maintain self-tolerance due to elimination of T cells specific for self-antigens, and they restrain the amplitude of T cells to prevent a stronger response against foreign pathogens than is necessary. However, they can be contra productive for a successful development of anti-tumor immunity. One immunological checkpoint is conveyed by the cytotoxic-T-lymphocyte-associated protein 4 (CTLA-4) counter-regulatory receptor, which is expressed by activated T cells [62]. Another important immunological checkpoint is the molecule B7-H1, which is one of the ligands for the PD-1 receptor. B7-H1 is an immunological molecule that is expressed on different cell types, like DC, macrophages etc. and is known to have suppressive functions on T cells [63]. Moreover, B7-H1 could be found on tumor cells and some types of immune suppressive cells.

Taking together, the immune system can be an attractive therapeutic target in pancreatic cancer. However to improve the results of immunotherapy, it is necessary to gain a more detailed understanding of the immune system as a whole, covering its activation and suppressive aims.

### **1.7 The immune system**

The immune system represents a complex network composed of several organs, different cell types as well as a variety of cytokines and molecules.

This system protects the body from damage by infectious agents and other harmful substances through a variety of effector cells and molecules, and can be divided into the innate and the adaptive system. The innate immune response is always immediately available to combat a wide range of pathogens, but does not respond to specific pathogens and does not lead to long lasting immunity. The adoptive system provides a specific response which requires the recognition of specific "non-self" antigens that develop during a lifetime and confers protective immunity to reinfection with the same pathogen.

Taken together, the immune system fulfills several main tasks. It provides immunological recognition carried out by lymphocytes and white blood cells, as well as immune effector functions, achieved by the complement system of blood proteins, antibodies and lymphocytes allowing an elimination of the infection. Beyond that, it is involved in processes of immune regulation, such as the ability of self-regulation to protect the body from allergies and autoimmune diseases. Furthermore, the immune system provides immunological memory, which protects the individual against recurring disease and allows for the development of an immediate and stronger response against a causing pathogen [64].

### **1.8 Cells of the immune system**

All cells of the immune system derive from pluripotent hematopoietic stem cells of the bone marrow, and then develop into mature cells of either the lymphoid or the myeloid lineages. The myeloid lineage comprises most of the cells of the innate immune system such as macrophages, granulocytes or dendritic cells, whereas the lymphoid lineage is composed of natural killer cells of innate immunity and lymphocytes of the adaptive immune system [64]. In following, the cell compartments most relevant for this work are described here in detail.

#### **1.8.1 Lymphocytes**

Lymphocytes belong to the leukocytes and are an important component of the adaptive immune response. They can be divided into two groups: B lymphocytes (B

cells) and T lymphocytes (T cells). Lymphocytes originate in the bone marrow. While B lymphocytes mature in the bone marrow as well, precursor T lymphocytes migrate for their maturation to the thymus. Mature lymphocytes circulate in the lymph and blood, and large numbers of these cells are found in lymphoid tissues or organs.

Cells that have not yet been activated by antigens represent naive lymphocytes, whereas antigen-activated, differentiated and entirely functional cells are known as effector lymphocytes. B cells convert into plasma cells after binding of an antigen to a B-cell receptor. This plasma cell is the effector form of B cells, which produces and secretes antibodies. T cells activated by a specific antigen, differentiate into effector T cells and proliferate. Various types of effector T lymphocytes have been described that can functionally be associated with either killing, activation or regulation [64].

The expression of specific cell surface receptors and functional specialization enables additional classification of T lymphocytes. All of them have a TCR/CD3 complex, crucial for their activation, with a corresponding antigen-MHC conglomerate, but only one group of the cells expresses the CD4 molecule (T helper cells) whereas the other fraction is characterized by CD8 expression (Cytotoxic T cells) [64].

CD4<sup>+</sup> T lymphocytes are also called T helper cells since they have a function of assisting and activating other effector cells in the immune system [65]. Two major subsets of T helper cells have been described in detail. The first group, Type 1 helper cells (TH1), is known to produce IL-2, interferon-gamma (IFN- $\gamma$ ) and tumor necrosis factor-beta (TNF- $\beta$ ) and acts in cancer, delayed-type hypersensitivity reactions and also activates infected macrophages to become more efficient in killing pathogens or cancer cells. Whereas the Type 2 helper cells (TH2) express IL-4, IL-5, IL-6 and IL-10 and function in stimulating of B cells by antibody production and secretion (reviewed in [66]).

CD8<sup>+</sup> T cells fulfill the task of killing infected cells as well as cancer cells. They recognize modified cells by binding to their MHC-I-molecule [64] and kill the cells by production of perforin and granzymes, which leads to apoptosis of infected cells [67]. Furthermore, they secrete IFN $\gamma$ , which increases the expression of MHC I molecules on other cells [68].

Whereas most cells in a tumor environment or when fighting infection die due to an apoptosis, a small proportion differentiates into memory cells. T lymphocytes have the ability to differentiate into two different subsets of memory cells: T effector memory cells ( $T_{em}$ ) and T central memory cells ( $T_{cm}$ ), which also can differentiate into T effector cells ( $T_{eff}$ ) after renewed antigen contact and then provide long lasting immunity [64, 69, 70]. In the process of T cell activation, an important role is played by antigen-presenting cells (APC). One of the most potent APC are dendritic cells.

### 1.8.2 Dendritic cells (DC)

Dendritic cells (DC) arise from lymphoid and myeloid progenitor cells in the bone marrow, serve as a messenger between innate and adaptive immunity and represent the most efficient inducers of a T cell response. Immature dendritic cells migrate from the bone marrow through the bloodstream to enter tissues, and they have the ability to phagocytose pathogens. Should they encounter invading microorganisms, they mature into cells that are able to migrate to the lymph nodes and to activate lymphocytes by presenting pathogen antigens on their surface [64]. The activation capacity of DC depends on the expression of the co-stimulatory molecules B7.1 (CD80) and B7.2 (CD86). These membrane-bound molecules are widely expressed on antigen-presenting cells and can interact with the T cell counter receptors CD28 and CTLA-4 [71, 72]. Additionally, DC can express regulatory molecules, such as B7-H1, which gives added input to their stimulation capacity.

There are at least two major groups in which dendritic cells can be categorized: the conventional myeloid dendritic cells (cDC), which are involved in antigen presentation and activation of naïve T cells, and plasmacytoid dendritic cells (pDC), which are not that important for activating naïve T cells but can produce high amounts of Class I interferon [64, 73].

Human plasmacytoid and myeloid DC can be characterized as followed:  $CD11c^{-/low} CD123^+ CD45RA^+ HLA-DR^+$  and  $CD11c^{high} CD11b^{low}$  cells [74]. Plasmacytoid dendritic cells in mice are described as  $CD45R/B220^+ CD11c^{int/low} CD11b^-$  whereas conventional DC are characterized by the  $CD11b^+ CD11c^{high}$  expression [75].

Thus, the complexity and variety of specific cell populations enables a fast and effective immune response, whenever it is necessary.

### **1.8.3. Natural killer cells**

Natural killer cells (NK cells) develop in the bone marrow from the common myeloid lymphoid progenitor and circulate in the blood. NK cells are able to kill other cells by releasing cytotoxic granules containing cytotoxic granzymes and pore-forming protein perforin. Killing is triggered by germline-encoded receptors and therefore NK cells are classified as part of the innate immune system because of those invariant receptors. Several interferons and cytokines are able to activate NK cells, for example IFN $\alpha$ , IFN $\beta$  or IL-12 [64] .

### **1.8.4. Immune regulation**

Both the strength and efficiency of the immune response have to be controlled. Mechanisms of immune regulation ensure that pathogens can be effectively combated without causing autoimmunity and tissue damage. Immune regulation can be viewed at different levels, for example on molecular levels and the levels of different cytokines and mediators as well as on the cellular level, which is for example represented by regulatory T cells (Treg) and myeloid derived suppressor cells (MDSC).

#### **1.8.4.1 Regulatory T cells (Treg)**

Regulatory T cells (Treg) can be divided into two subsets: naturally occurring Treg (nTreg), and adaptive or inducible Treg (iTreg) (reviewed in [76]). Treg have a capability to reduce the immune response by suppressing other cells of the immune system, either by direct cell-cell contact or through the production of suppressive cytokines, for example restraining the differentiation of naïve T cells to T helper cells [64].

nTreg constitute 5-10% of the total CD4<sup>+</sup> T cell population in healthy humans as well as in mice. These cells are produced in the thymus, then enter the peripheral blood circulation and are found in the lymph nodes and the spleen [77]. Treg are the part of

CD4-compartment and express the  $\alpha$ -chain of the IL-2 receptor (CD25) as well as the transcription factor Forkhead-Box-Protein P3 (Foxp3) [25, 64, 78].

While in mice Foxp3 represent an unique marker for Treg, in humans the Foxp3 is not limited to Treg but is also expressed by activated CD4<sup>+</sup> effector T cells [79-81].

iTreg differentiate from naïve FoxP3<sup>-</sup> CD4<sup>+</sup> T cells due to the impact of IL-10 but also from activated effector T cells [76, 82] undergoing anergy, and can be found in increased numbers in some cancers, for example in melanoma or renal cell carcinoma [83].

Other characteristic surface markers or mediators characteristic for Treg include co-stimulatory and co-inhibitory molecules like CD28 or cytotoxic T lymphocyte antigen 4 (CTLA-4), PD-1 as well as several Toll-like receptors and a variety of immunosuppressive cytokines such as IL-10 or transforming growth factors (TGF)- $\beta$  [84-86].

Due to their immunosuppressive function, Treg are involved in tumorigenic processes. An enrichment of Treg in the tumor environment has been demonstrated in several types of cancer, resulting in a suppression of the immune response due to the inhibitory effect of released cytokines like TGF- $\beta$  and IL-10, or due to direct cell contact with the target cell [87-90]. Furthermore, an accumulation of Treg correlates with poor prognosis for patients (tumor growth and survival rates) [91, 92].

In a PDAC model in mice, it was shown that a tumor environment favors the accumulation of regulatory T cells [90]. In this process several mechanisms are involved, to include conversion of non-regulatory T cells into Treg or the activation of naïve Treg [93, 94].

### **1.8.4.2 Myeloid derived suppressor cells (MDSC)**

Another important group of immunoregulatory cells involved in cancer progression are myeloid derived suppressor cells (MDSC). MDSC is a heterogeneous group of cells that consists of myeloid progenitor cells and immature myeloid cells (IMC) from the bone marrow. In healthy individuals IMC quickly differentiate into mature granulocytes, macrophages or dendritic cells, but in pathological situations such as

infectious diseases, trauma, sepsis or cancer the differentiation into mature cells can be blocked, resulting in expansion of MDSC [95]. In humans, MDSC express the myeloid marker CD33 but lack the expression of lymphoid markers and some markers of maturation, like the MHC-II-molecule HLA-DR [96, 97]. In mice, they are characterized by the co-expression of the myeloid-cell lineage differentiation antigen Gr-1 and CD11b [98]. Based on the expression of the two epitopes of Gr-1, Ly-6G and Ly-6C, the MDSC in mice can be further divided more precisely into two subsets: the granulocytic MDSC (gMDSC, CD11b<sup>+</sup>LY6G<sup>+</sup>LYC6<sup>low</sup>) and the monocytic MDSC (mMDSC, CD11b<sup>+</sup>LY6G<sup>-</sup>LY6C<sup>high</sup>) [99].

During pathological situations such as in cancer, the activation of IMCs enhances the expression of immune suppressive factors like the reactive oxygen species (ROS), arginase 1 (ARG1) and inducible nitric oxide synthase (iNOS), leading to augmentation of nitric oxide (NO) production [95]. iNOS plays an important role in the MDSC suppressive pathways [100]. One mechanism requires the synergistic interaction with ARG1 and the production of super-oxide and NO by iNOS, and a second one depends completely on iNOS [101].

Previously, L-arginine was known to be the major target of the suppressive activity of MDSC. This substrate is metabolized by two enzymes, iNOS and ARG1. Arginase 1 increases the L-arginine catabolism, which causes a shortage of L-arginine in the tumor microenvironment and therefore inhibits T cell proliferation by decreasing their expression of the CD3  $\zeta$  chains [102] and by inducing T cell apoptosis [103].

Nowadays, additional mechanisms of MDSC-provided immune suppression are described. One is the production of ROS by MDSCs which can cause oxidative stress [104], DNA damage in immune cells of the tumor environment, recruitment of MDSCs to the tumor site and preventing the maturation of immature MDSC into DC [95, 105, 106].

Another strategy is the expansion of regulatory T cells. MDSC are able to promote the clonal expansion of nTreg as well as the conversion of naïve CD4<sup>+</sup> T cells into iTreg [107].

Both described subsets of MDSC use different mechanisms to suppress T cell function: granulocytic MDSC express high levels of ROS and very small amounts of NO, whereas monocytic MDSC express high levels of NO and only a little ROS.

However, despite their different mechanisms the suppressive capacity of both subsets is equal [99].

Lately, MDSC were also described in dogs as an immunosuppressive cell population with the markers CD11b<sup>low</sup>/CADO48A<sup>low</sup>. This population was increased in the peripheral blood of tumor-bearing dogs [108]. This population has a polymorphonuclear granulocytic character and equates the granulocytic subset of MDSC in humans or mice [109]. Beyond that, it is specified that in dogs with advanced or metastatic cancer, the fraction of putative MDSC is higher than in healthy dogs or in dogs with early-stage, non-metastatic tumors [109].

The MDSC can also express several surface molecules such as CD115, CD124 or CD80 [99]. Beyond that, as well as some other cells, they can express the important immunoregulatory molecule B7-H1 [99].

### **1.8.4.3 The B7-H1 molecule**

On a molecular level, the immune suppression is regulated by numbers of immunosuppressive molecules, one of them is B7-H1.

B7-H1 (PD-L1, CD274) is a member of the B7 family. This molecule together with B7-DC (PD-L2, CD273) acts as a ligand for the programmed death-1 receptor (PD-1). PD-1 is induced on monocytes, B cells and T cells during activation and plays a role in regulating peripheral tolerance and autoimmunity [63, 110].

B7-H1 expression was described on T cells, B cells, DC and macrophages as well as on parenchymal cells, including pancreatic islet cells and vascular endothelial cells [111]. In contrast, B7-DC is nearly only expressed on the surface of dendritic cells and macrophages [110]. Both ligands are considered to participate mainly in the negative regulation of the immune system by linking to PD-1 [110].

As it was demonstrated, B7-H1 can also be expressed on tumor cells, and B7-H1 promotes tumor growth and induces apoptosis of PD-1 expressing T cells in the tumor environment [112]. It is also suggested that the interaction of PD-1/PD-L1 causes the conversion of Helper 1 T cells into regulatory T cells, which could be an

explanation for the increased number of Treg in the tumoral environment where B7-H1 is strongly expressed [113].

Moreover, the engagement of B7-H1 with PD-1 receptors on activated T cells promotes the production of IL-10 [112], which has immunosuppressive effects due to the inhibition of the IFN $\gamma$  and IL-2 cytokines [114, 115]. The expression of B7-H1 in cancers like carcinomas of the lung, breast, stomach, kidney and pancreas is associated with rapid tumor progression, poor prognosis and higher mortality [116-120]. In patients with PDAC, the expression of B7-H1 correlates with the stage of a tumor and serum level of the tumor marker CA 19-9 [121]. Additionally, cytokines, like IFN $\gamma$  can induce negative feedback loops and upregulate the expression of B7-H1 in pancreatic cancer tissue; and the concentration of IFN $\gamma$  in the pancreatic tumor environment correlates with expressed levels of B7-H1 [120]. Together with the data received in our group that another activating cytokine can also upregulate B7-H1 expression [122, 123]+[unpublished observation], this allows one to assume that some activating immune therapy approaches could be in part restricted due to undesirable B7-H1 expression.

### **1.9. The goal of this thesis**

In summary, the immune system plays an important role in cancer development and progression, also in PDAC. The complicated network of different immunological mechanisms can shift the balance in the direction of suppression or attenuation of an immune response. Therefore, the analysis of immune cells, their regulatory molecules and the understanding of crosslinks between the different cells, as well as advanced knowledge about immunological checkpoints are of great importance for the development of new treatment approaches of pancreatic cancer. Because of that, the aim of this thesis is to analyze the precise role of the B7-H1 expression on cells of the immune system with the main focus on MDSC in the context of anti-tumor immunity in PDAC. In order to achieve this aim, different experiments in vitro as well as in vivo were carried out using a mouse orthotopic model of pancreatic cancer using C57BL/6 Wild Type (WT) mice and transgene B7-H1 knockout (KO) mice.

## 2. Material and Methods

### 2.1 Material

#### 2.1.1 Mice

In the experiments, two types of mice age 8-12 weeks were used. The C57BL/6 WT mice were purchased by Charles River, Sulzbach. The B7-H1 KO mice were originally created by Dong and colleagues by homolog recombination in embryonic stem cells in a C57/Bl6 background [124] and kindly provided by Dr. Linda Diehl and Prof. Percy Knolle. Both types of mice were kept in the animal facility of University Heidelberg (IBF, Heidelberg) under specific pathogen-free (SPF) conditions. Homozygous B7-H1 KO mice were checked for the KO genotype stability in regular intervals. Experiments with animals were carried out after approval by the authorities (Regierungspraesidium Karlsruhe).

#### 2.1.2 Pancreas carcinoma cells

The syngeneic ductal pancreatic carcinoma cell line Panc02 was used for the tumor cell implantation [125].

#### 2.1.3 Pharmaceutical products

<b><i>Pharmaceutical products</i></b>	<b><i>Manufacturer</i></b>
Mouse Interferon Alpha A	R&D Systems®
Isofluran Baxter (Isofluran)	Baxter GmbH
Ketanest S 25mg/ml (Ketamin)	Pfizer AG
Rimadyl® ad us. vet., Injection solution (Carprofen)	Pfizer AG
Rompun 2% (Xylazin)	Bayer

5-FU 50 mg/ml (5 Fluorouracil)	medac GmbH
--------------------------------	------------

Tab.2.1.3. 1 Pharmaceutical products

### 2.1.4 Anti-mouse Antibodies for the flow cytometry

<i>Specificity</i>	<i>Conjugate</i>	<i>Clone</i>	<i>Isotype</i>	<i>End volume in <math>\mu</math>l *</i>	<i>Manufacturer</i>
CD62L	APC	MEL-14	Rat (Fischer) IgG <sub>2a</sub> , $\kappa$	1	BD Pharmingen
CD25	APC	3C7	Rat (Outbred OFA) IgG <sub>1</sub> , $\lambda$	1.5	BD Pharmingen
CD11c	APC	HL3	Armenian Hamster IgG1, $\lambda$ 2	1	BD Pharmingen
CD115	APC	AFS98	Rat IgG <sub>2a</sub> , $\kappa$	1	eBioscience
Gr-1	APC-Cy 7	RB6-8C5	Rat IgG <sub>2b</sub> , $\kappa$	0.25	BD Pharmingen
CD3e	APC-Cy 7	145-2C11	Armenian Hamster IgG1, $\kappa$	2	BD Pharmingen
CD44	FITC	IM7	Rat IgG <sub>2b</sub> , $\kappa$	0.5	BD Pharmingen
FoxP3	FITC	FJK-16s	Rat IgG <sub>2a</sub> , $\kappa$	1	eBioscience
CD80	FITC	16-10A1	Armenian Hamster IgG <sub>2</sub> , $\kappa$	1	BD Pharmingen
F4/80	FITC	BM8	Rat IgG <sub>2a</sub> , $\kappa$	1	eBioscience
Purified Arginase-1	N/A**	19/Arginase1	Mouse IgG1	2	BD Pharmingen
Ig for Arginase-1	FITC	N/A**	Goat Ig	0,5	BD Pharmingen
CD45R/B220	Pacific Blue	RA3-6B2	Rat IgG <sub>2a</sub> , $\kappa$	1	BD Pharmingen
CD45RB	PE	16A	Rat IgG <sub>2a</sub> , $\kappa$	1	BD Pharmingen
CD44	PE	IM7	Rat IgG <sub>2b</sub> , $\kappa$	1,25	BD Pharmingen
I-A[b]	PE	AF6-120.1	Mouse (BALB/c) IgG <sub>2a</sub> , $\kappa$	0.5	BD Pharmingen
CD 274 (B7-H1)	PE	MIH5	Mouse IgG1	3	eBioscience
CD 273 (B7-DC)	PE	TY25	Rat IgG <sub>2a</sub> , $\kappa$	3	eBioscience
Ly-6G	PE	1A8	Rat (LEW/N) IgG <sub>2a</sub> , $\kappa$	0.5	BD Pharmingen
CD62L	PE	MEL-14	Rat(F344) IgG <sub>2a</sub> , $\kappa$	1	BD Pharmingen

Material and Methods

CD69	PE	H1.2F3	Armenian Hamster IgG1, λ3	3	BD Pharmingen
CD86	PE-Cy 7	GL1	Rat (Louvain) IgG <sub>2a</sub> , κ	1	BD Pharmingen
CD8a	PerCP-Cy 5.5	53-6.7	Rat (LOU/Ws1/M) IgG <sub>2a</sub> , κ	1	BD Pharmingen
CD69	PerCP-Cy 5.5	H1.2F3	Armenian Hamster IgG1, λ3	1.5	BD Pharmingen
CD11b	PerCP-Cy 5.5	M1/70	Rat (DA) IgG <sub>2b</sub> , κ	1	BD Pharmingen
FoxP3	PerCP-Cy 5.5	FJK-16s	Rat IgG2a ,κ	2,5	eBioscience
CD4	V450	RM4-5	Rat (DA) IgG <sub>2a</sub> , κ	1	BD Horizon
Ly-6C	V450	AL-21	Rat IgM, κ	0.1	BD Horizon
CD45	V500	30-F11	Rat (LOU/Ws1/M) IgG <sub>2b</sub> , κ	2	BD Horizon
CFSE	FITC	N/A**	N/A**	0,5 μM	eBioscience
CD16/ CD32	N/A**	93	Rat IgG2a, λ	2	eBioscience
CD28 Functional Grade Purified	N/A**	37.51	Golden Syrian Hamster IgG	2 μl/ml medium	eBioscience
CD3 Functional Grade Purified	N/A**	17A2	Rat IgG2b, κ	1 μl/ml medium	eBioscience

**Tab.2.1.4. 1 Anti-mouse antibodies for flow cytometry**

\* volume pro  $2 \times 10^6$  cells/50 μl

\*\* N/A not applicable

### 2.1.5 Laboratory Equipment

<b>Laboratory Equipment</b>	<b>Manufacturer</b>
Bio Vortex V1	Lab-4 you
Counting chamber Neubauer Improved	neoLab Laborbedarf GmbH
Digital Timer	neoLab
Flow cytometer (FACS) Canto II	Becton Dickinson
Freezer -20°C	Liebherr
Freezer -80°C	Thermo Scientific
GASTIGHT Syringe 25μl	Hamilton Company

Incubator HeraCell	Heraeus
Wash stations	Millipore GmbH
Luminex® 100/200 System	Bio-Rad
Multipette® plus	Eppendorf
Optical microscope Axiostar <sub>plus</sub>	Zeiss
Optical microscope Axiovert 25	Zeiss
Pipette Proline	Biohit GmbH
Pipettes Pipetman	Gilson
Pipetus®-akku	Hirschmann Laborgeräte
Refrigerator 4°C	Liebherr
Scale EW600-2M	Kern & Sohn GmbH
Sterile bench Hera <sub>Safe</sub>	Heraeus
Vortex Genie 2	Scientific Industries
Zentrifuge 5810 R	Eppendorf

Tab.2.1.5 1 Laboratory Equipment

### 2.1.6 Laboratory consumables

<b>Laboratory consumables</b>	<b>Manufacturer</b>
aluminum foil	Roth GmbH
cell scraper 25 cm	Sarstedt
cell strainer (100 µm, 40 µm)	Becton Dickinson
Combitips Plus (0.1 ml, 0.5 ml, 2.5 ml, 5 ml)	Eppendorf
Costar® Stripette (5 ml, 10 ml, 25 ml)	Corning Incorporated
Eppendorf Tubes 1,5 ml	Eppendorf
FACS Tubes 5 ml	Becton Dickinson
Falcon Tubes (15 ml, 50 ml)	Becton Dickinson
Millex sterile filter 33 mm Diameter	Millipore
Microlance Needle 26G x1/2	Becton Dickinson
Polysorb™ USP 5-0	Covidien AG
Staple remover	Fine Science Tools
Surgical Skin Staplers Reflex 7 mm	Fine Science Tools
Suture Slip Reflex 7 mm	Fine Science Tools
Syringe 50 ml	B.Braun

Syringe 5 ml	Becton Dickinson
Syringe 1 ml	B.Braun
Transferpipettes 3 ml	Becton Dickinson
Well Plates (6-well, 96-well)	Becton Dickinson

**Tab.2.1.6. 1 Laboratory consumables**

### 2.1.7 Laboratory solutions

<b><i>Laboratory solutions</i></b>	<b><i>Manufacturer</i></b>
Collagenase III	Biochrom AG
Collagenase IV	Biochrom AG
DNase I	Roche
Dulbecco`s PBS Solution (10x)	PAA Laboratories GmbH
EDTA 0.5 M; pH 8.0	SERVA Electrophoresis GmbH
Foxp3 Staining Buffer Set	eBioscience
HBSS Buffer	PAA Laboratories GmbH
Hyaluronidase	Linaris GmbH
H-Insulin	Aventis Pharma AG
RBC Lysis Buffer(10x)	BioLegend
RPMI 1640	PAA Laboratories GmbH
Trypan Blue 0.5 %	Biochrom AG

**Tab.2.1.7. 1 Laboratory solutions**

### 2.1.8 Media and Buffers

#### 2.1.8.1 Buffers for the flow cytometry

##### Stain Buffer:

- 1x PBS buffer solution + 2 mM EDTA

Fixation buffer for intracellular FACS-Staining:

- 1:4 Dilution of Fixation/Permeabilization Concentrate (eBioscience) + Fixation/Permeabilization Diluent (eBioscience)

Wash buffer for intracellular FACS-Staining ("Perm-Wash"):

- 1:10 Dilution of Permeabilization Buffer (eBioscience) + distilled H<sub>2</sub>O

**2.1.8.2 Medium, buffer and solutions for the cell culture**

Wash buffer for the cell culture:

- PBS buffer (1x), sterile

Medium for the cell culture:

- RPMI 1640 + 10 % Fetal Calf Serum (heat-inactivated at 56°C for 30 min)

Interferon stock solution

- Mouse IFN $\alpha$  stock solution was purchased from R&D Systems<sup>®</sup> and was used for the treatment of cultures in a concentration of 1000U/ml.

5-FU stock solution

- The original stock solution was purchased from Medac. For the treatment of cultures it was used in a concentration of 65  $\mu$ g/ml.

CFSE stock solution

- The CFSE (Carboxyfluorescein Succinimidyl Ester) Proliferation Dye was from eBioscience, and originally reconstituted to 10 mM with DMSO. For the titration the concentrations of 0.25  $\mu$ M, 0.5  $\mu$ M and 1.0  $\mu$ M were tested. The most suitable concentration of 0.5  $\mu$ M was used for cell labeling.

Digestion solution

- The components of this solution are: 0.05 mg/ml DNase I, 0.24 mg/ml Collagenase III, 0.56 mg/ml Collagenase IV, 0.2 mg/ml Hyaluronidase, 0.08 U/ml H-Insulin in HBSS Buffer. Aliquots were made and stored at -20°C.

### 2.1.8.3 Buffer for MACS

#### MACS Buffer

- 1x PBS buffer solution + 0.5 % bovine serum albumin + 2 mM EDTA

### 2.1.9 Software

<b>Software</b>	<b>Manufacturer</b>
Bio-Plex Manager 4.0	Bio-Rad
EndNote X6	Thompson Reuters
FlowJo (Version 7.6.1) Diva	Tree Star
GraphPad PRISM (Version 5)	GraphPad Software

Tab.2.1.9. 1 Software

## 2.2 Methods

### 2.2.1 Orthotopic mouse model

Mice were anesthetized by inhalation anesthesia. For the induction, Isoflurane in the concentration of 5 Vol% was used together with 95 Vol% of oxygen. The maintenance of the status was achieved by using 3.5 Vol% Isoflurane and 96.5 Vol% of oxygen. Bepanthen eye ointment was used to protect the eyes from desiccation. Also 50 µl Rimadyl (5 mg/kg s.c., 1:10 diluted with 0.9 % NaCl) was injected preoperatively for pain relief/analgesia.

Tumor cells (Panc02) in a concentration of  $2 \times 10^7$ /ml were diluted in PBS and a volume of 5 µl was injected using a GASTIGHT Syringe (25 µl). The mice were

fixated in dorsal position, then the abdomen and substernal region were shaved, disinfected with alcohol and cut open in the linea alba to prevent heavy bleeding. After dislocation of the pancreas, Panc02 cells were implanted. Following the implantation a forceps was used to clamp the point of injection for 30 seconds and then the pancreas was located back to its original position.

After those steps, the abdomen was stitched in two-layers by continuous sutures. For both sutures an absorbable polyfil needle-thread combination (Polysorb 5-0 rounded needle) was used. Besides that, the skin was also stapled with clamps that were removed 10 days after the surgery.

### **2.2.2 Treatment of the mice with IFN $\alpha$ , with 5-FU or with the combination of IFN $\alpha$ +5-FU**

For treatment, the mice received therapeutics at Day 5, 7 and 9 after the surgery. The mice were injected intraabdominally with 50  $\mu$ l of either IFN $\alpha$  or 5-FU. The group of mice which got the combined therapy received 50  $\mu$ l of IFN $\alpha$  and 50  $\mu$ l of 5-FU.

The injection solution of IFN $\alpha$  was diluted to a concentration of  $2 \times 10^5$ /ml. For the 5-FU treatment the concentration of 14 mg/ml was prepared.

After four weeks the mice were killed by cervical dislocation. In cases of acute suffering incompatible with animal health and welfare, the mice were killed beforehand. Criteria for this were a bad general state of health like scrubby hair, hypothermia or refusing the food intake, apathy, icterus, ascites or an abnormal posture as well as a high loss of weight.

### **2.2.3 Preparation of tumors and spleens, collecting blood samples**

Four weeks after the implantation of Panc02 cells, the mice were killed by cervical dislocation. If serum was needed, the mice were first anesthetized by Ketamin-Xylazin and blood samples were taken directly by heart puncture. Afterwards, the mice were killed by cervical dislocation.

Spleens and tumors were dissected and kept in PBS for further use. The size of pancreatic tumors was determined using a slide vernier caliper.

Additionally, the abdomen was examined for the presence of metastasis in the liver, intestines and peritoneum as well as any adhesions or abnormalities. The size of the metastasis was graded from + to +++.

After they were allowed to clot, the blood samples were centrifuged at 6000 g for 25 min. The clear serum supernatant was centrifuged again at 9300 g for 10 min. Afterwards the serum was frozen at -20°C until it was analyzed by Luminex approach.



**Fig.2.2.3. 1** Photos of blood sample collection, dissection and measuring of organs

### **2.2.4 Preparation of a single-cell suspension**

To prepare a single-cell suspension from spleen and tumor, tissue was pressed through a 100  $\mu\text{m}$  cell strainer and flushed with 10 ml of PBS to collect as many cells as possible. Then the samples were centrifuged at 4°C, 400 g, 5 min and the supernatant was discarded. After adding 1 ml of erythrolysis buffer, the samples were resuspended and incubated for 2 min. As a result, the erythrocytes were destroyed and an unspecific binding to antibodies was prevented. Following this incubation time, 10 ml of PBS was added to stop erythrolysis. After another centrifugation step (4°C, 400 g, 5 min) the cells were resuspended in 10 ml of PBS and flowed through a 40  $\mu\text{m}$  cell strainer. The tumor samples passed through the 40  $\mu\text{m}$  cell strainer twice, since tumor cells are generally more likely to generate clumps. Subsequent to another centrifugation, the cell number was detected by using trypan blue and a Neubauer counting chamber. Finally the cell concentration was adjusted to the requested concentration of  $2 \times 10^6$  cells/50  $\mu\text{l}$  [126].

### 2.2.5 Flow cytometry

Flow cytometry is a method that can be used to determine cells based on their characteristics of size (FSC- Forward Scatter), granularity (SSC- Side Scatter) and intensity of antibody-bound fluorescence. Flow cytometry is also called FACS (“Fluorescence activated cell sorting”) and is based on an antigen-antibody reaction using fluorescence conjugated antibodies. The cells are excited by a laser and the emitted signals are transformed into an electrical signal that can be recorded and analyzed.

Prior to the measurement of the samples, compensation was made to minimize the overlap of fluorescence spectra, produced by different types of fluorescence. The principle of this compensation is to measure the single fluorescence-coupled antibodies separately, to calculate the overlap and to compensate for it.

#### 2.2.5.1 Immunophenotyping

The splenocytes and tumor cells were stained with different antibody combinations in several panels to enable a detailed look at the individual cell populations. In tumor-bearing mice, CD45 was used to differentiate between tumor cells (CD45<sup>-</sup>) and tumor-infiltrating leucocytes (CD45<sup>+</sup>). CD4/CD8 panel: CD4/CD8 T cells as well as their subsets, naïve T cells (CD62L<sup>+</sup>CD44<sup>-</sup>), effector T cells (CD62L<sup>-</sup>CD44<sup>-</sup>), central memory T cells (CD62L<sup>+</sup>CD44<sup>+</sup>), and effector memory T cells (CD62L<sup>-</sup>CD44<sup>+</sup>) were analyzed. DC panel: in this panel the following subsets, conventional DC (CD11c<sup>high</sup>CD11b<sup>+</sup>, cDC) and plasmacytoid DC (CD11c<sup>int</sup>CD45R<sup>+</sup>, pDC) were characterized, and the expression of MHC-II molecules (I-A[b]) or B7-H1 molecules (B7-H1) on their surface was investigated. The activation state of the dendritic cells was verified by the expression of CD80 and CD86 costimulatory molecules. For the analysis of suppressive cell population, the Treg panel was used as well as the MDSC panel. Treg panel: in the Treg panel the T regulatory cells were gated as Foxp3<sup>+</sup>CD25<sup>+</sup> within the CD4 T cell population. MDSC panels: in the panels for MDSC it was first gated on total MDSC (CD11b<sup>+</sup>Gr-1<sup>+</sup>) and this population was further divided in two subsets. The granulocytic MDSC are characterized as Ly-6C<sup>low</sup>Ly-6G<sup>+</sup> and the monocytic MDSC as Ly-6C<sup>high</sup>Ly-6G<sup>-</sup>. To test functional status of

MDSC, the expression of Arginase-1 (Arg-1) and inducible Nitric Oxide Synthase (iNOS) was examined.

### **2.2.5.2 Extracellular staining**

First, the cells were incubated for 10 min with 1  $\mu$ l of anti-CD16/CD32 in order to inhibit unspecific binding of antibodies by the Fc-receptors. Afterwards, 50  $\mu$ l of the cell suspension was plated in 96-well plates, the appropriate antibodies for cell surfaces molecules were added to each well and incubated for 15 min at 4°C in the dark. After this incubation the samples were washed twice with 200  $\mu$ l of stain buffer. In between and afterwards the samples were centrifuged and the supernatant was discarded. After the washing steps the cells were resuspended in 100  $\mu$ l stain buffer and then transferred to FACS tubes already containing 300  $\mu$ l stain buffer. The tubes were stored on ice until they were analyzed on the BD Canto II Flow cytometer.

### **2.2.5.3 Intracellular staining**

For intracellular staining it is necessary that the cells are fixated and permeabilised so the antibodies are able to bind to the intracellular antigen. First, extracellular staining with non-conjugated antibodies was performed and the cells were fixed with 1 ml of the Fixation/Permeabilisation Buffer. The samples were then incubated for at least 3 hours at 4°C avoiding light. Afterwards, two washing steps with 2 ml of Permeabilisation Buffer were performed. The centrifuge was set at 4°C, 400 g, 5 min. After those washing steps the intracellular and also the conjugated extracellular antibodies were pipetted to the samples. The reason for this is that conjugated extracellular antibodies are more instable than non-conjugated and therefore could easily fall apart throughout the fixation. Finally, after two more washing steps with Permeabilisation Buffer, the cells were resuspended in 300  $\mu$ l of stain buffer and analyzed on the BD FACS Canto II.

### **2.2.6 Treatment of splenocytes in culture**

After preparation of a single-cell suspension of the spleen cells, they were resuspended in the medium (RMPI 1640+10% FCS) in the concentration of  $2 \times 10^6$  cells/ml. Afterwards, the cells were plated using a 6-well plate with 5ml per well and incubated at 37°C for 1 hour in order to allow them to recover before treatment. After this the cultures were treated either with IFN $\alpha$  in the concentration of 1000 U/ml or 5-FU in the concentration of 65  $\mu$ g/ml or the combination of IFN $\alpha$ +5-FU. Some of the wells were left as vehicle controls with 5  $\mu$ l PBS. After an incubation time of 24 hours at 37°C in the incubator, the cells were harvested by using a gentle scraper. Finally, the cells were prepared for FACS staining following the usual staining protocol.

### **2.2.7 Investigation of MDSC suppressive activity**

In order to investigate whether the MDSC have a suppressive effect on the proliferation of splenocytes, these cells had been cocultured in different constellations. CFSE (Carboxyfluorescein succinimidyl ester) labeled splenocytes from either WT or B7-H1 KO mice were plated with or without the activation with CD3/CD28. Afterwards, MDSC from WT or B7-H1 KO mice were added to the splenocytes.

#### **2.2.7.1 CFSE cell labeling of splenocytes**

In order to trace proliferative capacity of splenocytes, they were labeled with CFSE. CFSE is a marker for proliferation and cell tracking and is able to cross the intact cell membranes. The cell division can be seen because only half of the fluorescence intensity is found in the next cell generation.

CFSE in the optimized concentration of 0.5  $\mu$ M was added to the single cell suspension of splenocytes, then the samples were incubated for 10 min at room temperature protected from light. To stop the labeling process, first 5 volumes of complete cold medium was added and the samples were incubated on ice for another 5 min. Afterwards, the samples were washed 3 times with a cold medium. The washing steps were always carried out as followed: 4°C, 400 g, 5 min. After this, the splenocytes were put in cell culture.

### **2.2.7.2. Digestion of tumors**

Digestion solution (see 2.1.8.2.) was used to digest the tumors and therefore reduce their stickiness, in particular of the more necrotic tumor regions. First, the isolated tumors were cut into small pieces and incubated in 5 ml of the digestion solution at 37°C in the water bath with the shaker function. Afterwards, the tumors were treated in the usual way using the FACS protocol.

### **2.2.7.3 Magnetic activated cell sorting (MACS)**

The MACS separation was used to isolate the MDSC from the tumor cell suspension according to manufacturer instructions. The basic principle of MACS is that specific cell fractions can be magnetically labeled due to the expression of specific receptors. Thus, during the isolation procedure positive cells will remain on the column due to the magnetic field while the negative cells flow through. Afterwards, the positive cells can be removed with a plunger. The MDSC subpopulations are characterized by the differential expression of Ly-6G and Ly-6C cell surface. In our case first Gr-1<sup>high</sup>Ly-6G<sup>+</sup> cells can be magnetically labeled by Anti-Ly-6G-Biotin antibody and Anti-Biotin MicroBeads. Therefore, the first flow through is pre-enriched in Gr-1<sup>dim</sup>Ly-6G<sup>-</sup> cells. Afterwards, this first flow through is magnetically labeled with Anti-Gr-1-Biotin antibodies and Streptavidin MicroBeads, which allows for isolating Gr-1<sup>dim</sup>Ly-6G<sup>-</sup> cells by positive selection.

The samples for isolation were prepared as a single-cell suspension. After the first centrifugation step (4°C, 300 g, 10 min) the cells were resuspended in MACS buffer. Then, a FcR Blocking Reagent was added. Afterwards, the samples were vortexed and incubated in the refrigerator for 10 min. Anti-Ly-6G-Biotin antibody was added, the cells were mixed again and incubated in the refrigerator for another 10 min. Then the cells were washed with MACS buffer and centrifuged at 4°C, 300 g, 10 min. The supernatant was discarded and the cells were resuspended in an appropriate amount of buffer. Afterwards, Anti-Biotin MicroBeads were added to the samples, followed by an incubation step of 15 min at 4°C. After another washing step, the cells were centrifuged and resuspended in MACS buffer in order to pass through the column.

The LS Column was first placed in the magnetic field of the MACS Separator and rinsed with MACS buffer. The cell suspension ran through the column and the flow-through was collected. After three washing steps, all flow through were combined with the flow through of unlabeled cells and this suspension of unlabeled cells (pre-enriched of Gr-1<sup>dim</sup>Ly-6G<sup>-</sup>) were labeled in a second step.

The positive cells from the column were removed from the outside magnetic field using the MACS buffer and a plunger.

To increase the purity of Gr-1<sup>high</sup>Ly-6G<sup>+</sup> cells, the cells were allowed to pass through once more using a new column.

In the second step, the cells from the first flow through were labeled with Anti-Gr1-Biotin antibody and incubated for 10 min. Afterwards, the samples were washed with MACS buffer, and after another centrifugation, the supernatant was discarded. After resuspending the cells in MACS buffer, Streptavidin Micro Beads were added. Another 10-min incubation step and one washing step followed. Finally, the cells were resuspended in an appropriate amount of MACS buffer.

For this isolation, an MS Column was used. The cell suspension was applied on the column and washed three times with buffer. Then the Gr-1<sup>dim</sup>Ly-6G<sup>-</sup> cells were flushed out of the column by using the plunger.

Again to increase the purity of Gr-1<sup>dim</sup>Ly-6G<sup>-</sup> cells they were run through a new second column.

### **2.2.7.4 Coculture**

For the cocultures, 96-well round bottom plates were used. The CFSE labeled splenocytes were seeded in a concentration of  $2 \times 10^5$ /200  $\mu$ l Medium and the MDSC in a concentration of  $2 \times 10^5$ /50  $\mu$ l Medium. To activate the cells, CD3 antibody (1  $\mu$ l/ml) and CD28 antibody (2  $\mu$ l/ml) were used as activation stimuli and were added to the appropriate wells 1 hour after the cells were plated.

After an incubation time of 72 hours at 37°C, the medium supernatant was collected and stored at -20°C until it was analyzed by the Luminex approach. The cells were harvested and the cell concentration was adjusted to  $2 \times 10^6$ /50  $\mu$ l. Afterwards, the

cells were stained with appropriate antibodies and their fluorescence was measured by flow cytometry on the BD FACS Canto II.

### **2.2.8 Luminex (Bioplex) assay**

Samples of collected sera and culture supernatants were analyzed by Luminex assay for the presence of the following cytokines: IL-6, IFN $\gamma$ , IL-10, IL-1 $\beta$ , IL-2 and VEGF by 6plex with magnetic beads and TGF- $\beta$ 1 with non-magnetic beads.

According to the manufacturer instructions, the samples were centrifuged at 800 g for 5 min to allow debris to deposit at the bottom of the Eppendorf tube.

The plates were first prewashed with wash buffer and shaken off for 10 min at room temperature followed by removing the buffer using a magnetic (for magnetic beads) or the vacuum (for non-magnetic beads) wash stations.

Afterwards, the following reagents were added: Assay buffer to background and sample wells, serum matrix to background, standard and control wells, standard to the appropriate standard wells and the quality controls to the control wells. Then the samples were added to the relevant wells. The samples used for the TGF- $\beta$ 1 detection were treated with HCL and NaOH prior to plating. Finally, the appropriate beads were added to each well. The plate was sealed and placed on the plate shaker at 4°C overnight.

On the next day, all contents were removed and the plates washed twice with buffer. Afterwards, the Detection antibody was added to each well for 1 hour. The secondary antibody, Streptavidin-Phycoerythrin was directly added to each well and incubated for another 30 min. After two washing steps, Sheath fluid was added to each well and the plates were measured by the Luminex<sup>®</sup> 100/200 System.

### **2.2.9 Statistical analysis**

All statistical analyses were performed using GraphPad Prism Version 5.01. Distributions of continuous variables were described by standard error of mean, SEM, median, 25% and 75% percentiles, and were presented as box-and-whiskers

plots or as column bar graphs. D'Agostino and Pearson omnibus normality tests were conducted to estimate the distribution of data. The null hypothesis (mean values were equal) versus the alternative hypothesis (mean values were not equal) was tested for more than two groups by one-way ANOVA with the Dunnett's post-hoc test, and for two groups by unpaired, two-tailed *t*-test for normal distributed variants or by the Mann-Whitney test for nonparametric distributed data. Survival analysis was done with Kaplan-Meier curves and statistically analyzed with the Log-rank test. All statistical tests were two-tailed. The significance level was  $\alpha=5\%$ .

### 3. Results

#### **3.1 Effects of chemo (5-FU) - and immunotherapy (IFN $\alpha$ ) on the constellation of leukocyte subsets and on the expression of B7-H1/B7-DC molecules on splenocytes of healthy WT and B7-H1 KO mice in *in vitro* cultures**

In this experiment series we wanted to investigate whether 5-FU and IFN $\alpha$  could directly influence the frequency and phenotype of leukocytes subsets in healthy WT and B7-H1 KO mice. Moreover, we wanted to examine if this could be also accompanied by a direct effect on B7-H1 or B7-DC expression in the different leukocytes subpopulations of WT and B7-H1 KO mice respectively. To achieve this, we isolated splenocytes of healthy WT and B7-H1 KO mice and treated them in a culture with either 5-FU, IFN $\alpha$  or the combination of IFN $\alpha$ +5-FU. After incubation for 24 hours, we collected the cells, analyzed them by flow cytometry and compared WT and B7-H1 KO mice in terms of the constellation of different immune cells as well as the expression of the B7-H1/B7-DC molecules.

##### **3.1.1 Analysis of CD4<sup>+</sup>/CD8<sup>+</sup> T cells**

First, we took a look at the frequency of lymphocytes in all live cells. In all treatment groups as well as in the control group, the percentage of lymphocytes was significantly lower in WT mice than in B7-H1 KO mice (Fig.3.1.1.1 A). By looking at WT and B7-H1 KO separately, no significant difference was seen between controls and the therapy groups, neither in WT nor B7-H1 KO mice (Fig.3.1.1.1 B,C).

## Results

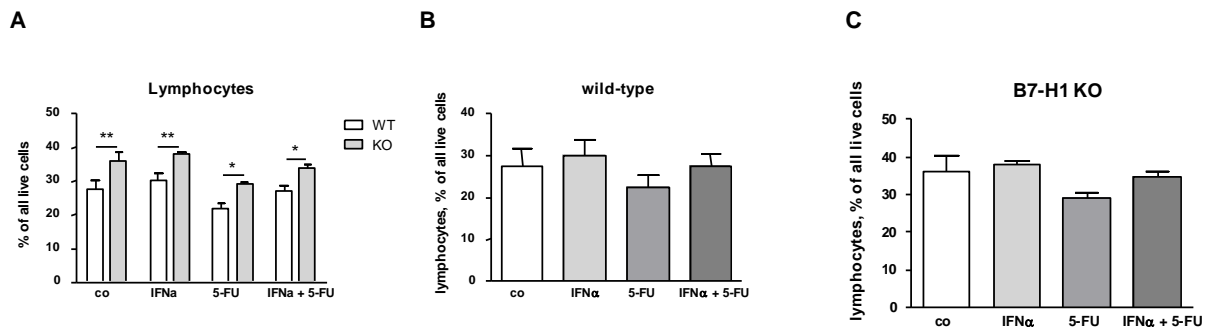
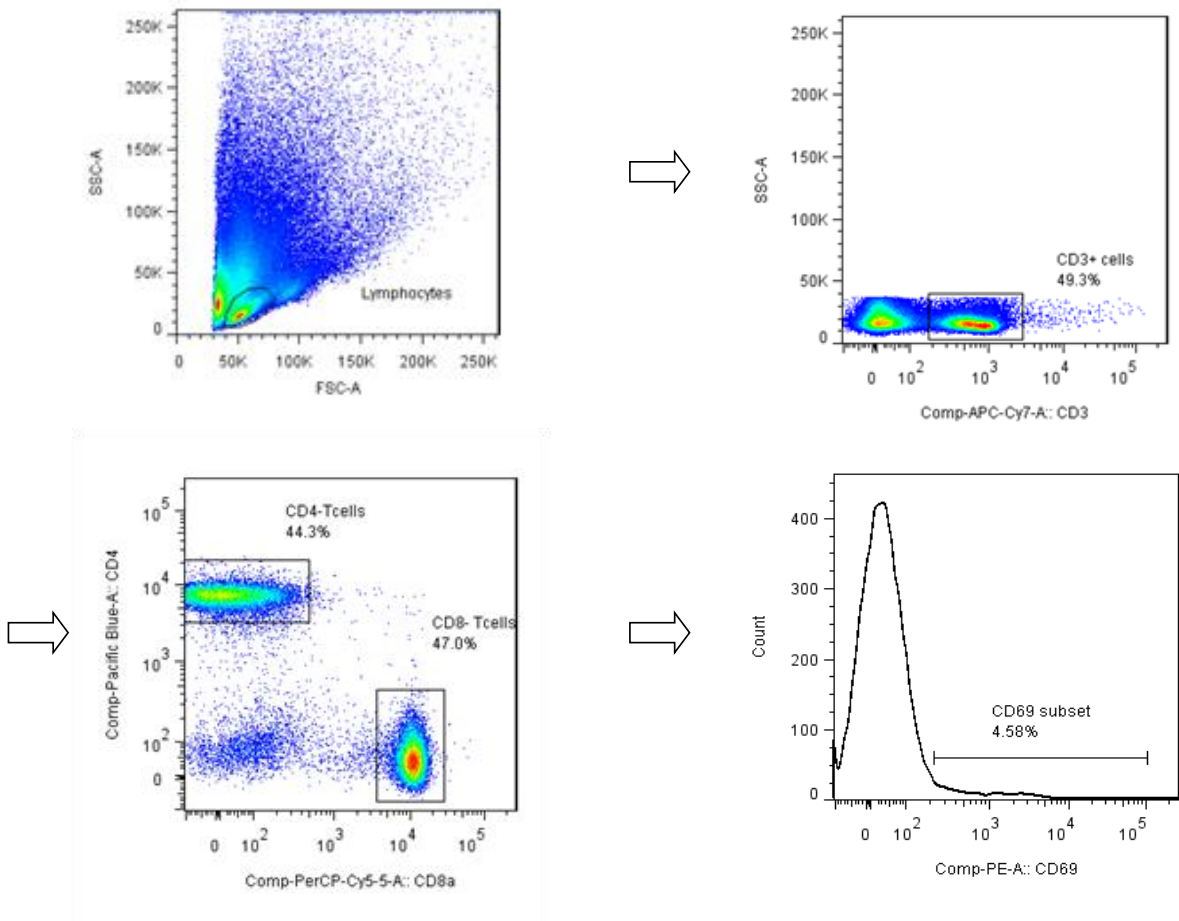


**Fig.3.1.1. 1** Quantification of lymphocytes from WT and B7-H1 KO mice in control groups (without treatment, co) and after the treatment of splenocytes in *in vitro* cultures with IFN $\alpha$ , 5-FU and IFN $\alpha$ +5-FU.

Freshly isolated splenocytes were put in a culture and treated with IFN $\alpha$ , 5-FU and IFN $\alpha$ +5-FU for 24 hours. Afterwards, the cells were stained with fluorescence labeled specific antibodies and analyzed by flow cytometry. Data from four independent experiments are presented as column bar graphs with standard error of mean (SEM) (n = 16; \*p<0.05, \*\*p<0.01; control group vs. treatment groups; two-way (A) and one-way (B,C) ANOVA)

In a second step, we determined the frequency of T cell populations, CD4<sup>+</sup> T cells and CD8<sup>+</sup> T cells, out of CD3<sup>+</sup> cells. The performed gating strategy for the CD4/CD8 panel in this *in vitro* experiment is shown in Fig.3.1.1.2., the FACS data (dot-plot, histogram) represent one typical result out of four independent experiments.

Gating Strategy for CD4<sup>+</sup>/CD8<sup>+</sup> T cells



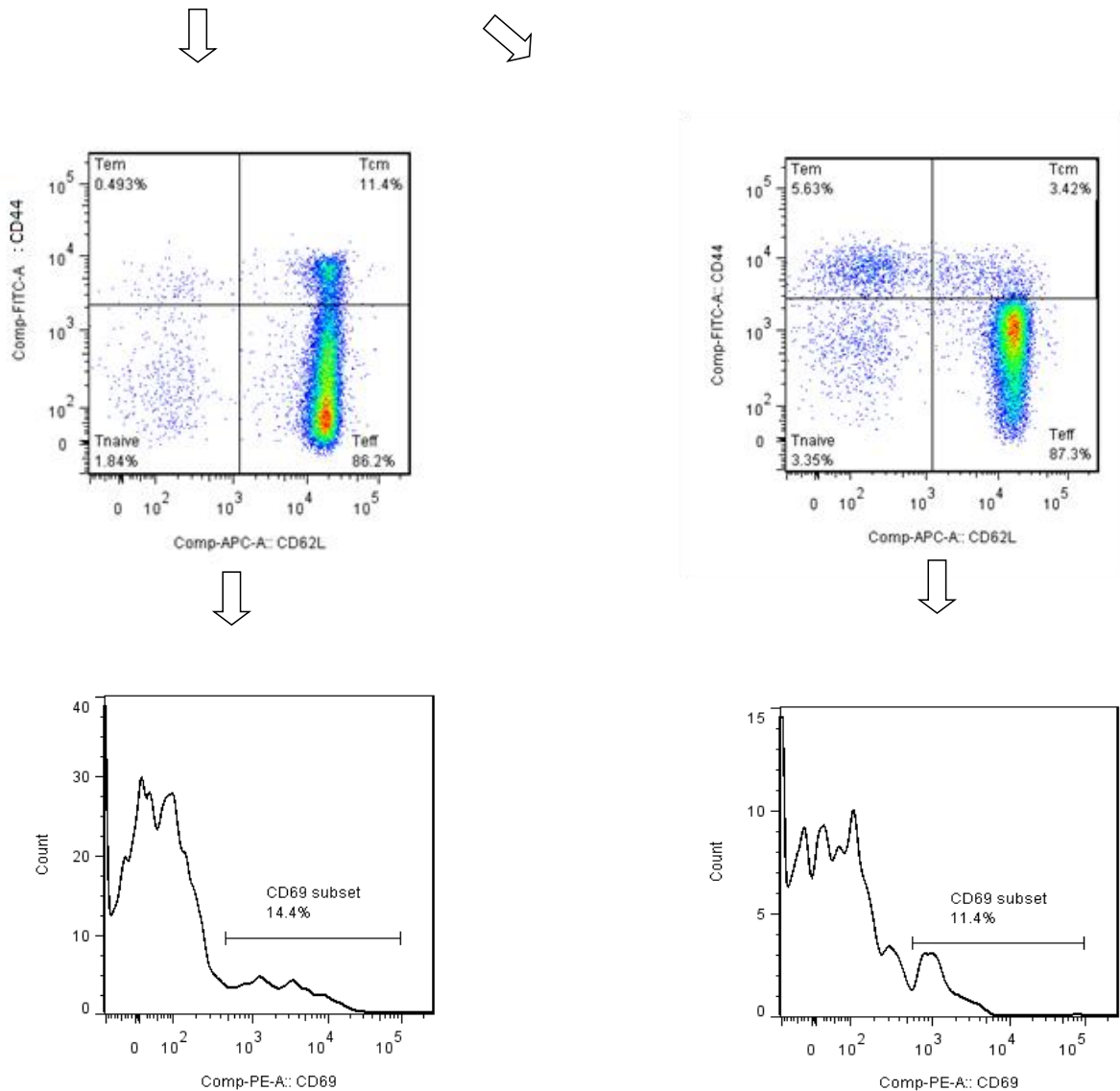


**Fig.3.1.1. 2 Gating strategy for CD4<sup>+</sup>/CD8<sup>+</sup> T cells in splenocytes using flow cytometry.**

Lymphocytes were gated out using FSC/SSC dot plot. Next, the CD3<sup>+</sup> cells were selected and the CD4<sup>+</sup>/CD8<sup>+</sup> T cells were gated out from CD3<sup>+</sup> cells. Furthermore, the CD4<sup>+</sup>/CD8<sup>+</sup> T cells were divided into naïve T cells (Tnaive), effector T cells (Teff), effector memory cells (Tem) and central memory cells (Tcm). The activation status of different subpopulations was determined by analyzing the expression of the CD69 early activation marker. All positive gates were set according to FMO controls.

Concerning the CD4<sup>+</sup> T cells, a significantly higher frequency of CD4<sup>+</sup> T cells out of CD3<sup>+</sup> cells was seen in the treatment groups of 5-FU and IFN $\alpha$ +5-FU in WT compared to B7-H1 KO mice. In control and IFN $\alpha$  treated groups, only a tendency

towards an increase in CD4<sup>+</sup> T cells was seen (Fig.3.1.1.3 A). No significant difference was determined between control and treatment groups for both WT and B7-H1 KO mice, when investigated separately (Fig.3.1.1.3 B,C).

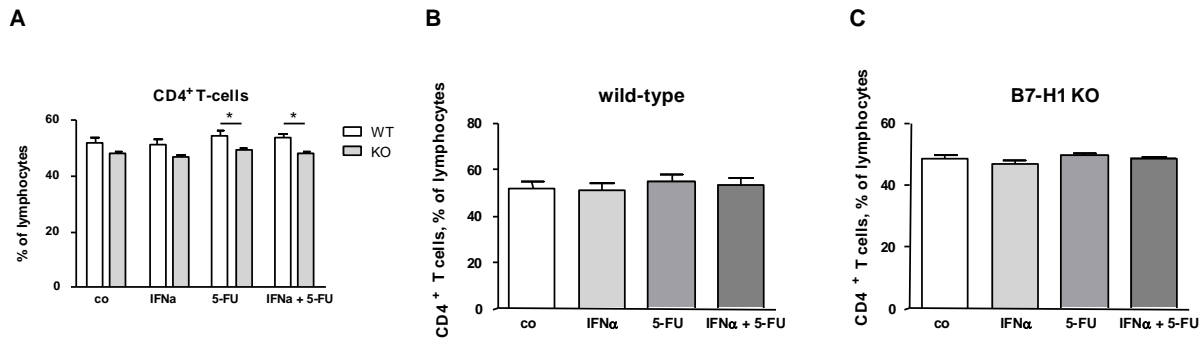


**Fig.3.1.1. 3 Quantification of CD4<sup>+</sup> T cells from WT and B7-H1 KO mice in control groups (without treatment, co) and after the treatment of splenocytes in *in vitro* cultures with IFN $\alpha$ , 5-FU and IFN $\alpha$ +5-FU.**

Freshly isolated splenocytes were put in a culture and treated with IFN $\alpha$ , 5-FU and IFN $\alpha$ +5-FU for 24 hours. Afterwards, the cells were stained with fluorescence labeled specific antibodies and analyzed by flow cytometry. Data from four independent experiments are presented as column bar graphs with SEM (n = 16; \*p<0.05; control group vs. treatment groups; two-way (A) and one-way (B,C) ANOVA)

We also looked at the activation status of CD4<sup>+</sup> T cells by analyzing the expression of the CD69 early activation marker. WT and B7-H1 KO showed no significant difference in their activation status when compared with each other (Fig.3.1.1.4 A). By looking at WT mice in detail, the expression of CD69 was higher in IFN $\alpha$  and IFN $\alpha$ +5-FU treatment groups as compared to the control. Between control and the 5-FU treatment group, no significant difference was recognized (Fig.3.1.1.4 B). In B7-H1 KO, a significant increase of CD69 expression was found in the treatment groups of IFN $\alpha$  and IFN $\alpha$ +5-FU compared with control (Fig.3.1.1.4 C). Considering the MFI (mean fluorescent intensity) for CD69 on CD4<sup>+</sup> T cells, a significant difference was found between WT and B7-H1 KO in the treatments with IFN $\alpha$  and IFN $\alpha$ +5-FU (Fig.3.1.1.4 D). In WT mice, a significantly lower CD69 MFI was recorded in the group of IFN $\alpha$ +5-FU compared to control (Fig.3.1.1.4 E). However, in cells of B7-H1 KO mice no significant difference was seen (Fig.3.1.1.4 F).

## Results

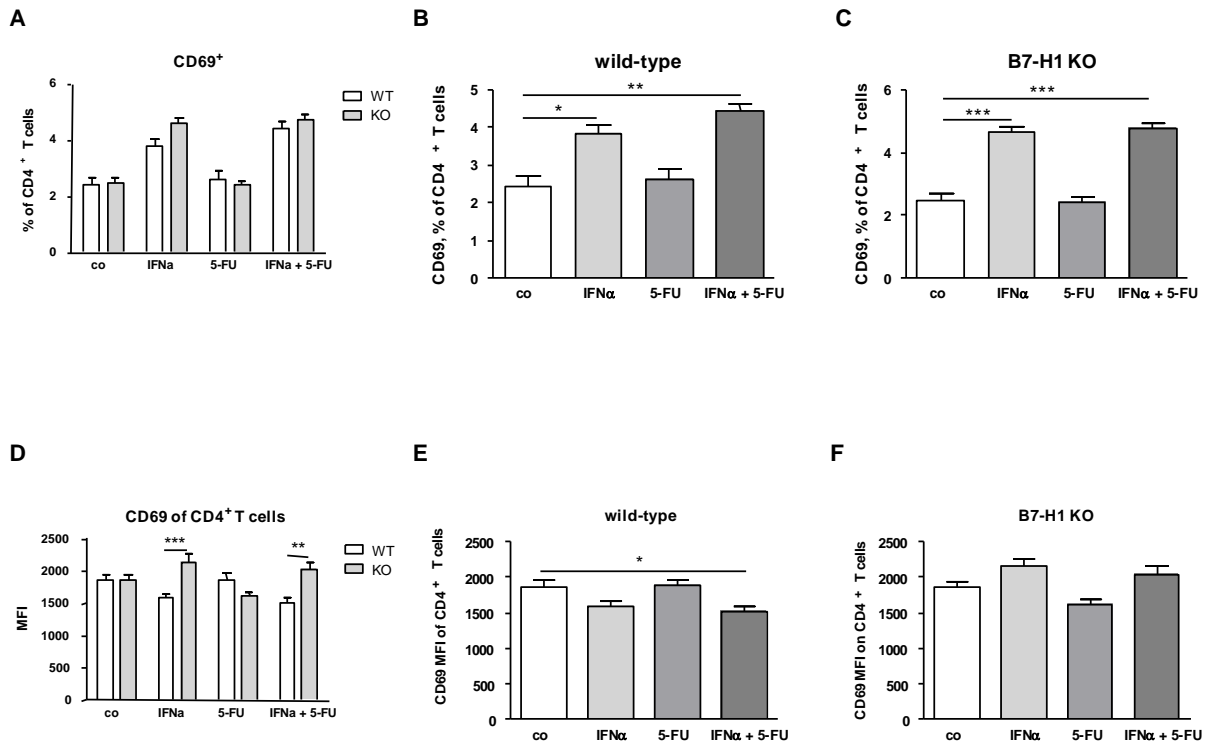


**Fig.3.1.1. 4 Quantification of CD69 expression on CD4<sup>+</sup>T cells from WT and B7-H1 KO mice in control groups (without treatment, co) and after the treatment of splenocytes in *in vitro* cultures with IFN $\alpha$ , 5-FU and IFN $\alpha$ +5-FU.**

Freshly isolated splenocytes were put in a culture and treated with IFN $\alpha$ , 5-FU and IFN $\alpha$ +5-FU for 24 hours. Afterwards, the cells were stained with fluorescence labeled specific antibodies. The frequency of CD69<sup>+</sup> CD4<sup>+</sup> T cells together with the MFI of CD69 was analyzed by flow cytometry. Data from four independent experiments are presented as column bar graphs with SEM (n = 16; \*p<0.05, \*\*p<0.01, \*\*\*p<0.001; control group vs. treatment groups; two-way (A,D) and one-way (B,C,E,F) ANOVA )

Next, we examined the individual subsets of CD4<sup>+</sup> T cells (Tnaive, Teff, Tem, Tcm) and their activation status based on CD69 expression. In WT mice, the percentage of naïve cells was significantly higher in the control as well as in all treatment groups compared to B7-H1 KO (Fig.3.1.1.5 A). Between the treatments and control in the WT group, no significant change in percentage of Tnaive could be shown (Fig.3.1.1.5 B). For the B7-H1 KO mice in the groups of IFN $\alpha$  and IFN $\alpha$ +5-FU, a significant increase in percentages of Tnaive was registered compared with the control group (Fig.3.1.1.5 C).

## Results

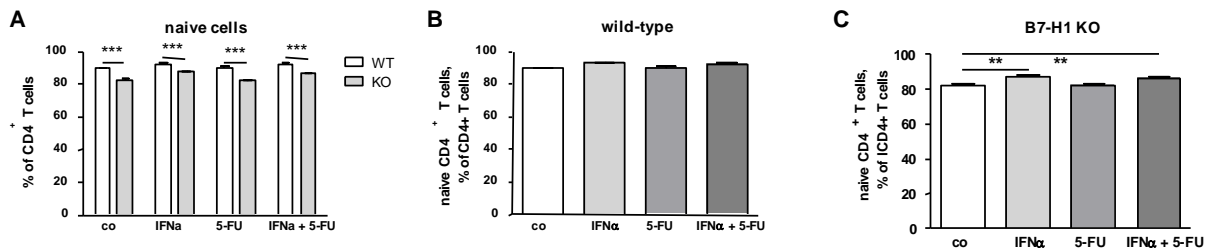


**Fig.3.1.1. 5** Quantification of naïve CD4<sup>+</sup>T cells from WT and B7-H1 KO mice in control groups (without treatment, co) and after the treatment of splenocytes in *in vitro* cultures with IFN $\alpha$ , 5-FU and IFN $\alpha$ +5-FU.

Freshly isolated splenocytes were put in a culture and treated with IFN $\alpha$ , 5-FU and IFN $\alpha$ +5-FU for 24 hours. Afterwards, the cells were stained with fluorescence labeled specific antibodies and analyzed by flow cytometry. Data from four independent experiments are presented as column bar graphs with SEM (n = 16; \*\*p<0.01, \*\*\*p<0.001; control group vs. treatment groups; two-way (A) and one-way (B,C) ANOVA)

The second subset we analyzed was the population of effector T cells (Teff) out of all CD4<sup>+</sup> T cells. The statistical analysis showed a tendency towards higher percentages of Teff in the B7-H1 KO groups in comparison to WT (Fig.3.1.1.6 A). By looking at WT groups separately, no significant difference was seen between control and treatment groups (Fig.3.1.1.6 B). For B7-H1 KO groups, a significant increase in Teff frequency was found in the 5-FU group compared to control (Fig.3.1.1.6 C).

## Results

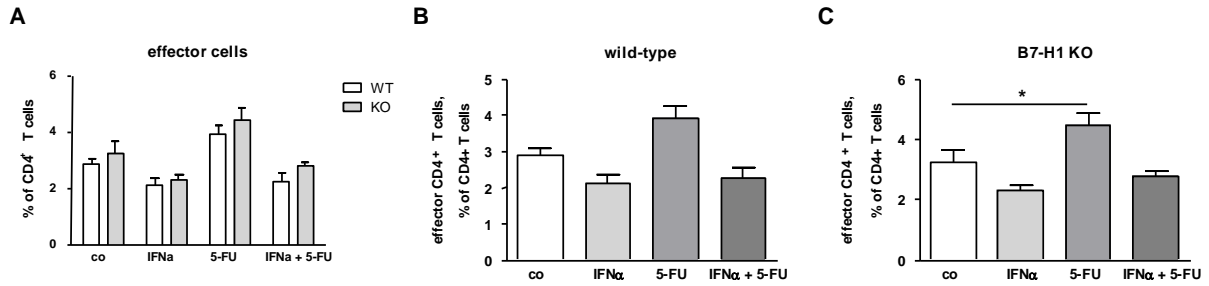


**Fig.3.1.1. 6 Quantification of effector CD4<sup>+</sup>T cells from WT and B7-H1 KO mice in control groups (without treatment, co) and after the treatment of splenocytes in *in vitro* cultures with IFN $\alpha$ , 5-FU and IFN $\alpha$ +5-FU.**

Freshly isolated splenocytes were put in a culture and treated with IFN $\alpha$ , 5-FU and IFN $\alpha$ +5-FU for 24 hours. Afterwards, the cells were stained with fluorescence labeled specific antibodies and analyzed by flow cytometry. Data from four independent experiments are presented as column bar graphs with SEM (n = 16; \*p<0.05; control group vs. treatment groups; two-way (A) and one-way (B,C) ANOVA)

Contemplating the activation status of CD4<sup>+</sup> Teff cells, no significant difference was measured between WT and B7-H1 KO mice (Fig.3.1.1.7 A). Analyzing the different treatments of WT compared to control, significantly higher percentages of CD69<sup>+</sup> Teff were achieved in the groups of IFN $\alpha$  and IFN $\alpha$ +5-FU (Fig.3.1.1.7 B). Also in the groups of B7-H1 KO mice, significantly higher frequencies of activated Teff were found after treatment with IFN $\alpha$  and IFN $\alpha$ +5-FU compared to control (Fig.3.1.1.7 C). For the MFI of CD69 on Teff, no significant difference was seen between WT and B7-H1 KO mice (Fig.3.1.1.7 D). Furthermore, no significant change in the value of CD69 MFI was found between treatment groups and control by looking at WT and B7-H1 KO mice separately (Fig.3.1.1.7 E,F).

## Results

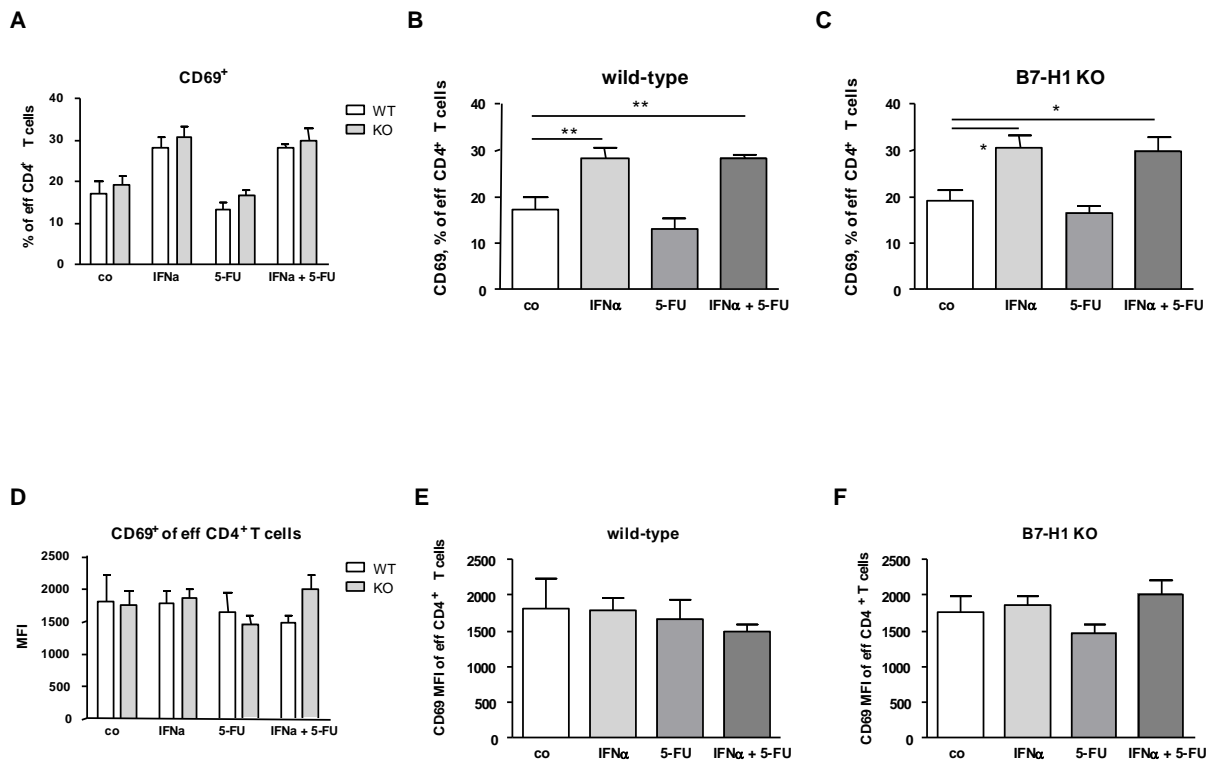


**Fig.3.1.1.7 Quantification of CD69 expression on effector CD4<sup>+</sup>T cells from WT and B7-H1 KO mice in control groups (without treatment, co) and after the treatment of splenocytes in *in vitro* cultures with IFN $\alpha$ , 5-FU and IFN $\alpha$ +5-FU.**

Freshly isolated splenocytes were put in a culture and treated with IFN $\alpha$ , 5-FU and IFN $\alpha$ +5-FU for 24 hours. Afterwards, the cells were stained with fluorescence labeled specific antibodies. The frequency of CD69<sup>+</sup> effector CD4<sup>+</sup> T cells together with the MFI of CD69 was analyzed by flow cytometry. Data from four independent experiments are presented as column bar graphs with SEM (n = 16; \*p<0.05, \*\*p<0.01; control group vs. treatment groups; two-way (A,D) and one-way (B,C,E,F) ANOVA)

For the subset of effector memory cells (Tem) within the CD4<sup>+</sup> T cell population, we observed significantly higher percentages of Tem in B7-H1 KO compared to WT mice, both in the control and in all treatment groups (Fig.3.1.1.8 A). Between the treatment groups of WT mice, no significant difference was determined for the frequency of CD4<sup>+</sup> Tem (Fig.3.1.1.8 B). Within the groups of B7-H1 KO mice, significantly lower percentages of Tem were found in the treatment groups of IFN $\alpha$  and IFN $\alpha$ +5-FU compared to control (Fig.3.1.1.8 C).

## Results

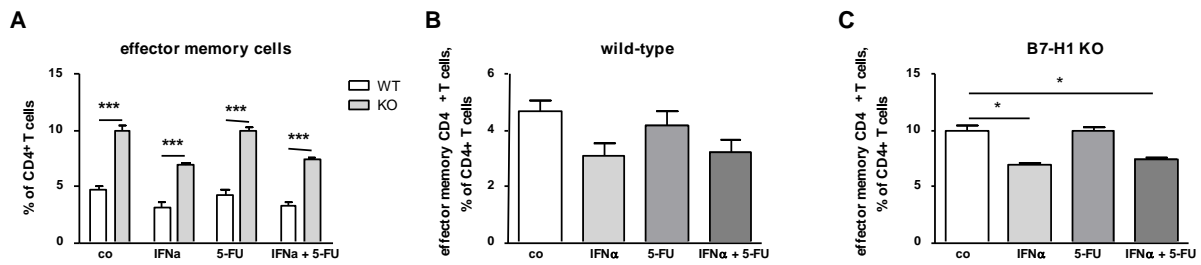


**Fig.3.1.1. 8 Quantification of effector memory CD4<sup>+</sup>T cells from WT and B7-H1 KO mice in control groups (without treatment, co) and after the treatment of splenocytes in *in vitro* cultures with IFN $\alpha$ , 5-FU and IFN $\alpha$ +5-FU.**

Freshly isolated splenocytes were put in a culture and treated with IFN $\alpha$ , 5-FU and IFN $\alpha$ +5-FU for 24 hours. Afterwards, the cells were stained with fluorescence labeled specific antibodies and analyzed by flow cytometry. Data from four independent experiments are presented as column bar graphs with SEM (n = 16; \*p<0.05, \*\*\*p<0.001; control group vs. treatment groups; two-way (A) and one-way (B,C) ANOVA)

The analysis of CD69<sup>+</sup> cells out of CD4<sup>+</sup> Tem revealed a tendency to lower percentages in all four groups of WT as compared to B7-H1 KO (Fig.3.1.1.9 A). When looking at the WT groups in detail, significantly higher levels of CD69<sup>+</sup>Tem were observed in IFN $\alpha$  and IFN $\alpha$ +5-FU groups compared to controls (Fig.3.1.1.8 B). In the B7-H1 KO, a significant increase of CD69 expression was found after the treatment with IFN $\alpha$  and IFN $\alpha$ +5-FU compared to control (Fig.3.1.1.9 C). The analyzed MFI of CD69 revealed no significant difference between control and treatment groups of WT and B7-H1 KO (Fig.3.1.1.9 D). By looking at WT and B7-H1 KO separately, significantly higher values of CD69 MFI were determined for the groups of IFN $\alpha$  and IFN $\alpha$ +5-FU compared to controls in both WT and B7-H1 KO mice (Fig.3.1.1.9 E,F).

## Results

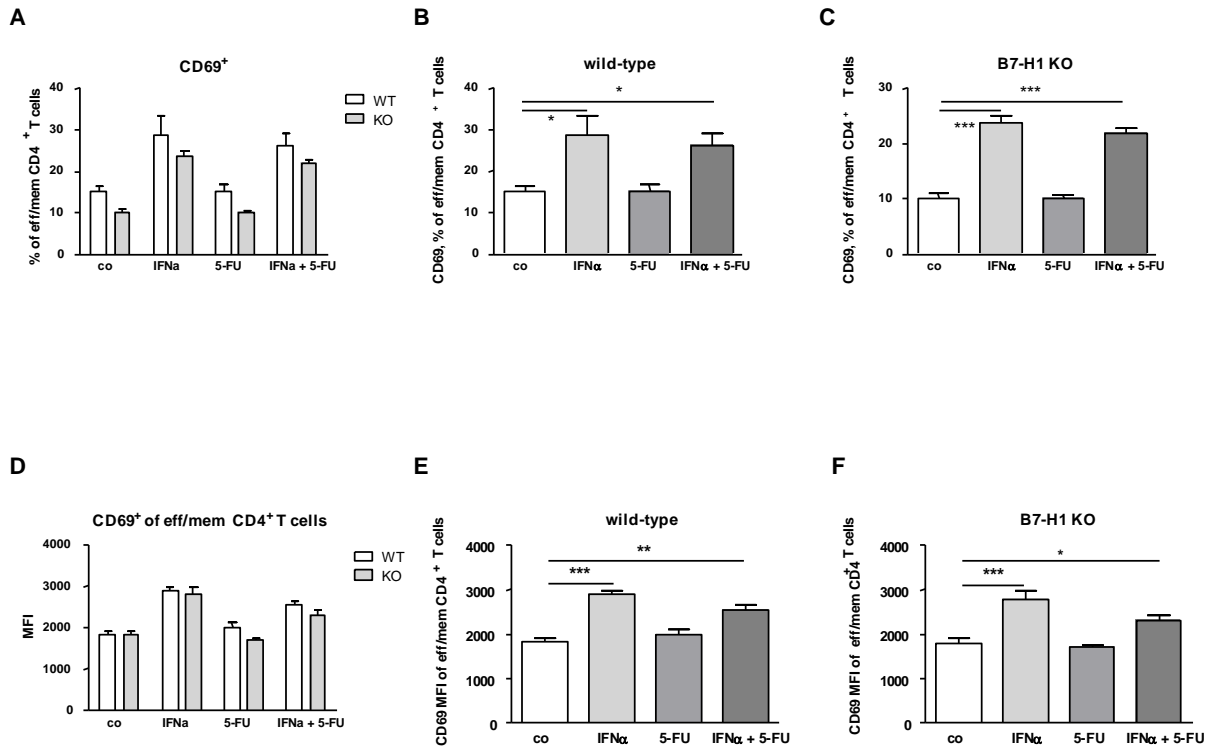


**Fig.3.1.1. 9 Quantification of CD69 expression on effector memory CD4<sup>+</sup>T cells from WT and B7-H1 KO mice in control groups (without treatment, co) and after the treatment of splenocytes in *in vitro* cultures with IFN $\alpha$ , 5-FU and IFN $\alpha$ +5-FU.**

Freshly isolated splenocytes were put in a culture and treated with IFN $\alpha$ , 5-FU and IFN $\alpha$ +5-FU for 24 hours. Afterwards, the cells were stained with fluorescence labeled specific antibodies. The frequency of CD69<sup>+</sup> effector memory CD4<sup>+</sup> T cells together with the MFI of CD69 was analyzed by flow cytometry. Data from four independent experiments are presented as column bar graphs with SEM (n = 16; \*p<0.05,\*\*p<0.01,\*\*\*p<0.001; control group vs. treatment groups; two-way (A,D) and one-way (B,C,E,F) ANOVA)

The last analyzed fraction of CD4<sup>+</sup> T cells were the central memory cells (Tcm). The percentages of this cell population were significantly higher in the control and all therapy groups in B7-H1 KO compared to WT mice (Fig.3.1.1.10 A). In WT, the differences between control and treatment groups were not of significance (Fig.3.1.1.10 B), whereas in B7-H1 KO mice, significantly lower frequencies of Tcm were determined for all treatment groups compared to control (Fig.3.1.1.10 C).

## Results

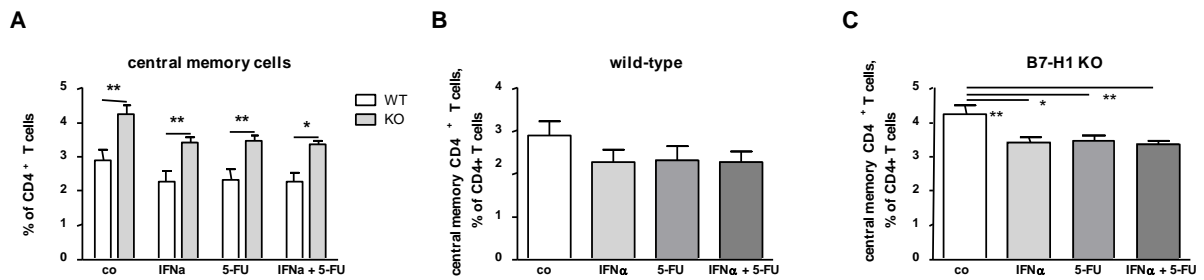


**Fig.3.1.1.10** Quantification of central memory CD4<sup>+</sup>T cells from WT and B7-H1 KO mice in control groups (without treatment, co) and after the treatment of splenocytes in *in vitro* cultures with IFN $\alpha$ , 5-FU and IFN $\alpha$ +5-FU.

Freshly isolated splenocytes were put in a culture and treated with IFN $\alpha$ , 5-FU and IFN $\alpha$ +5-FU for 24 hours. Afterwards, the cells were stained with fluorescence labeled specific antibodies and analyzed by flow cytometry. Data from four independent experiments are presented as column bar graphs with SEM (n = 16; \*p<0.05, \*\*p<0.01; control group vs. treatment groups; two-way (A) and one-way (B,C) ANOVA)

As indicated by investigation of CD69 expression, the activation status of Tcm cells was similar between the groups of WT and B7-H1 KO mice (Fig.3.1.1.11 A). By looking at WT in detail, significantly higher percentages of activated cells were determined for IFN $\alpha$  and IFN $\alpha$ +5-FU groups compared to control (Fig.3.1.1.11 B). In B7-H1 KO, such a significant increase in frequency of activated cells was also found in the treatment groups of IFN $\alpha$  and IFN $\alpha$ +5-FU compared to control (Fig.3.1.1.11 C). The statistical analysis showed no significant difference between WT and B7-H1 KO for the different treatments in respect of CD69 MFI (Fig.3.1.1.11 D). Besides, in WT, no significant difference between control and treated groups was determined for the MFI of CD69 (Fig.3.1.1.11 E). Instead, for groups of B7-H1 KO mice, significant differences in the values of CD69 MFI were seen between control and IFN $\alpha$ , IFN $\alpha$ +5-FU groups (Fig.3.1.1.11 F).

## Results

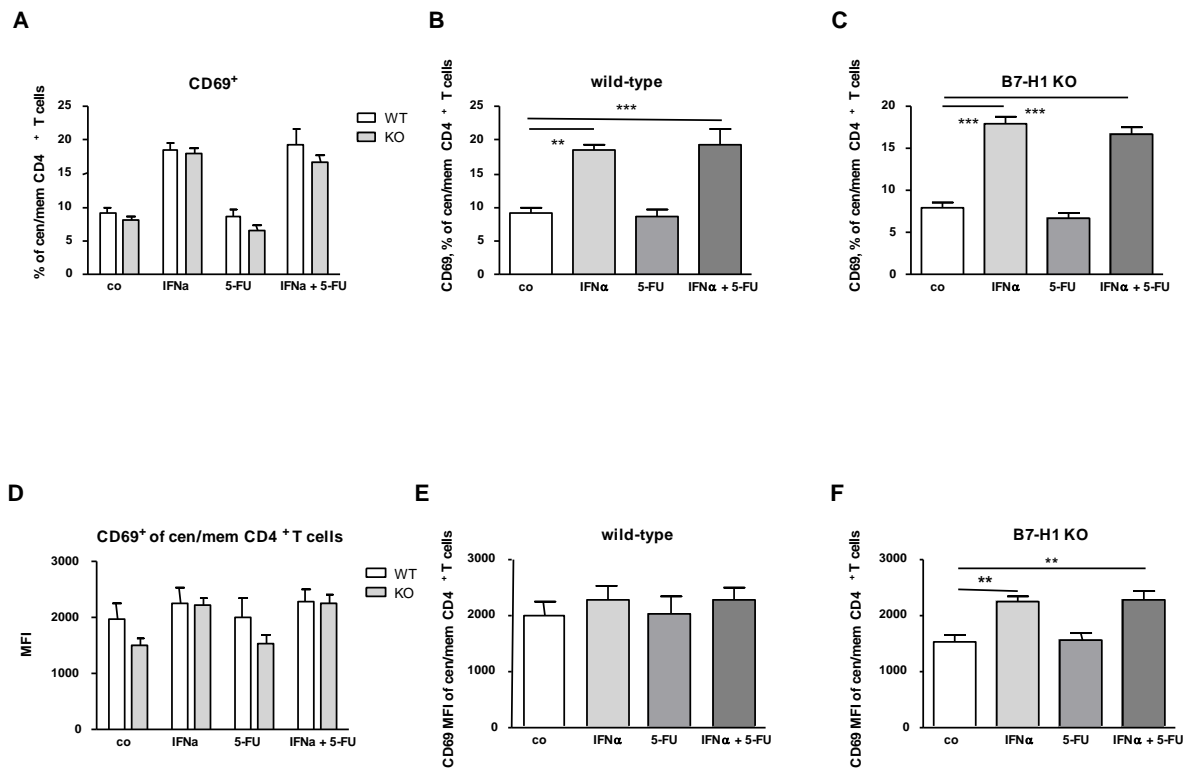


**Fig.3.1.1.11 Quantification of CD69 expression on central memory CD4<sup>+</sup>T cells from WT and B7-H1 KO mice in control groups (without treatment, co) and after the treatment of splenocytes in *in vitro* cultures with IFN $\alpha$ , 5-FU and IFN $\alpha$ +5-FU.**

Freshly isolated splenocytes were put in a culture and treated with IFN $\alpha$ , 5-FU and IFN $\alpha$ +5-FU for 24 hours. Afterwards, the cells were stained with fluorescence labeled specific antibodies. The frequency of CD69<sup>+</sup> central memory CD4<sup>+</sup> T cells together with the MFI of CD69 was analyzed by flow cytometry. Data from four independent experiments are presented as column bar graphs with SEM (n = 16; \*\*p<0.01, \*\*\*p<0.001; control group vs. treatment groups; two-way (A,D) and one-way (B,C,E,F) ANOVA)

Afterwards, we took a closer look at the CD8<sup>+</sup> T cells. For this cell population, gated out of CD3<sup>+</sup> lymphocytes, the comparison between WT and B7-H1 KO groups showed no significant difference between the control and treatment groups of both mouse strains (Fig.3.1.1.12 A). In WT, no significant difference in CD8<sup>+</sup> T cell frequency was seen between control and treatment groups (Fig.3.1.1.12 B), whereas in the B7-H1 KO groups, a significant decrease was found in 5-FU treated cells compared to the control (Fig.3.1.1.12 C).

## Results

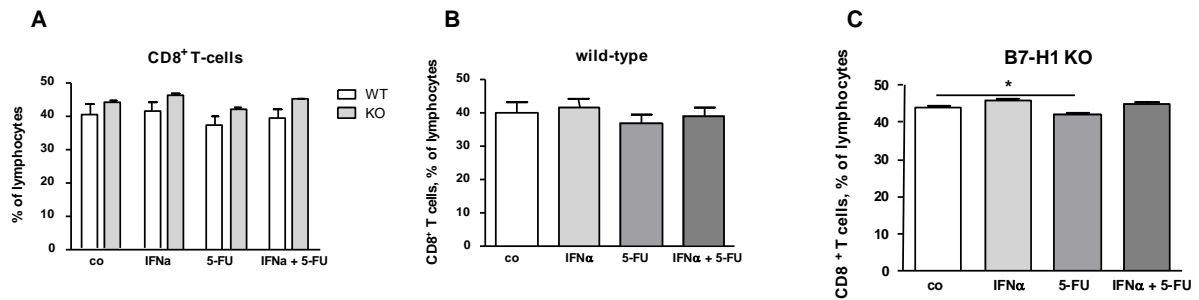


**Fig.3.1.1.12 Quantification of CD8<sup>+</sup> T cells from WT and B7-H1 KO mice in control groups (without treatment, co) and after the treatment of splenocytes in *in vitro* cultures with IFN $\alpha$ , 5-FU and IFN $\alpha$ +5-FU.**

Freshly isolated splenocytes were put in a culture and treated with IFN $\alpha$ , 5-FU and IFN $\alpha$ +5-FU for 24 hours. Afterwards, the cells were stained with fluorescence labeled specific antibodies and analyzed by flow cytometry. Data from four independent experiments are presented as column bar graphs with SEM (n = 16; \*p<0.05; control group vs. treatment groups; two-way (A) and one-way (B,C) ANOVA)

Next we analyzed the activation status of CD8<sup>+</sup> T cells by measuring the expression of the CD69 early activation marker. The comparison between WT and B7-H1 KO showed no significant difference for the controls and treatment groups (Fig.3.1.1.13 A). In both, WT and B7-H1 KO groups, significantly higher frequencies of CD69<sup>+</sup> CD8<sup>+</sup> T cells were observed after IFN $\alpha$  and IFN $\alpha$ +5-FU treatment compared to the control (Fig.3.1.1.13 B,C). The MFI of CD69 revealed significantly lower values in the control and 5-FU treatment group of B7-H1 KO compared to the same groups of WT (Fig.3.1.1.13 D). For the control and treatment groups of WT mice, no significant difference in the value of CD69 MFI was determined (Fig.3.1.1.13 E). Between control and IFN $\alpha$  treatment group of B7-H1 KO, a significant increase in CD69 MFI was found after the treatment (Fig.3.1.1.13 F).

## Results

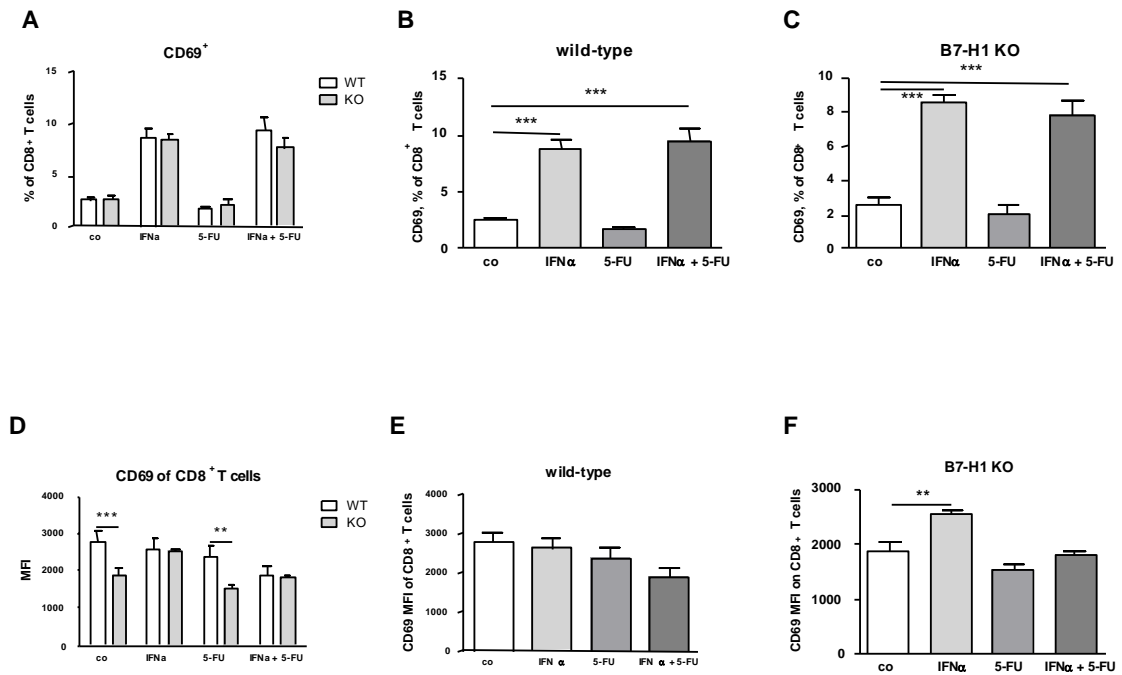


**Fig.3.1.1.13 Quantification of CD69 expression on CD8<sup>+</sup> T cells from WT and B7-H1 KO mice in control groups (without treatment, co) and after the treatment of splenocytes in *in vitro* cultures with IFN $\alpha$ , 5-FU and IFN $\alpha$ +5-FU.**

Freshly isolated splenocytes were put in a culture and treated with IFN $\alpha$ , 5-FU and IFN $\alpha$ +5-FU for 24 hours. Afterwards, the cells were stained with fluorescence labeled specific antibodies. The frequency of CD69<sup>+</sup> CD8<sup>+</sup> T cells together with the MFI of CD69 was analyzed by flow cytometry. Data from four independent experiments are presented as column bar graphs with SEM (n = 16; \*\*p<0.01, \*\*\*p<0.001; control group vs. treatment groups, two-way (A) and one-way (B,C) ANOVA)

Afterwards, we looked at the four subsets of CD8<sup>+</sup> T cells in more detail: Tnaive, T<sub>eff</sub>, T<sub>em</sub> and T<sub>cm</sub> as well as their activation status were analyzed. We observed significantly lower percentages of naïve CD8<sup>+</sup> T cells in all four groups of B7-H1 KO compared to WT cells (Fig.3.1.1.14 A). By looking at WT and B7-H1 KO separately, no significant differences in the frequency of naïve CD8<sup>+</sup> T cells were seen between the treatments and control in both WT and B7-H1 KO groups (Fig.3.1.1.14 B,C).

## Results

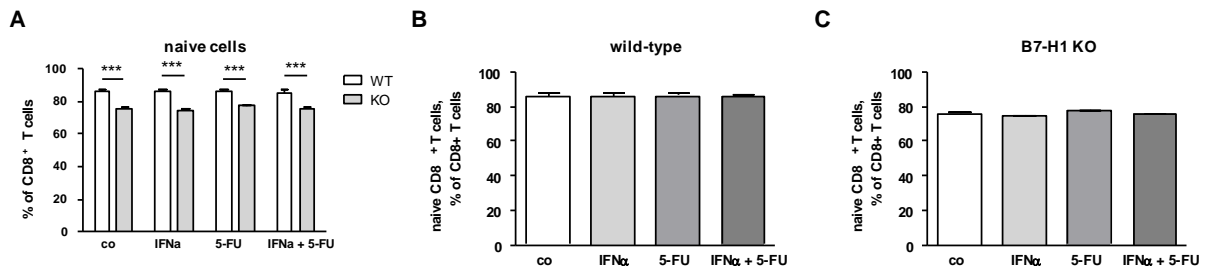


**Fig.3.1.1.14** Quantification of naïve CD8<sup>+</sup> T cells from WT and B7-H1 KO mice in control groups (without treatment, co) and after the treatment of splenocytes in *in vitro* cultures with IFN $\alpha$ , 5-FU and IFN $\alpha$ +5-FU.

Freshly isolated splenocytes were put in a culture and treated with IFN $\alpha$ , 5-FU and IFN $\alpha$ +5-FU for 24 hours. Afterwards, the cells were stained with fluorescence labeled specific antibodies and analyzed by flow cytometry. Data from four independent experiments are presented as column bar graphs with SEM (n = 16; \*\*\*p<0.001; control group vs. treatment groups; two-way (A) and one-way (B,C) ANOVA)

Assessing the percentage of Teff out of the CD8<sup>+</sup> T cell population, we detected a tendency towards higher values of these cells in all of the B7-H1 KO groups compared to WT (Fig.3.1.1.15 A). By looking at WT and B7-H1 KO separately, increased CD8<sup>+</sup> Teff frequencies were observed in the group of 5-FU compared to control in both WT and B7-H1 KO (Fig.3.1.1.15 B,C).

## Results

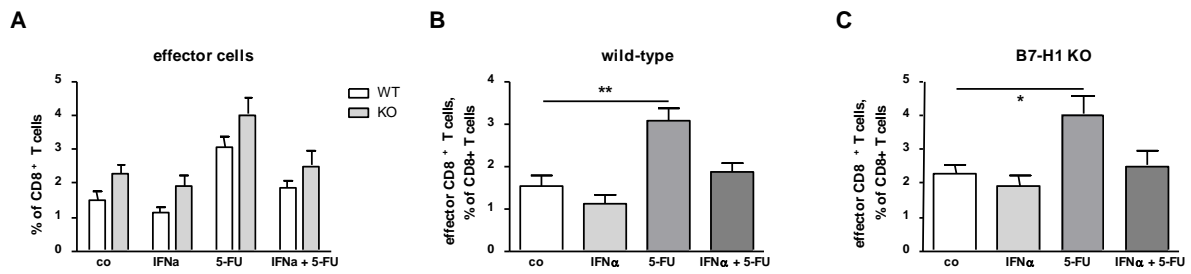


**Fig.3.1.1. 15 Quantification of effector CD8<sup>+</sup> T cells from WT and B7-H1 KO mice in control groups (without treatment, co) and after the treatment of splenocytes in *in vitro* cultures with IFN $\alpha$ , 5-FU and IFN $\alpha$ +5-FU.**

Freshly isolated splenocytes were put in a culture and treated with IFN $\alpha$ , 5-FU and IFN $\alpha$ +5-FU for 24 hours. Afterwards, the cells were stained with fluorescence labeled specific antibodies and analyzed by flow cytometry. Data from four independent experiments are presented as column bar graphs with SEM (n = 16; \*p<0.05, \*\*p<0.01; control group vs. treatment groups; two-way (A) and one-way (B,C) ANOVA)

The analysis of the activation status of Teff revealed significantly higher frequencies of CD69<sup>+</sup> cells in all groups of B7-H1 KO cells compared to WT groups (Fig.3.1.1.16 A). For WT, increased percentages of CD69<sup>+</sup> Teff were measured in IFN $\alpha$  and IFN $\alpha$ +5-FU treatment groups compared to control (Fig.3.1.1.16 B). In B7-H1 KO groups, significantly higher percentages of CD69<sup>+</sup> cells were found after IFN $\alpha$  treatment compared to control, whereas the CD69 expression was significantly lower in the group of 5-FU treatment in comparison to control (Fig.3.1.1.16 C). The MFI of CD69 expression on CD8<sup>+</sup>Teff had lower values in B7-H1 KO groups compared to WT groups. This result is highly significant for all samples, except for controls where only a tendency was determined (Fig.3.1.1.16 D). Between the control and therapy groups of WT, no significant difference in CD69 MFI was found (Fig.3.1.1.16 E). For the groups of B7-H1 KO cells, significant increase in MFI values were registered in IFN $\alpha$  and IFN $\alpha$ +5-FU treatment groups compared to the control (Fig.3.1.1.16 F).

## Results

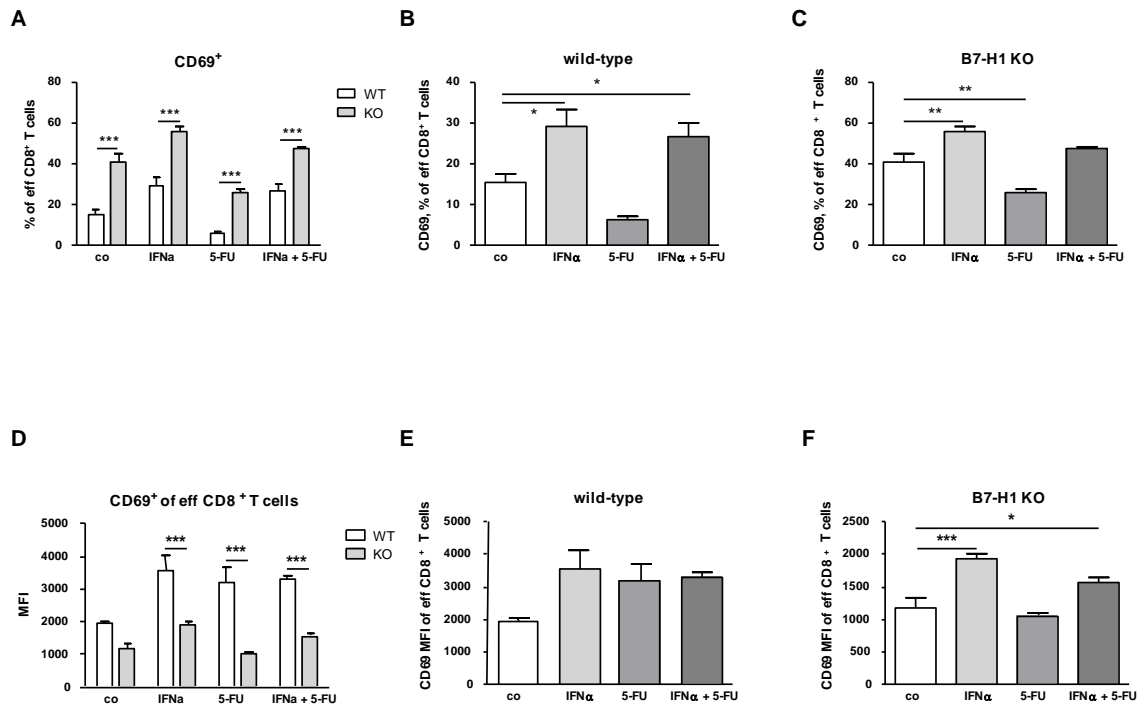


**Fig.3.1.1.16 Quantification of CD69 expression on effector CD8<sup>+</sup> T cells from WT and B7-H1 KO mice in control groups (without treatment, co) and after the treatment of splenocytes in *in vitro* cultures with IFN $\alpha$ , 5-FU and IFN $\alpha$ +5-FU.**

Freshly isolated splenocytes were put in a culture and treated with IFN $\alpha$ , 5-FU and IFN $\alpha$ +5-FU for 24 hours. Afterwards, the cells were stained with fluorescence labeled specific antibodies. The frequency of CD69<sup>+</sup> effector CD8<sup>+</sup> T cells together with the MFI of CD69 was analyzed by flow cytometry. Data from four independent experiments are presented as column bar graphs with SEM (n = 16; \*p<0.05, \*\*p<0.01, \*\*\*p<0.001; control group vs. treatment groups; two-way (A,D) and one-way (B,C,E,F) ANOVA)

As far as Tem, we saw significantly higher Tem frequencies in the groups of B7-H1 KO compared to WT groups (Fig.3.1.1.17 A). When looking at the WT in detail, significantly higher percentages of CD8<sup>+</sup> Tem were measured in the treatment group of 5-FU compared to the control (Fig.3.1.1.17 B). In the B7-H1 KO groups, no significant differences in percentages of Tem were seen between the control and treatment groups (Fig.3.1.1.17 C).

## Results

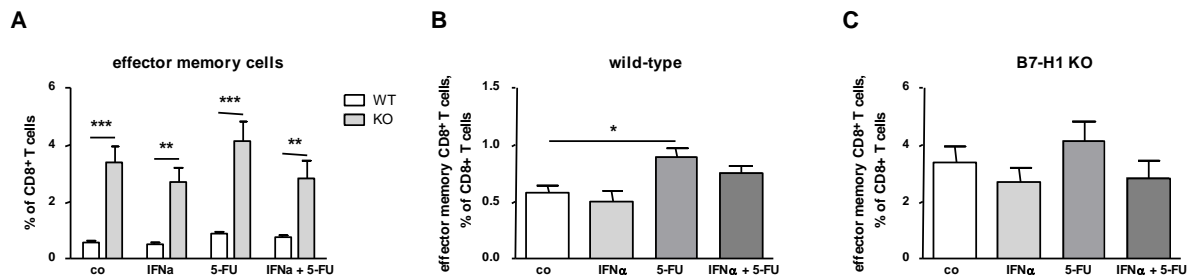


**Fig.3.1.1.17** Quantification of effector memory CD8<sup>+</sup> T cells from WT and B7-H1 KO mice in control groups (without treatment, co) and after the treatment of splenocytes in *in vitro* cultures with IFN $\alpha$ , 5-FU and IFN $\alpha$ +5-FU.

Freshly isolated splenocytes were put in a culture and treated with IFN $\alpha$ , 5-FU and IFN $\alpha$ +5-FU for 24 hours. Afterwards, the cells were stained with fluorescence labeled specific antibodies and analyzed by flow cytometry. Data from four independent experiments are presented as column bar graphs with SEM (n = 16; \*p<0.05, \*\*p<0.01, \*\*\*p<0.001; control group vs. treatment groups; two-way (A) and one-way (B,C) ANOVA)

When analyzing the expression of CD69 on Tem, no significant difference in the frequency of CD69<sup>+</sup> Tem was determined between cells of all WT and B7-H1 KO groups (Fig.3.1.1.18 A). In both WT and B7-H1 KO mice, a significant increase in activated CD8<sup>+</sup> Tem cells was measured in the treatment groups of IFN $\alpha$  and IFN $\alpha$ +5FU compared to the controls (Fig.3.1.1.18 B,C). The MFI of CD69 showed a significantly higher value in the 5-FU WT group compared to the same group of B7-H1 KO cells (Fig.3.1.1.18 D). In WT, significantly higher values in CD69 MFI were seen in the group of 5-FU treatment compared to the control (Fig.3.1.1.18 E). Whereas in the groups of B7-H1 KO, no significant difference in CD69 MFI was noted between the control and treatment groups (Fig.3.1.1.18 F).

## Results

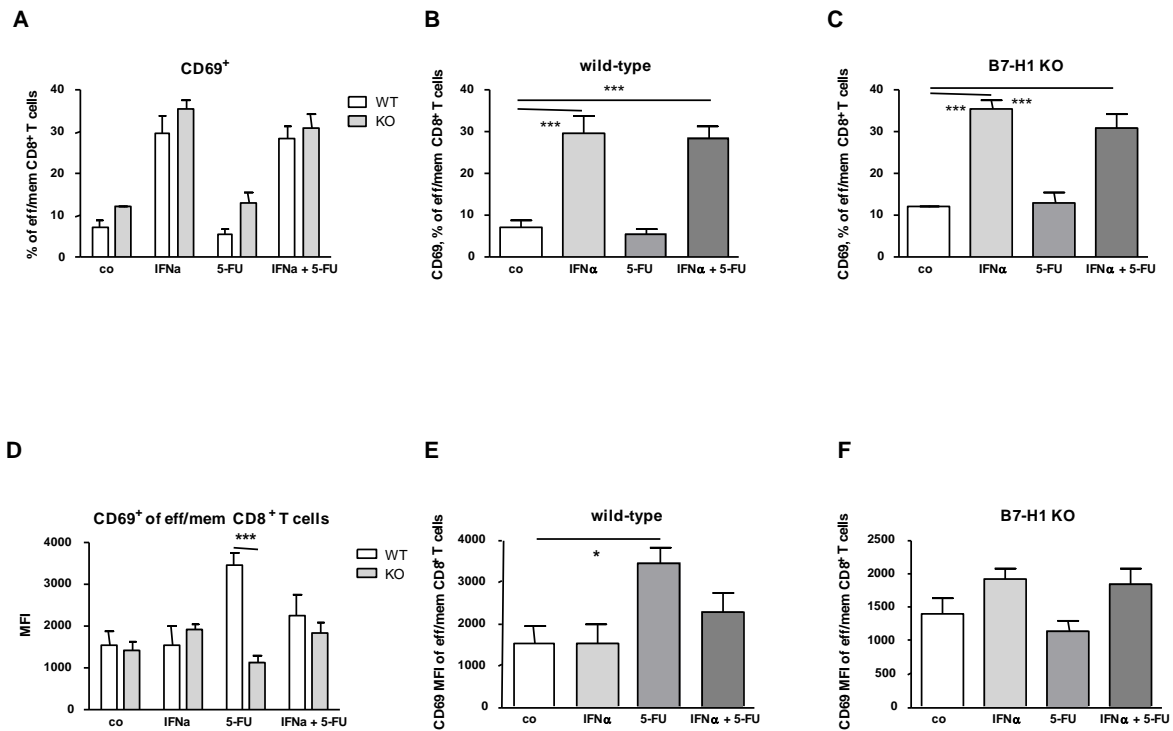


**Fig.3.1.1.18 Quantification of CD69 expression on effector memory CD8<sup>+</sup> T cells from WT and B7-H1 KO mice in control groups (without treatment, co) and after the treatment of splenocytes in *in vitro* cultures with IFN $\alpha$ , 5-FU and IFN $\alpha$ +5-FU.**

Freshly isolated splenocytes were put in a culture and treated with IFN $\alpha$ , 5-FU and IFN $\alpha$ +5-FU for 24 hours. Afterwards, the cells were stained with fluorescence labeled specific antibodies. The frequency of CD69<sup>+</sup> effector memory CD8<sup>+</sup>T cells together with the MFI of CD69 was analyzed by flow cytometry. Data from four independent experiments are presented as column bar graphs with SEM (n = 16; \*p<0.05, \*\*\*p<0.001; control group vs. treatment groups; two-way (A,D) and one-way (B,C,E,F) ANOVA)

Tcm were the last analyzed subset of CD8<sup>+</sup> T cells. The comparison between WT and B7-H1 KO groups showed significantly higher frequencies of CD8<sup>+</sup> Tcm in the controls, IFN $\alpha$  and IFN $\alpha$ +5-FU groups of B7-H1 KO. In the treatment group of 5-FU, a tendency towards higher percentages was found in cells of B7-H1 KO mice (Fig.3.1.1.19 A). In the WT groups, no significant difference between the treatments and the control was observed (Fig.3.1.1.19 B). In the B7-H1 KO group, IFN $\alpha$  treatment significantly increased the percentages of Tcm, and 5-FU significantly decreased Tcm frequencies compared to the control (Fig.3.1.1.19 C).

## Results

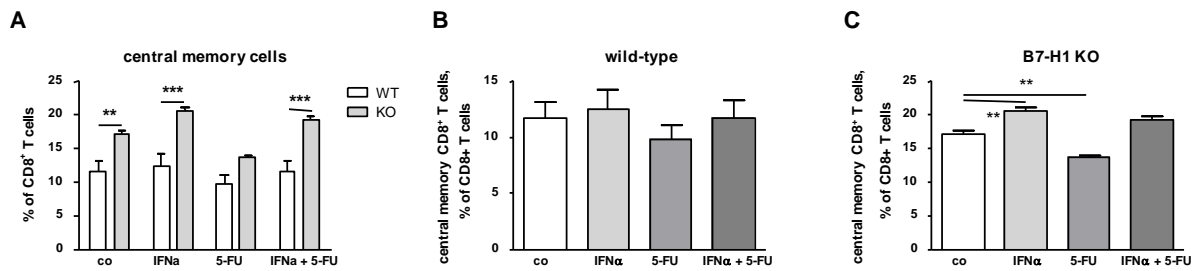


**Fig.3.1.1. 19 Quantification of central memory CD8<sup>+</sup> T cells from WT and B7-H1 KO mice in control groups (without treatment, co) and after the treatment of splenocytes in *in vitro* cultures with IFN $\alpha$ , 5-FU and IFN $\alpha$ +5-FU.**

Freshly isolated splenocytes were put in a culture and treated with IFN $\alpha$ , 5-FU and IFN $\alpha$ +5-FU for 24 hours. Afterwards, the cells were stained with fluorescence labeled specific antibodies and analyzed by flow cytometry. Data from four independent experiments are presented as column bar graphs with SEM (n = 16; \*\*p<0.01, \*\*\*p<0.001; control group vs. treatment groups; two-way (A) and one-way (B,C) ANOVA)

When analyzing the activation status of CD8<sup>+</sup> Tcm, significantly higher percentages of CD69<sup>+</sup> Tcm were found in the IFN $\alpha$  and IFN $\alpha$ +5-FU treatment groups of B7-H1 KO compared to those groups of WT. For controls and 5-FU groups, a tendency towards decreased cell numbers was seen in the B7-H1 KO group compared to WT (Fig.3.1.1.20 A). Taking a closer look at the WT and B7-H1 KO separately, significantly higher percentages of CD69<sup>+</sup> Tcm were observed in the groups of IFN $\alpha$  and IFN $\alpha$ +5-FU compared to controls in both WT and B7-H1 KO mice (Fig.3.1.1.20 B,C). The statistical analysis of the MFI of CD69 on Tcm revealed no significant difference between the groups of WT and B7-H1 KO cells (Fig.3.1.1.20 D). Also between the treatment groups and the control of either WT or B7-H1 KO, no significant change in values of CD69 MFI was determined (Fig.3.1.1.20 E,F).

## Results

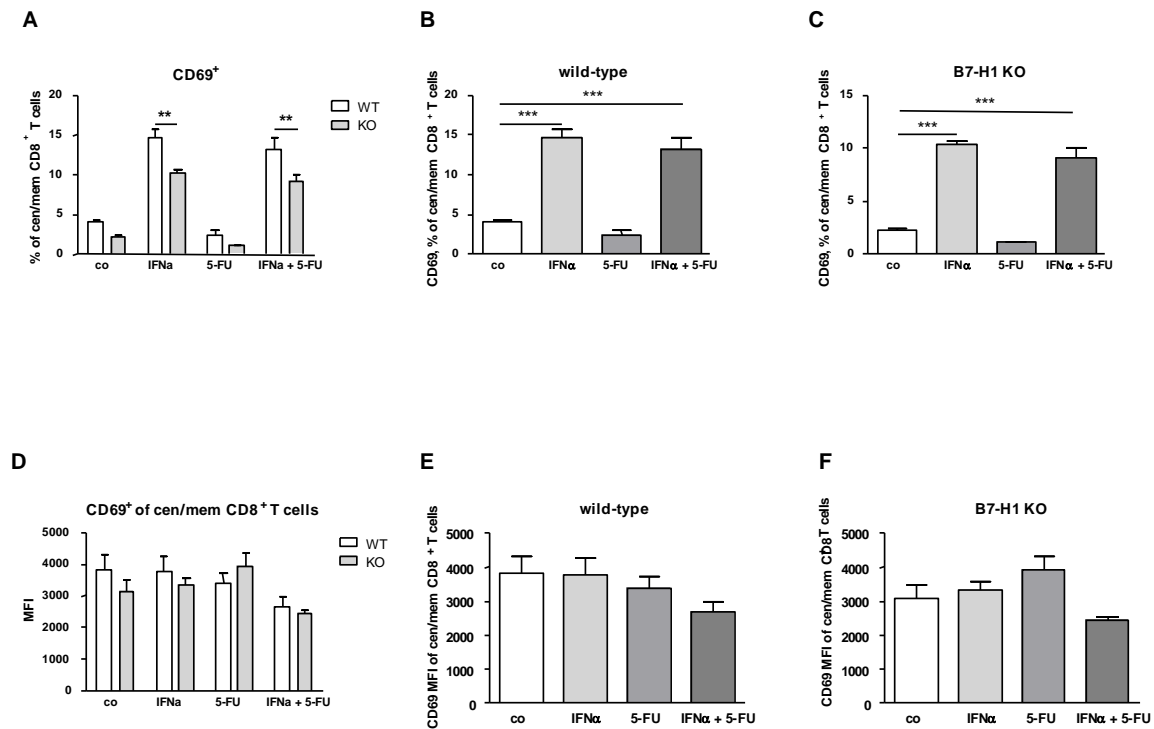


**Fig.3.1.1. 20 Quantification of CD69 expression on central memory CD8<sup>+</sup> T cells from WT and B7-H1 KO mice in control groups (without treatment, co) and after the treatment of splenocytes in *in vitro* cultures with IFN $\alpha$ , 5-FU and IFN $\alpha$ +5-FU.**

Freshly isolated splenocytes were put in a culture and treated with IFN $\alpha$ , 5-FU and IFN $\alpha$ +5-FU for 24 hours. Afterwards, the cells were stained with fluorescence labeled specific antibodies. The frequency of CD69<sup>+</sup> central memory CD8<sup>+</sup> T cells together with the MFI of CD69 was analyzed by flow cytometry. Data from four independent experiments are presented as column bar graphs with SEM (n = 16; \*\*p<0.01, \*\*\*p<0.001; control group vs. treatment groups; two-way (A) and one-way (B,C) ANOVA)

Taken together, our main findings for the CD4<sup>+</sup>/CD8<sup>+</sup> T cells were higher frequencies of lymphocytes in spleens of B7-H1 KO mice compared to WT mice. Furthermore, in spleens of B7-H1 KO mice we found higher ratios of Tem and Tcm throughout all treatments compared to spleens of WT mice. In the treatment groups of IFN $\alpha$  and IFN $\alpha$ +5-FU, higher concentrations of activated CD69<sup>+</sup> cell populations were found throughout the entire experiment series in both mouse strains, WT and B7-H1KO.

### 3.1.2 Analysis of regulatory T cells (Treg)

After analyzing the CD4<sup>+</sup> and CD8<sup>+</sup> T cells, we decided to next take a detailed look at an important subset of the CD4<sup>+</sup> T cells, the regulatory T cells (Treg). As well we analyzed their non-regulatory counterparts, Tcon and activated Tcon. The gating strategy for these cell populations is presented in Fig.3.1.2.1. The FACS data (dot-plot) represent one typical result out of four independent experiments.

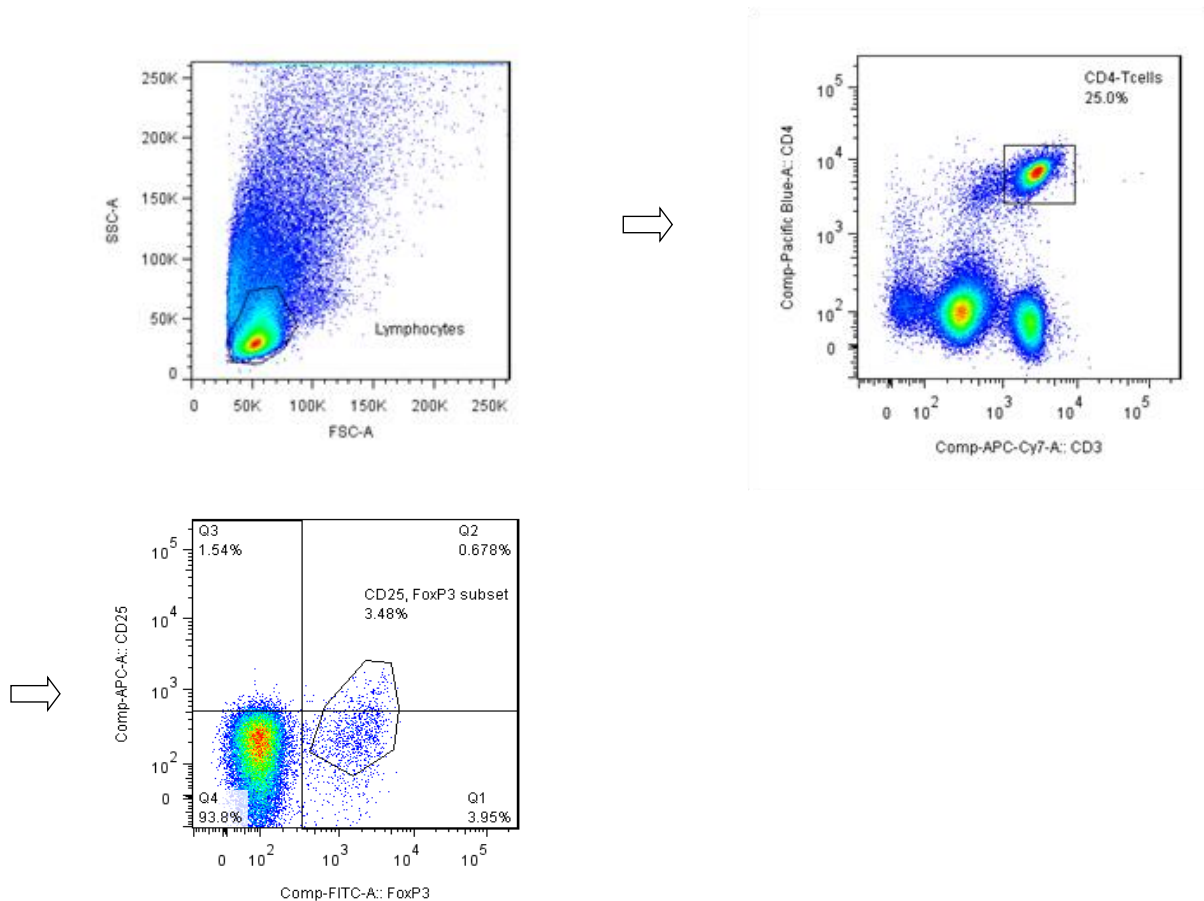


**Fig.3.1.2. 1 Gating strategy for regulatory T cells and Tcon in splenocytes using flow cytometry.**

The first gate was set on lymphocytes using FSC/SSC dot plot; afterwards CD4<sup>+</sup>Tcells were determined. Out of this cell population Treg, Tcon, activated Tcon were determined using CD25 and FoxP3 expression.

The percentages of Treg out of all CD4<sup>+</sup> T cells were significantly higher in all treatment groups and in the control of B7-H1 KO mice compared to WT groups

(Fig.3.1.2.2 A). Analyzing WT and B7-H1 KO groups separately, no significant difference in frequencies of Treg was found between control and treatment groups, neither in WT nor in B7-H1 KO (Fig.3.1.2.2 B,C).

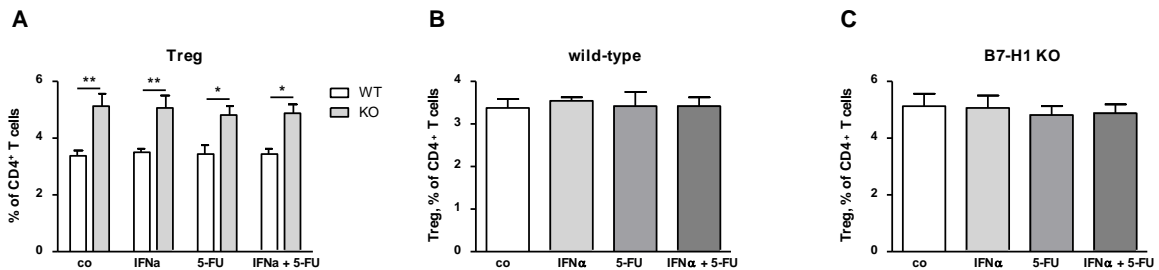


**Fig.3.1.2. 2 Quantification of Treg from WT and B7-H1 KO mice in control groups (without treatment, co) and after the treatment of splenocytes in *in vitro* cultures with IFN $\alpha$ , 5-FU and IFN $\alpha$ +5-FU.**

Freshly isolated splenocytes were put in a culture and treated with IFN $\alpha$ , 5-FU and IFN $\alpha$ +5-FU for 24 hours. Afterwards, the cells were stained with fluorescence labeled specific antibodies and analyzed by flow cytometry. Data from four independent experiments are presented as column bar graphs with SEM (n = 16; \*p<0.05, \*\*p<0.01; control group vs. treatment groups; two-way (A) and one-way (B,C) ANOVA)

For the Tcon population out of CD4<sup>+</sup> T cells, no significant differences in frequencies were seen between WT and B7-H1 KO groups (Fig.3.1.2.3 A). Also by taking a detailed look at WT and B7-H1 KO groups, in both there were no significant differences in the percentages of Tcon measured between the control and treatment groups (Fig.3.1.2.3 B,C).

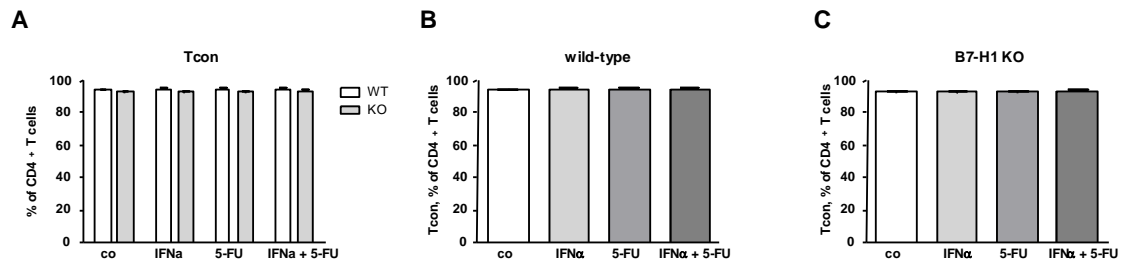


**Fig.3.1.2. 3 Quantification of Tcon from WT and B7-H1 KO mice in control groups (without treatment, co) and after the treatment of splenocytes in *in vitro* cultures with IFN $\alpha$ , 5-FU and IFN $\alpha$ +5-FU.**

Freshly isolated splenocytes were put in a culture and treated with IFN $\alpha$ , 5-FU and IFN $\alpha$ +5-FU for 24 hours. Afterwards, the cells were stained with fluorescence labeled specific antibodies and analyzed by flow cytometry. Data from four independent experiments are presented as column bar graphs with SEM (n = 16; control group vs. treatment groups; two-way (A) and one-way (B,C) ANOVA)

Analyzing the frequencies of activated Tcon out of all CD4<sup>+</sup> T cells, no significant difference was determined between the groups of WT and B7-H1 KO (Fig.3.1.2.4 A). In WT, between the control and treatment groups, no significant difference in the frequency of activated Tcon was seen (Fig.3.1.2.4 B). The analysis of the groups of B7-H1 KO splenocytes revealed no significant change in percentages of activated Tcon between the therapies and the control (Fig.3.1.2.4 C).

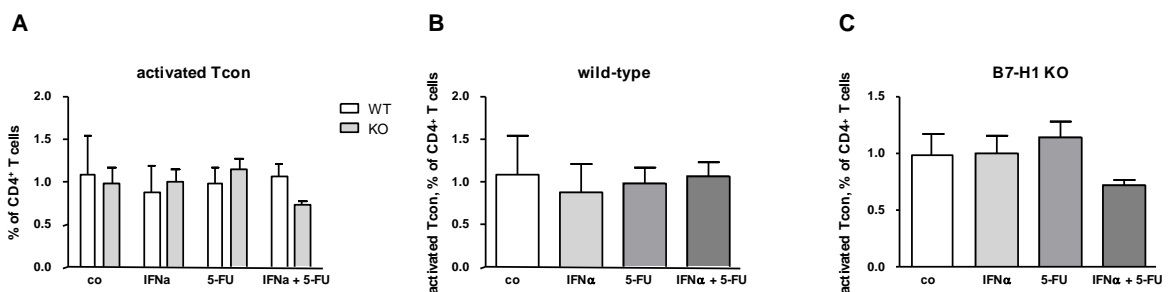


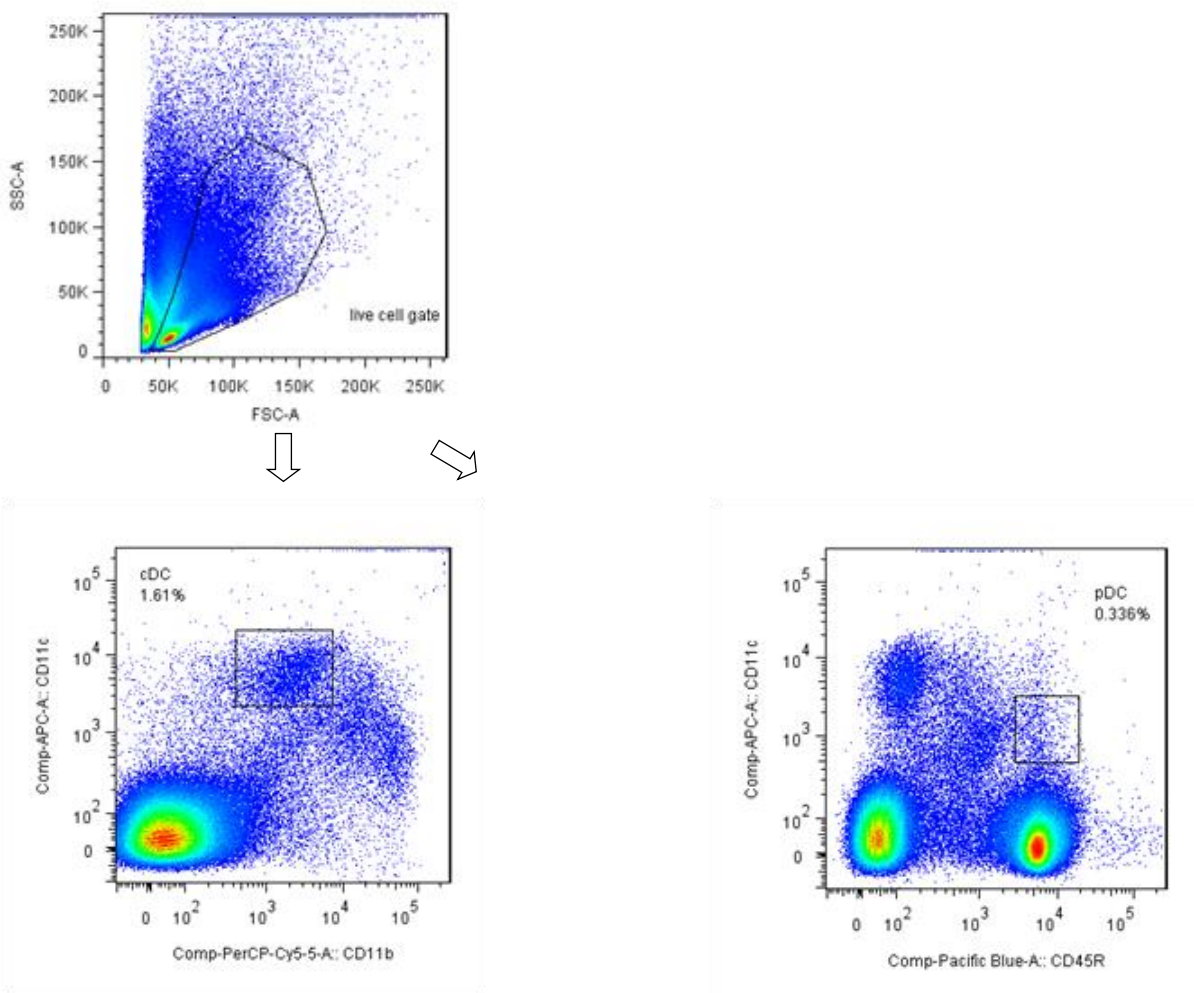
**Fig.3.1.2. 4 Quantification of activated Tcon from WT and B7-H1 KO mice in control groups (without treatment, co) and after the treatment of splenocytes in *in vitro* cultures with IFN $\alpha$ , 5-FU and IFN $\alpha$ +5-FU.**

Freshly isolated splenocytes were put in a culture and treated with IFN $\alpha$ , 5-FU and IFN $\alpha$ +5-FU for 24 hours. Afterwards the cells were stained with fluorescence labeled specific antibodies and analyzed by flow cytometry. Data from four independent experiments are presented as column bar graphs with SEM (n = 16; control group vs. treatment groups; two-way (A) and one-way (B,C) ANOVA)

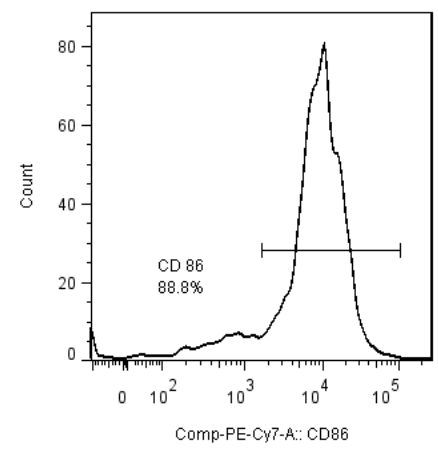
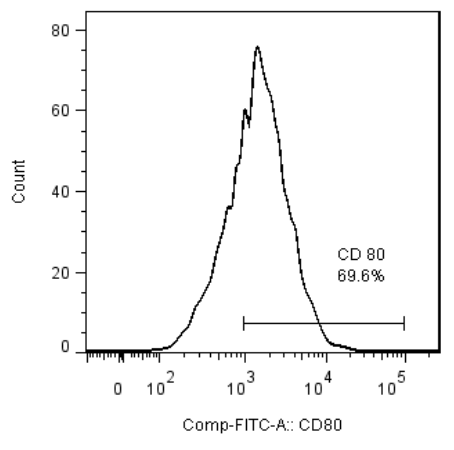
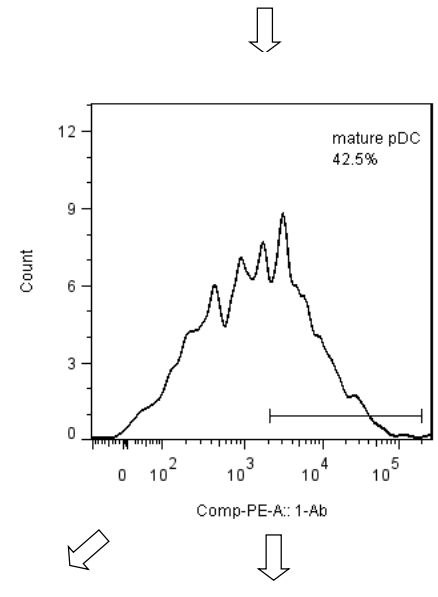
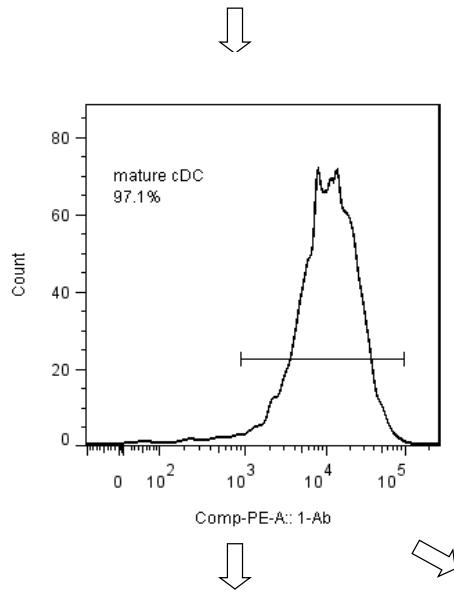
To summarize, our analysis of the Treg population revealed higher frequencies of Treg in spleens of B7-H1 KO mice compared to WT spleens, independent of the applied therapy.

### 3.1.3 Analysis of dendritic cells (DC)

Another analyzed cell population were the dendritic cells (DC) with their two subsets, conventional DC (cDC) and plasmacytoid DC (pDC). The gating strategy for the DC panel is shown in Fig.3.1.3.1. The FACS data (dot-plot, histogram) represent one typical result out of four independent experiments.



# Results



or

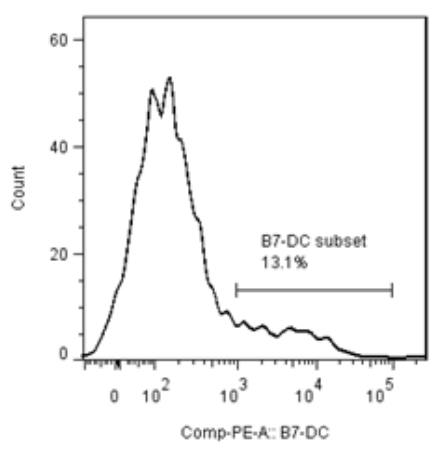
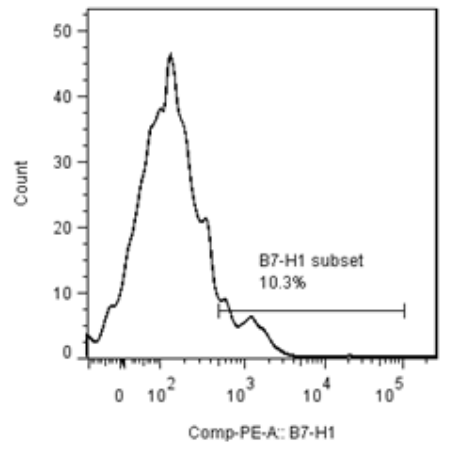


### **Fig.3.1.3. 1 Gating strategy for dendritic cells in splenocytes using flow cytometry.**

The first gate was set on all live leukocytes cells using FSC/SSC dot plot. Then the two subsets of DC, conventional DC (cDC) and plasmacytoid DC (pDC), were gated according to the expression of CD11c and either CD11b or CD45R markers. The I-Ab antibody was used to define the maturation status of cDC and pDC. Mature cDC and pDC were further analyzed for the expression of CD80 and CD86 costimulatory as well as the expression of B7-H1/B7-DC regulatory molecules. All positive gates were set according to FMO controls.

First, we analyzed the percentages of cDC out of all live cells. By comparing WT and B7-H1 KO groups to each other, we saw that no significant difference in percentages of cDC occurred (Fig.3.1.3.2 A). Furthermore, we showed that in both WT and B7-H1 KO mice, significantly lower frequencies of cDC were measured in the IFN $\alpha$  treatment group compared to control (Fig.3.1.3.2 B,C). When looking at the pDC, no significant differences in percentages of pDC were found between the groups of WT and B7-H1 KO (Fig.3.1.3.2 D). In WT, no significant change in frequencies of pDC in the treatment groups compared to control was determined (Fig.3.1.3.2 E). Also in the groups of B7-H1 KO, the difference in pDC ratio between the treated groups and the control was of no significance (Fig.3.1.3.2 F).

## Results

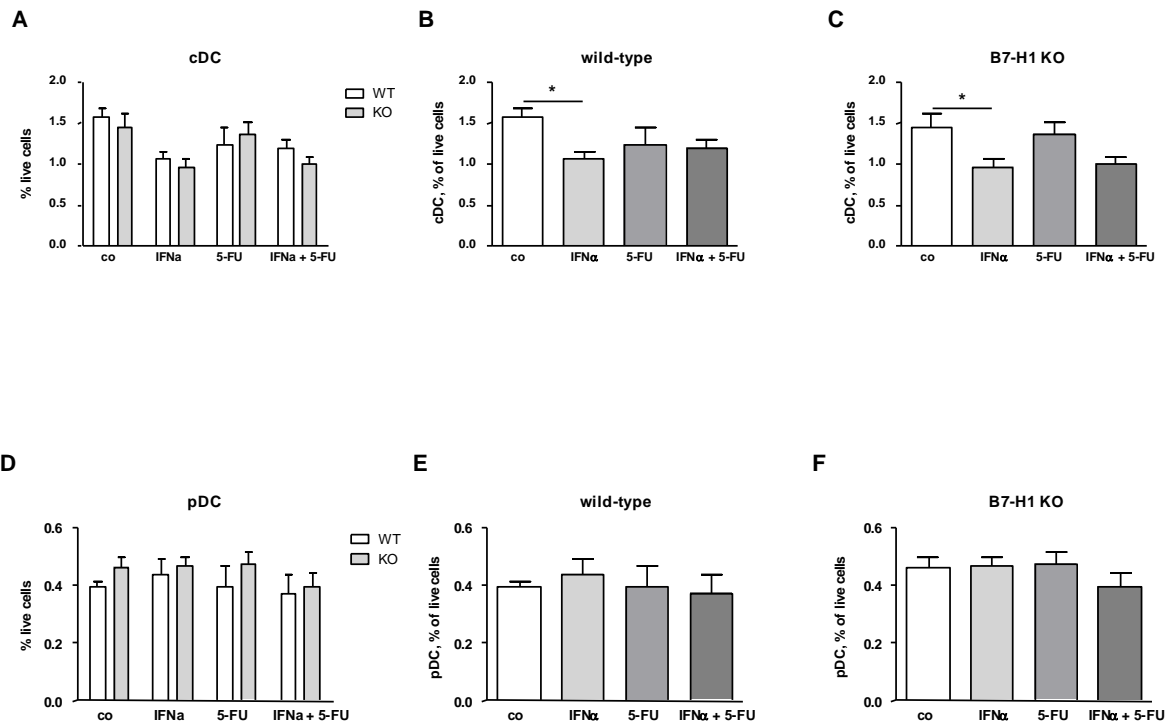


**Fig.3.1.3. 2 Quantification of cDC and pDC from WT and B7-H1 KO mice in control groups (without treatment, co) and after the treatment of splenocytes in *in vitro* cultures with IFN $\alpha$ , 5-FU and IFN $\alpha$ +5-FU.**

Freshly isolated splenocytes were put in a culture and treated with IFN $\alpha$ , 5-FU and IFN $\alpha$ +5-FU for 24 hours. Afterwards, the cells were stained with fluorescence labeled specific antibodies and analyzed by flow cytometry. Data from four independent experiments are presented as column bar graphs with SEM (n = 16; \*p<0.05; control group vs. treatment groups; two-way (A,D) and one-way (B,C,E,F) ANOVA)

Furthermore, we analyzed the maturation status of cDC and pDC with the help of the I-Ab antibody. In the cDC population, the analysis of the maturation status revealed no significant difference between WT and B7-H1 KO throughout all groups (Fig.3.1.3.3 A). In WT and B7-H1 KO on their own, no significant difference was seen between the treatment groups compared to controls in both WT and B7-H1 KO mice (Fig.3.1.3.3 B,C). The analysis of the maturation status of the pDC population revealed no significant change in percentages between WT and B7-H1 KO groups throughout all treatments (Fig.3.1.3.3 D). Also between control and treatment groups of either WT or B7-H1 KO mice, no significant difference in the frequency of mature pDC was determined (Fig.3.1.3.3 E,F).

## Results

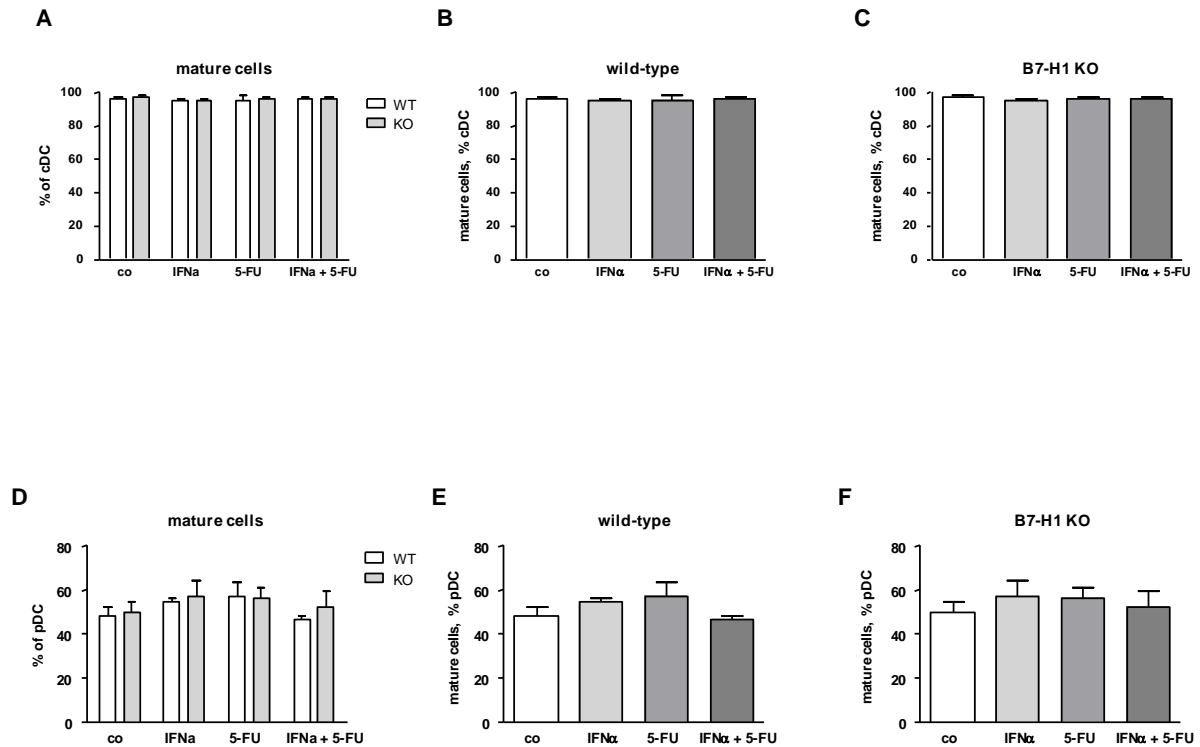


**Fig.3.1.3. 3 Quantification of mature cDC and pDC from WT and B7-H1 KO mice in control groups (without treatment, co) and after the treatment of splenocytes in *in vitro* cultures with IFN $\alpha$ , 5-FU and IFN $\alpha$ +5-FU.**

Freshly isolated splenocytes were put in a culture and treated with IFN $\alpha$ , 5-FU and IFN $\alpha$ +5-FU for 24 hours. Afterwards, the cells were stained with fluorescence labeled specific antibodies and analyzed by flow cytometry. Data from four independent experiments are presented as column bar graphs with SEM (n = 16; control group vs. treatment groups; two-way (A,D) and one-way (B,C,E,F) ANOVA)

After analyzing the maturation status of cDC and pDC, we investigated the expression of CD80 and CD86 co-stimulatory molecules on mature cDC and pDC, starting with the population of cDC. Between the four groups of WT and B7-H1 KO, the percentage of CD80<sup>+</sup> cDC showed no significant difference (Fig.3.1.3.4 A). In WT, no significant change in frequencies of CD80<sup>+</sup> cDC was observed between the control and treatment groups (Fig.3.1.3.4 B). In the B7-H1 KO groups, no significant difference in the percentage of CD80<sup>+</sup> cDC was found between the treatment groups and the control (Fig.3.1.3.4 C). The MFI of CD80 for the cell population of mature cDC showed no significant difference between the groups of WT compared to those of B7-H1 KO (Fig.3.1.3.4 D). However, when we looked at WT and B7-H1 groups

## Results

separately, we saw a significant increase in CD80 MFI values in all treatment groups of WT compared to the control group (Fig.3.1.3.4 E). In the groups of B7-H1 KO mice, significantly higher values were observed between control and 5-FU, IFN $\alpha$ +5-FU treatment groups (Fig.3.1.3.4 F).

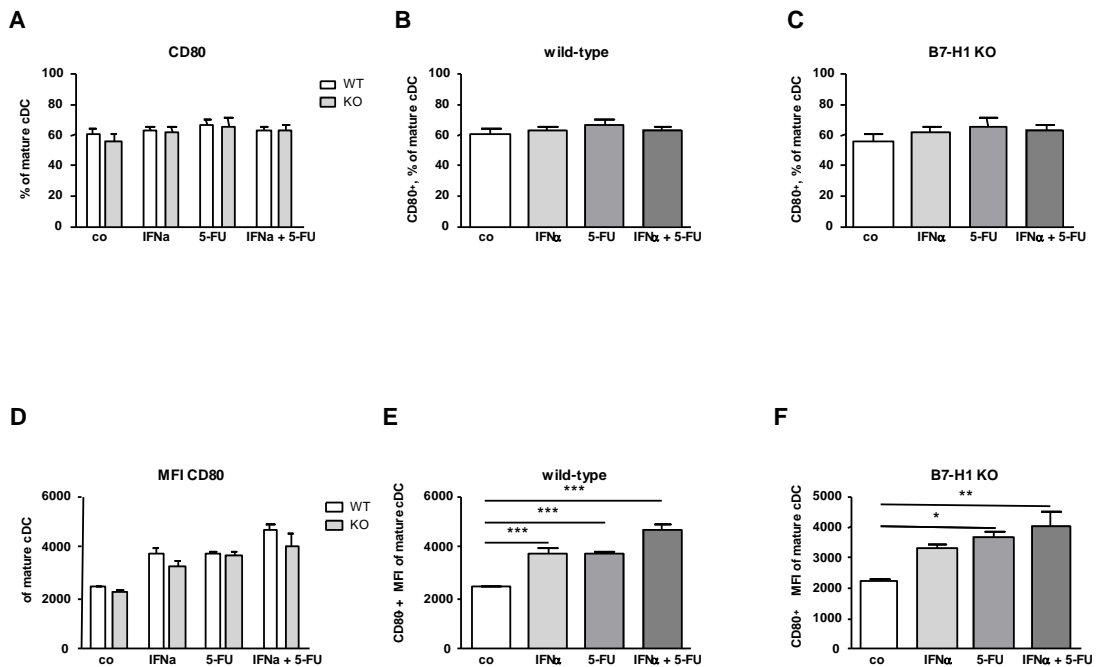


**Fig.3.1.3. 4 Quantification of CD80 expression on mature cDC from WT and B7-H1 KO mice in control groups (without treatment, co) and after the treatment of splenocytes in *in vitro* cultures with IFN $\alpha$ , 5-FU and IFN $\alpha$ +5-FU.**

Freshly isolated splenocytes were put in a culture and treated with IFN $\alpha$ , 5-FU and IFN $\alpha$ +5-FU for 24 hours. Afterwards, the cells were stained with fluorescence labeled specific antibodies. The frequency of CD80<sup>+</sup> mature cDC together with the MFI of CD80 was analyzed by flow cytometry. Data from four independent experiments are presented as column bar graphs with SEM (n = 16; \*p<0.05, \*\*p<0.01, \*\*\*p<0.001; control group vs. treatment groups; two-way (A,D) and one-way (B,C,E,F) ANOVA)

For the CD86 expression on mature cDC, no significant difference in respect of CD86<sup>+</sup> cDC frequencies was determined for all four groups of WT mice in comparison to the groups of B7-H1 KO mice (Fig.3.1.3.5 A). In the WT as well as the B7-H1 KO groups, no significant change in frequencies of the CD86<sup>+</sup> mature cDC

## Results

was determined between treatment groups and controls (Fig.3.1.3.5 B,C). The analysis of CD86 MFI revealed no significant difference in all subgroups between the groups of WT and B7-H1 KO (Fig.3.1.3.5 D). However, in the groups of WT mice, significantly higher values of CD86 MFI were measured in the groups of IFN $\alpha$  and IFN $\alpha$ +5-FU compared to the control (Fig.3.1.3.5 E). In B7-H1 KO groups, a significant increase of the CD86 MFI was revealed after the treatment of the cells with IFN $\alpha$  and IFN $\alpha$ +5-FU compared to the control (Fig.3.1.3.5 F).

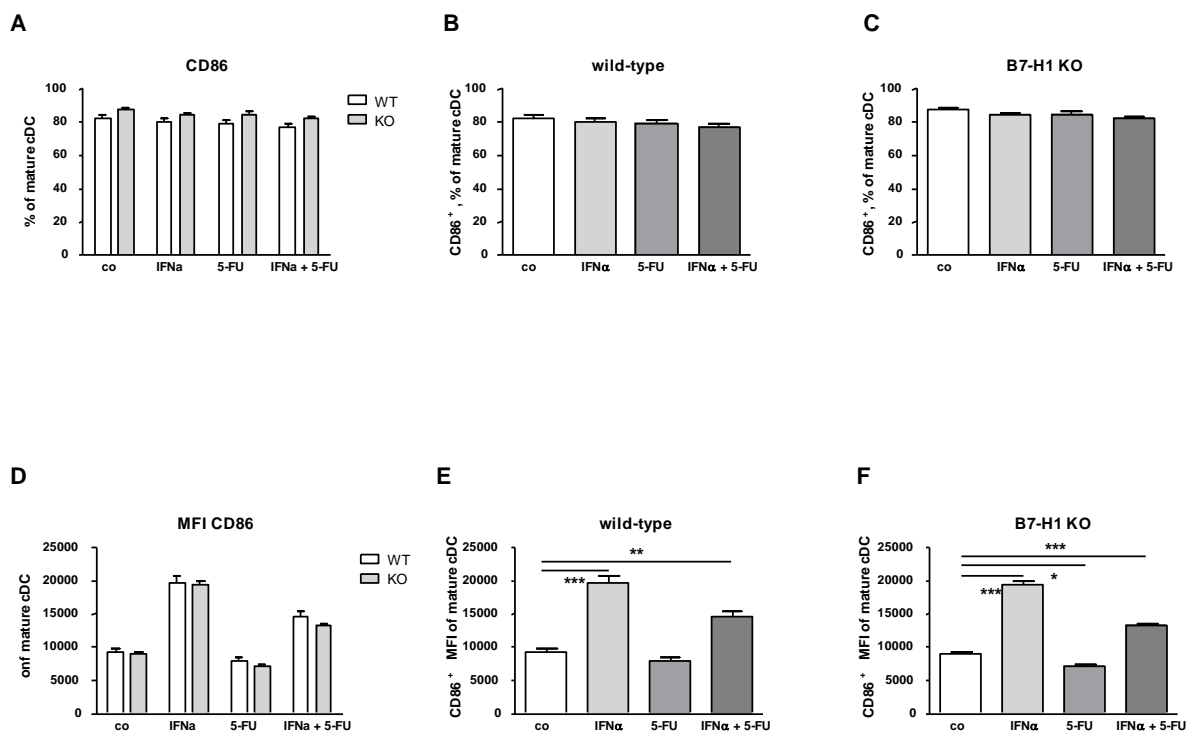


**Fig.3.1.3. 5 Quantification of CD86 expression on mature cDC from WT and B7-H1 KO mice in control groups (without treatment, co) and after the treatment of splenocytes in *in vitro* cultures with IFN $\alpha$ , 5-FU and IFN $\alpha$ +5-FU.**

Freshly isolated splenocytes were put in a culture and treated with IFN $\alpha$ , 5-FU and IFN $\alpha$ +5-FU for 24 hours. Afterwards, the cells were stained with fluorescence labeled specific antibodies. The frequency of CD86<sup>+</sup> mature cDC together with the MFI of CD86 was analyzed by flow cytometry. Data from four independent experiments are presented as column bar graphs with SEM (n = 16; \*p<0.05, \*\*p<0.01, \*\*\*p<0.001; control group vs. treatment groups; two-way (A,D) and one-way (B,C,E,F) ANOVA)

## Results

As presented in Fig.3.1.3.6 A, a tendency towards higher percentages of CD80<sup>+</sup> mature pDC was seen in all subgroups of WT compared to those of B7-H1 KO groups. The groups of WT and B7-H1 KO, when investigated separately, showed no significant difference between control and treatment groups, neither in WT nor in B7-H1 KO (Fig.3.1.3.6 B,C). Concerning the MFI of CD80 on mature pDC, we found no significant difference in values when we compared WT groups to B7-H1 KO groups (Fig.3.1.3.6 D). In the groups of WT mice, no significant changes in the values of the CD80 MFI were determined between treatment groups and control (Fig.3.1.3.6 E). In the B7-H1 KO groups on their own, significantly higher CD80 MFI values were found for IFN $\alpha$  and IFN $\alpha$ +5-FU groups compared to the control (Fig.3.1.3.6 F).

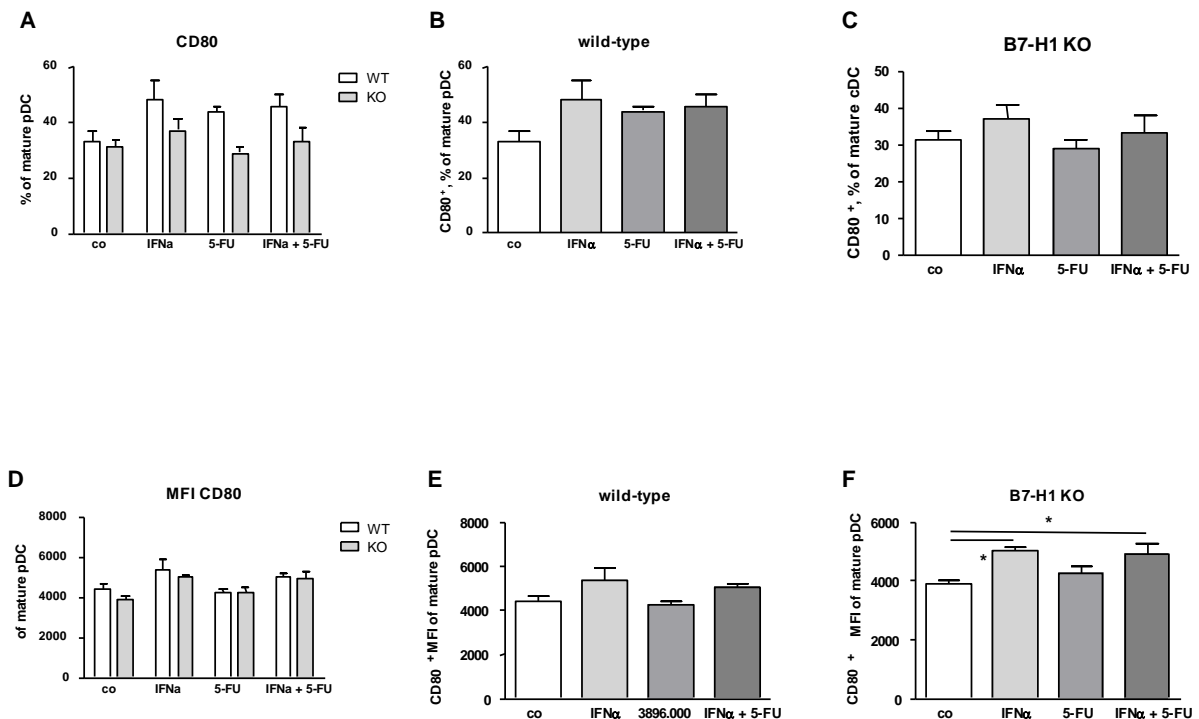


**Fig.3.1.3. 6 Quantification of CD80 expression on mature pDC from WT and B7-H1 KO mice in control groups (without treatment, co) and after the treatment of splenocytes in *in vitro* cultures with IFN $\alpha$ , 5-FU and IFN $\alpha$ +5-FU.**

Freshly isolated splenocytes were put in a culture and treated with IFN $\alpha$ , 5-FU and IFN $\alpha$ +5-FU for 24 hours. Afterwards, the cells were stained with fluorescence labeled specific antibodies. The frequency of CD80<sup>+</sup> mature pDC together with the MFI of CD80 was analyzed by flow cytometry. Data from four independent experiments are presented as column bar graphs with SEM (n = 16; \*p<0.05; control group vs. treatment groups; two-way (A,D) and one-way (B,C,E,F) ANOVA)

For the frequencies of CD86<sup>+</sup> cells among mature pDC, no significant difference was seen between the groups of WT and B7-H1 KO mice (Fig.3.1.3.7 A). Beyond that, in WT and B7-H1 KO groups on their own, no significant difference in frequencies of CD86<sup>+</sup> mature pDC was determined between the single treatment groups and the control in both the WT and B7-H1 KO groups (Fig.3.1.3.7 B,C). The analysis of CD86 MFI on mature pDC revealed significantly lower values in cells of B7-H1 KO for the groups of IFN $\alpha$ , 5-FU and IFN $\alpha$ +5-FU compared to those groups of WT. For the control of WT and B7-H1 KO, a tendency towards lower values in B7-H1 KO was observed (Fig.3.1.3.7 D). In WT, the MFI of CD86 was significantly increased after IFN $\alpha$  and IFN $\alpha$ +5-FU treatment compared to control (Fig.3.1.3.7 E). In B7-H1 KO, significantly higher intensity values of CD86 MFI were found in the group of IFN $\alpha$  treatment compared to control (Fig.3.1.3.7 F).

## Results

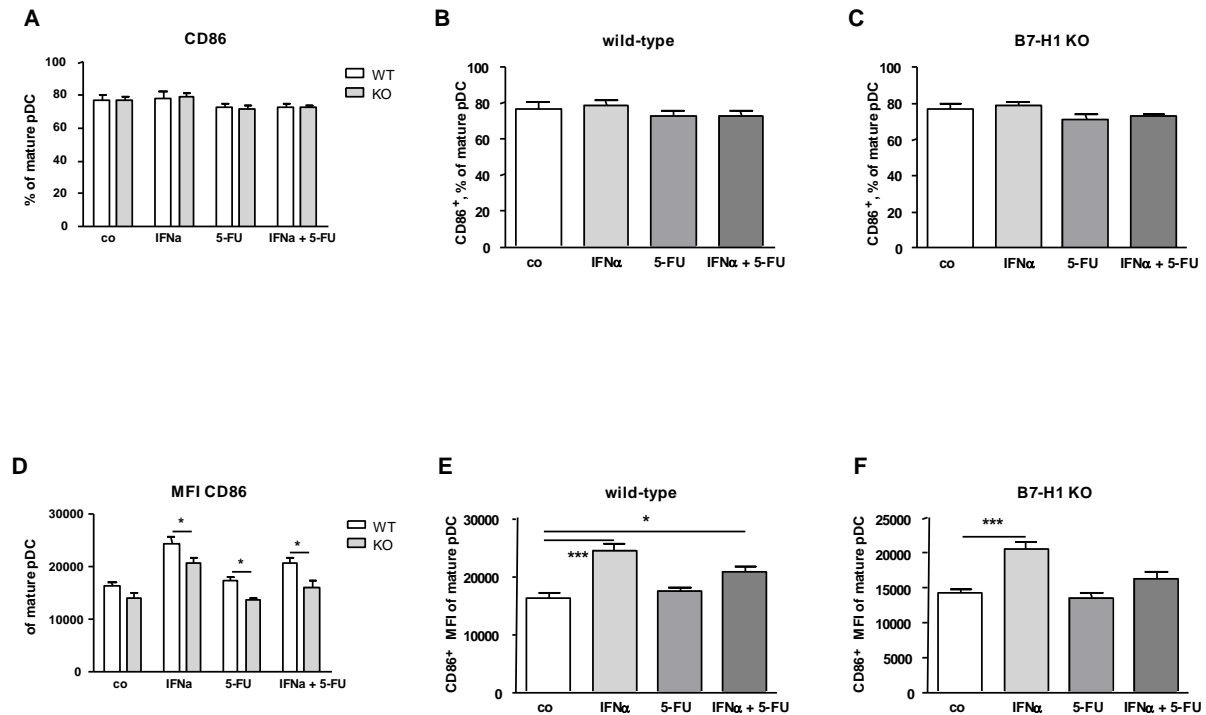


**Fig.3.1.3. 7** Quantification of CD86 expression on mature pDC from WT and B7-H1 KO mice in control groups (without treatment, co) and after the treatment of splenocytes in *in vitro* cultures with IFN $\alpha$ , 5-FU and IFN $\alpha$ +5-FU.

Freshly isolated splenocytes were put in a culture and treated with IFN $\alpha$ , 5-FU and IFN $\alpha$ +5-FU for 24 hours. Afterwards, the cells were stained with fluorescence labeled specific antibodies. The frequency of CD86<sup>+</sup> mature cDC together with the MFI of CD86 was analyzed by flow cytometry. Data from four independent experiments are presented as column bar graphs with SEM (n = 16; \*p<0.05, \*\*\*p<0.001; control group vs. treatment groups; two-way (A,D) and one-way (B,C,E,F) ANOVA)

In addition to co-stimulatory molecules, also regulatory molecules can be expressed by DC. Therefore, the next aspect we were interested in was the expression of B7-H1 regulatory molecules on mature cDC and pDC in the cells of WT mice, respectively the B7-DC expression on mature cDC and pDC in the cells of B7-H1 KO mice. In WT groups, no significant difference in B7-H1 expression on mature cDC was seen between the control group and the different treatments (Fig.3.1.3.8 A). The measured MFI of B7-H1 on mature cDC from WT showed no significant difference between the treatment groups and the control (Fig.3.1.3.8 B). When assessing the B7-DC expression of mature cDC in B7-H1 KO groups, significantly higher levels of B7-DC expression were seen in IFN $\alpha$  and IFN $\alpha$ +5-FU groups compared to control

(Fig.3.1.3.8 C). The MFI of B7-DC expression on mature cDC was increased in the group of 5-FU compared to the control (Fig.3.1.3.8 D).

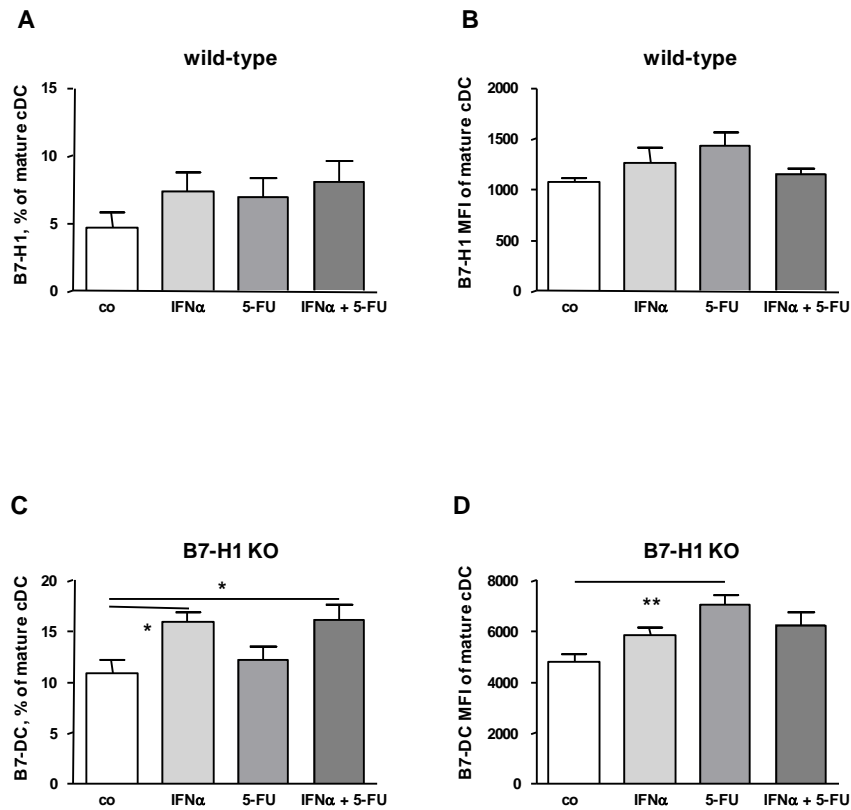


**Fig.3.1.3. 8 Quantification of B7-H1/B7-DC expression on mature cDC from WT and B7-H1 KO mice in control groups (without treatment, co) and after the treatment of splenocytes in *in vitro* cultures with IFN $\alpha$ , 5-FU and IFN $\alpha$ +5-FU.**

Freshly isolated splenocytes were put in a culture and treated with IFN $\alpha$ , 5-FU and IFN $\alpha$ +5-FU for 24 hours. Afterwards, the cells were stained with fluorescence labeled specific antibodies. The frequency of B7-H1/B7-DC<sup>+</sup> mature cDC together with the MFI of B7-H1/B7-DC was analyzed by flow cytometry. Data from four independent experiments are presented as column bar graphs with SEM (n = 16; \*p<0.05, \*\*p<0.01; control group vs. treatment groups; one-way (A-D) ANOVA)

Analysis of the B7-H1/B7-DC expression on mature pDC is demonstrated in Fig.3.1.3.9. In WT mice, no significant difference in the frequency of B7-H1<sup>+</sup> mature pDC between control and treatments groups was registered (Fig.3.1.3.9 A). The analysis of the MFI of B7-H1 expression on mature pDC, showed that the values were not significantly different between the controls and therapy groups (Fig.3.1.3.9 B). In the groups of B7-H1 KO mice, we determined no significant differences in the

B7-DC expression on mature pDC between the control and treatment groups (Fig.3.1.3.9 C). For the B7-DC MFI values, we saw no significant differences between treatment groups and control (Fig.3.1.3.9 D).

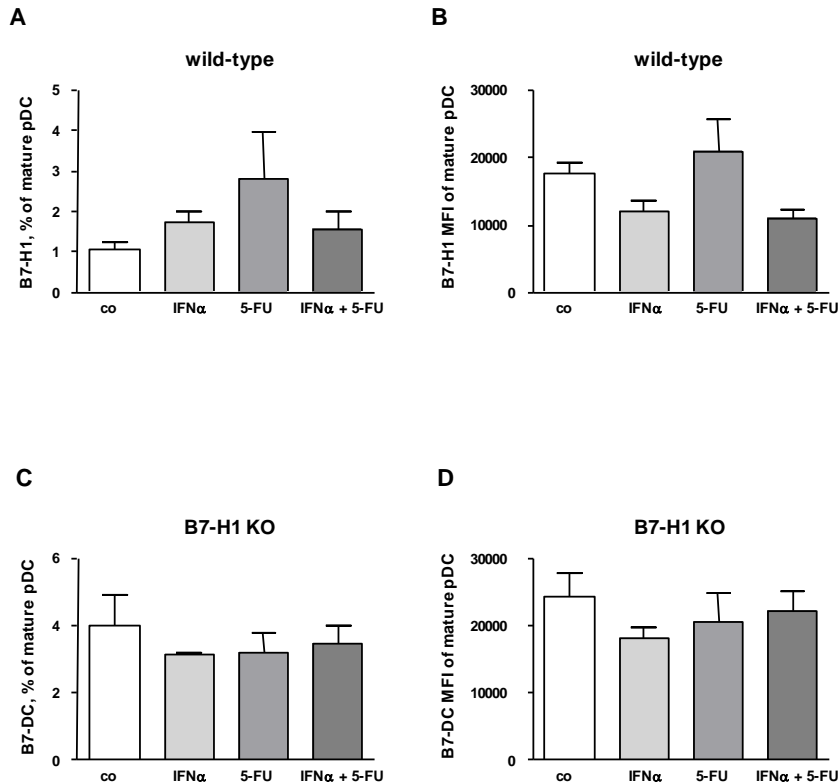


**Fig.3.1.3. 9 Quantification of B7-H1/B7-DC expression on mature pDC from WT and B7-H1 KO mice in control groups (without treatment, co) and after the treatment of splenocytes in *in vitro* cultures with IFN $\alpha$ , 5-FU and IFN $\alpha$ +5-FU.**

Freshly isolated splenocytes were put in a culture and treated with IFN $\alpha$ , 5-FU and IFN $\alpha$ +5-FU for 24 hours. Afterwards, the cells were stained with fluorescence labeled specific antibodies. The frequency of B7-H1/B7-DC<sup>+</sup> mature pDC together with the MFI of B7-H1/B7-DC was analyzed by flow cytometry. Data from four independent experiments are presented as column bar graphs with SEM (n = 16; control group vs. treatment groups; one-way (A-D) ANOVA)

Taken together, the data of the examined DC cell populations did not show significant differences in the frequencies of cDC, pDC, as well as their activation status between spleens of healthy WT or B7-H1 KO mice. Beyond that, the analysis of the molecules B7-H1/B7-DC revealed significantly higher frequencies in B7-DC<sup>+</sup>

mature cDC in spleens of B7-H1 KO mice after the IFN $\alpha$ , IFN $\alpha$ +5-FU treatment compared to the control.

### **3.1.4 Analysis of Gr-1<sup>+</sup>CD11b<sup>+</sup> cells**

The last analyzed cell population in this *in vitro* experiment was the population of Gr-1<sup>+</sup>CD11b<sup>+</sup> cells, which corresponds to myeloid derived suppressor cells (MDSC) in tumor-bearing mice.

The gating strategy for this panel is shown in Fig.3.1.4.1. FACS data (dot-plot, histogram) represent one typical result out of four independent experiments.

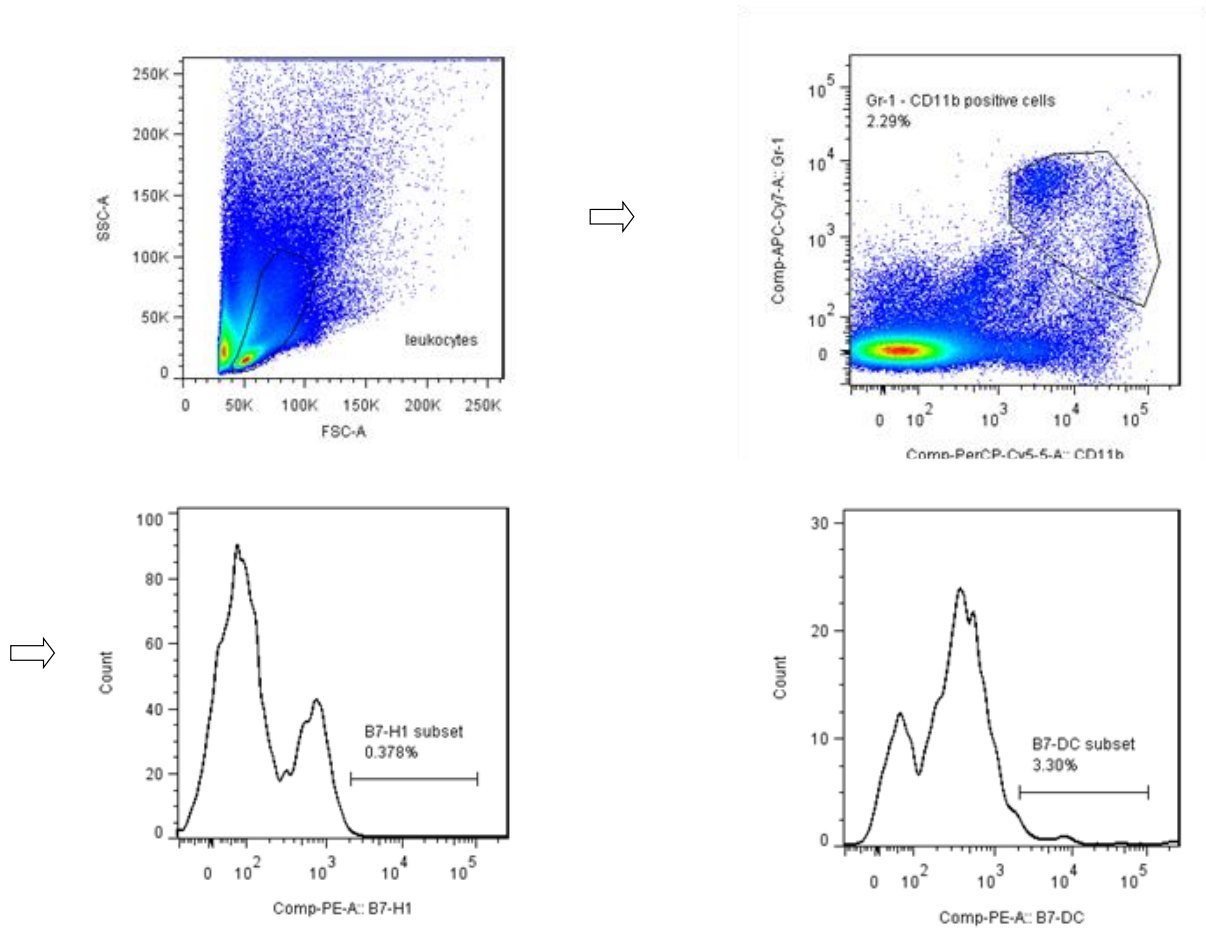


**Fig.3.1.4. 1 Gating strategy for Gr-1<sup>+</sup>CD11b<sup>+</sup> cell population in splenocytes using flow cytometry.**

The first gate was set on leukocytes using FSC/SSC dot plot; afterwards, the Gr-1<sup>+</sup>CD11b<sup>+</sup> cell population was gated. From this population furthermore the expression of the molecule B7-H1 in WT, B7-DC in B7-H1 KO was analyzed using histograms. All positive gates were set according to FMO controls.

First, we analyzed the frequency of Gr-1<sup>+</sup>CD11b<sup>+</sup> cells out of all leukocytes. When comparing the groups of WT and B7-H1 KO mice with each other, only for the group with the 5-FU treatment, could a significant difference be seen with decreased percentages of Gr-1<sup>+</sup>CD11b<sup>+</sup> cells in the 5-FU group of B7-H1 KO mice (Fig.3.1.4.2 A). If we just looked at the treatment groups of WT, no significant difference was determined between the different treatment groups and control (Fig.3.1.4.2 B). For

the groups of B7-H1 KO, there were also no significant differences seen between the control and treatment groups (Fig.3.1.4.2 C).

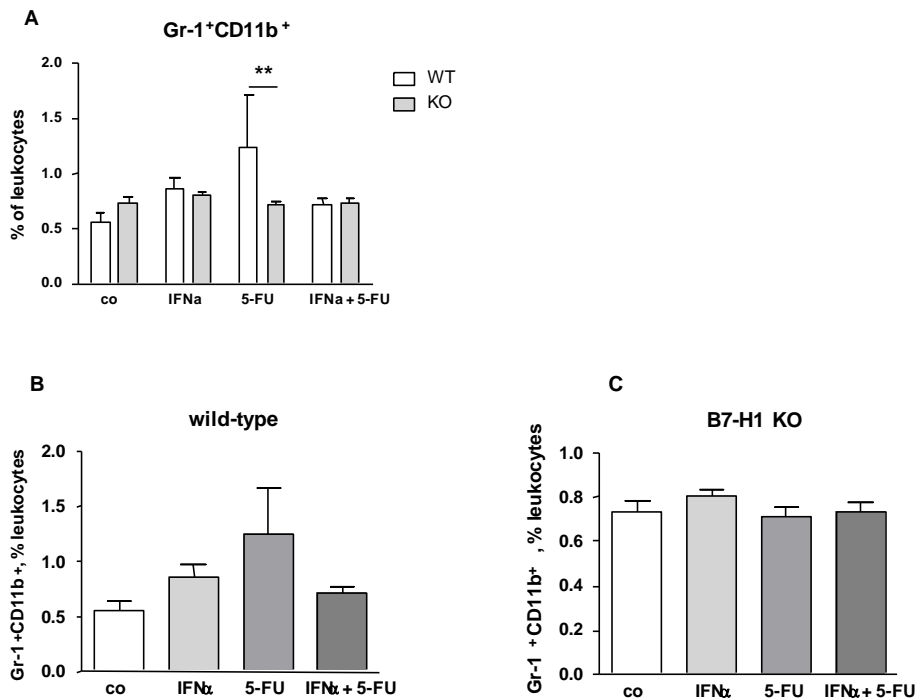


**Fig.3.1.4. 2 Quantification of Gr-1<sup>+</sup>CD11b<sup>+</sup> cells from WT and B7-H1 KO mice in control groups (without treatment, co) and after the treatment of splenocytes in *in vitro* cultures with IFN $\alpha$ , 5-FU and IFN $\alpha$ +5-FU.**

Freshly isolated splenocytes were put in a culture and treated with IFN $\alpha$ , 5-FU and IFN $\alpha$ +5-FU for 24 hours. Afterwards, the cells were stained with fluorescence labeled specific antibodies and analyzed by flow cytometry. Data from four independent experiments are presented as column bar graphs with SEM (n = 16; \*\*p<0.01; control group vs. treatment groups; two-way (A) and one-way (B,C) ANOVA)

We furthermore determined the MFI of B7-H1 respectively of B7-DC expression on Gr-1<sup>+</sup>CD11b<sup>+</sup> cells. In groups of WT mice, the MFI of B7-H1 did not show a significant difference in values between control and treated groups (Fig.3.1.4.3 A). For the groups of B7-H1 KO mice, no significant differences in values of the MFI of B7-DC on Gr-1<sup>+</sup>CD11b<sup>+</sup> cells were seen between control and treatment groups (Fig.3.1.4.3 B).

## Results

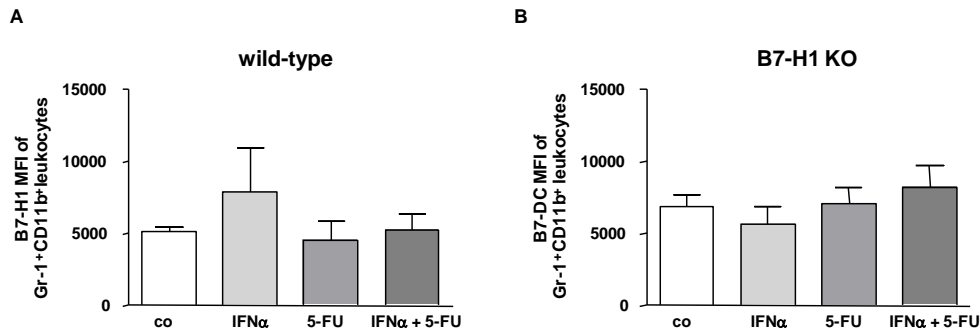


**Fig.3.1.4. 3 Quantification of B7-H1/B7-DC MFI of Gr-1<sup>+</sup>CD11b<sup>+</sup> cells from WT and B7-H1 KO mice in control groups (without treatment, co) and after the treatment of splenocytes in *in vitro* cultures with IFN $\alpha$ , 5-FU and IFN $\alpha$ +5-FU.**

Freshly isolated splenocytes were put in a culture and treated with IFN $\alpha$ , 5-FU and IFN $\alpha$ +5-FU for 24 hours. Afterwards, the cells were stained with fluorescence labeled specific antibodies. The MFI of B7-H1<sup>+</sup>/B7-DC<sup>+</sup> Gr-1<sup>+</sup>CD11b<sup>+</sup> cells was analyzed by flow cytometry. Data from four independent experiments are presented as column bar graphs with SEM (n = 16; control group vs. treatment groups; one-way (A,B) ANOVA)

Summarizing the data of Gr-1<sup>+</sup>CD11b<sup>+</sup> cell population, in cultures of spleens of healthy WT and B7-H1 KO mice, only in the treatment group of 5-FU a significantly lower ratio of Gr-1<sup>+</sup>CD11b<sup>+</sup> cells was seen in spleens of B7-H1 KO mice compared to those of WT mice.

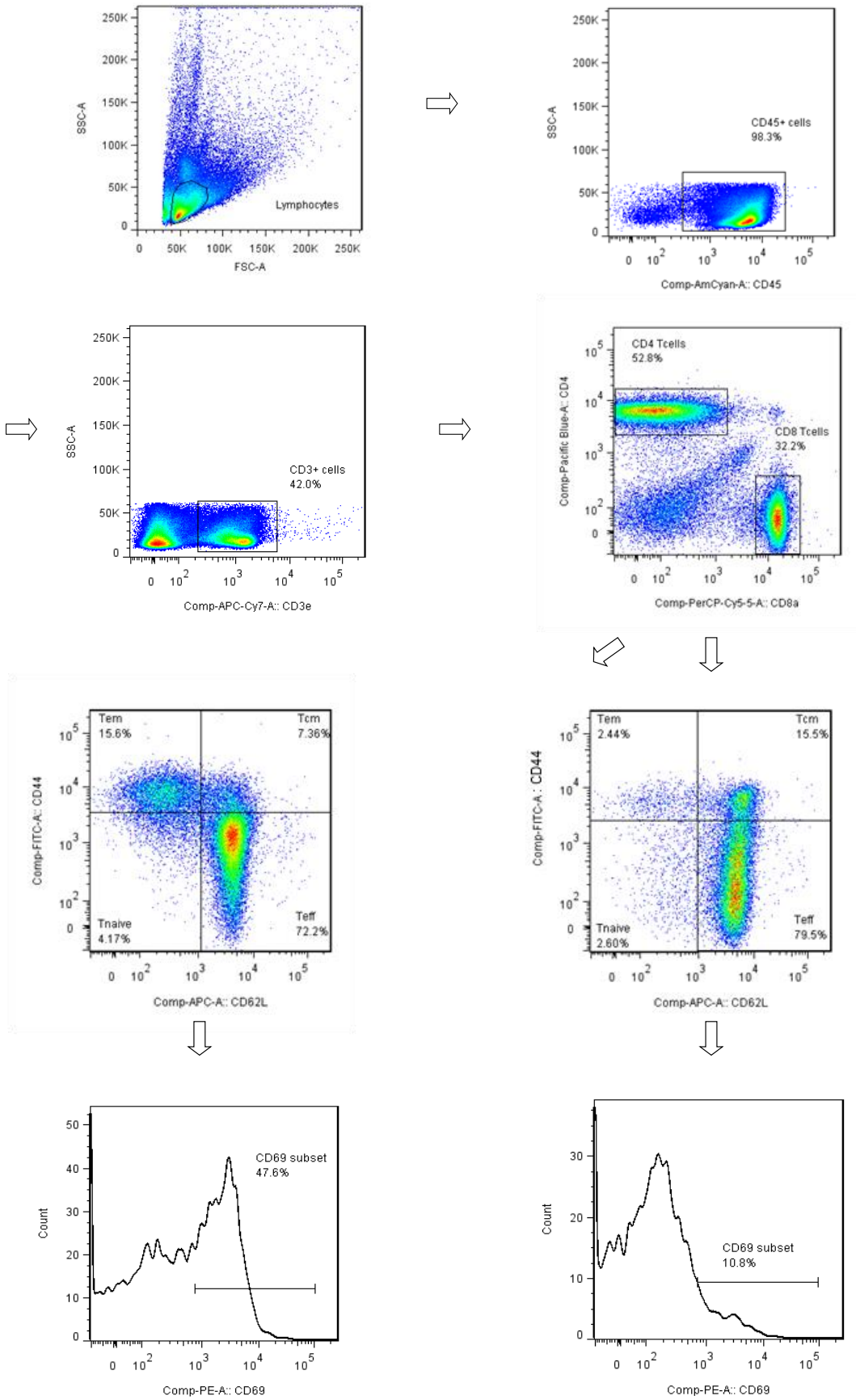
### **3.2 *In vivo* Effects of chemo (5-FU) - and immunotherapy (IFN $\alpha$ ) on the constellation of leukocyte subsets and the expression of B7-H1/B7-DC molecules in tumor-bearing WT and B7-H1 KO mice**

Since we have seen that chemotherapy can affect the constellation of leukocyte subsets in healthy mice, in this experiment series we wanted to examine whether 5-FU and IFN $\alpha$  could directly influence the constellation of immune cells in tumor-bearing WT and B7-H1 KO mice. Furthermore, we wanted to investigate if this could also be accompanied by a direct effect of 5-FU and IFN $\alpha$  on B7-H1 or B7-DC expression on the different leukocyte subpopulations of WT and B7-H1 KO mice respectively. To achieve this, we treated tumor-bearing WT and B7-H1 KO mice with either IFN $\alpha$ , or 5-FU alone or in the combination of IFN $\alpha$ +5-FU on Day 5, 7 and 9 after Panc02 implantation. One group was kept untreated and used as the control. After a period of four weeks, the mice were killed and the spleens and tumors eviscerated. With the help of flow cytometry, we analyzed and compared treated WT and B7-H1 KO mice in terms of the constellation of different immune cells as well as the expression of B7-H1/B7-DC molecules.

#### **3.2.1 Analysis of CD4<sup>+</sup>/CD8<sup>+</sup> T cells**

The performed gating strategy for CD4/CD8 Panel is shown in Fig.3.2.1.1. The FACS data (dot-plot, histogram) represent one typical result out of four independent experiments.

# Results



and

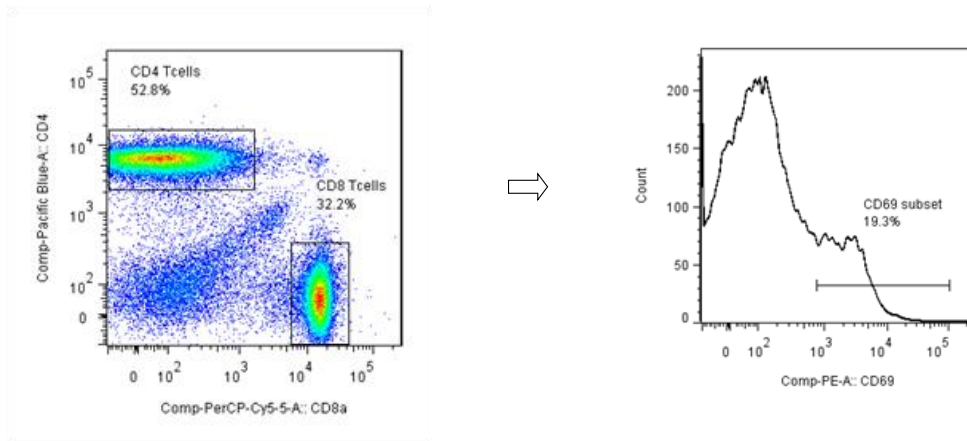


**Fig.3.2.1.1 Gating strategy for CD4<sup>+</sup>/CD8<sup>+</sup> T cells in spleens and tumors using flow cytometry.**

Lymphocytes were gated out using FSC/SSC dot plot. Afterwards, we marked CD45<sup>+</sup> cells to discriminate tumor cells (CD45<sup>-</sup>) and tumor-infiltrating leukocytes (CD45<sup>+</sup>). The CD3<sup>+</sup> cells were determined and the CD4<sup>+</sup>/CD8<sup>+</sup> T cells were gated out of CD3<sup>+</sup> cells. Furthermore, the CD4<sup>+</sup>/CD8<sup>+</sup> T cells were divided into naïve T cells (Tnaive), effector T cells (Teff), effector memory cells (Tem) and central memory cells (Tcm). The activation status of different subpopulations was determined by analyzing the expression of CD69 early activation marker. All positive gates were set according to FMO controls.

First, we analyzed the frequency of CD8<sup>+</sup> T cells out of all CD3<sup>+</sup> lymphocytes within the splenocytes of tumor-bearing mice. The analysis of WT and B7-H1 KO groups in comparison showed significantly higher percentages of CD8<sup>+</sup> T cells in the treatment groups of 5-FU and IFN $\alpha$ +5-FU in B7-H1 KO mice compared to those groups of WT mice (Fig.3.2.1.2 A). In WT spleens, no significant difference in the ratio of CD8<sup>+</sup> T cells was observed between control and treatment groups (Fig.3.2.1.2 B). However, in B7-H1 KO spleens, significantly increased percentages of CD8<sup>+</sup> T cells were measured in the group of IFN $\alpha$ +5-FU compared to the control (Fig.3.2.1.2 D).

When taking a detailed look at the tumors of WT mice, significantly higher frequencies of CD8<sup>+</sup> T cells were found in mice treated with IFN $\alpha$  compared to the control mice (Fig.3.2.1.2 C).

## Results

Here and further on in this experiment series, the B7-H1 effect on the tumor growth was so strong that we had nearly no visible tumors from the B7-H1 KO mice so we could isolate tumor-infiltrating cells and take a more detailed look. The only available tumor material was used for MDSC characterization, described later on (3.4.1).

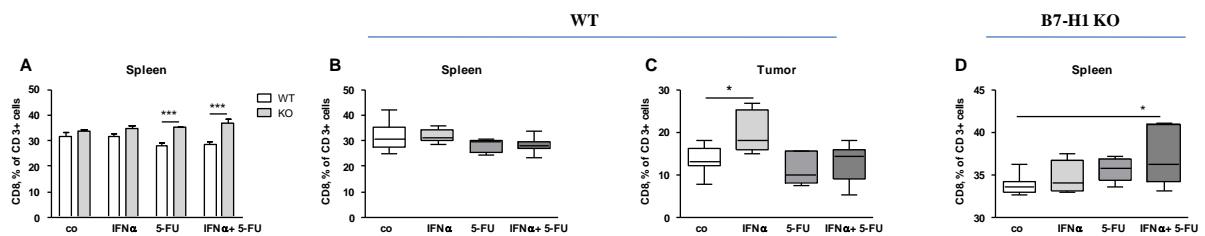


**Fig.3.2.1.2 Quantification of CD8<sup>+</sup> T cells in spleens and tumors from tumor bearing WT and B7-H1 KO mice with and without treatment (co).**

Mice were treated with IFN $\alpha$ , 5-FU or the combination of IFN $\alpha$ +5-FU on Day 5, 7 and 9 after Panc02 implantation. Untreated mice were used as the control. Four weeks after surgery, the mice were killed and the organs were eviscerated. Single-cell suspensions of spleens and tumors were stained with fluorescence labeled specific antibodies. The frequency of CD8<sup>+</sup> T cells out of CD3<sup>+</sup> lymphocytes was analyzed by flow cytometry. Data from four independent experiments are presented as column bar graphs and box plots with SEM ((spleens: n = 9 for co, and n = 6 for IFN $\alpha$ ; 5-FU; IFN $\alpha$ +5-FU; tumors: n = 7 for co, n = 4-6 for IFN $\alpha$ ; 5-FU; IFN $\alpha$ +5-FU); \*p<0.05, \*\*\*p<0.001; control group vs. treatment groups; two-way (A) and one-way (B,C,D) ANOVA)

The activation status of CD8<sup>+</sup> T cells from spleens and tumors was determined by the expression of the CD69 early activation marker. When comparing the groups of WT splenocytes with those of B7-H1 KO, no significant difference was seen throughout all four groups (Fig.3.2.1.3 A). When we looked at the groups of WT and B7-H1 KO spleens in detail, no significant difference was registered between the control and the treatment groups in both the WT and B7-H1 KO groups (Fig.3.2.1.3 B,D).

The analysis of WT tumors showed no significant difference between control and treatment groups in respect of proportion of CD69<sup>+</sup> CD8<sup>+</sup> T cells (Fig.3.2.1.3 C).

## Results

The measured MFI of CD69 on CD8<sup>+</sup> T cells of the spleens reached significantly higher values in all four groups of WT compared to groups of B7-H1 KO tumor-bearing mice (Fig.3.2.1.3 E). Alone in the WT and B7-H1 KO groups, the analyzed MFI of CD69 revealed no significant difference between the treatment groups and the control (Fig.3.2.1.3 F,H).

In the tumors of WT mice, no significant difference in CD69 MFI was observed between control and treatment groups (Fig.3.2.1.3 G).

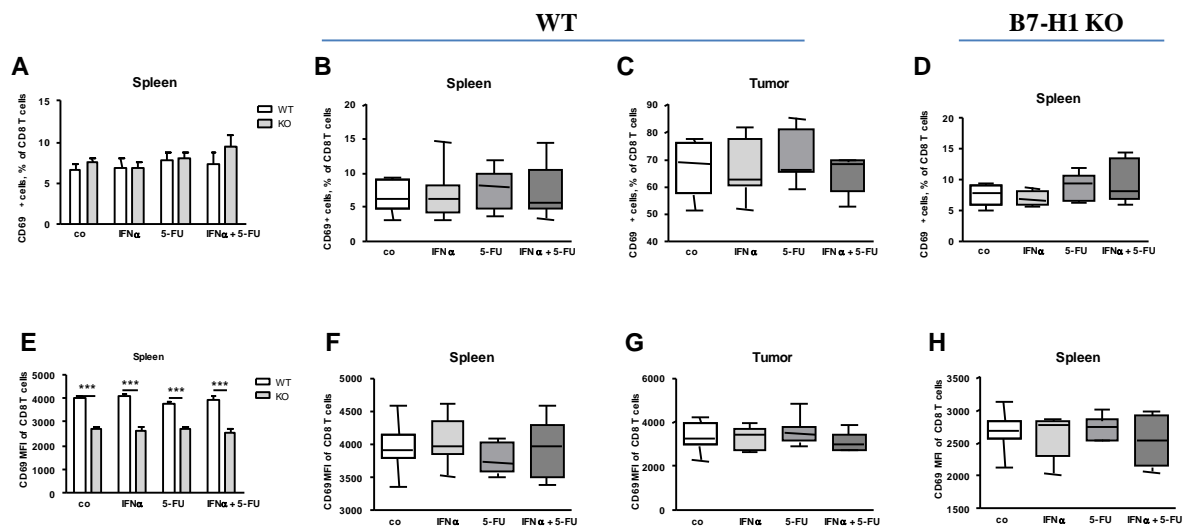


**Fig.3.2.1.3 Quantification of CD69 expression on CD8<sup>+</sup> T cells in spleens and tumors from tumor-bearing WT and B7-H1 KO mice with and without treatment (co).**

Mice were treated with IFN $\alpha$ , 5-FU or the combination of IFN $\alpha$ +5-FU on Day 5, 7 and 9 after Panc02 implantation. Untreated mice were used as the control. Four weeks after surgery, the mice were killed and the organs were eviscerated. Single-cell suspensions of spleens and tumors were stained with fluorescence labeled specific antibodies. The frequency of CD69<sup>+</sup> CD8<sup>+</sup> T cells out of CD3<sup>+</sup> lymphocytes together with the MFI of CD69 was analyzed by flow cytometry. Data from four independent experiments are presented as column bar graphs and box plots with SEM ((spleens: n = 9 for co, and n = 6 for IFN $\alpha$ ; 5-FU; IFN $\alpha$ +5-FU; tumors: n = 7 for co, n = 4-6 for IFN $\alpha$ ; 5-FU; IFN $\alpha$ +5-FU); \*\*\*p<0.001; control group vs. treatment groups; two-way (A,E) and one-way (B,C,D,F,G,H) ANOVA)

## Results

Next, we analyzed the four subsets of CD8<sup>+</sup> T cells, Tnaive, Teff, Tem, and Tcm. The CD8<sup>+</sup> Tnaive in spleens achieved lower percentages in the B7-H1 KO groups compared to the WT groups. For the controls, as well as for the therapies with IFN $\alpha$  and IFN $\alpha$ +5-FU, this difference is of significance. In the group of 5-FU, a tendency towards lower percentages of Tnaive was found in spleens of B7-H1 KO mice compared to those of WT mice (Fig.3.2.1.4 A). Analyzing splenocytes of treated WT and B7-H1 KO tumor-bearing mice separately, a significant decrease of Tnaive was found in the treatment of IFN $\alpha$ +5-FU compared to control in spleens of both the WT and B7-H1 KO tumor-bearing mice (Fig.3.2.1.4 B,D).

The analysis of WT tumors demonstrated no significant difference in percentages of Tnaive between control and treatment groups (Fig.3.2.1.4 C).

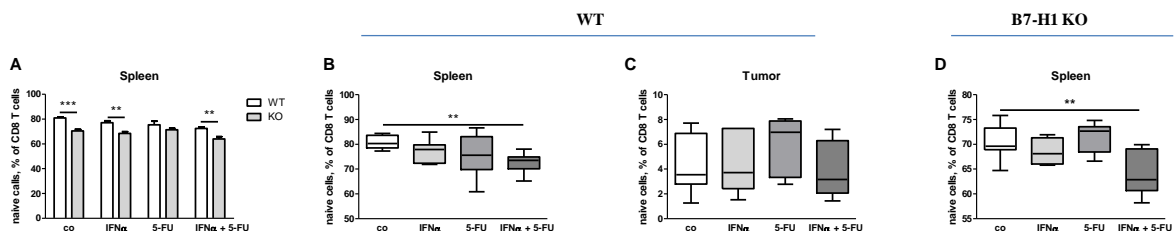


**Fig.3.2.1.4 Quantification of naïve CD8<sup>+</sup> T cells in spleens and tumors from tumor-bearing WT and B7-H1 KO mice with and without treatment (co).**

Mice were treated with IFN $\alpha$ , 5-FU or the combination of IFN $\alpha$ +5-FU on Day 5, 7 and 9 after Panc02 implantation. Untreated mice were used as the control. Four weeks after surgery, the mice were killed and the organs were eviscerated. Single-cell suspensions of spleens and tumors were stained with fluorescence labeled specific antibodies. The frequency of naïve CD8<sup>+</sup> T cells was analyzed by flow cytometry. Data from four independent experiments are presented as column bar graphs and box plots with SEM ((spleens: n = 9 for co, and n = 6 for IFN $\alpha$ ; 5-FU; IFN $\alpha$ +5-FU; tumors: n = 7 for co, n = 4-6 for IFN $\alpha$ ; 5-FU; IFN $\alpha$ +5-FU);\*\*p<0.01, \*\*\*p<0.001; control group vs. treatment groups; two-way (A) and one-way (B,C,D) ANOVA)

Considering the Teff population of CD8<sup>+</sup> T cells in spleens, in all four groups significantly increased WT frequencies of Teff were found in the groups of B7-H1 KO mice compared to groups of WT mice (Fig.3.2.1.5 A).

## Results

By looking at CD8<sup>+</sup> Teff of spleens in WT mice in detail, significantly lower frequencies were determined for the groups of IFN $\alpha$ ,5-FU and IFN $\alpha$ +5-FU in comparison to the control (Fig.3.2.1.5 B). In the spleens of B7-H1 KO tumor-bearing mice, no significant differences in the ratio of Teff were recognized between the control and the treatment groups (Fig.3.2.1.5 D).

The analysis of tumors of WT mice revealed significantly lower percentages of Teff in the groups of IFN $\alpha$  and IFN $\alpha$ +5-FU compared to the control (Fig.3.2.1.5.C).

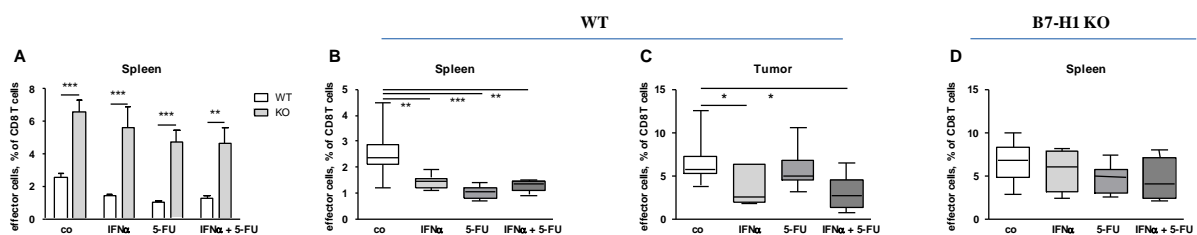


**Fig.3.2.1.5 Quantification of effector CD8<sup>+</sup> T cells in spleens and tumors from tumor-bearing WT and B7-H1 KO mice with and without treatment (co).**

Mice were treated with IFN $\alpha$ , 5-FU or the combination of IFN $\alpha$ +5-FU on Day 5, 7 and 9 after Panc02 implantation. Untreated mice were used as control. Four weeks after surgery, the mice were killed and the organs were eviscerated. Single-cell suspensions of spleens and tumors were stained with fluorescence labeled specific antibodies. The frequency of effector CD8<sup>+</sup> T cells was analyzed by flow cytometry. Data from four independent experiments are presented as column bar graphs and box plots with SEM ((spleens: n = 9 for co, and n = 6 for IFN $\alpha$ ; 5-FU; IFN $\alpha$ +5-FU; tumors: n = 7 for co, n = 4-6 for IFN $\alpha$ ; 5-FU; IFN $\alpha$ +5-FU); \*p<0.05, \*\*p<0.01, \*\*\*p<0.001; control group vs. treatment groups; two-way (A) and one-way (B,C,D) ANOVA)

The proportion of CD69<sup>+</sup> Teff was significantly higher in all four groups of B7-H1 KO spleens compared to WT spleens (Fig.3.2.1.6 A). As one can see in Fig.3.2.1.6 B, in WT spleens we found that all treatment groups achieved significantly higher frequencies of CD69<sup>+</sup> cells as compared to the control. In spleens of B7-H1 KO tumor bearing mice, a significant increase in the percentage of CD69<sup>+</sup> Teff was seen between the control and the IFN $\alpha$ +5-FU treatment group (Fig.3.2.1.6 D).

## Results

In the analysis of the tumors of WT mice, it was observed that the treatment group of IFN $\alpha$  has significantly less CD69<sup>+</sup> Teff compared to the control group (Fig.3.2.1.6 C).

The measured MFI of CD69 expression on Teff showed significantly higher values in WT spleens in all four groups compared to the same B7-H1 KO groups (Fig.3.2.1.6 E). No significant changes in CD69 MFI were observed when comparing the control to treatment groups of either WT or B7-H1 KO tumor-bearing mice separately (Fig.3.2.1.6 F,H).

In tumors of WT mice, no significant differences in the MFI of CD69 were seen between the control and treatment groups (Fig.3.2.1.6 G).

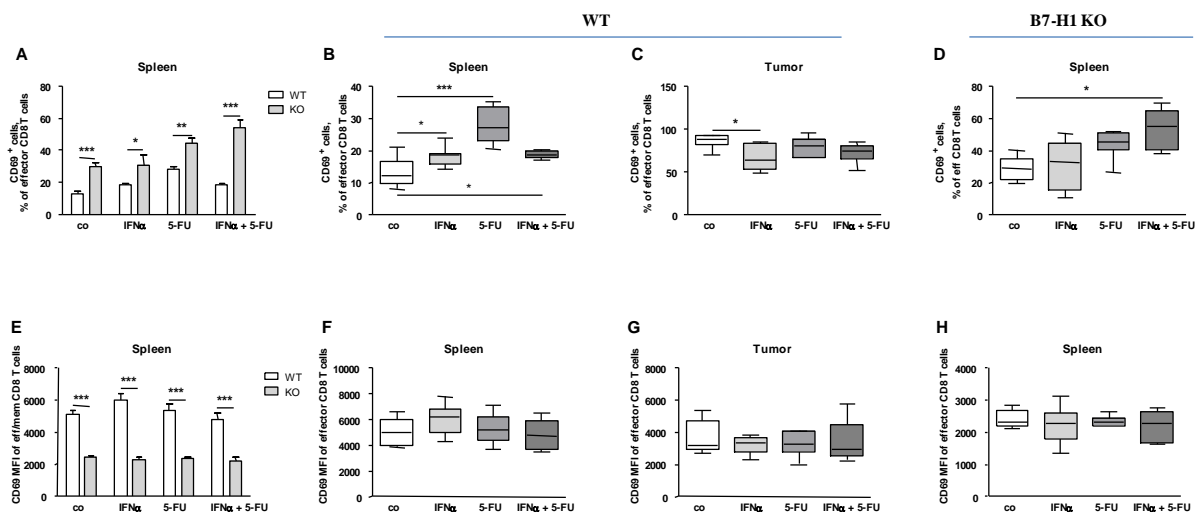


**Fig.3.2.1.6 Quantification of CD69 expression on effector CD8<sup>+</sup> T cells in spleens and tumors from tumor-bearing WT and B7-H1 KO mice with and without treatment (co).**

Mice were treated with IFN $\alpha$ , 5-FU or the combination of IFN $\alpha$ +5-FU on Day 5, 7 and 9 after Panc02 implantation. Untreated mice were used as control. Four weeks after surgery, the mice were killed and the organs were eviscerated. Single-cell suspensions of spleens and tumors were stained with fluorescence labeled specific antibodies. The frequency of CD69<sup>+</sup> CD8<sup>+</sup> effector T cells together with the MFI of CD69 was analyzed by flow cytometry. Data from four independent experiments are presented as column bar graphs and box plots with SEM ((spleens: n = 9 for co, and n = 6 for IFN $\alpha$ ; 5-FU; IFN $\alpha$ +5-FU; tumors: n = 7 for co, n = 4-6 for IFN $\alpha$ ; 5-FU; IFN $\alpha$ +5-FU); \*p<0.05, \*\*p<0.01, \*\*\*p<0.001; control group vs. treatment groups; two-way (A,E) and one-way (B,C,D,F,G,H) ANOVA)

## Results

The analysis of the frequency of Tem out of all CD8<sup>+</sup> T cells in spleens revealed highly significant greater percentages in all groups of B7-H1 KO mice compared to the ones of WT tumor-bearing mice (Fig.3.2.1.7 A). In WT spleens, IFN $\alpha$ +5-FU treatment induced significantly higher frequencies of Tem compared to the control (Fig.3.2.1.7 B). Whereas in groups of B7-H1 KO, no significant difference in frequencies of Tem was seen between the therapies and the control (Fig.3.2.1.7 D).

For the Tem, out of all CD8<sup>+</sup> T cells in WT tumors, we found a significant increase in percentages in the IFN $\alpha$ +5-FU treated WT mice compared to the control mice (Fig.3.2.1.7 C).

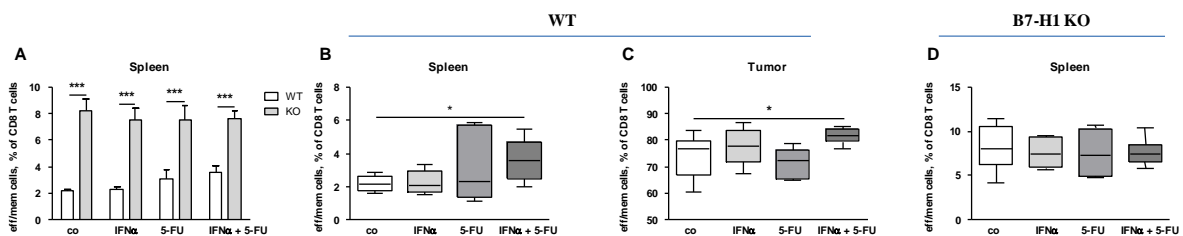


**Fig.3.2.1.7 Quantification of effector memory CD8<sup>+</sup> T cells in spleens and tumors from tumor-bearing WT and B7-H1 KO mice with and without treatment (co).**

Mice were treated with IFN $\alpha$ , 5-FU or the combination of IFN $\alpha$ +5-FU on Day 5, 7 and 9 after Panc02 implantation. Untreated mice were used as control. Four weeks after surgery, the mice were killed and the organs were eviscerated. Single-cell suspensions of spleens and tumors were stained with fluorescence labeled specific antibodies. The frequency of effector memory CD8<sup>+</sup> T cells was analyzed by flow cytometry. Data from four independent experiments are presented as column bar graphs and box plots with SEM ((spleens: n = 9 for co, and 3 n = 6 for IFN $\alpha$ ; 5-FU; IFN $\alpha$ +5-FU; tumors: n = 7 for co, n = 4-6 for IFN $\alpha$ ; 5-FU; IFN $\alpha$ +5-FU); \*p<0.05,\*\*\*p<0.001; control group vs. treatment groups; two-way (A) and one-way (B,C,D) ANOVA)

When analyzing the frequency of CD69<sup>+</sup> cells, out of all the CD8<sup>+</sup> Tem in the spleens of WT and B7-H1 KO tumor-bearing mice, significantly lower percentages were seen in B7-H1 KO spleens in the control and 5-FU treatment groups compared to those groups of WT mice. In IFN $\alpha$  and IFN $\alpha$ +5-FU treatment groups, no significant difference was observed between WT and B7-H1 KO mice (Fig.3.2.1.8 A).

The analysis of either WT or B7-H1 KO spleens showed no significant increases or decreases in percentages between control and treatment groups in both mouse strains, WT and B7-H1 KO (Fig.3.2.1.8 B,D).

Between treatment groups and the control of WT tumors, no significant difference in the frequency of CD69<sup>+</sup> Tem was determined (Fig.3.2.1.8 C).

As we looked at the values of CD69 MFI of CD8<sup>+</sup> Tem in spleens, lower values were determined for the groups of B7-H1 KO compared to WT tumor-bearing mice. For IFN $\alpha$ , 5-FU and IFN $\alpha$ +5-FU treatments, this result was statistically significant, whereas the comparison between the controls of WT and B7-H1 KO tumor-bearing mice showed a tendency towards lower values (Fig.3.2.1.8 E). In WT mice, the comparison between control and treatment groups revealed no significant difference in CD69 MFI (Fig.3.2.1.8 F). In B7-H1 KO groups, the difference in CD69 MFI between the treatment groups and the control was of no significance (Fig.3.2.1.8 H).

Analyzing WT tumors, no significant difference in the values of CD69 MFI of CD8<sup>+</sup> Tem was seen between the control and treatment groups (Fig.3.2.1.8 G).

## Results

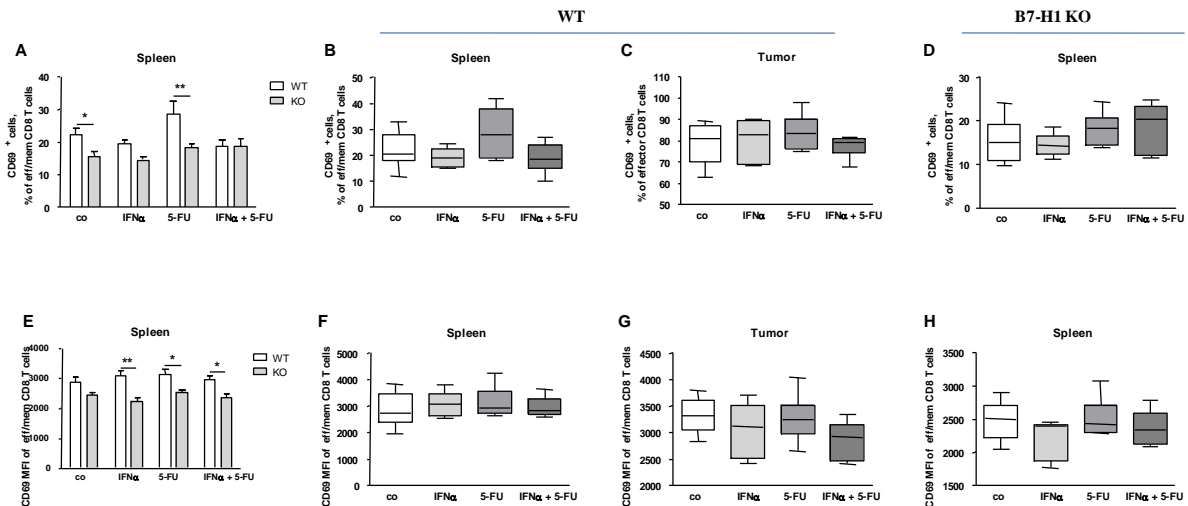


**Fig.3.2.1.8 Quantification of CD69 expression on effector memory CD8<sup>+</sup> T cells in spleens and tumors from tumor-bearing WT and B7-H1 KO mice with and without treatment (co).**

Mice were treated with IFN $\alpha$ , 5-FU or the combination of IFN $\alpha$ +5-FU on Day 5, 7 and 9 after Panc02 implantation. Untreated mice were used as control. Four weeks after surgery, the mice were killed and the organs were eviscerated. Single-cell suspensions of spleens and tumors were stained with fluorescence labeled specific antibodies. The frequency of CD69<sup>+</sup> effector memory CD8<sup>+</sup> T cells together with the MFI of CD69 was analyzed by flow cytometry. Data from four independent experiments are presented as column bar graphs and box plots with SEM ((spleens: n = 9 for co, and n = 6 for IFN $\alpha$ ; 5-FU; IFN $\alpha$ +5-FU; tumors: n = 7 for co, n = 4-6 for IFN $\alpha$ ; 5-FU; IFN $\alpha$ +5-FU); \*p<0.05, \*\*p<0.01; control group vs. treatment groups; two-way (A,E) and one-way (B,C,D,F,G,H) ANOVA)

Analyzing the cell fraction of Tcm out of CD8<sup>+</sup> T cells, no significant difference was seen between WT and B7-H1 KO spleens throughout all four groups (Fig.3.2.1.9 A). In spleens of WT tumor-bearing mice, a significant increase of Tcm frequencies was registered in the groups of IFN $\alpha$  and IFN $\alpha$ +5-FU treatment compared to the control (Fig.3.2.1.9 B). In the B7-H1 KO spleens, a significant increase in the frequency of Tcm was detected after treatment with IFN $\alpha$ +5-FU compared to the control (Fig.3.2.1.9 D).

The analysis of Tcm in WT tumors showed significantly higher percentages of Tcm in the treatment group of 5-FU compared to the control group (Fig.3.2.1.9 C).

## Results

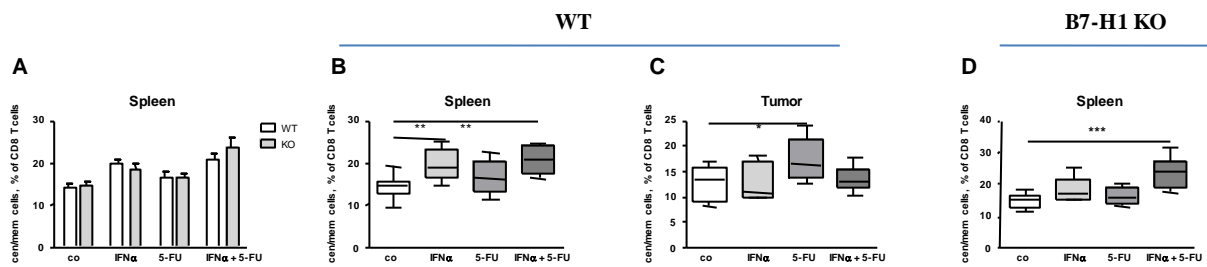


**Fig.3.2.1.9 Quantification of central memory CD8<sup>+</sup> T cells in spleens and tumors from tumor-bearing WT and B7-H1 KO mice with and without treatment (co).**

Mice were treated with IFN $\alpha$ , 5-FU or the combination of IFN $\alpha$ +5-FU on Day 5, 7 and 9 after Panc02 implantation. Untreated mice were used as control. Four weeks after surgery, the mice were killed and the organs were eviscerated. Single-cell suspensions of spleens and tumors were stained with fluorescence labeled specific antibodies. The frequency of central memory CD8<sup>+</sup> T cells was analyzed by flow cytometry. Data from four independent experiments are presented as column bar graphs and box plots with SEM ((spleens: n = 9 for co, and n = 6 for IFN $\alpha$ ; 5-FU; IFN $\alpha$ +5-FU; tumors: n = 7 for co, n = 4-6 for IFN $\alpha$ ; 5-FU; IFN $\alpha$ +5-FU); \*p<0.05, \*\*p<0.01, \*\*\*p<0.001; control group vs. treatment groups; two-way (A) and one-way (B,C,D) ANOVA)

Examining the activation status of CD8<sup>+</sup> Tcm, a tendency towards lower percentages of CD69<sup>+</sup>CD8<sup>+</sup> Tcm was recorded in B7-H1 KO mice compared to WT mice throughout all groups (Fig.3.2.1.10 A). When analyzing the spleens of WT and B7-H1 KO tumor-bearing mice in detail, no significant change in percentages in CD69<sup>+</sup>CD8<sup>+</sup> Tcm was observed between the control and the treatment groups, neither in spleens of WT mice nor the B7-H1 KO mice (Fig.3.2.1.10 B,D).

Tumors of WT mice showed an increase in activated Tcm in the group of 5-FU treatment compared to the control recorded by the increase of CD69<sup>+</sup> cells (Fig.3.2.1.10 C).

The analysis of CD69 MFI of CD8<sup>+</sup> Tcm revealed similar values in groups of WT and B7-H1 KO spleens (Fig.3.2.1.10 E). The comparison between control and treatment groups of either WT and B7-H1 KO spleens demonstrated no significant difference in the MFI of CD69 (Fig.3.2.1.10 F,H).

For the MFI of CD69 on Tcm in WT tumors, we determined no significant difference in values between the control and treatment groups (Fig.3.2.1.10 G).

## Results

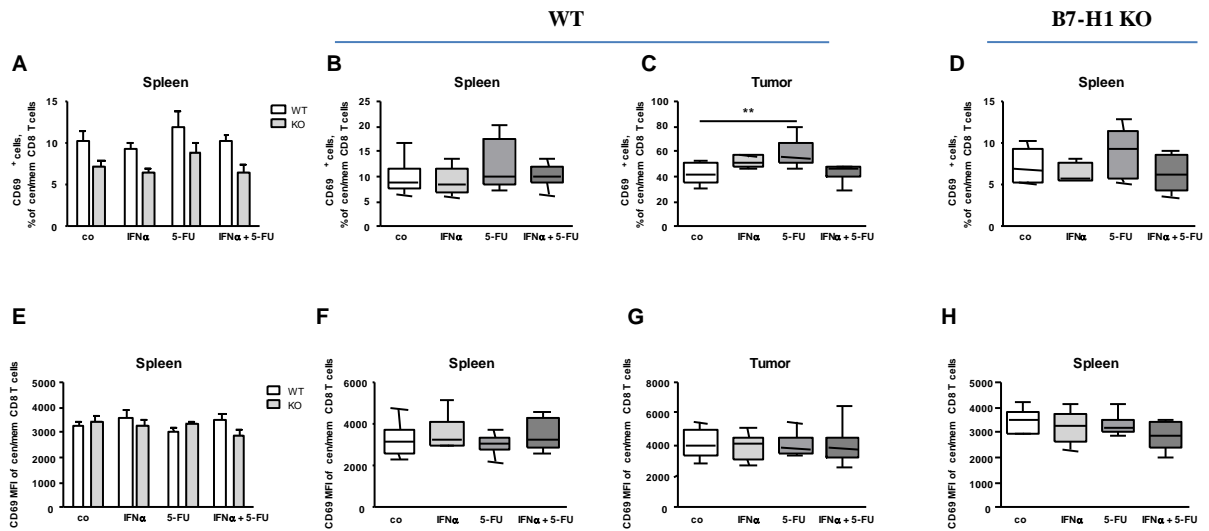


**Fig.3.2.1.10 Quantification of CD69 expression on central memory CD8<sup>+</sup> T cells in spleens and tumors from tumor-bearing WT and B7-H1 KO mice with and without treatment (co).**

Mice were treated with IFN $\alpha$ , 5-FU or the combination of IFN $\alpha$ +5-FU on Day 5, 7 and 9 after Panc02 implantation. Untreated mice were used as control. Four weeks after surgery, the mice were killed and the organs were eviscerated. Single-cell suspensions of spleens and tumors were stained with fluorescence labeled specific antibodies. The frequency of CD69<sup>+</sup> central memory CD8<sup>+</sup> T cells together with the MFI of CD69 was analyzed by flow cytometry. Data from four independent experiments are presented as column bar graphs and box plots with SEM ((spleens: n = 9 for co, and n = 6 for IFN $\alpha$ ; 5-FU; IFN $\alpha$ +5-FU; tumors: n = 7 for co, n = 4-6 for IFN $\alpha$ ; 5-FU; IFN $\alpha$ +5-FU); \*\*p<0.01; control group vs. treatment groups; two-way (A,E) and one-way (B,C,D,F,G,H) ANOVA)

After we finished the analysis of CD8<sup>+</sup> cells and their subsets, we followed the same procedure to analyze the CD4<sup>+</sup> T cells as well as their activation status and subsets. The gating strategy is shown above in Fig.3.2.1.1. First, we investigated the percentages of CD4<sup>+</sup> T cells out of CD3<sup>+</sup> lymphocytes in spleens. No significant difference in the ratio of CD4<sup>+</sup> T cells was seen between the groups of WT and B7-H1 KO spleens (Fig.3.2.1.11 A). In the WT and B7-H1 KO groups on their own, no significant change in frequencies was found in both mouse strains between the single treatments compared to the controls (Fig.3.2.1.11 B,D).

For the tumors of WT mice, we determined significantly lower percentages of CD4<sup>+</sup> T cells for the group of IFN $\alpha$  treatment compared to control (Fig.3.2.1.11 C).

## Results

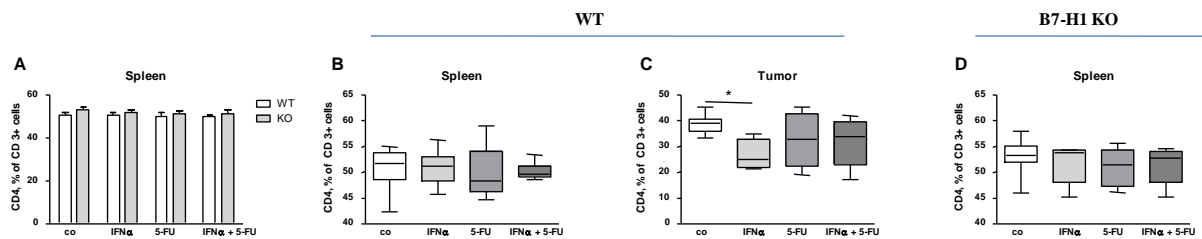


**Fig.3.2.1.11 Quantification of CD4<sup>+</sup> T cells in spleens and tumors from tumor-bearing WT and B7-H1 KO mice with and without treatment (co).**

Mice were treated with IFN $\alpha$ , 5-FU or the combination of IFN $\alpha$ +5-FU on Day 5, 7 and 9 after Panc02 implantation. Untreated mice were used as control. Four weeks after surgery, the mice were killed and the organs were eviscerated. Single-cell suspensions of spleens and tumors were stained with fluorescence labeled specific antibodies. The frequency of CD4<sup>+</sup> T cells was analyzed by flow cytometry. Data from four independent experiments are presented as column bar graphs and box plots with SEM ((spleens: n = 9 for co, and n = 6 for IFN $\alpha$ ; 5-FU; IFN $\alpha$ +5-FU; tumors: n = 7 for co, n = 4-6 for IFN $\alpha$ ; 5-FU; IFN $\alpha$ +5-FU); \*p<0.05; control group vs. treatment groups; two-way (A) and one-way (B,C,D) ANOVA)

Analysis of the activation status of the CD4<sup>+</sup> T cell population revealed no significant difference in the ratio of CD69<sup>+</sup> cells between groups of WT and B7-H1 KO spleens (Fig.3.2.1.12 A). When analyzing the single treatments compared to the control, in both WT and B7-H1 KO splenocytes no significant difference in the ratio of CD69<sup>+</sup> cells was seen (Fig.3.2.1.12 B,D).

The percentage of CD69<sup>+</sup> cells out of CD4<sup>+</sup> T cells in tumors of WT mice was not significantly different between the control and the single treatments (Fig.3.2.1.12 C).

For the MFI of CD69, no significant difference in values was found between the subgroups of WT and B7-H1 KO spleens (Fig.3.2.1.12 E). Furthermore, between the control and treatments of either WT or B7-H1 KO spleens, no significant difference in CD69 MFI was determined (Fig.3.2.1.12 F,H).

For WT tumors, no significant difference between the control and treatment group was measured determining the CD69 MFI of CD4<sup>+</sup> T cells (Fig.3.2.1.12 G).

## Results

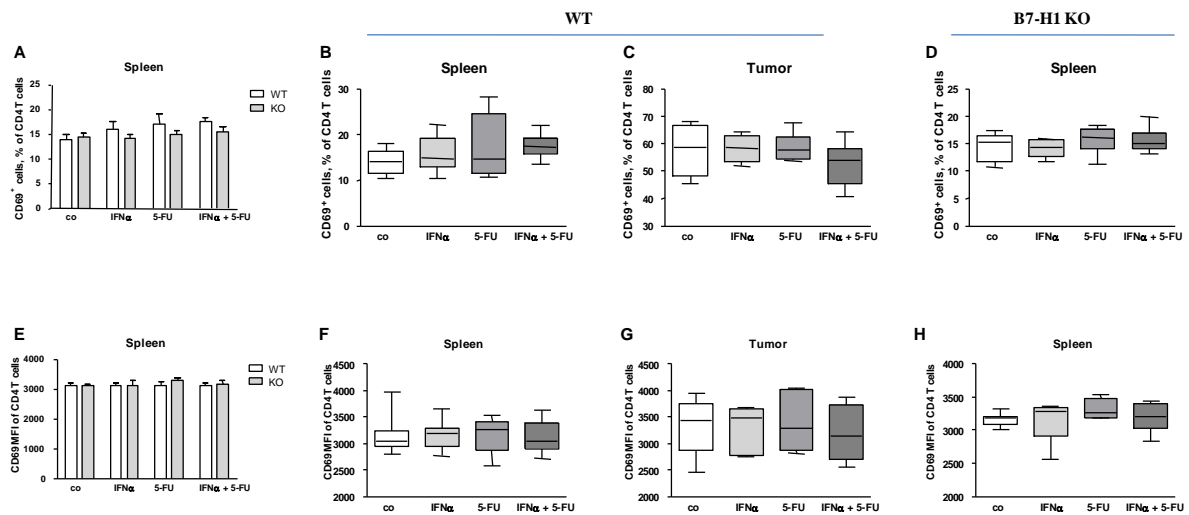


**Fig.3.2.1.12 Quantification of CD69 expression on CD4<sup>+</sup> T cells in spleens and tumors from tumor-bearing WT and B7-H1 KO mice with and without treatment (co).**

Mice were treated with IFN $\alpha$ , 5-FU or the combination of IFN $\alpha$ +5-FU on Day 5, 7 and 9 after Panc02 implantation. Untreated mice were used as control. Four weeks after surgery, the mice were killed and the organs were eviscerated. Single-cell suspensions of spleens and tumors were stained with fluorescence labeled specific antibodies. The frequency of CD69<sup>+</sup> CD4<sup>+</sup> T cells together with the MFI of CD69 was analyzed by flow cytometry. Data from four independent experiments are presented as column bar graphs and box plots with SEM ((spleens: n = 9 for co, and n = 6 for IFN $\alpha$ ; 5-FU; IFN $\alpha$ +5-FU; tumors: n = 7 for co, n = 4-6 for IFN $\alpha$ ; 5-FU; IFN $\alpha$ +5-FU); control group vs. treatment groups; two-way (A,E) and one-way (B,C,D,F,G,H) ANOVA)

In the analysis of Tnaive out of CD4<sup>+</sup> T cells in spleens, significantly higher frequencies were seen in the group of controls in WT compared to B7-H1 KO tumor-bearing mice. The comparison of the treatment groups between WT and B7-H1 KO spleens indicated no significant difference (Fig.3.2.1.13 A). Looking at the single treatment groups in spleens of WT mice, significantly lower percentages of Tnaive were measured between control and 5-FU treatment and even lower for IFN $\alpha$ +5-FU treatment (Fig.3.2.1.13 B). In the spleens of B7-H1 KO mice, significantly lower frequencies of CD4<sup>+</sup> Tnaive were registered in the groups of 5-FU and IFN $\alpha$ +5-FU treatment compared to control (Fig.3.2.1.13 D).

As one can see in the analysis of WT tumors, a significantly higher percentage of Tnaive was found in WT mice treated with IFN $\alpha$  compared to control (Fig.3.2.1.13 C).

## Results

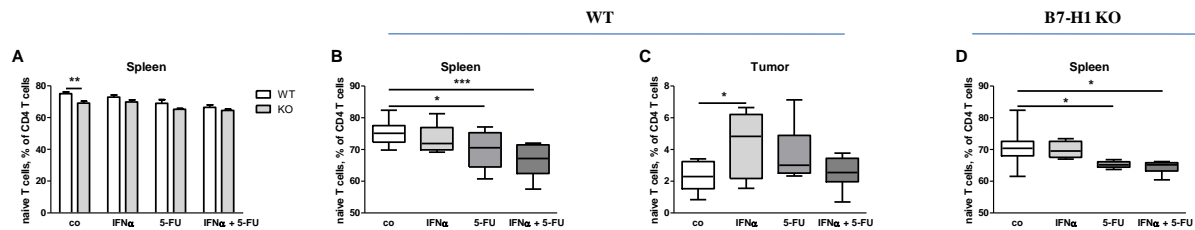


**Fig.3.2.1.13 Quantification of naïve CD4<sup>+</sup> T cells in spleens and tumors from tumor-bearing WT and B7-H1 KO mice with and without treatment (co).**

Mice were treated with IFN $\alpha$ , 5-FU or the combination of IFN $\alpha$ +5-FU on Day 5, 7 and 9 after Panc02 implantation. Untreated mice were used as control. Four weeks after surgery, the mice were killed and the organs were eviscerated. Single-cell suspensions of spleens and tumors were stained with fluorescence labeled specific antibodies. The frequency of naïve CD4<sup>+</sup> T cells was analyzed by flow cytometry. Data from four independent experiments are presented as column bar graphs and box plots with SEM ((spleens: n = 9 for co, and n = 6 for IFN $\alpha$ ; 5-FU; IFN $\alpha$ +5-FU; tumors: n = 7 for co, n = 4-6 for IFN $\alpha$ ; 5-FU; IFN $\alpha$ +5-FU); \*p<0.05, \*\*p<0.01, \*\*\*p<0.001; control group vs. treatment groups; two-way (A) and one-way (B,C,D) ANOVA)

The analysis of Teff out of CD4<sup>+</sup> T cells demonstrated a significant difference between the controls of WT and B7-H1 KO spleens, with higher percentages of CD4<sup>+</sup> Teff in the B7-H1 KO group (Fig.3.2.1.14 A). Between the single treatments and the control of WT spleens, frequencies of Teff were similar to each other (Fig.3.2.1.14 B). When comparing the treatment groups of B7-H1 KO spleens to the control, a significant increase in percentage of Teff was found after therapy with IFN $\alpha$  and IFN $\alpha$ +5-FU (Fig.3.2.1.14 D).

By taking a closer look at the tumors of WT mice, we have seen significantly higher ratios of Teff in the group of 5-FU treatment compared to control (Fig.3.2.1.14 C).

## Results

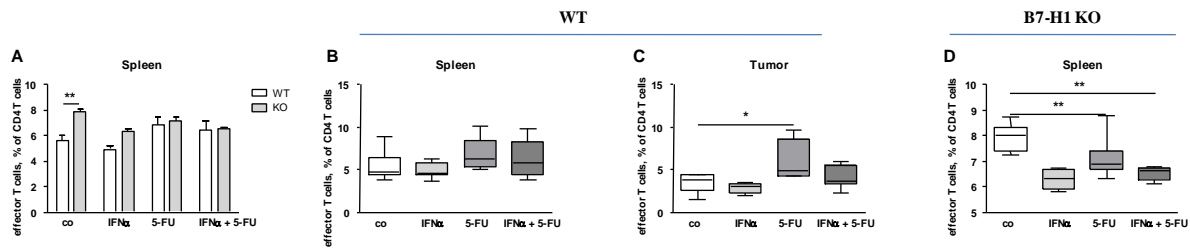


**Fig.3.2.1.14 Quantification of effector CD4<sup>+</sup> T cells in spleens and tumors from tumor-bearing WT and B7-H1 KO mice with and without treatment (co).**

Mice were treated with IFN $\alpha$ , 5-FU or the combination of IFN $\alpha$ +5-FU on Day 5, 7 and 9 after Panc02 implantation. Untreated mice were used as control. Four weeks after surgery, the mice were killed and the organs were eviscerated. Single-cell suspensions of spleens and tumors were stained with fluorescence labeled specific antibodies. The frequency of effector CD4<sup>+</sup> T cells was analyzed by flow cytometry. Data from four independent experiments are presented as column bar graphs and box plots with SEM ((spleens: n = 9 for co, and n = 6 for IFN $\alpha$ ; 5-FU; IFN $\alpha$ +5-FU; tumors: n = 7 for co, n = 4-6 for IFN $\alpha$ ; 5-FU; IFN $\alpha$ +5-FU); \*p<0.05, \*\*p<0.01; control group vs. treatment groups; two-way (A) and one-way (B,C,D) ANOVA)

The activation status of CD4<sup>+</sup> Teff, investigated by measuring of CD69 expression, was not significantly different between WT and B7-H1 KO spleens throughout all four groups (Fig.3.2.1.15 A). The analysis of both the WT and B7-H1 KO spleens revealed no significant difference between controls and treatment groups (Fig.3.2.1.15 B,D).

Furthermore, in tumors of WT mice, no significant difference in the percentages of Teff was found between treated mice and the control group (Fig.3.2.1.15 C).

The measurements of the CD69 MFI of CD4<sup>+</sup> Teff in spleens showed no significant difference between WT and B7-H1 KO spleens in all four groups (Fig.3.2.1.15 E). When looking at WT and B7-H1 KO groups in more detail, no significant difference in CD69 MFI was found between control and treatment groups, in both the WT and B7-H1 KO spleens (Fig.3.2.1.15 F,H).

Nearly equal values of CD69 MFI of CD4<sup>+</sup> T cells were observed for the treatment groups of WT tumors compared to the control group (Fig.3.2.1.15 G).

## Results

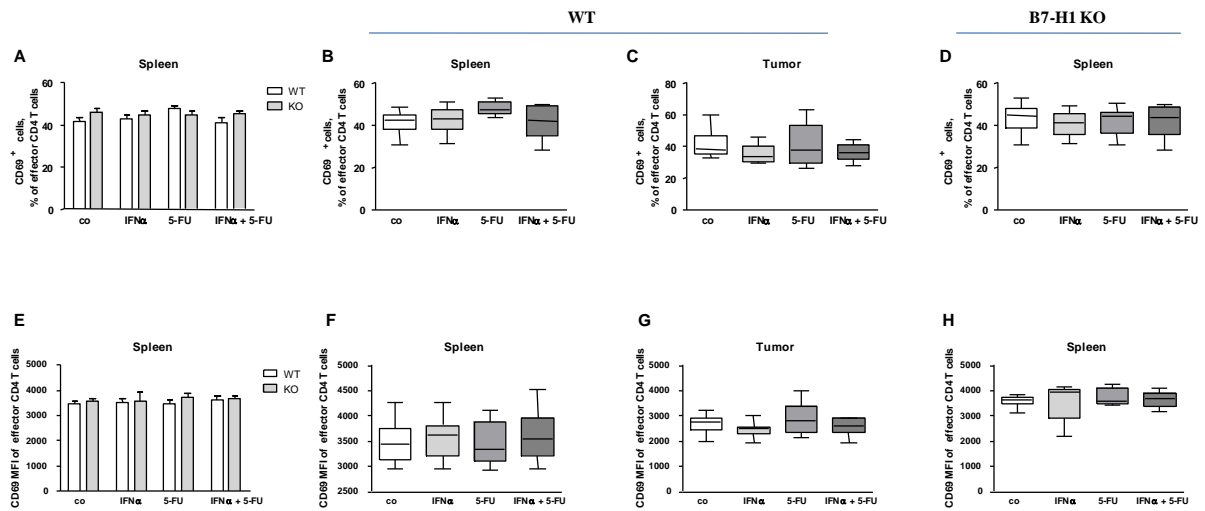


**Fig.3.2.1.15 Quantification of CD69 expression on effector CD4<sup>+</sup> T cells in spleens and tumors from tumor-bearing WT and B7-H1 KO mice with and without treatment (co).**

Mice were treated with IFN $\alpha$ , 5-FU or the combination of IFN $\alpha$ +5-FU on Day 5, 7 and 9 after Panc02 implantation. Untreated mice were used as control. Four weeks after surgery, the mice were killed and the organs were eviscerated. Single-cell suspensions of spleens and tumors were stained with fluorescence labeled specific antibodies. The frequency of CD69<sup>+</sup> effector CD4<sup>+</sup> T cells together with the MFI of CD69 was analyzed by flow cytometry. Data from four independent experiments are presented as column bar graphs and box plots with SEM ((spleens: n = 9 for co, and n = 6 for IFN $\alpha$ ; 5-FU; IFN $\alpha$ +5-FU; tumors: n = 7 for co, n = 4-6 for IFN $\alpha$ ; 5-FU; IFN $\alpha$ +5-FU); control group vs. treatment groups; two-way (A,E) and one-way (B,C,D,F,G,H) ANOVA)

Next, we examined the cell fraction of Tem out of CD4<sup>+</sup> T cells. Between WT and B7-H1 KO spleens, higher cell frequencies were found in the spleens of B7-H1 KO tumor-bearing mice in all four groups. For controls, IFN $\alpha$  and 5-FU treatments were used, whose result was of a statistical significance (Fig.3.2.1.16 A). In WT spleens, a significant increase in the frequency of Tem was found in the groups of 5-FU and IFN $\alpha$ +5-FU compared to the control (Fig.3.2.1.16 B). In spleens of B7-H1 KO tumor-bearing mice, a significant increase in Tem was observed in the group of IFN $\alpha$ +5-FU treatment compared to control (Fig.3.2.1.16 D).

When analyzing the tumors of WT mice, no significant difference in the frequency of Tem was seen between the control group and treatment groups (Fig.3.2.1.16 C).

## Results

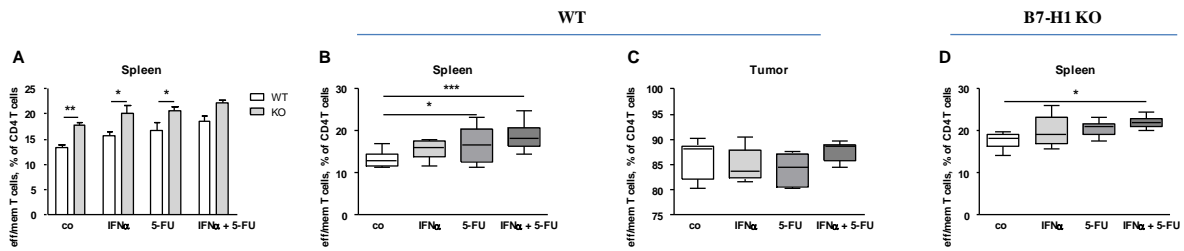


**Fig.3.2.1.16 Quantification of effector memory CD4<sup>+</sup> T cells in spleens and tumors from tumor-bearing WT and B7-H1 KO mice with and without treatment (co).**

Mice were treated with IFN $\alpha$ , 5-FU or the combination of IFN $\alpha$ +5-FU on Day 5, 7 and 9 after Panc02 implantation. Untreated mice were used as control. Four weeks after surgery, the mice were killed and the organs were eviscerated. Single-cell suspensions of spleens and tumors were stained with fluorescence labeled specific antibodies. The frequency of effector memory CD4<sup>+</sup> T cells was analyzed by flow cytometry. Data from four independent experiments are presented as column bar graphs and box plots with SEM ((spleens: n = 9 for co, and n = 6 for IFN $\alpha$ ; 5-FU; IFN $\alpha$ +5-FU; tumors: n = 7 for co, n = 4-6 for IFN $\alpha$ ; 5-FU; IFN $\alpha$ +5-FU); \*p<0.05, \*\*p<0.01, \*\*\*p<0.001; control group vs. treatment groups; two-way (A) and one-way (B,C,D) ANOVA)

Determining the expression of CD69 on Tem, a tendency towards lower ratios of CD69<sup>+</sup> Tem was found in the groups of B7-H1 KO spleens compared to WT groups. Between the groups of 5-FU treatments, this result was significant (Fig.3.2.1.17 A). When analyzing the treatments for the WT and B7-H1 KO groups on their own, the observed proportion of CD69<sup>+</sup> cells showed no significant difference between the treatments compared to controls, in the spleens of both the WT and B7-H1 KO tumor-bearing mice (Fig.3.2.1.17 B,D).

In the tumors of WT mice, no significant difference in the ratio of CD69<sup>+</sup> Tem was seen between the treatment groups and the control (Fig.3.2.17 C).

Afterwards, we took a closer look at the MFI of CD69 of Tem in the spleens of WT and B7-H1 KO tumor-bearing mice. No significant difference was seen in the comparison of WT and B7-H1 KO spleens to each other (Fig.3.2.1.17 E) as well as between the single groups compared to the control of either WT or B7-H1 KO spleens (Fig.3.2.1.17 F,H).

## Results

Analyzing the MFI of CD69 of Teff in WT tumors, no significant difference was observed between the control and the treatment groups (Fig.3.2.1.17 G).

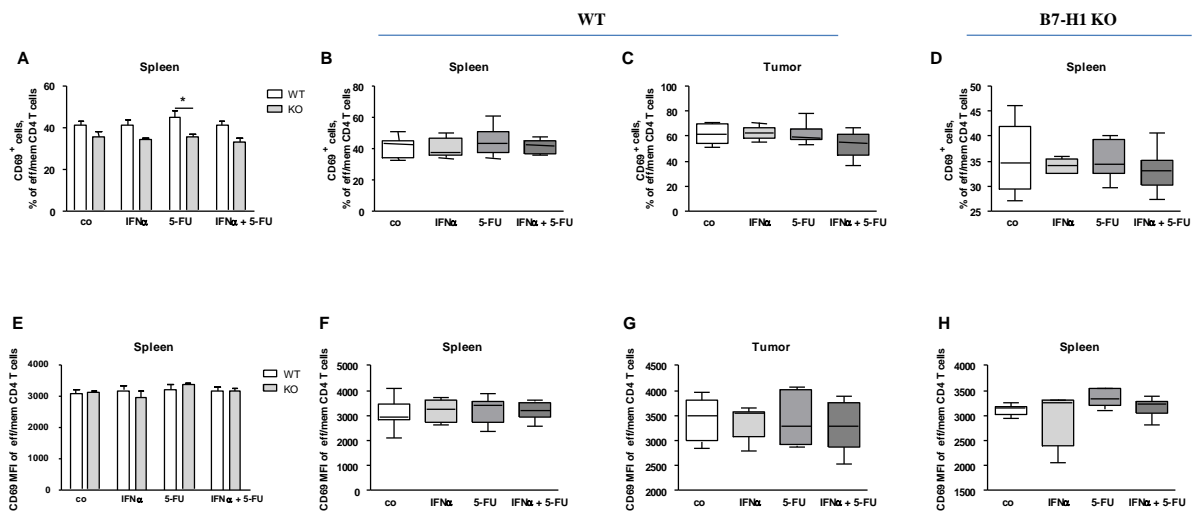


**Fig.3.2.1.17 Quantification of CD69 expression on effector memory CD4<sup>+</sup> T cells in spleens and tumors from tumor-bearing WT and B7-H1 KO mice with and without treatment (co).**

Mice were treated with IFN $\alpha$ , 5-FU or the combination of IFN $\alpha$ +5-FU on Day 5, 7 and 9 after Panc02 implantation. Untreated mice were used as control. Four weeks after surgery, the mice were killed and the organs were eviscerated. Single-cell suspensions of spleens and tumors were stained with fluorescence labeled specific antibodies. The frequency of CD69<sup>+</sup> effector memory CD4<sup>+</sup> T cells together with the MFI of CD69 was analyzed by flow cytometry. Data from four independent experiments are presented as column bar graphs and box plots with SEM ((spleens: n = 9 for co, and n = 6 for IFN $\alpha$ ; 5-FU; IFN $\alpha$ +5-FU; tumors: n = 7 for co, n = 4-6 for IFN $\alpha$ ; 5-FU; IFN $\alpha$ +5-FU); \*p<0.05; control group vs. treatment groups; two-way (A,E) and one-way (B,C,D,F,G,H) ANOVA)

The analysis of Tcm out of CD4<sup>+</sup> T cells in spleens of tumor-bearing mice revealed highly significant differences between WT and B7-H1 KO spleens in all four groups, with higher percentages of CD4<sup>+</sup> Tcm in the B7-H1 KO groups compared to WT groups (Fig.3.2.1.18 A). In groups of WT spleens alone, significantly higher cell frequencies of Tcm were measured in the group of IFN $\alpha$ +5-FU treatment compared to the control (Fig.3.2.1.18 B). Between treatment groups and the control of B7-H1 KO spleens, no significant difference in Tcm percentages was seen (Fig.3.2.1.18 D).

## Results

By analyzing the tumors of WT mice, significantly higher percentages of CD4<sup>+</sup> Tcm were found in the group of IFN $\alpha$ +5-FU treated animals in comparison to control animals (Fig.3.2.1.18 C).

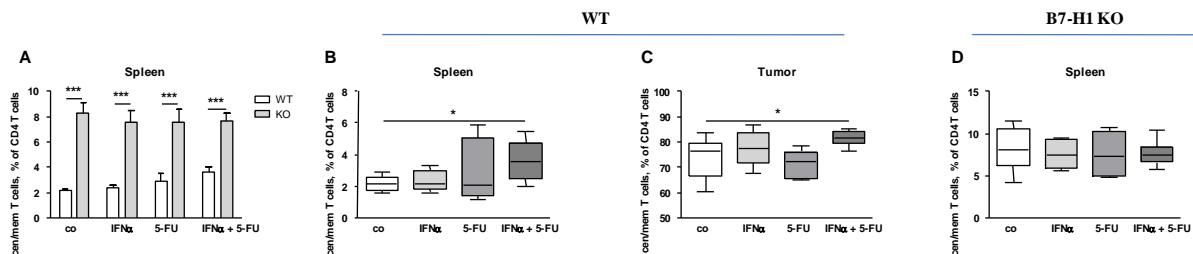


**Fig.3.2.1.18 Quantification of central memory CD4<sup>+</sup> T cells in spleens and tumors from tumor-bearing WT and B7-H1 KO mice with and without treatment (co).**

Mice were treated with IFN $\alpha$ , 5-FU or the combination of IFN $\alpha$ +5-FU on Day 5, 7 and 9 after Panc02 implantation. Untreated mice were used as control. Four weeks after surgery, the mice were killed and the organs were eviscerated. Single-cell suspensions of spleens and tumors were stained with fluorescence labeled specific antibodies. The frequency of central memory CD4<sup>+</sup> T cells was analyzed by flow cytometry. Data from four independent experiments are presented as column bar graphs and box plots with SEM ((spleens: n = 9 for co, and n = 6 for IFN $\alpha$ ; 5-FU; IFN $\alpha$ +5-FU; tumors: n = 7 for co, n = 4-6 for IFN $\alpha$ ; 5-FU; IFN $\alpha$ +5-FU); \*p<0.05,\*\*\*p<0.001; control group vs. treatment groups; two-way (A) and one-way (B,C,D) ANOVA)

When determining the activation status of CD4<sup>+</sup> Tcm, no significant difference in percentages of CD69<sup>+</sup> Tcm was found between the spleens of WT and B7-H1 KO tumor-bearing mice in all treatments and the control group. A tendency towards lower percentages was determined for the control and IFN $\alpha$  and 5-FU treatments in spleens of B7-H1 KO mice compared to the same groups of WT mice (Fig.3.2.1.19 A). When we looked at the single groups of either WT or B7-H1 KO, no significant difference in the ratio of Tcm was found between the treatments and the control, in the spleens of both WT and B7-H1 KO tumor-bearing mice (Fig.3.2.1.19 B,D).

The analysis of tumors of WT mice revealed no statistical difference in the frequency of Tcm between the treated and control mice (Fig.3.2.1.19 C).

## Results

In the analysis of the MFI of CD69 of Tcm, one can see significantly lower values measured in the groups of IFN $\alpha$ , 5-FU and IFN $\alpha$ +5-FU treatment for the spleens of B7-H1 KO mice compared to WT spleens (Fig.3.2.1.19 E). In comparison of the treatment groups to the control, the values were not of a significant difference, in both groups of WT and B7-H1 KO spleens (Fig.3.2.1.19 F,H).

Furthermore, no significant difference in the MFI of CD69 was observed in WT tumors between the control and treatment groups (Fig.3.2.1.19 G).

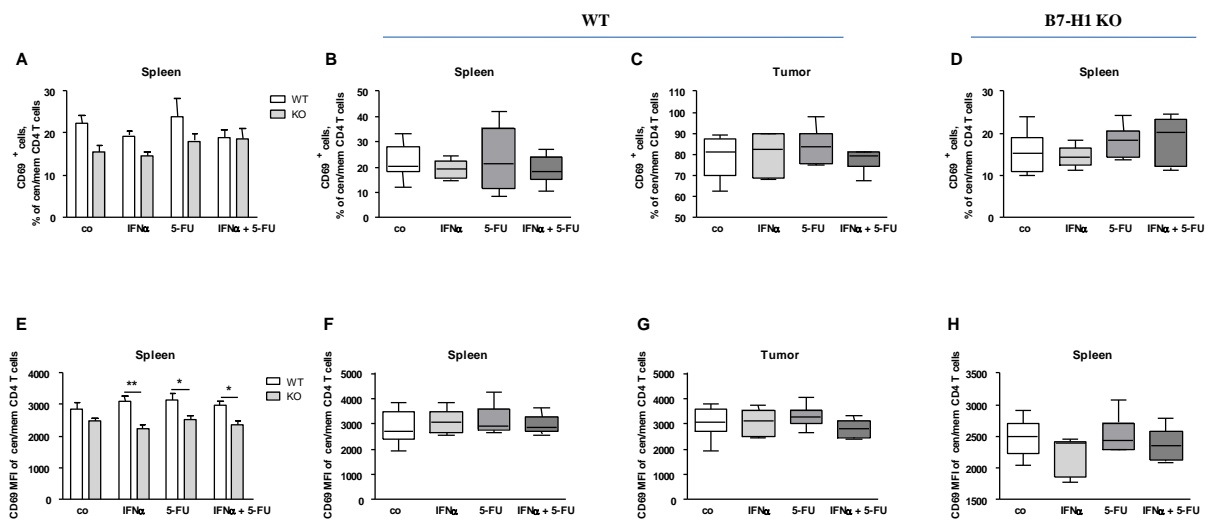


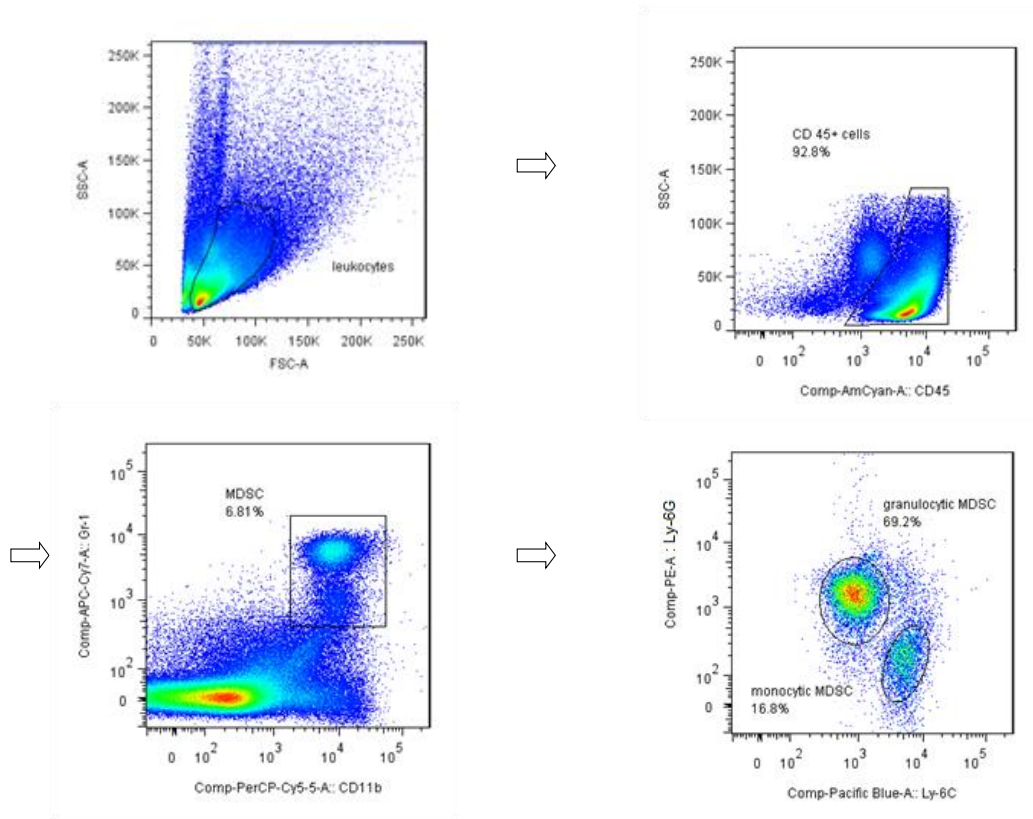
**Fig.3.2.1.19 Quantification of CD69 expression on central memory CD4<sup>+</sup> T cells in spleens and tumors from tumor-bearing WT and B7-H1 KO mice with and without treatment (co).**

Mice were treated with IFN $\alpha$ , 5-FU or the combination of IFN $\alpha$ +5-FU on Day 5, 7 and 9 after Panc02 implantation. Untreated mice were used as control. Four weeks after surgery, the mice were killed and the organs were eviscerated. Single-cell suspensions of spleens and tumors were stained with fluorescence labeled specific antibodies. The frequency of CD69<sup>+</sup> central memory CD4<sup>+</sup> T cells together with the MFI of CD69 was analyzed by flow cytometry. Data from four independent experiments are presented as column bar graphs and box plots with SEM ((spleens: n = 9 for co, and n = 6 for IFN $\alpha$ ; 5-FU; IFN $\alpha$ +5-FU; tumors: n = 7 for co, n = 4-6 for IFN $\alpha$ ; 5-FU; IFN $\alpha$ +5-FU); \*p<0.05, \*\*p<0.01; control group vs. treatment groups; two-way (A,E) and one-way (B,C,D,F,G,H) ANOVA)

Summarizing the data of CD4<sup>+</sup>/CD8<sup>+</sup> T cells, we observed higher frequencies of CD4<sup>+</sup>/CD8<sup>+</sup> Tem and Tcm in spleens of B7-H1 KO compared to those of WT tumor-bearing mice.

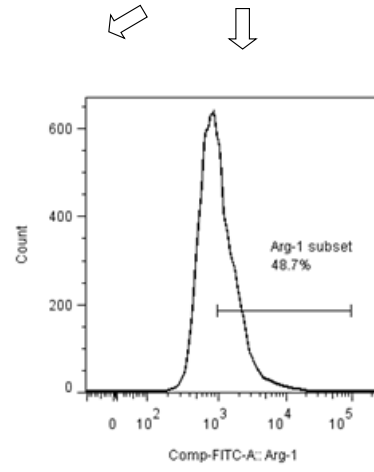
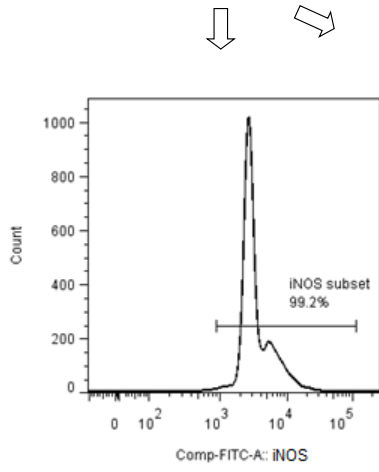
### 3.2.2 Analysis of Myeloid derived suppressor cells (MDSC)

Since the MDSC play an important role in the establishment and development of tumors, we wanted to know which impact the application of different therapies has on the constellation of these cells in presence and absence of B7-H1. In Fig.3.2.2.1, the gating strategy for MDSC is shown. The FACS data (dot-plot, histogram) represent one typical result out of four independent experiments.



# Results

---



and

## Results

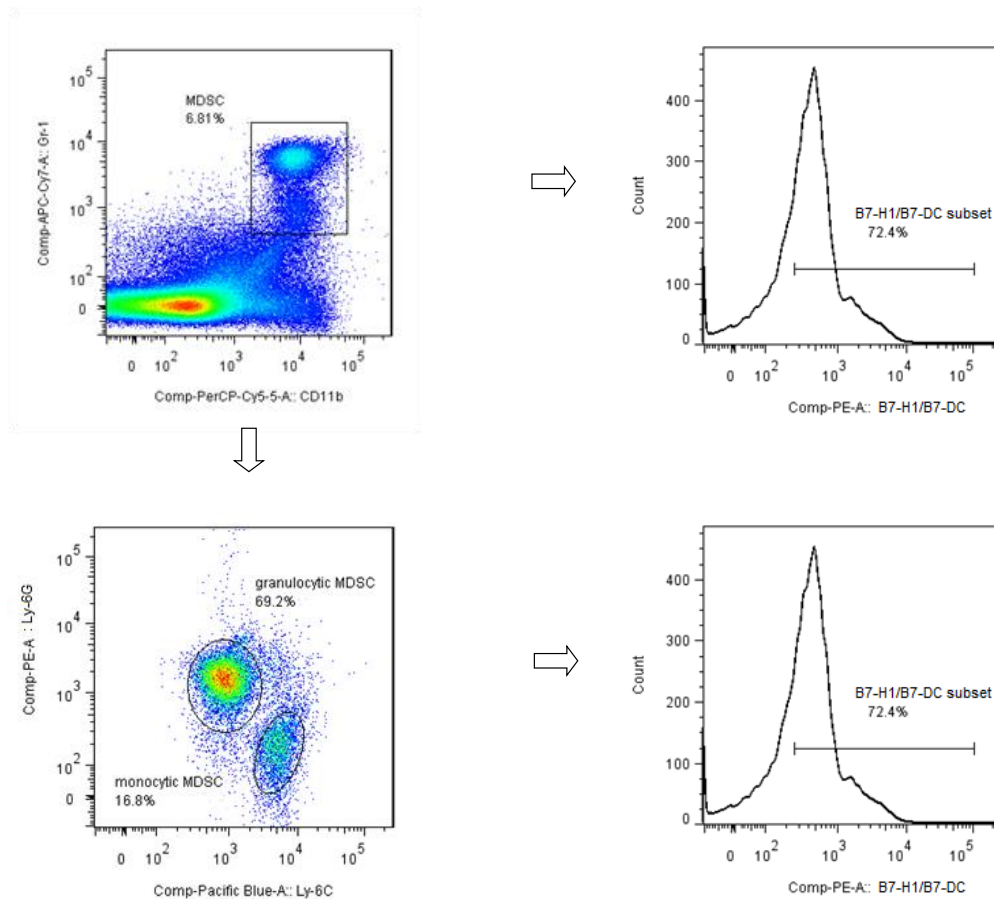


**Fig.3.2.2. 1 Gating strategy for Myeloid derived suppressor cells (MDSC) in spleens and tumors from tumor-bearing WT and B7-H1 KO mice using flow cytometry.**

First, lymphocytes were gated using FSC/SSC dot plot. Afterwards, we gated on CD45<sup>+</sup> cells, and out of this cell population, Gr-1<sup>+</sup>CD11b<sup>+</sup> MDSC were marked. The two subsets of MDSC, granulocytic and monocytic MDSC were gated according to the expression of Ly-6G and Ly-6C. For the functional status, the iNOS and Arginase subsets were determined from total MDSC as well as from both subsets using histograms. Furthermore, the expression of the B7-H1/B7-DC molecules was analyzed for all MDSC as well as for the two subsets using histograms. All positive gates were set according to FMO controls.

First, we determined the frequency of MDSC out of all leukocytes in spleens of WT and B7-H1 KO tumor-bearing mice. A tendency towards lower frequencies of MDSC for all treatment groups and the controls was determined in B7-H1 KO spleens compared to WT spleens. Between the groups of IFN $\alpha$ +5-FU treatment, this difference was statistically significant (Fig.3.2.2.2 A). In spleens of WT mice, no

significant difference between the treatment groups and control was observed (Fig.3.2.2.2 B). In contrast, in the spleens of B7-H1 KO mice, a significant increase in the percentage of MDSC was measured for IFN $\alpha$  and IFN $\alpha$ +5-FU treatment groups compared to control (Fig.3.2.2.2 D).

Furthermore, in the tumors of WT mice, a significantly higher percentage of MDSC was found after IFN $\alpha$ +5-FU treatment in comparison to the control (Fig.3.2.2.2 C).

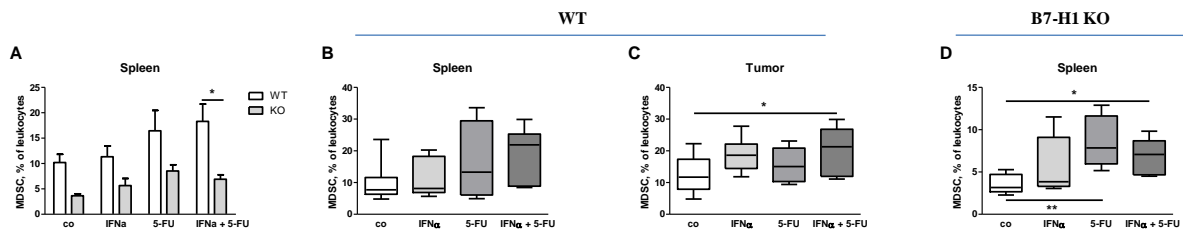


**Fig.3.2.2. 2 Quantification of MDSC in spleens and tumors from tumor-bearing WT and B7-H1 KO mice with and without treatment (co).**

Mice were treated with IFN $\alpha$ , 5-FU or the combination of IFN $\alpha$ +5-FU on Day 5, 7 and 9 after Panc02 implantation. Untreated mice were used as control. Four weeks after surgery, the mice were killed and the organs were eviscerated. Single-cell suspensions of spleens and tumors were stained with fluorescence labeled specific antibodies. The frequency of MDSC was analyzed by flow cytometry. Data from four independent experiments are presented as column bar graphs and box plots with SEM ((spleens: n = 9 for co, and n = 6 for IFN $\alpha$ ; 5-FU; IFN $\alpha$ +5-FU; tumors: n = 7 for co, n = 4-6 for IFN $\alpha$ ; 5-FU; IFN $\alpha$ +5-FU); \*p<0.05; control group vs. treatment groups; two-way (A) and one-way (B,C,D) ANOVA)

Afterwards, we examined the percentages of granulocytic MDSC (gMDSC) and monocytic MDSC (mMDSC) out of total MDSC in spleens of WT and B7-H1 KO mice. Between WT and B7-H1 KO spleens, a significantly higher percentage of gMDSC was found in the B7-H1 KO IFN $\alpha$  group compared to this group of WT spleens. For the other groups no significant difference was seen (Fig.3.2.2.3 A). By looking at the spleens in more detail, in the groups of WT spleens a significant decrease in frequency of gMDSC was seen in 5-FU treated animals compared to control animals

(Fig.3.2.2.3 B). In the B7-H1 KO spleens, an increase of gMDSC was observed in the group of IFN $\alpha$  treatment compared to the control group (Fig.3.2.2.3 D).

The analysis of tumors from WT mice showed no significant difference in the ratio of gMDSC between untreated and treated mice (Fig.3.2.2.3 C).

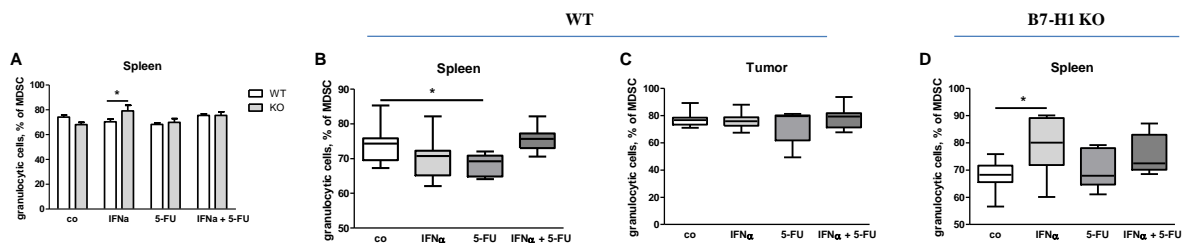


**Fig.3.2.2. 3 Quantification of gMDSC in spleens and tumors from tumor-bearing WT and B7-H1 KO mice with and without treatment (co).**

Mice were treated with IFN $\alpha$ , 5-FU or the combination of IFN $\alpha$ +5-FU on Day 5, 7 and 9 after Panc02 implantation. Untreated mice were used as control. Four weeks after surgery, the mice were killed and the organs were eviscerated. Single-cell suspensions of spleens and tumors were stained with fluorescence labeled specific antibodies. The frequency of gMDSC was analyzed by flow cytometry. Data from four independent experiments are presented as column bar graphs and box plots with SEM ((spleens: n = 9 for co, and n = 6 for IFN $\alpha$ ; 5-FU; IFN $\alpha$ +5-FU; tumors: n = 7 for co, n = 4-6 for IFN $\alpha$ ; 5-FU; IFN $\alpha$ +5-FU); \*p<0.05; control group vs. treatment groups; two-way (A) and one-way (B,C,D) ANOVA)

When assessing the monocytic MDSC subpopulation out of the total MDSC in spleens of WT and B7-H1 KO tumor-bearing mice, significantly decreased ratios of mMDSC were found in B7-H1 KO spleens in the group of IFN $\alpha$  treatment compared to the corresponding group of WT spleens (Fig.3.2.2.4 A). When comparing the single groups of WT spleens to each other, a significantly lower frequency of mMDSC was found in the group of IFN $\alpha$ +5-FU compared to the control group (Fig.3.2.2.4 B). In spleens of B7-H1 KO mice, significantly lower percentages of mMDSC were registered in the treatment groups of IFN $\alpha$ , 5-FU and IFN $\alpha$ +5-FU compared to control (Fig.3.2.2.4 D).

## Results

In the tumors of WT animals, no significant difference in the frequency of mMDSC was observed between control and the treatment groups (Fig.3.2.2.4 C).

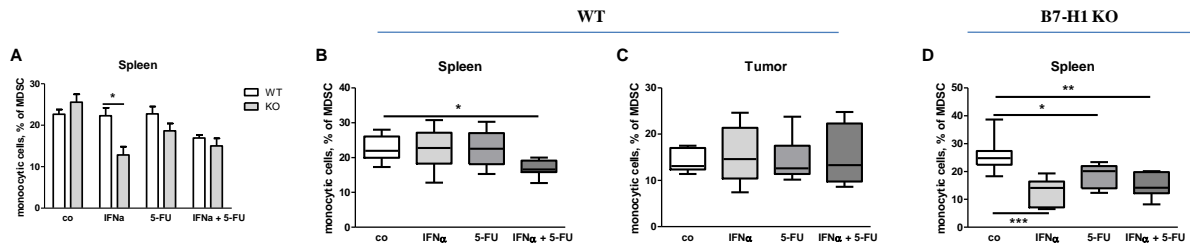


**Fig.3.2.2. 4 Quantification of mMDSC in spleens and tumors from tumor-bearing WT and B7-H1 KO mice with and without treatment (co).**

Mice were treated with IFN $\alpha$ , 5-FU or the combination of IFN $\alpha$ +5-FU on Day 5, 7 and 9 after Panc02 implantation. Untreated mice were used as control. Four weeks after surgery, the mice were killed and the organs were eviscerated. Single-cell suspensions of spleens and tumors were stained with fluorescence labeled specific antibodies. The frequency of mMDSC was analyzed by flow cytometry. Data from four independent experiments are presented as column bar graphs and box plots with SEM ((spleens: n = 9 for co, and n = 6 for IFN $\alpha$ ; 5-FU; IFN $\alpha$ +5-FU; tumors: n = 7 for co, n = 4-6 for IFN $\alpha$ ; 5-FU; IFN $\alpha$ +5-FU); \*p<0.05, \*\*p<0.01; control group vs. treatment groups; two-way (A) and one-way (B,C,D) ANOVA)

Furthermore, we analyzed the functional status of MDSC and their two subsets. Therefore, we examined the iNOS as well as the Arginase expression of these cell populations, starting with the analysis of iNOS production in total MDSC, gMDSC and mMDSC. In total MDSC, one can see similar iNOS levels between the subgroups of WT and B7-H1 KO spleens (Fig.3.2.2.5 A). In the analysis of the single groups of WT spleens, a significantly lower percentage of iNOS<sup>+</sup> cells was seen in the group of IFN $\alpha$ +5-FU treatment compared to the control (Fig.3.2.2.5 B). Between the single treatments and the control in B7-H1 KO spleens, no significant difference in the ratio of iNOS<sup>+</sup> MDSC was observed (Fig.3.2.2.5 D).

The comparison of treatment groups to the control of WT tumors showed no significant difference in iNOS<sup>+</sup> MDSC (Fig.3.2.2.5 C).

## Results

For the MFI of iNOS<sup>+</sup> MDSC, a significantly lower value was determined for the B7-H1 KO IFN $\alpha$  treatment group compared to the corresponding WT group. For the other groups, the MFI of iNOS<sup>+</sup> MDSC revealed a tendency towards lower values in groups of B7-H1 KO spleens compared to groups of WT spleens (Fig.3.2.2.5 E). No significant differences in the iNOS MFI were measured when we compared the treatment groups of either WT or B7-H1 KO spleens to the respective control group (Fig.3.2.2.5 F,H).

The comparison of treatment groups with the control in WT tumors revealed no significant difference in the values of iNOS MFI as seen in Fig.3.2.2.5 G.

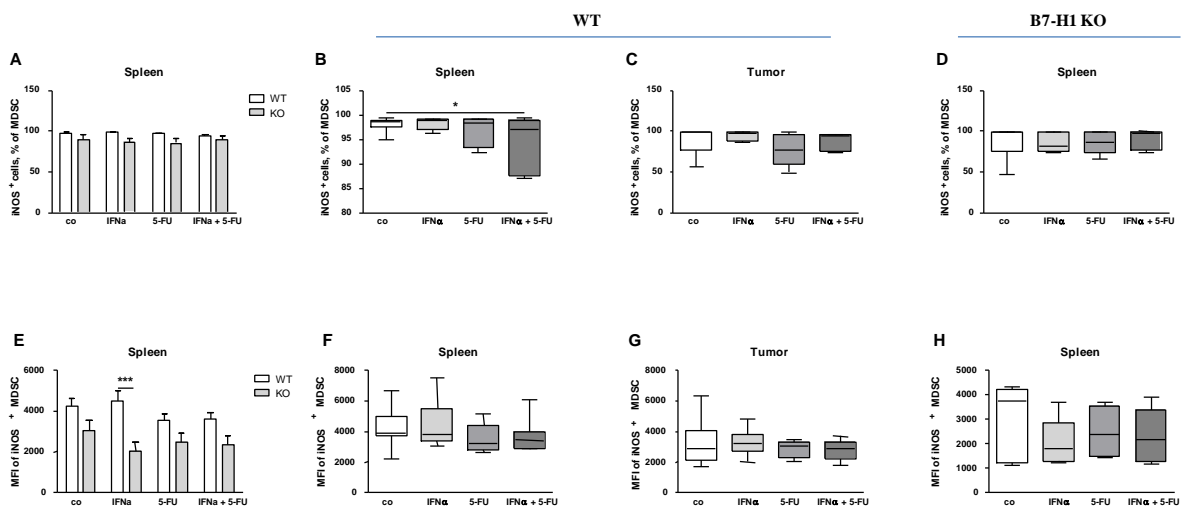


**Fig.3.2.2. 5 Quantification of iNOS expression of MDSC in spleens and tumors from tumor-bearing WT and B7-H1 KO mice with and without treatment (co).**

Mice were treated with IFN $\alpha$ , 5-FU or the combination of IFN $\alpha$ +5-FU on Day 5, 7 and 9 after Panc02 implantation. Untreated mice were used as control. Four weeks after surgery, the mice were killed and the organs were eviscerated. Single-cell suspensions of spleens and tumors were stained with fluorescence labeled specific antibodies. The frequency of iNOS<sup>+</sup> MDSC together with the MFI of iNOS was analyzed by flow cytometry. Data from four independent experiments are presented as column bar graphs and box plots with SEM ((spleens: n = 9 for co, and n = 6 for IFN $\alpha$ ; 5-FU; IFN $\alpha$ +5-FU; tumors: n = 7 for co, n = 4-6 for IFN $\alpha$ ; 5-FU; IFN $\alpha$ +5-FU);\*\*\*p<0.001; control group vs. treatment groups; two-way (A,E) and one-way (B,C,D,F,G,H) ANOVA)

In spleens of WT and B7-H1 KO mice, similar frequencies of iNOS<sup>+</sup> gMDSC were determined in all four groups (Fig.3.2.2.6 A). By looking at WT and B7-H1 KO spleens separately, no significant difference was observed between the control group compared to the treatments, in spleens of both the WT and B7-H1 KO tumor-bearing mice (Fig.3.2.2.6 B,D).

Beyond that, no significant change in percentages of iNOS<sup>+</sup> gMDSC was found for the treatment groups in tumors of WT mice compared to the control group (Fig.3.2.2.6 C).

For the MFI of iNOS<sup>+</sup> gMDSC, a significantly lower value was observed in the group of IFN $\alpha$  treatment in B7-H1 KO spleens compared to WT spleens. In the other groups, no significant difference was seen between the groups of WT spleens compared to those of B7-H1 KO spleens (Fig.3.2.2.6 E). Comparing the groups of either WT or B7-H1 KO spleens separately, no significant difference in the MFI of iNOS was seen between control and treated animals, in both WT and B7-H1 KO spleens (Fig.3.2.2.6 F,H).

In the tumors of WT mice, we found no significant difference in the iNOS MFI between the control group and treatment groups (Fig.3.2.2.6 G).

## Results

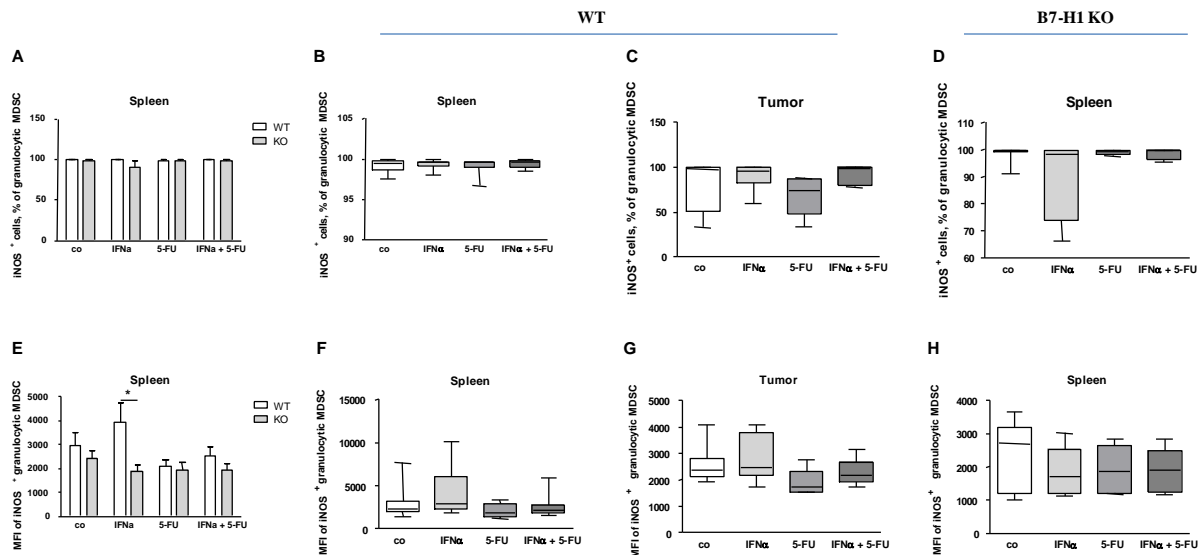


**Fig.3.2.2.6 Quantification of iNOS expression of gMDSC in spleens and tumors from tumor-bearing WT and B7-H1 KO mice with and without treatment (co).**

Mice were treated with IFN $\alpha$ , 5-FU or the combination of IFN $\alpha$ +5-FU on Day 5, 7 and 9 after Panc02 implantation. Untreated mice were used as control. Four weeks after surgery, the mice were killed and the organs were eviscerated. Single-cell suspensions of spleens and tumors were stained with fluorescence labeled specific antibodies. The frequency of iNOS<sup>+</sup> gMDSC together with the MFI of iNOS was analyzed by flow cytometry. Data from four independent experiments are presented as column bar graphs and box plots with SEM ((spleens: n = 9 for co, and n = 6 for IFN $\alpha$ ; 5-FU; IFN $\alpha$ +5-FU; tumors: n = 7 for co, n = 4-6 for IFN $\alpha$ ; 5-FU; IFN $\alpha$ +5-FU); \*p<0.05; control group vs. treatment groups; two-way (A,E) and one-way (B,C,D,F,G,H) ANOVA)

When looking at the iNOS<sup>+</sup> mMDSC in spleens of WT and B7-H1 KO tumor-bearing mice in comparison, no significant difference was seen throughout all four groups (Fig.3.2.2.7 A). The detailed analysis of WT as well as B7-H1 KO spleens, revealed no significant difference in the frequency of iNOS<sup>+</sup> mMDSC between the control and treated mice (Fig.3.2.2.7 B,D).

In WT tumors, the change in percentage of iNOS<sup>+</sup> mMDSC between the control and treatment groups was of no statistical significance (Fig.3.2.2.7 C).

As one can see in the Fig.3.2.2.7 E, the MFI of iNOS<sup>+</sup> mMDSC demonstrated no significant difference between all groups of WT spleens compared to B7-H1 KO spleens. In the spleens of WT tumor-bearing mice, a significantly lower MFI of iNOS

## Results

was determined for the group of 5-FU treated animals compared to control animals (Fig.3.2.2.7 F). The analysis of iNOS MFI in B7-H1 KO spleens showed no significant difference between the control and treatment groups (Fig.3.2.2.7 H).

For the MFI of iNOS in WT tumors, no significant difference in values was found between the control and treatment groups (Fig.3.2.2.7 G).

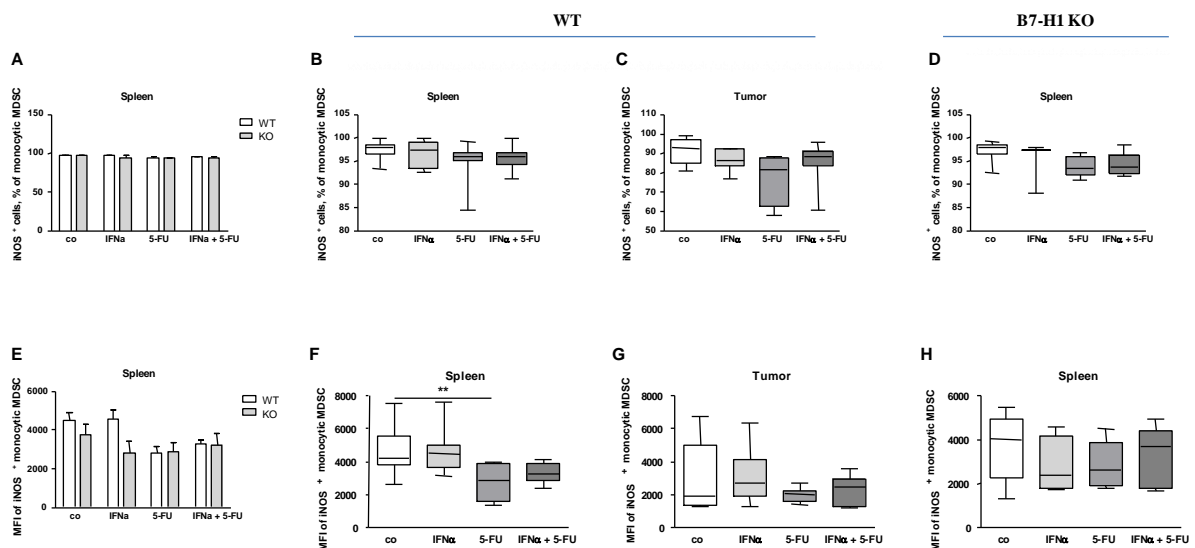


**Fig.3.2.2. 7 Quantification of iNOS expression of mMDSC in spleens and tumors from tumor-bearing WT and B7-H1 KO mice with and without treatment (co).**

Mice were treated with IFN $\alpha$ , 5-FU or the combination of IFN $\alpha$ +5-FU on Day 5, 7 and 9 after Panc02 implantation. Untreated mice were used as control. Four weeks after surgery, the mice were killed and the organs were eviscerated. Single-cell suspensions of spleens and tumors were stained with fluorescence labeled specific antibodies. The frequency of iNOS $^+$  mMDSC together with the MFI of iNOS was analyzed by flow cytometry. Data from four independent experiments are presented as column bar graphs and box plots with SEM ((spleens: n = 9 for co, and n = 6 for IFN $\alpha$ ; 5-FU; IFN $\alpha$ +5-FU; tumors: n = 7 for co, n = 4-6 for IFN $\alpha$ ; 5-FU; IFN $\alpha$ +5-FU); \*\*p < 0.01; control group vs. treatment groups; two-way (A,E) and one-way (B,C,D,F,G,H) ANOVA)

After we finished the analysis of iNOS expression, we next analyzed the Arginase expression in total MDSC, as well as their subsets. No difference in Arg $^+$  MDSC was seen between WT and B7-H1 KO tumor-bearing mice for all four groups when we compared spleens of WT to the B7-H1 KO spleens (Fig.3.2.2.8 A). When comparing

the single-treatment groups of either WT or B7-H1 KO spleens to the control groups separately, no significant difference in the frequency of Arg<sup>+</sup> MDSC was determined in the spleens from both the WT and B7-H1 KO tumor-bearing mice (Fig.3.2.2.8 B,D).

The analysis of WT tumors showed no significant difference in the ratio of Arg<sup>+</sup> MDSC between the control group and the treatment groups (Fig.3.2.2.8 C).

The measured MFI of Arg<sup>+</sup> MDSC in spleens showed significantly lower values in the group of IFN $\alpha$ +5-FU treated animals of B7-H1 KO spleens compared to WT spleens. For the other groups, a tendency towards lower intensities was found in B7-H1 KO spleens compared to WT spleens (Fig.3.2.2.8 E). Between the control and treatment groups in spleens from both the WT and B7-H1 KO mice, we did not see a significant difference in the values of Arg MFI (Fig.3.2.2.8 F,H).

In the groups of WT tumors, no significant difference in the Arg MFI was registered when we compared the control group to the treatment groups (Fig.3.2.2.8 G).

## Results

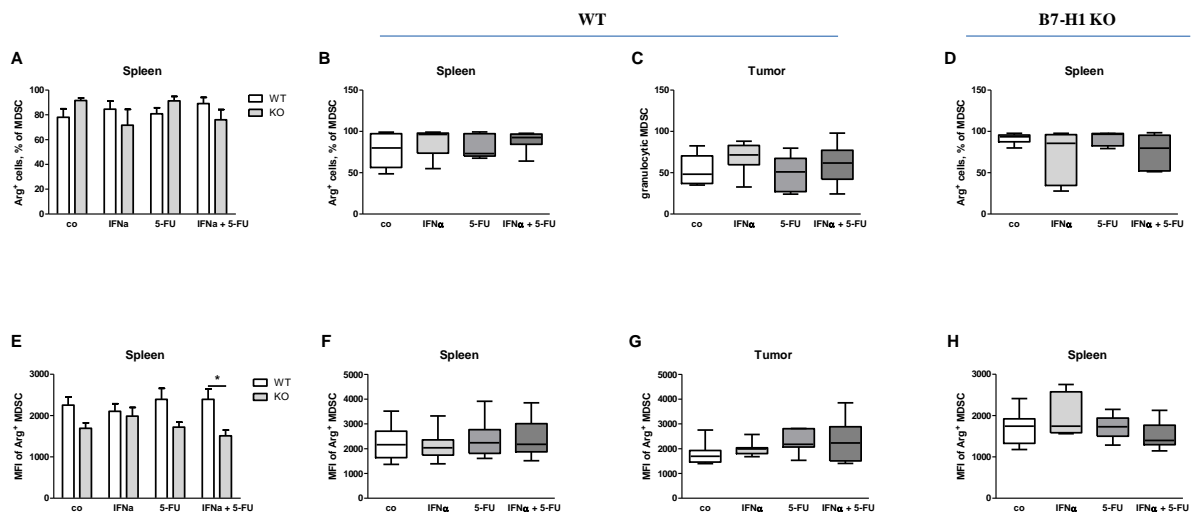


**Fig.3.2.2. 8 Quantification of Arg expression of MDSC in spleens and tumors from tumor-bearing WT and B7-H1 KO mice with and without treatment (co).**

Mice were treated with IFN $\alpha$ , 5-FU or the combination of IFN $\alpha$ +5-FU on Day 5, 7 and 9 after Panc02 implantation. Untreated mice were used as control. Four weeks after surgery, the mice were killed and the organs were eviscerated. Single-cell suspensions of spleens and tumors were stained with fluorescence labeled specific antibodies. The frequency of Arg<sup>+</sup> MDSC together with the MFI of Arg was analyzed by flow cytometry. Data from four independent experiments are presented as column bar graphs and box plots with SEM ((spleens: n = 9 for co, and n = 6 for IFN $\alpha$ ; 5-FU; IFN $\alpha$ +5-FU; tumors: n = 7 for co, n = 4-6 for IFN $\alpha$ ; 5-FU; IFN $\alpha$ +5-FU); \*p<0.05; control group vs. treatment groups; two-way (A,E) and one-way (B,C,D,F,G,H) ANOVA)

When we took a detailed look at the Arginase expression in gMDSC in spleens of WT and B7-H1 KO tumor-bearing mice in comparison, similar percentages were determined for all four groups (Fig.3.2.2.9 A). Within the single groups of WT and B7-H1 KO spleens, no significant difference in the ratio of Arg<sup>+</sup> gMDSC was seen between the controls and applied therapies in spleens of WT as well as B7-H1 KO tumor-bearing mice (Fig.3.2.2.9 B,D).

When analyzing WT tumor groups, no statistically significant difference was revealed after applied treatments compared to the control (Fig.3.2.2.9 C).

For the MFI of Arg, significantly lower values were determined in the B7-H1 KO group of IFN $\alpha$ +5-FU treatment compared to the respective WT group (Fig.3.2.2.9 E). The comparison of the single groups of either WT or B7-H1 KO spleens showed no

## Results

significant difference in Arg MFI between the controls and treatment groups, in both mouse strains (Fig.3.2.2.9 F,H).

In the analysis of WT tumors, one can see a significant increase in the value of Arg MFI in the 5-FU treatment group compared to the control group (Fig.3.2.2.9 G).

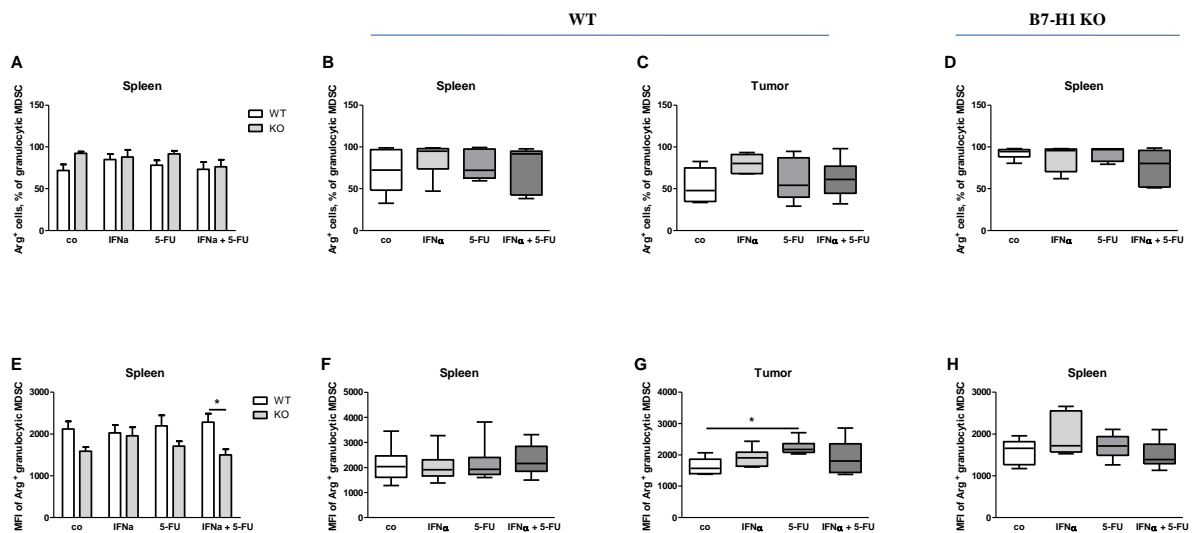


**Fig.3.2.2. 9 Quantification of Arg expression of gMDSC in spleens and tumors from tumor-bearing WT and B7-H1 KO mice with and without treatment (co).**

Mice were treated with IFN $\alpha$ , 5-FU or the combination of IFN $\alpha$ +5-FU on Day 5, 7 and 9 after Panc02 implantation. Untreated mice were used as control. Four weeks after surgery, the mice were killed and the organs were eviscerated. Single-cell suspensions of spleens and tumors were stained with fluorescence labeled specific antibodies. The frequency of Arg<sup>+</sup> granulocytic MDSC together with the MFI of Arg was analyzed by flow cytometry. Data from four independent experiments are presented as column bar graphs and box plots with SEM ((spleens: n = 9 for co, and n = 6 for IFN $\alpha$ ; 5-FU; IFN $\alpha$ +5-FU; tumors: n = 7 for co, n = 4-6 for IFN $\alpha$ ; 5-FU; IFN $\alpha$ +5-FU); \*p<0.05; control group vs. treatment groups; two-way (A,E) and one-way (B,C,D,F,G,H) ANOVA)

The analysis of MDSC demonstrated lower frequencies of total MDSC in all four groups in the spleens of B7-H1 KO compared to WT spleens of tumor-bearing mice.

### 3.2.3 Analysis of B7-H1/B7-DC expression on MDSC

We also analyzed the expression of the regulatory molecules B7-H1 on total MDSC, as well as on the MDSC subsets in WT spleens and tumors. Additionally, we were interested whether different treatments can have an impact on the expression of B7-H1 on MDSC. In WT spleens as well as in WT tumors, no significant difference in the frequency of B7-H1<sup>+</sup> MDSC was seen between control groups and treatment groups (Fig.3.2.3.1 A,B).

When determining the MFI of B7-H1 of total MDSC, a significantly lower value was observed in WT spleens in the group IFN $\alpha$ +5-FU treatment compared to the control (Fig.3.2.3.1 C). The measured MFI of B7-H1 on total MDSC of WT tumors showed no significant difference between the control group and the treatment groups (Fig.3.2.3.1 D).

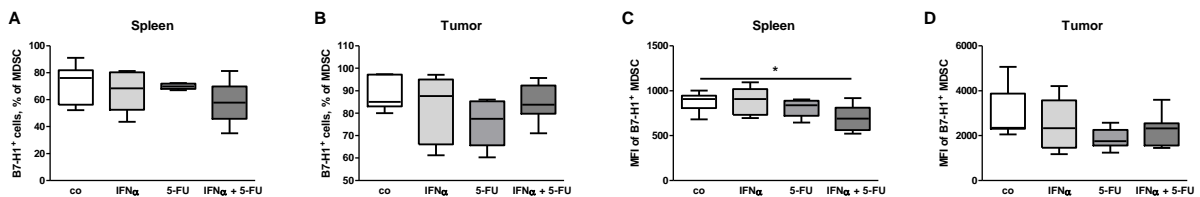


**Fig.3.2.3. 1 Quantification of B7-H1 expression on MDSC in spleens and tumors from tumor-bearing WT mice with and without treatment (co).**

Mice were treated with IFN $\alpha$ , 5-FU or the combination of IFN $\alpha$ +5-FU on Day 5, 7 and 9 after Panc02 implantation. Untreated mice were used as control. Four weeks after surgery, the mice were killed and the organs were eviscerated. Single-cell suspensions of spleens and tumors were stained with fluorescence labeled specific antibodies. The frequency of B7-H1<sup>+</sup> MDSC together with the MFI of B7-H1 was analyzed by flow cytometry. Data from four independent experiments are presented as box plots with SEM ((spleens: n = 9 for co, and n = 6 for IFN $\alpha$ ; 5-FU; IFN $\alpha$ +5-FU; tumors: n = 7 for co, n = 4-6 for IFN $\alpha$ ; 5-FU; IFN $\alpha$ +5-FU); \*p<0.05; control group vs. treatment groups; one-way (A,B,C,D) ANOVA)

Next, we examined the percentage of B7-H1<sup>+</sup> cells out of gMDSC in spleens and tumors of WT mice. No significant difference in the frequency of B7-H1<sup>+</sup> gMDSC was found between the single treatment groups and the control group, neither in spleens nor in tumors from WT mice (Fig.3.2.3.2 A,B).

The analyzed MFI of B7-H1 did not point out a significant difference between control mice and treated mice, in both the spleens and tumors of WT mice (Fig.3.2.3.2 C,D).

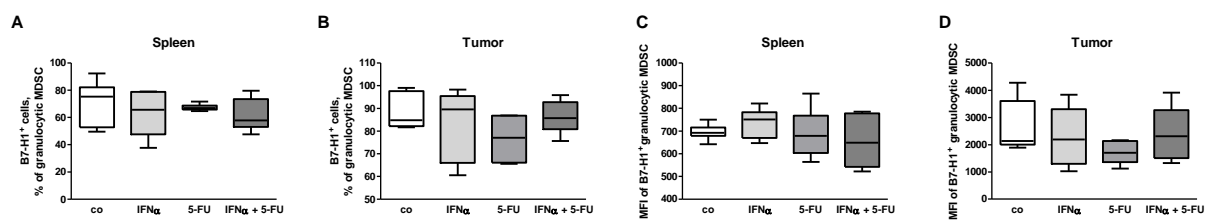


**Fig.3.2.3. 2 Quantification of B7-H1 expression on gMDSC in spleens and tumors from tumor-bearing WT mice with and without treatment (co).**

Mice were treated with IFN $\alpha$ , 5-FU or the combination of IFN $\alpha$ +5-FU on Day 5, 7 and 9 after Panc02 implantation. Untreated mice were used as control. Four weeks after surgery, the mice were killed and the organs were eviscerated. Single-cell suspensions of spleens and tumors were stained with fluorescence labeled specific antibodies. The frequency of B7-H1<sup>+</sup> gMDSC together with the MFI of B7-H1 was analyzed by flow cytometry. Data from four independent experiments are presented as box plots with SEM ((spleens: n = 9 for co, and n = 6 for IFN $\alpha$ ; 5-FU; IFN $\alpha$ +5-FU; tumors: n = 7 for co, n = 4-6 for IFN $\alpha$ ; 5-FU; IFN $\alpha$ +5-FU); control group vs. treatment groups; one-way (A,B,C,D) ANOVA)

For the expression of B7-H1 molecule on mMDSC, we found no significant change in frequencies of B7-H1<sup>+</sup> mMDSC in WT spleens of treated animals compared to control animals (Fig.3.2.3.3 A). In WT tumors, the difference in the ratio of B7-H1<sup>+</sup> mMDSC between the control group and treatment groups is of no statistical significance (Fig.3.2.3.3 B).

Analyzing the measured B7-H1 MFI of mMDSC, no significant difference between the control group and treatment groups was determined for both the spleens and tumors of WT mice (Fig.3.2.3.3 C,D).

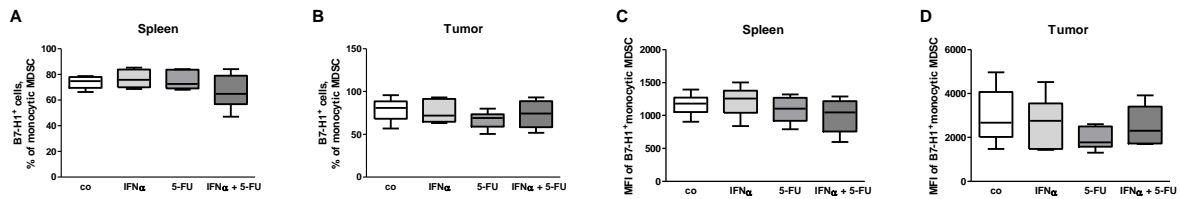


**Fig.3.2.3. 3 Quantification of B7-H1 expression on mMDSC in spleens and tumors from tumor-bearing WT mice with and without treatment (co).**

Mice were treated with IFN $\alpha$ , 5-FU or the combination of IFN $\alpha$ +5-FU on Day 5, 7 and 9 after Panc02 implantation. Untreated mice were used as control. Four weeks after surgery, the mice were killed and the organs were eviscerated. Single-cell suspensions of spleens and tumors were stained with fluorescence labeled specific antibodies. The frequency of B7-H1<sup>+</sup> mMDSC together with the MFI of B7-H1 was analyzed by flow cytometry. Data from four independent experiments are presented as box plots with SEM ((spleens: n = 9 for co, and n = 6 for IFN $\alpha$ ; 5-FU; IFN $\alpha$ +5-FU; tumors: n = 7 for co, n = 4-6 for IFN $\alpha$ ; 5-FU; IFN $\alpha$ +5-FU); control group vs. treatment groups; one-way (A,B,C,D) ANOVA)

Furthermore, we looked at the B7-DC expression on total MDSC and MDSC subsets in spleens of B7-H1 KO mice. In the analysis of B7-DC expression on total MDSC, no significant difference in percentages of B7-DC<sup>+</sup> MDSC was seen between the control and treatment groups (Fig.3.2.3.4 A). The MFI of B7-DC of total MDSC was not significantly different between the control group and the treatment groups (Fig.3.2.3.4 B).

For the B7-DC expression on gMDSC, similar percentages were found in all treatment groups compared to the control group (Fig.3.2.3.4 C). The MFI of B7-DC on this cell population showed no statistically difference between the control and treatment groups (Fig.3.2.3.4 D).

For mMDSC, we found no significant difference in frequencies of B7-DC<sup>+</sup> mMDSC between the control and treatment groups in spleens of B7-H1 KO mice (Fig.3.2.3.4 E). Furthermore, for the B7-DC MFI of mMDSC, similar values were registered for the treatment groups compared to the control group (Fig.3.2.3.4 F).

## Results

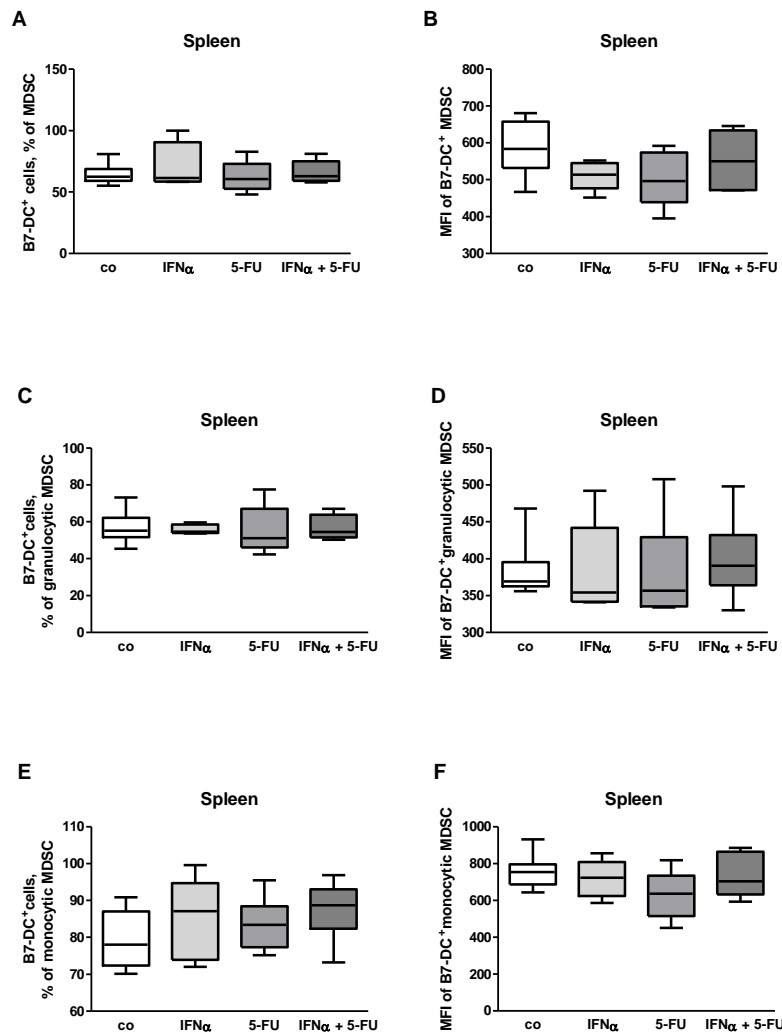


**Fig.3.2.3. 4 Quantification of B7-DC expression on MDSC, gMDSC and mMDSC in spleens from tumor-bearing B7-H1 KO mice with and without treatment (co).**

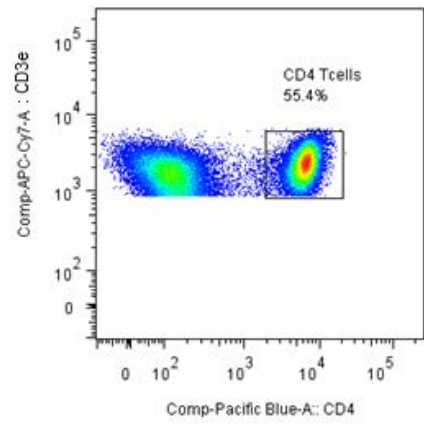
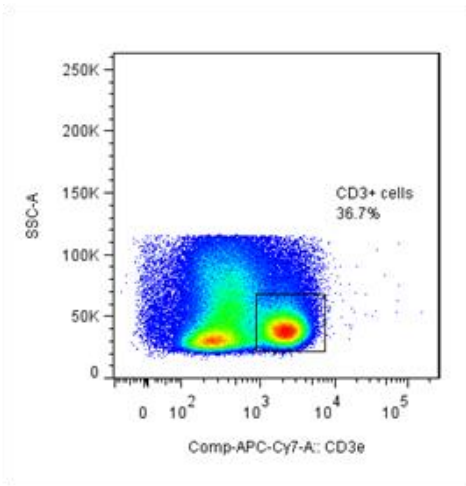
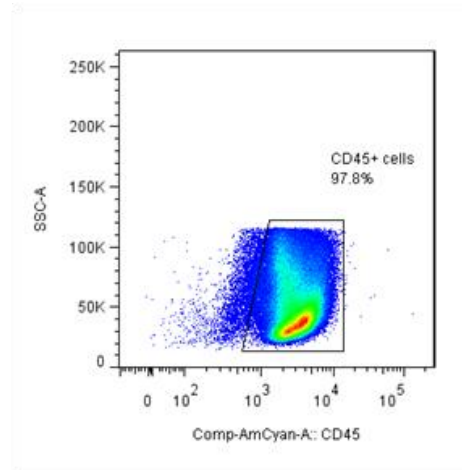
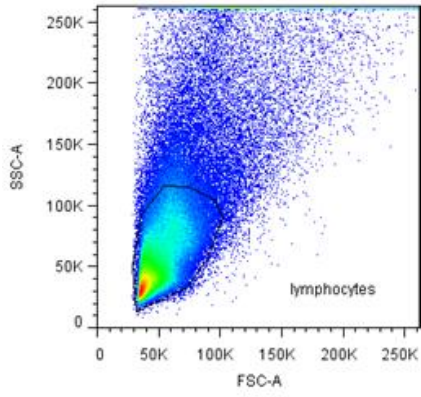
Mice were treated with IFN $\alpha$ , 5-FU or the combination of IFN $\alpha$ +5-FU on Day 5, 7 and 9 after Panc02 implantation. Untreated mice were used as control. Four weeks after surgery, the mice were killed and the organs were eviscerated. Single-cell suspensions of spleens were stained with fluorescence labeled specific antibodies. The frequencies of B7-DC<sup>+</sup> MDSC, gMDSC and mMDSC together with the MFI of B7-DC were analyzed by flow cytometry. Data from four independent experiments are presented as box plots with SEM ((spleens: n = 9 for co, and n = 6 for IFN $\alpha$ ; 5-FU; IFN $\alpha$ +5-FU; tumors: n = 7 for co, n = 4-6 for IFN $\alpha$ ; 5-FU; IFN $\alpha$ +5-FU); control group vs. treatment groups; one-way (A,B,C,D,F,G,) ANOVA)

Summarizing the data concerning the regulatory molecules B7-H1/B7-DC in spleens and tumors of tumor-bearing WT and B7-H1 KO mice, no significant difference in the expression of this molecule was seen between the control and treated mice.

### **3.2.4 Analysis of regulatory T cells (Treg)**

Another suppressive cell population we analyzed in detail was the population of Treg. We examined Treg, as well as Tcon and activated Tcon, in spleens of WT and B7-H1 KO mice (control and treated with IFN $\alpha$ , 5-FU, IFN $\alpha$ +5-FU) as well as in WT tumors. Our gating strategy is presented below in Fig.3.2.4.1. The FACS data (dot-plot, histogram) represent one typical result out of four independent experiments.

# Results



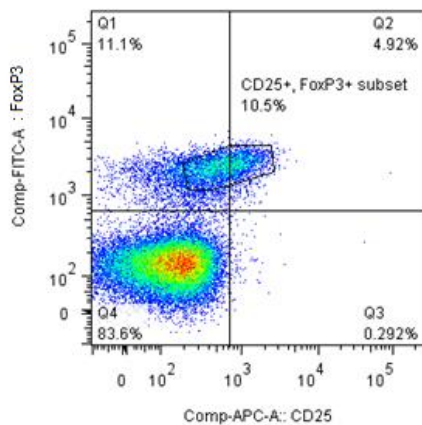


**Fig.3.2.4. 1 Gating strategy for regulatory T cells in spleens and tumors using flow cytometry.**

The first gate was set on lymphocytes using FSC/SSC dot plot; afterwards CD4<sup>+</sup> T cells were marked. Out of this cell population of regulatory T cells (Treg), Tcon, activated Tcon and CD25<sup>-</sup>FoxP3<sup>+</sup> the cells were determined using CD25 and FoxP3 expression.

First, we looked at the frequencies of Treg out of all CD4<sup>+</sup> T cells in spleens from WT and B7-H1 KO tumor-bearing mice. When comparing the groups of splenocytes of treated WT and B7-H1 KO tumor-bearing mice, no significant difference in Treg frequencies was found for all four groups (Fig.3.2.4.2 A). By taking a detailed look at the single groups of WT or B7-H1 KO spleens, no significant difference in the ratio of Treg was observed between the control group and the treatment groups in the spleens from both the WT and B7-H1 KO tumor-bearing mice (Fig.3.2.4.2 B,D).

The comparison of the treatment groups to the control of WT tumors, showed no significant difference in the percentages of Treg (Fig.3.2.4.2 C).

## Results

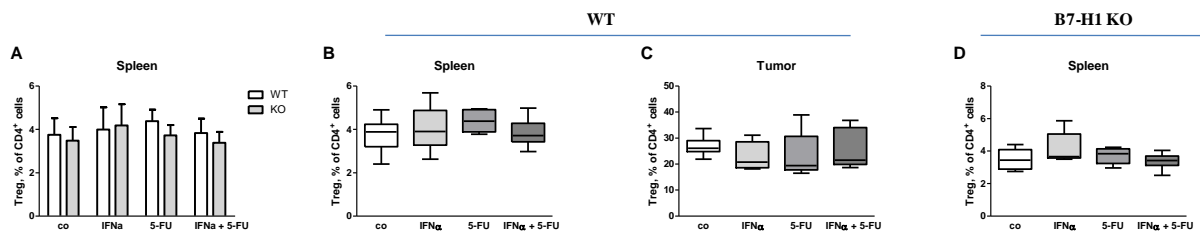


**Fig.3.2.4. 2 Quantification of Treg in spleens and tumors from tumor-bearing WT and B7-H1 KO mice with and without treatment (co).**

Mice were treated with IFN $\alpha$ , 5-FU or the combination of IFN $\alpha$ +5-FU on Day 5, 7 and 9 after Panc02 implantation. Untreated mice were used as control. Four weeks after surgery, the mice were killed and the organs were eviscerated. Single-cell suspensions of spleens and tumors were stained with fluorescence labeled specific antibodies. The frequency of Treg was analyzed by flow cytometry. Data from four independent experiments are presented as column bar graphs and box plots with SEM ((spleens: n = 9 for co, and n = 6 for IFN $\alpha$ ; 5-FU; IFN $\alpha$ +5-FU; tumors: n = 7 for co, n = 4-6 for IFN $\alpha$ ; 5-FU; IFN $\alpha$ +5-FU); control group vs. treatment groups; two-way (A) and one-way (B,C,D) ANOVA)

Analyzing the proportion of Tcon out of the CD4<sup>+</sup> T cells in spleens of WT and B7-H1 KO tumor-bearing mice, one can see similar percentages of Tcon between WT and B7-H1 KO spleens throughout all groups (Fig.3.2.4.3 A). By looking at the groups of WT spleens alone, we registered a significant decrease in the frequency of Tcon in the groups of IFN $\alpha$  and IFN $\alpha$ +5-FU treatment compared to the control (Fig.3.2.4.3 B). In B7-H1 KO spleens, a significantly lower percentage of Tcon was seen in the group of 5-FU treatment compared to the control (Fig.3.2.4.3 D).

The analysis of WT tumors revealed a significant increase in Tcon ratio in the group of IFN $\alpha$ +5-FU treatment compared to the control group (Fig.3.2.4.3 C).

## Results

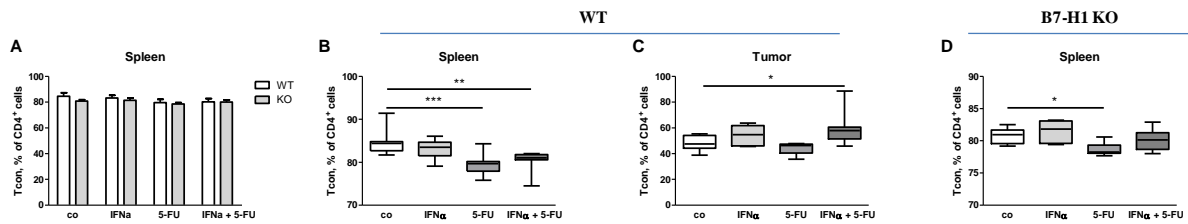


**Fig.3.2.4.3 Quantification of Tcon in spleens and tumors from tumor-bearing WT and B7-H1 KO mice with and without treatment (co).**

Mice were treated with IFN $\alpha$ , 5-FU or the combination of IFN $\alpha$ +5-FU on Day 5, 7 and 9 after Panc02 implantation. Untreated mice were used as control. Four weeks after surgery, the mice were killed and the organs were eviscerated. Single-cell suspensions of spleens and tumors were stained with fluorescence labeled specific antibodies. The frequency of Tcon was analyzed by flow cytometry. Data from four independent experiments are presented as column bar graphs and box plots with SEM ((spleens: n = 9 for co, and n = 6 for IFN $\alpha$ ; 5-FU; IFN $\alpha$ +5-FU; tumors: n = 7 for co, n = 4-6 for IFN $\alpha$ ; 5-FU; IFN $\alpha$ +5-FU); \*p<0.05, \*\*p<0.01, \*\*\*p<0.001; control group vs. treatment groups; two-way (A) and one-way (B,C,D) ANOVA)

Furthermore, the percentages of activated Tcon (CD25<sup>+</sup>) in WT and B7-H1 KO tumor-bearing mice were determined. The measured differences in frequencies of activated Tcon were not significant between all groups from the WT and B7-H1 KO spleens (Fig.3.2.4.4 A). In WT spleens in detail, no significant difference in the ratio of activated Tcon was seen in the treatment groups compared to the control group (Fig.3.2.4.4 B). For spleens of B7-H1 KO mice, a significantly lower percentage of activated Tcon was observed in the group of IFN $\alpha$  treatment compared to the control group (Fig.3.2.4.4 D).

The tumors of WT mice showed no significant difference in the percentages of Tcon between the control and treatment groups (Fig.3.2.4.4 C).

## Results

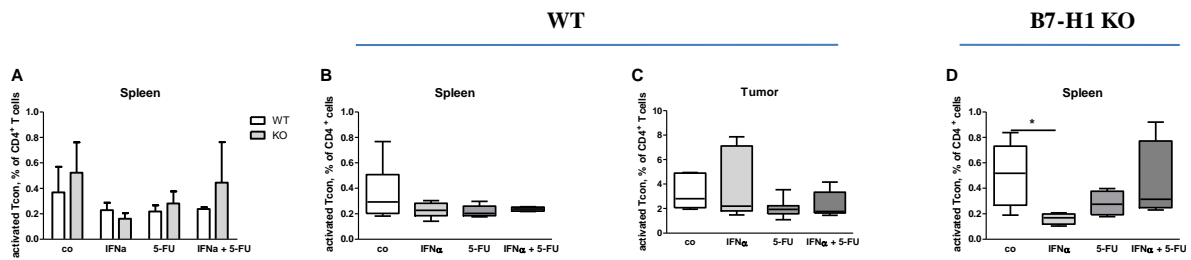


**Fig.3.2.4. 4 Quantification of activated Tcon in spleens and tumors from tumor-bearing WT and B7-H1 KO mice with and without treatment (co).**

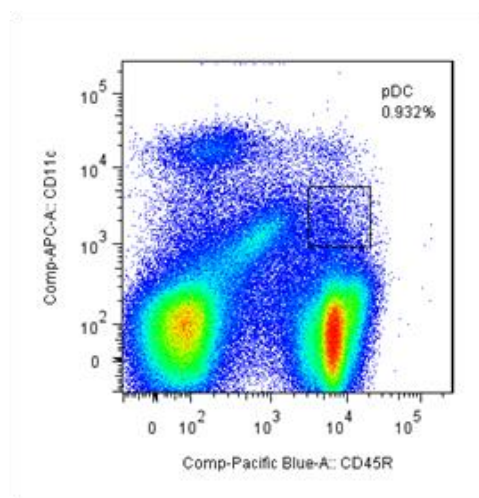
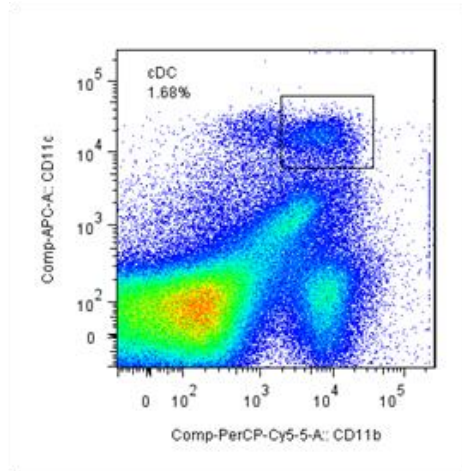
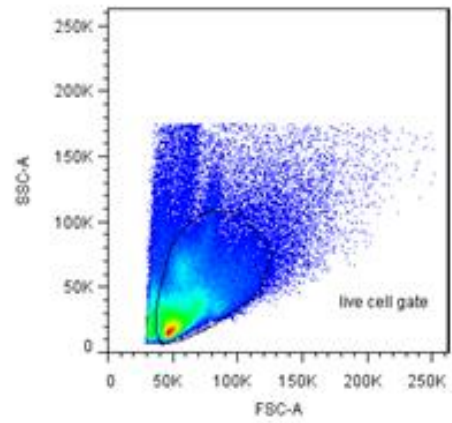
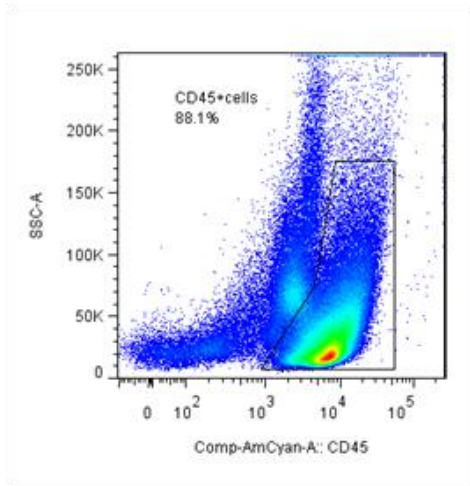
Mice were treated with IFN $\alpha$ , 5-FU or the combination of IFN $\alpha$ +5-FU on Day 5, 7 and 9 after Panc02 implantation. Untreated mice were used as control. Four weeks after surgery, the mice were killed and the organs were eviscerated. Single-cell suspensions of spleens and tumors were stained with fluorescence labeled specific antibodies. The frequency of activated Tcon was analyzed by flow cytometry. Data from four independent experiments are presented as column bar graphs and box plots with SEM ((spleens: n = 9 for co, and n = 6 for IFN $\alpha$ ; 5-FU; IFN $\alpha$ +5-FU; tumors: n = 7 for co, n = 4-6 for IFN $\alpha$ ; 5-FU; IFN $\alpha$ +5-FU); \*p<0.05; control group vs. treatment groups; two-way (A) and one-way (B,C,D) ANOVA)

Taken together, the analysis of Treg revealed no large impact in our different therapies on the frequencies of Treg in WT and B7-H1 KO tumor-bearing mice. Furthermore, no significant differences were observed when we compared the frequencies of Treg between WT and B7-H1 KO tumor-bearing mice.

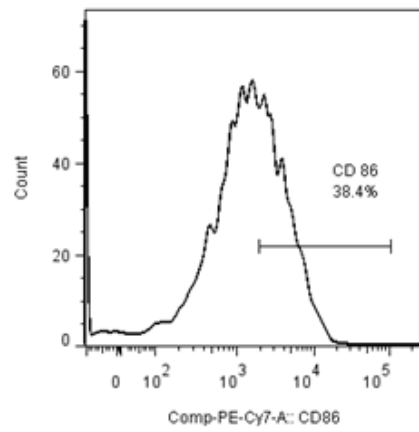
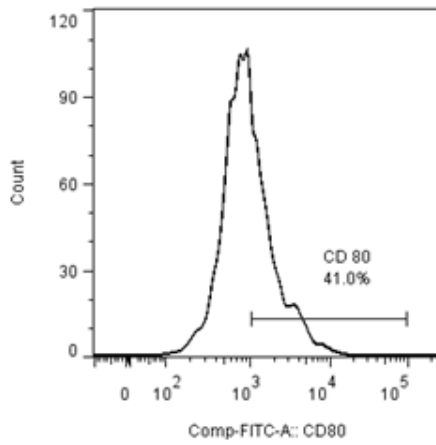
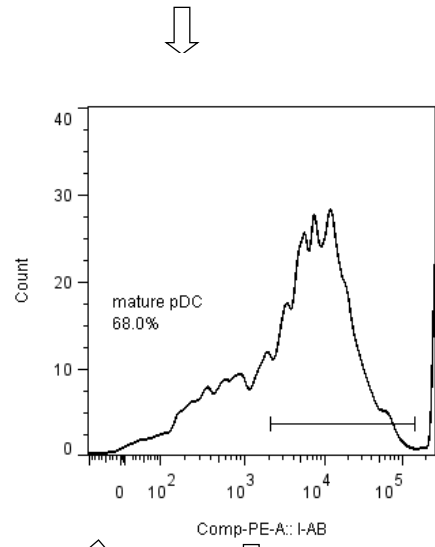
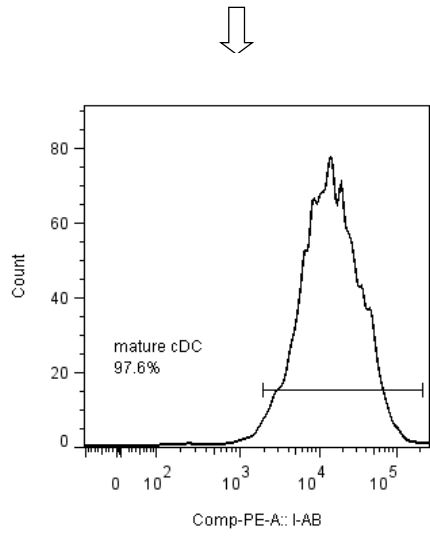
### 3.2.5 Analysis of dendritic cells (DC)

The last major cell population we analyzed was the population of DC with their subsets of conventional DC (cDC) and plasmacytoid DC (pDC). Furthermore, we took a closer look at their maturation status, analyzed the expression of the costimulatory molecules CD80/CD86 as well as the expression of the regulatory molecules B7-H1/B7-DC. The gating strategy for our DC panel is shown in Fig.3.2.5.1. The FACS data (dot-plot, histogram) represent one typical result out of four independent experiments.

# Results



# Results



or

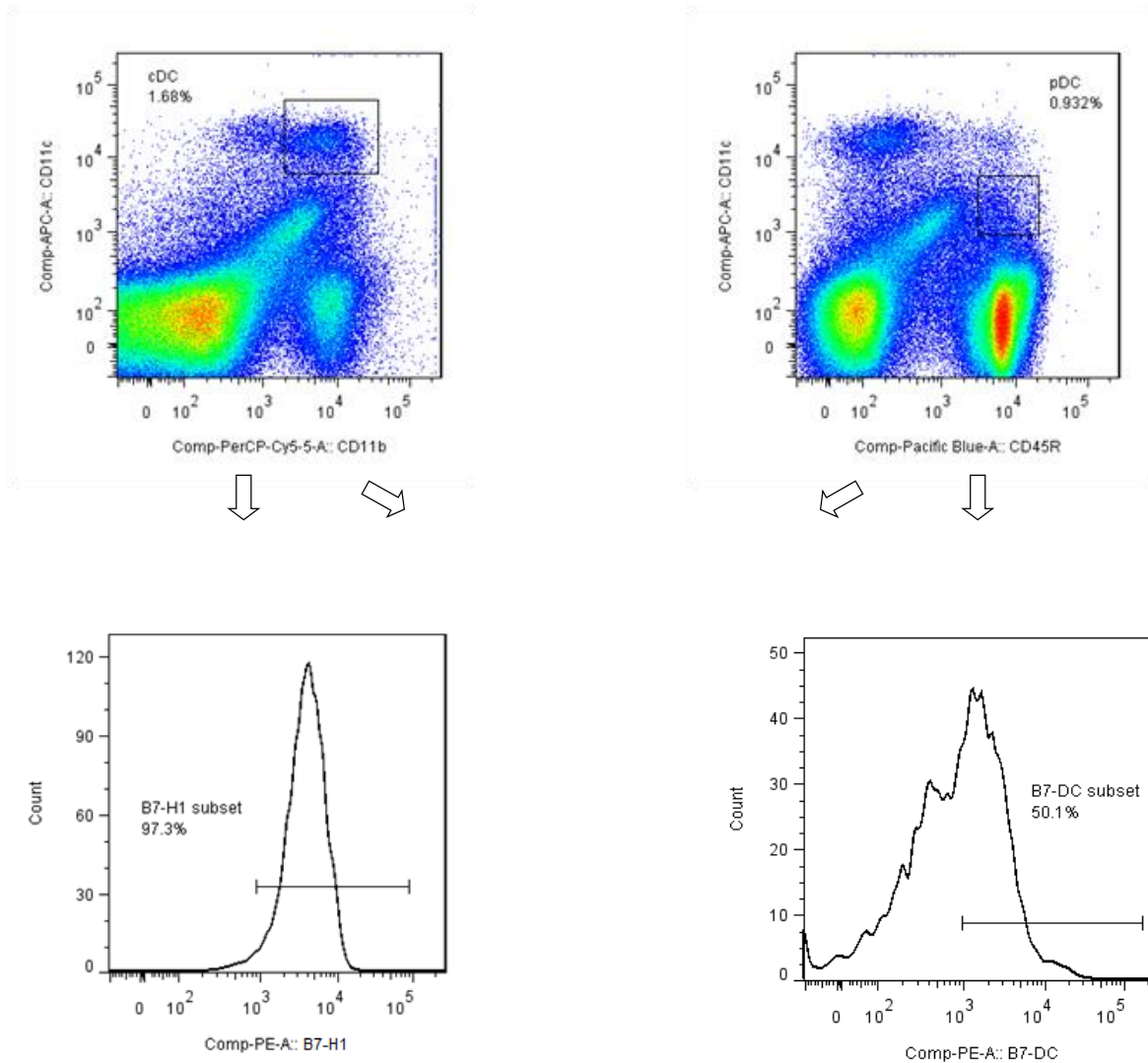


**Fig.3.2.5. 1 Gating strategy for dendritic cells in spleens and tumors using flow cytometry.**

The first gate was set on CD45<sup>+</sup> cells, and out of those, all the living cells were gated using FSC/SSC dot plot. Then the two subsets of DC, conventional DC (cDC) and plasmacytoid DC (pDC), were gated according to the expression of CD11c and either CD11b or CD45R markers. The I-Ab antibody was used to define the maturation status of cDC and pDC. Mature cDC and pDC, and further analyzed for the expression of CD80 and CD86 as well as the expression of B7-H1/B7-DC molecules. All positive gates were set according to FMO controls.

In the DC panel, we started with the analysis of the cDC cell population. WT and B7-H1 KO spleens from tumor-bearing mice in comparison showed no significant difference in the frequency of cDC between all four groups of both mouse strains (Fig.3.2.5.2 A). When looking at WT spleens in detail, no significant difference in percentage of cDC was seen between the control group and the treatment groups (Fig.3.2.5.2 B). In B7-H1 KO mice, significantly lower percentages of cDC were found in the groups of IFN $\alpha$  and IFN $\alpha$ +5-FU treatments compared to the control group (Fig.3.2.5.2 D).

In WT tumors, a significant decrease of cDC portion was determined in the IFN $\alpha$ +5-FU group compared to the control group (Fig.3.2.5.2 C)

After we analyzed the frequency of the cDC population, we also determined the maturation status of this cell fraction. For spleens from WT and B7-H1 KO tumor-bearing mice in comparison, similar values were reached between WT and B7-H1 KO throughout all treatments and the controls (Fig.3.2.5.2 E). In WT spleens, the treatment groups compared to the control in WT showed a significant decrease in percentage of mature cDC in the 5-FU and IFN $\alpha$ +5-FU treated animals (Fig.3.2.5.2 F). For the groups of B7-H1 KO spleens, we found no significant difference in the ratio of mature cDC between the treatments and the control (Fig.3.2.5.2 H).

In tumors of WT animals, significantly lower frequencies of mature cDC were found in the group of IFN $\alpha$  treatment compared to the control (Fig.3.2.5.2 G).

## Results

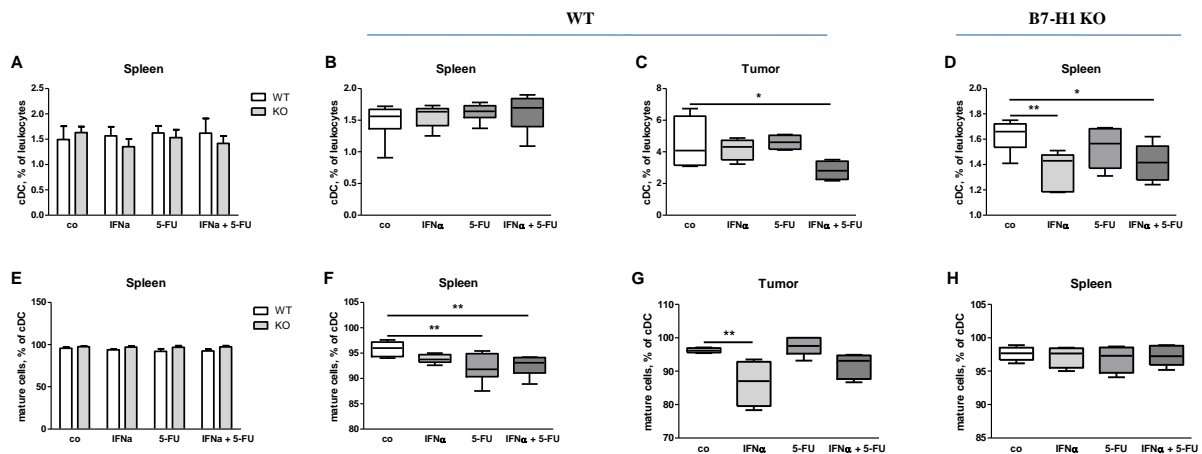


**Fig.3.2.5. 2 Quantification of cDC and their maturation status in spleens and tumors from tumor-bearing WT and B7-H1 KO mice with and without treatment (co).**

Mice were treated with IFN $\alpha$ , 5-FU or the combination of IFN $\alpha$ +5-FU on Day 5, 7 and 9 after Panc02 implantation. Untreated mice were used as control. Four weeks after surgery, the mice were killed and the organs were eviscerated. Single-cell suspensions of spleens and tumors were stained with fluorescence labeled specific antibodies. The frequencies of cDC and mature cDC were analyzed by flow cytometry. Data from four independent experiments are presented as column bar graphs and box plots with SEM ((spleens: n = 9 for co, and n = 6 for IFN $\alpha$ ; 5-FU; IFN $\alpha$ +5-FU; tumors: n = 7 for co, n = 4-6 for IFN $\alpha$ ; 5-FU; IFN $\alpha$ +5-FU); \*p<0.05, \*\*p<0.01; control group vs. treatment groups; two-way (A,E) and one-way (B,C,D,F,G,H) ANOVA)

After we determined the frequencies of mature cDC, we analyzed the costimulatory molecules CD80 and CD86, starting with the expression of CD80 molecule. In the groups of IFN $\alpha$ , 5-FU and IFN $\alpha$ +5-FU treatments, a significantly increased expression of the D80 molecule, revealed by the determined percentages, was seen in spleens of B7-H1 KO compared to WT mice (Fig.3.2.5.3 A). When looking at the WT spleen groups in more detail, no significant difference in percentage of CD80<sup>+</sup> mature cDC was seen between the treatment groups compared to the control, (Fig.3.2.5.3 B). Instead, in the spleens of B7-H1 KO mice a significant increase in the portion of CD80<sup>+</sup>, mature cDC was found in the groups of IFN $\alpha$  and 5-FU treatment compared to the control (Fig.3.2.5.3 D).

The analysis of CD80 molecule expression in WT tumors revealed no significant difference between the single treatments compared to the control (Fig.3.2.5.3 C).

## Results

The measured MFI of CD80 molecule showed highly significant lower values in the spleens of B7-H1 KO compared to spleens from WT tumor-bearing mice in all four groups (Fig.3.2.5.3 E). In the WT spleens, no significant difference in CD80 MFI was registered between control and treatment groups (Fig.3.2.5.3 F). In B7-H1 KO spleens, significantly higher values in the MFI of CD80 were found in the groups of IFN $\alpha$  and 5-FU treatment compared to control (Fig.3.2.5.3 H).

In tumors of WT mice, a significant increase in the value of CD80 MFI was recorded in the IFN $\alpha$  treated mice, whereas in the group of 5-FU treatment, a significant decrease in the value was seen compared to the control group (Fig.3.2.5.3 G).

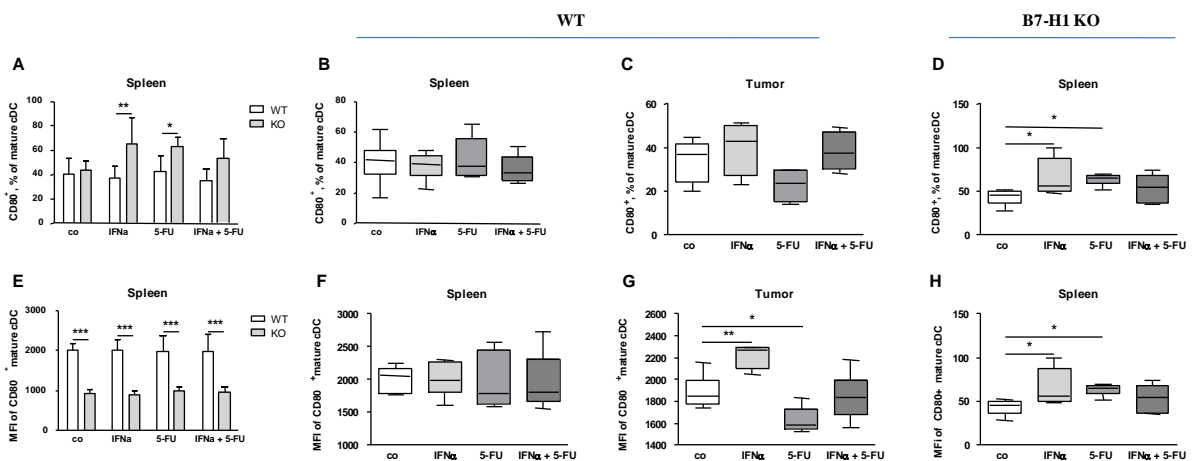


**Fig.3.2.5. 3 Quantification of CD80 expression on mature cDC in spleens and tumors from tumor-bearing WT and B7-H1 KO mice with and without treatment (co).**

Mice were treated with IFN $\alpha$ , 5-FU or the combination of IFN $\alpha$ +5-FU on Day 5, 7 and 9 after Panc02 implantation. Untreated mice were used as control. Four weeks after surgery, the mice were killed and the organs were eviscerated. Single-cell suspensions of spleens and tumors were stained with fluorescence labeled specific antibodies. The frequency of CD80<sup>+</sup> mature cDC together with the MFI of CD80 was analyzed by flow cytometry. Data from four independent experiments are presented as column bar graphs and box plots with SEM ((spleens: n = 9 for co, and n = 6 for IFN $\alpha$ ; 5-FU; IFN $\alpha$ +5-FU; tumors: n = 7 for co, n = 4-6 for IFN $\alpha$ ; 5-FU; IFN $\alpha$ +5-FU); \*p<0.05, \*\*p<0.01; control group vs. treatment groups; two-way (A,E) and one-way (B,C,D,F,G,H) ANOVA)

Next, we determined the differences in mature cDC that express CD86 molecules, between WT and B7-H1 KO spleens as well as between the single treatments compared to the control in both mouse strains. Significantly higher percentages of CD86 molecule expression were found in B7-H1 KO spleens in the groups of IFN $\alpha$ , 5-FU, and IFN $\alpha$ +5-FU compared to those groups of WT spleens from tumor-bearing mice (Fig.3.2.5.4 A). Between the treatment groups and the control of WT spleens, no significant difference in CD86<sup>+</sup> mature cDC was seen (Fig.3.2.5.4 B), whereas in the B7-H1KO spleens a significant increase in percentage of CD86<sup>+</sup> mature cDC was found in IFN $\alpha$  treated animals compared to untreated ones (Fig.3.2.5.4 D).

In the WT tumors, no significant difference in frequencies was determined between the treatment groups and the control group analyzing CD86<sup>+</sup> mature cDC (Fig.3.2.5.4 C).

As one can see in the analysis of the MFI of CD86 on mature cDC, significantly lower values were observed in B7-H1 KO spleens compared to WT spleens in all four groups (Fig.3.2.5.4 E). Between the single groups in spleens of treated WT and B7-H1 KO tumor-bearing mice, no significant difference in values of CD86 MFI was found between the control and the treatment groups in spleens from both the WT and B7-H1 KO mice (Fig.3.2.5.4 F,H).

Furthermore, for WT tumors, no significant difference was measured for the MFI of CD86 when we compared treatment groups to the control (Fig.3.2.5.4 G).

## Results

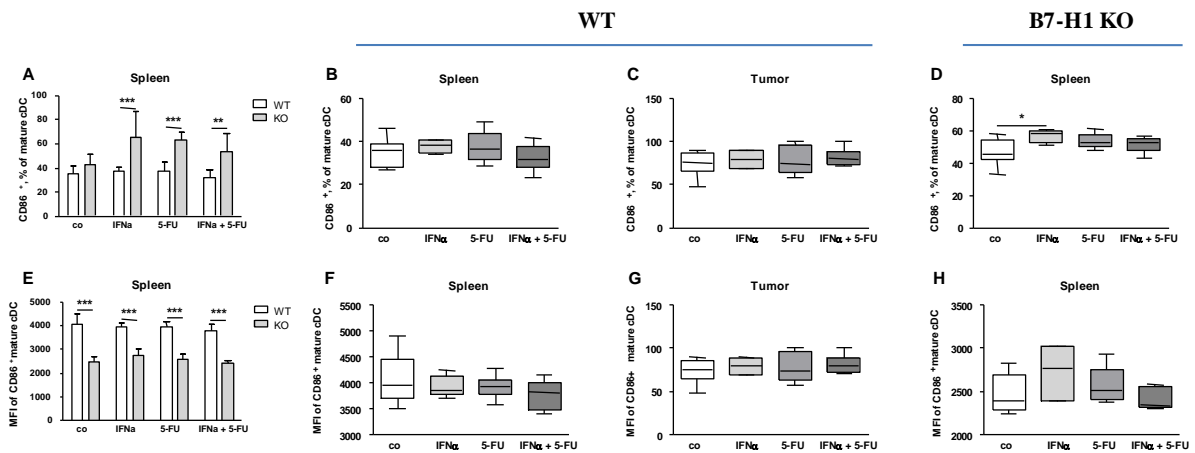


**Fig.3.2.5. 4 Quantification of CD86 expression on mature cDC in spleens and tumors from tumor-bearing WT and B7-H1 KO mice with and without treatment (co).**

Mice were treated with IFN $\alpha$ , 5-FU or the combination of IFN $\alpha$ +5-FU on Day 5, 7 and 9 after Panc02 implantation. Untreated mice were used as control. Four weeks after surgery, the mice were killed and the organs were eviscerated. Single-cell suspensions of spleens and tumors were stained with fluorescence labeled specific antibodies. The frequency of CD86<sup>+</sup> mature cDC was, together with the MFI of CD86, analyzed by flow cytometry. Data from four independent experiments are presented as column bar graphs and box plots with SEM ((spleens: n = 9 for co, and n = 6 for IFN $\alpha$ ; 5-FU; IFN $\alpha$ +5-FU; tumors: n = 7 for co, n = 4-6 for IFN $\alpha$ ; 5-FU; IFN $\alpha$ +5-FU); \*\*p<0.01, \*\*\*p<0.001; control groups vs. treatment groups; two-way (A,E) and one-way (B,C,D,F,G,H) ANOVA)

Next, we analyzed the expression of the regulatory molecule B7-H1 on cDC in WT, respectively B7-DC in B7-H1 KO tumor-bearing mice. In spleens of WT mice, no significant difference in the frequency of B7-H1<sup>+</sup> cDC was seen between treated and control animals (Fig.3.2.5.5 A). For the expression of B7-H1 molecule on cDC in WT tumors, similar values were found between the treatment groups and the control group (Fig.3.2.5.5 B). By comparing treatments and control of B7-H1 KO spleens, no significant difference in B7-DC expression on WT cDC was observed (Fig.3.2.5.5 C).

Analyzing the B7-H1 MFI on cDC in WT spleens, no significant difference was determined for the treatment groups compared to the control group (Fig.3.2.5.5 D). In WT tumors, we found no statistically significant difference in B7-H1 MFI of cDC between treated mice and control mice (Fig.3.2.5.5 E). However, in spleens of B7-H1

## Results

KO mice, a significantly higher B7-DC MFI was found in the group of IFN $\alpha$  treatment compared to control (Fig.3.2.5.5 F).

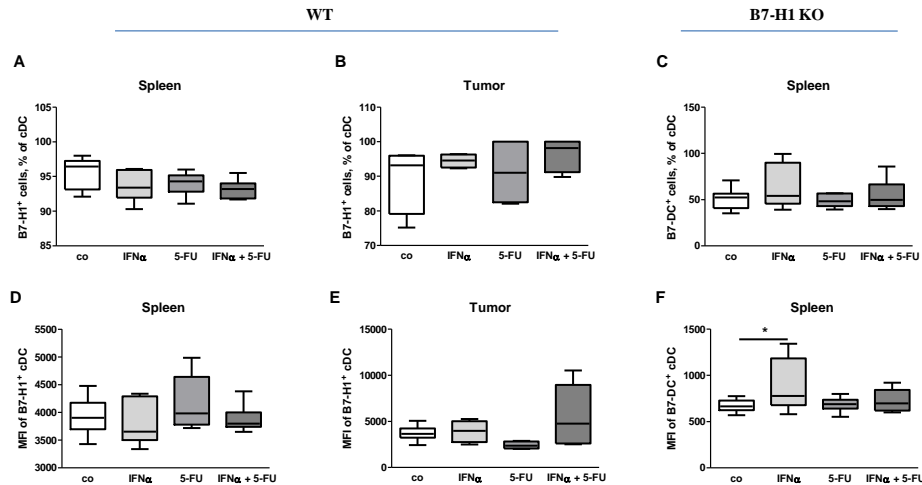


**Fig.3.2.5. 5 Quantification of B7-H1/B7-DC expression on cDC in spleens and tumors from tumor-bearing WT and B7-H1 KO mice with and without treatment (co).**

Mice were treated with IFN $\alpha$ , 5-FU or the combination of IFN $\alpha$ +5-FU on Day 5, 7 and 9 after Panc02 implantation. Untreated mice were used as control. Four weeks after surgery, the mice were killed and the organs were eviscerated. Single-cell suspensions of spleens and tumors were stained with fluorescence labeled specific antibodies. The frequency of B7-H1/B7-DC<sup>+</sup> cDC together with the MFI of B7-H1/B7-DC was analyzed by flow cytometry. Data from four independent experiments are presented as box plots with SEM ((spleens: n = 9 for co, and n = 6 for IFN $\alpha$ ; 5-FU; IFN $\alpha$ +5-FU; tumors: n = 7 for co, n = 4-6 for IFN $\alpha$ ; 5-FU; IFN $\alpha$ +5-FU); \*p<0.05; control group vs. treatment groups; one-way (A,B,C,D,F) ANOVA)

After we had analyzed the population of cDC, we then took a detailed look at the pDC population. By comparing the frequencies of pDC out of all leucocytes between spleens of WT and B7-H1 KO tumor-bearing mice, no significant difference was found between both mouse strains in all four groups (Fig.3.2.5.6 A). As we looked at the single groups of WT and B7-H1 KO in more detail, no significant difference in the ratio of pDC was seen between the treatment groups and control, in splenocytes from both the WT and B7-H1 KO tumor-bearing mice (Fig.3.2.5.6 B,D).

## Results

In tumors of WT mice, the percentages of pDC in the control showed no significant difference compared to the treatment groups (Fig.3.2.5.6 C).

The analysis of the frequencies of mature pDC revealed highly significant increases in the spleens of B7-H1 KO tumor-bearing mice compared to WT spleens throughout all four groups (Fig.3.2.5.6 E). Between the control and treatment groups in WT spleens, a significant decrease in percentage of mature pDC was found in the group of IFN $\alpha$ +5-FU compared to the control group (Fig.3.2.5.6 F). We observed no significant difference in the percentages of mature pDC between the control and treatment groups of B7-H1 KO (Fig.3.2.5.6 H).

In tumors of WT mice, no significant difference was seen for the frequencies of mature pDC between the treatment groups and the control (Fig.3.2.5.6 G).

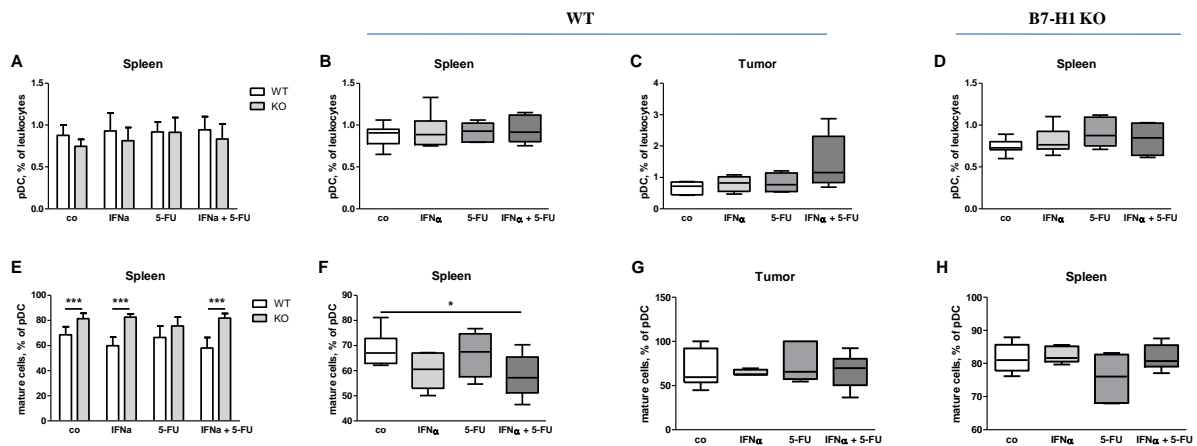


**Fig.3.2.5. 6 Quantification of pDC and their maturation status in spleens and tumors from tumor-bearing WT and B7-H1 KO mice with and without treatment (co).**

Mice were treated with IFN $\alpha$ , 5-FU or the combination of IFN $\alpha$ +5-FU on Day 5, 7 and 9 after Panc02 implantation. Untreated mice were used as control. Four weeks after surgery, the mice were killed and the organs were eviscerated. Single-cell suspensions of spleens and tumors were stained with fluorescence labeled specific antibodies. The frequencies of pDC and mature pDC were analyzed by flow cytometry. Data from four independent experiments are presented as column bar graphs and box plots with SEM ((spleens: n = 9 for co, and n = 6 for IFN $\alpha$ ; 5-FU; IFN $\alpha$ +5-FU; tumors: n = 7 for co, n = 4-6 for IFN $\alpha$ ; 5-FU; IFN $\alpha$ +5-FU); \*p<0.05; control group vs. treatment groups; two-way (A,E) and one-way (B,C,D,F,G,H) ANOVA)

The analysis of CD80 molecule expression on mature pDC revealed a tendency of higher percentages in spleens of WT mice compared to spleens of B7-H1 KO tumor-bearing mice throughout all treatment groups and the controls (Fig.3.2.5.7 A). Between the single groups of either WT or B7-H1 KO spleens in comparison, no significant difference in the ratio of CD80<sup>+</sup> mature pDC was determined between treatment groups and control, in both the WT and B7-H1 KO mice (Fig.3.2.5.7 B,D).

For WT tumors, no significant change in percentages of CD80<sup>+</sup> mature pDC was observed between the treatments and the control (Fig.3.2.5.7 C).

When examining the MFI of CD80 molecule on mature pDC, the comparison of the groups of WT and B7-H1 KO spleens (Fig.3.2.5.7 E), as well as the comparison of the single groups of either WT or B7-H1 KO spleens, no significant difference between treatment groups and the control (Fig.3.2.5.7 F,H) was revealed.

The MFI of CD80 on mature pDC of WT tumors showed no significant difference between the single treatment groups and the control group (Fig.3.2.5.7 G).

## Results

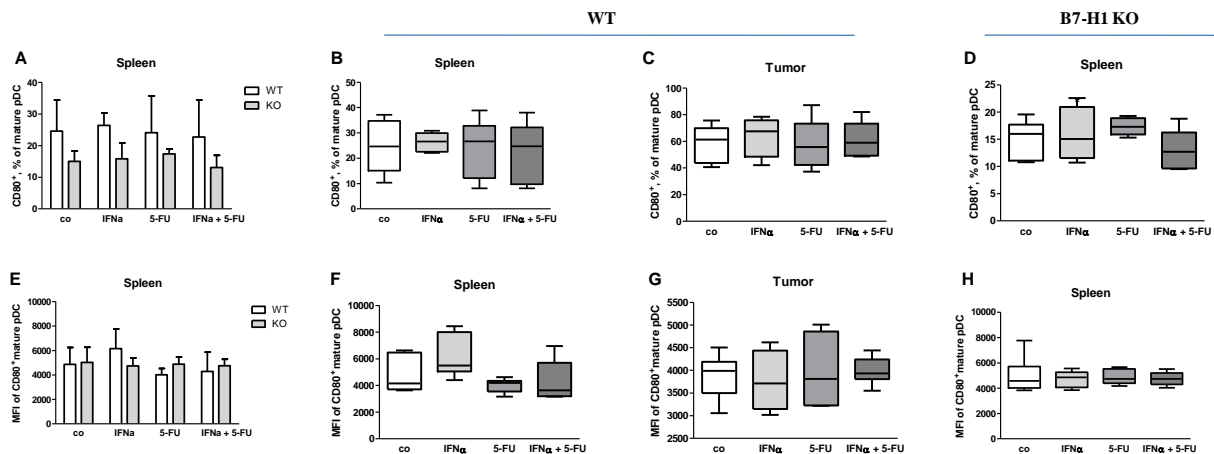


**Fig.3.2.5. 7 Quantification of CD80 expression on mature pDC in spleens and tumors from tumor-bearing WT and B7-H1 KO mice with and without treatment (co).**

Mice were treated with IFN $\alpha$ , 5-FU or the combination of IFN $\alpha$ +5-FU on Day 5, 7 and 9 after Panc02 implantation. Untreated mice were used as control. Four weeks after surgery, the mice were killed and the organs were eviscerated. Single-cell suspensions of spleens and tumors were stained with fluorescence labeled specific antibodies. The frequency of CD80<sup>+</sup> mature pDC together with the MFI of CD80 was analyzed by flow cytometry. Data from four independent experiments are presented as column bar graphs and box plots with SEM ((spleens: n = 9 for co, and n = 6 for IFN $\alpha$ ; 5-FU; IFN $\alpha$ +5-FU; tumors: n = 7 for co, n = 4-6 for IFN $\alpha$ ; 5-FU; IFN $\alpha$ +5-FU); \*p<0.05, \*\*p<0.01; control group vs. treatment groups; two-way (A,E) and one-way (B,C,D,F,G,H) ANOVA)

In addition to the molecule CD80, we analyzed the expression of CD86 molecule on mature pDC. In the analysis of WT and B7-H1 KO spleens in comparison, no significant difference in the frequency of CD86<sup>+</sup> mature pDC was recognized in all four groups (Fig.3.2.5.8 A). By looking at WT and B7-H1 KO spleens separately, similar ratios of CD86<sup>+</sup> mature pDC were found when we compared treatments to the control, in spleens from both groups of WT and B7-H1 KO tumor-bearing mice (Fig.3.2.5.8 B,D).

In WT tumors, no significant difference in percentages of CD86<sup>+</sup> mature pDC was registered between the treatment groups and the control (Fig.3.2.5.8 C).

Furthermore, the values of the measured MFI of CD86 of mature pDC showed no significant difference between the groups of WT and B7-H1 KO spleens (Fig.3.2.5.8 E). In groups of WT and B7-H1 KO spleens in detail, no significant difference in the

## Results

values of CD86 MFI was observed between the treatment groups compared to the control, in both of the tumor-bearing mouse strains (Fig.3.2.5.8 F,H).

The CD86 MFI of mature pDC in WT tumors showed no significant difference between the treatment groups and the control (Fig.3.2.5.8 G).

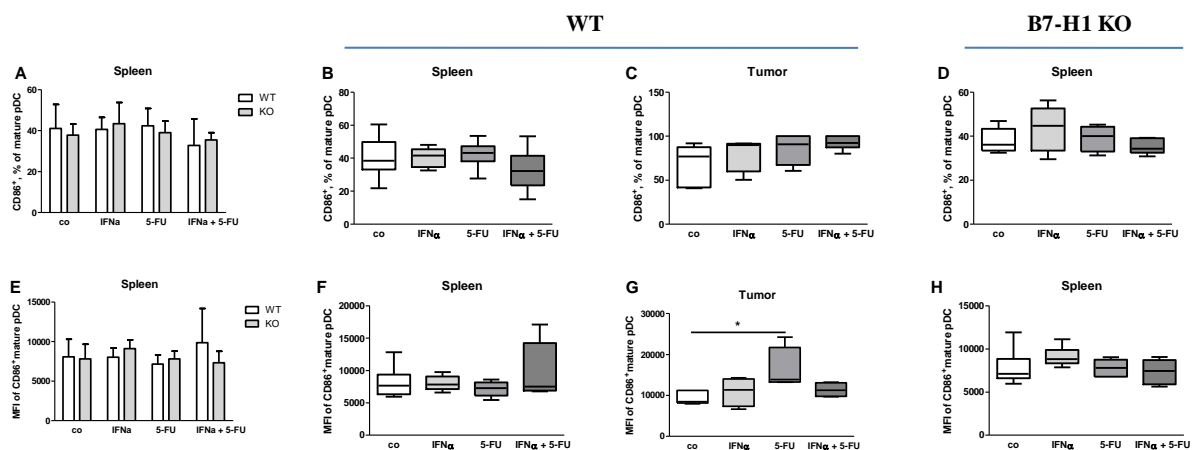


**Fig.3.2.5. 8 Quantification of CD86 expression on mature pDC in spleens and tumors from tumor-bearing WT and B7-H1 KO mice with and without treatment (co).**

Mice were treated with IFN $\alpha$ , 5-FU or the combination of IFN $\alpha$ +5-FU on Day 5, 7 and 9 after Panc02 implantation. Untreated mice were used as control. Four weeks after surgery, the mice were killed and the organs were eviscerated. Single-cell suspensions of spleens and tumors were stained with fluorescence labeled specific antibodies. The frequency of CD86<sup>+</sup> mature pDC together with the MFI of CD86 was analyzed by flow cytometry. Data from four independent experiments are presented as column bar graphs and box plots with SEM ((spleens: n = 9 for co, and n = 6 for IFN $\alpha$ ; 5-FU; IFN $\alpha$ +5-FU; tumors: n = 7 for co, n = 4-6 for IFN $\alpha$ ; 5-FU; IFN $\alpha$ +5-FU); control group vs. treatment groups; two-way (A,E) and one-way (B,C,D,F,G,H) ANOVA)

In this part of the experiment, we examined the B7-H1 expression on pDC in WT mice, and the B7-DC expression on pDC in B7-H1 KO tumor-bearing mice. The frequency of B7-H1 expression on pDC in WT spleens showed no significant difference between the control and treatment groups (Fig.3.2.5.9 A). In tumors of WT mice, the frequencies of B7-H1<sup>+</sup> pDC were similar between the treatment groups and the control (Fig.3.2.5.9 B). In spleens of B7-H1 KO mice, no significant difference in

## Results

the ratio of B7-DC<sup>+</sup> pDC was determined in the comparison of treatment groups to the control group (Fig.3.2.5.9 C).

The analysis of B7-H1 MFI of pDC revealed no significant difference in values between the treatment groups and the control in both spleens and tumors of WT mice (Fig.3.2.5.9 D,E). For the B7-DC MFI of pDC in B7-H1 KO spleens, similar values were determined for the treatment groups compared to the control (Fig.3.2.5.9 F).

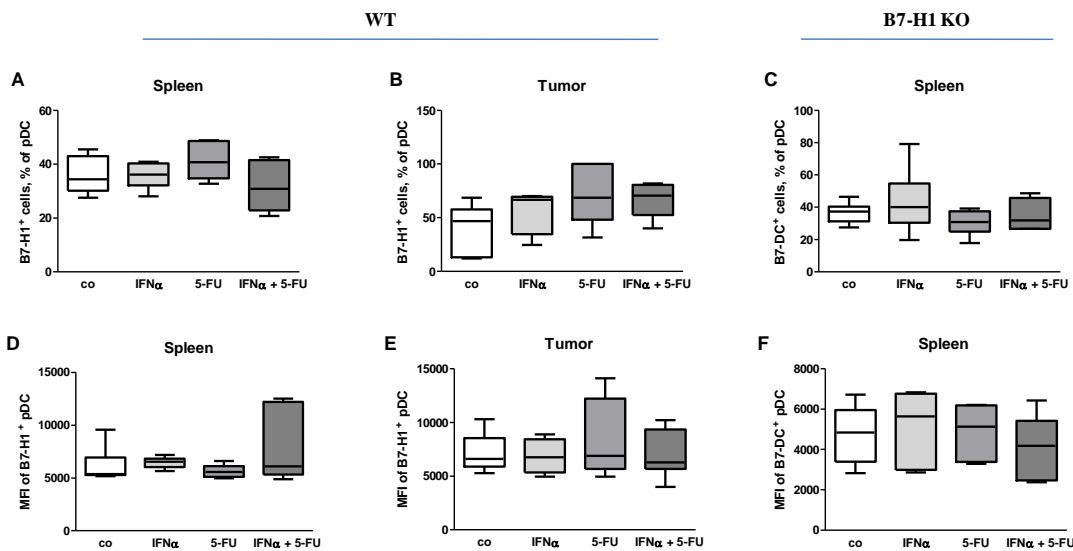


**Fig.3.2.5. 9 Quantification of B7-H1/B7-DC expression of pDC in spleens and tumors of tumor-bearing WT and B7-H1 KO mice with and without treatment (co).**

Mice were treated with IFN $\alpha$ , 5-FU or the combination of IFN $\alpha$ +5-FU on Day 5, 7 and 9 after Panc02 implantation. Untreated mice were used as control. Four weeks after surgery, the mice were killed and the organs were eviscerated. Single-cell suspensions of spleens and tumors were stained with fluorescence labeled specific antibodies. The frequency of B7-H1/B7-DC<sup>+</sup> pDC together with the MFI of B7-H1/B7-DC was analyzed by flow cytometry. Data from four independent experiments are presented as box plots with SEM ((spleens: n = 9 for co, and n = 6 for IFN $\alpha$ ; 5-FU; IFN $\alpha$ +5-FU; tumors: n = 7 for co, n = 4-6 for IFN $\alpha$ ; 5-FU; IFN $\alpha$ +5-FU); control group vs. treatment groups; one-way (A,B,C,D,F) ANOVA)

To summarize the results seen in the analysis of the DC populations, no significant differences were found in the comparison of WT and B7-H1 KO spleens from tumor-bearing mice. Between the different treatments compared to the control of either WT or B7-H1 KO spleens, occasional significant differences were observed.

### **3.3 Effects of chemo (5-FU) - and immunotherapy (IFN $\alpha$ ) on cytokine concentration in blood serum of tumor-bearing WT and B7-H1 KO mice**

In order to investigate the *in vivo* effect of 5-FU and IFN $\alpha$  treatment on systemic cytokine production in tumor-bearing WT and B7-H1 KO mice, we treated them with either IFN $\alpha$ , 5-FU or the combination of IFN $\alpha$ +5-FU on Day 5, 7 and 9 after Panc02 implantation. One group was kept untreated and used as the control. After a period of four weeks the mice were killed, the serum samples collected and analyzed for the presence of Transforming growth factor beta (TGF- $\beta$ ), Interleukin-1 beta (IL-1 $\beta$ ), Interleukin-2 (IL-2), Interleukin-6 (IL-6) and Vascular endothelial growth factor (VEGF) using Luminex approaches. We compared the determined cytokine production between WT and B7-H1 KO mice as well as between different treatment groups for WT or B7-H1 KO mice separately.

For TGF- $\beta$ , there was no significant difference measured between untreated control WT and B7-H1 KO tumor-bearing mice (Fig.3.3.1 A). Moreover, we did not find any significant differences between control and therapy groups for both the WT and B7-H1 KO mice (Fig.3.3.1 B,C).

## Results

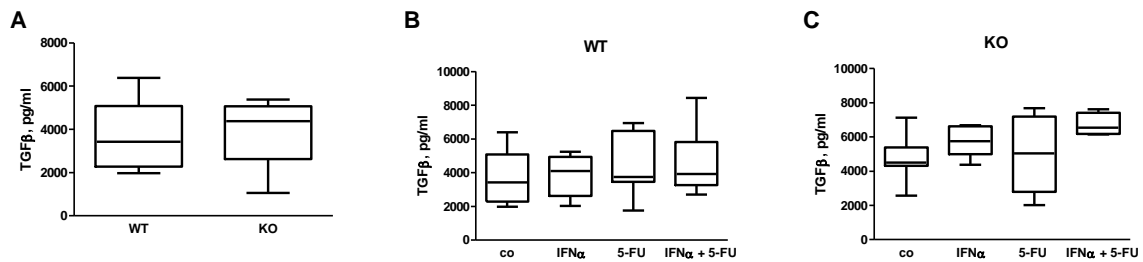


**Fig.3.3. 1 Quantification of TGF- $\beta$  in serum samples of WT and B7-H1 KO tumor-bearing mice with and without treatment (co).**

Mice were treated on Day 5, 7 and 9 after Panc02 implantation with IFN $\alpha$ , 5-FU or the combination of IFN $\alpha$ +5-FU. Four weeks after the surgery, blood was collected prior to killing of the mice. After clotting and centrifugation, the serum was processed by Luminex approach. The amount of TGF- $\beta$  was measured and analyzed using Bio-Plex Manager 4.0. Data from four independent experiments are presented as box plots with SEM ((splens: n = 9 for co, and n = 6 for IFN $\alpha$ ; 5-FU; IFN $\alpha$ +5-FU; tumors: n = 7 for co, n = 4-6 for IFN $\alpha$ ; 5-FU; IFN $\alpha$ +5-FU); control group vs. treatment groups; *T*-test (A) and one-way (B,C) ANOVA)

Assessing the cytokine IL-1 $\beta$ , significantly lower amounts of IL-1 $\beta$  were found in the untreated control B7-H1 KO compared to WT tumor-bearing mice (Fig.3.3.2 A). In the analysis of the WT groups, no significant difference was seen between the treated and control groups (Fig.3.3.2 B), whereas in B7-H1 KO mice, the concentration of IL-1 $\beta$  was significantly increased in IFN $\alpha$  and IFN $\alpha$ +5-FU groups as compared with the control (Fig.3.3.2 C).

## Results

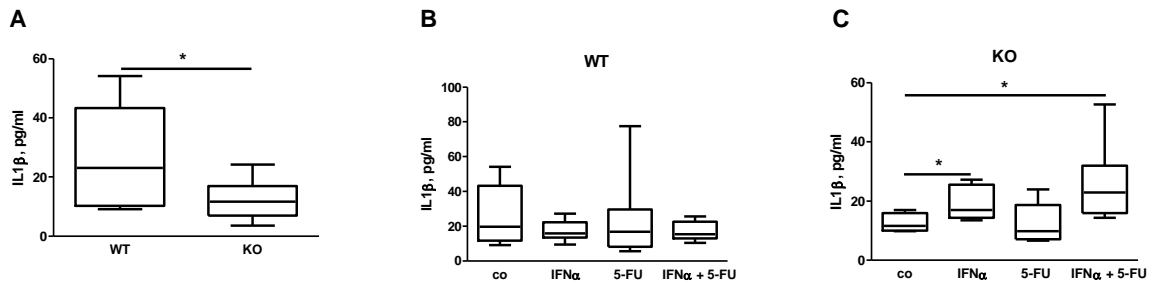


**Fig.3.3. 2 Quantification of IL-1 $\beta$  in serum samples of WT and B7-H1 KO mice with and without treatment (co).**

Mice were treated on Day 5, 7 and 9 after Panc02 implantation with IFN $\alpha$ , 5-FU or the combination of IFN $\alpha$ +5-FU. Four weeks after the surgery, blood was collected prior to killing of the mice. After clotting and centrifugation, the serum was processed by Luminex approach. The amount of IL-1 $\beta$  was measured and analyzed using Bio-Plex Manager 4.0. Data from four independent experiments are presented as box plots with SEM ((splens: n = 9 for co, and n = 6 for IFN $\alpha$ ; 5-FU; IFN $\alpha$ +5-FU; tumors: n = 7 for co, n = 4-6 for IFN $\alpha$ ; 5-FU; IFN $\alpha$ +5-FU); \*p<0.05; control group vs. treatment groups; T-test (A) and one-way (B,C) ANOVA)

The comparison between untreated control WT and B7-H1 KO tumor-bearing mice showed no significant difference in the concentration of IL-2 (Fig.3.3.3 A). Looking at WT alone, a significant increase of IL-2 concentration was measured in the samples of IFN $\alpha$ +5-FU treated animals as compared with WT control (Fig.3.3.3 B). However, in B7-H1 KO significantly higher amounts of IL-2 were seen in the group of 5-FU compared to the control (Fig3.3.3 C).

## Results

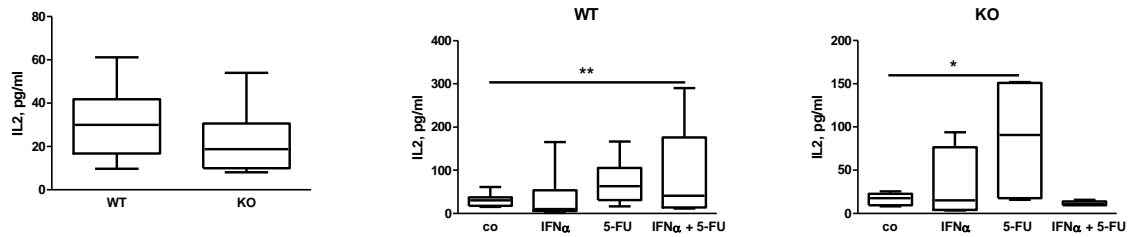


**Fig.3.3. 3 Quantification of IL-2 in serum samples of WT and B7-H1 KO mice with and without treatment (co).**

Mice were treated on Day 5, 7 and 9 after Panc02 implantation with IFN $\alpha$ , 5-FU or the combination of IFN $\alpha$ +5-FU. Four weeks after the surgery, blood was collected prior to killing of the mice. After clotting and centrifugation, the serum was processed by Luminex approach. The amount of IL-2 was measured and analyzed using Bio-Plex Manager 4.0. Data from four independent experiments are presented as box plots with SEM ((splens: n = 9 for co, and n = 6 for IFN $\alpha$ ; 5-FU; IFN $\alpha$ +5-FU; tumors: n = 7 for co, n = 4-6 for IFN $\alpha$ ; 5-FU; IFN $\alpha$ +5-FU); \*p<0.05, \*\*p<0.001; control group vs. treatment groups; T-test (A) and one-way (B,C) ANOVA)

For the IL-6 cytokine, no significant difference in the concentration was found between untreated control WT and B7-H1 KO tumor-bearing mice (Fig.3.3.4 A). A significant increase of the IL-6 amount was found in the WT animals treated with IFN $\alpha$ +5-FU as compared to the control (Fig.3.3.4 B). However, in the B7-H1 KO mice, a significant increase was found in the 5-FU group compared to the control (Fig.3.3.4 C).

## Results

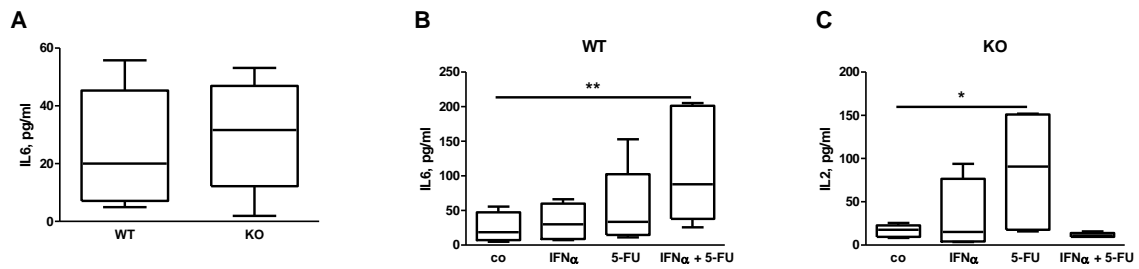


**Fig.3.3.4 Quantification of IL-6 in serum samples of WT and B7-H1 KO mice with and without treatment (co).**

Mice were treated on Day 5, 7 and 9 after Panc02 implantation with IFN $\alpha$ , 5-FU or the combination of IFN $\alpha$ +5-FU. Four weeks after the surgery, blood was collected prior to killing of the mice. After clotting and centrifugation, the serum was processed by Luminex approach. The amount of IL-6 was measured and analyzed using Bio-Plex Manager 4.0. Data from four independent experiments are presented as box plots with SEM ((splens: n = 9 for co, and n = 6 for IFN $\alpha$ ; 5-FU; IFN $\alpha$ +5-FU; tumors: n = 7 for co, n = 4-6 for IFN $\alpha$ ; 5-FU; IFN $\alpha$ +5-FU); \*p<0.05, \*\*p<0.01; control group vs. treatment groups; T-test (A) and one-way (B,C) ANOVA)

The last parameter we determined was VEGF. Between untreated control WT and B7-H1 KO tumor-bearing mice, a significantly lower amount of VEGF was found in B7-H1 KO mice compared to WT mice (Fig.3.3.5 A). Moreover, in WT samples, continued decreased levels were found between control, IFN $\alpha$ , 5-FU and IFN $\alpha$ +5-FU, with the lowest measured amounts of VEGF in the IFN $\alpha$ +5-FU sample (Fig.3.3.5 B). However, in B7-H1KO mice, no significant difference in VEGF concentration was determined between control and treatment groups (Fig.3.3.5 C).

## Results

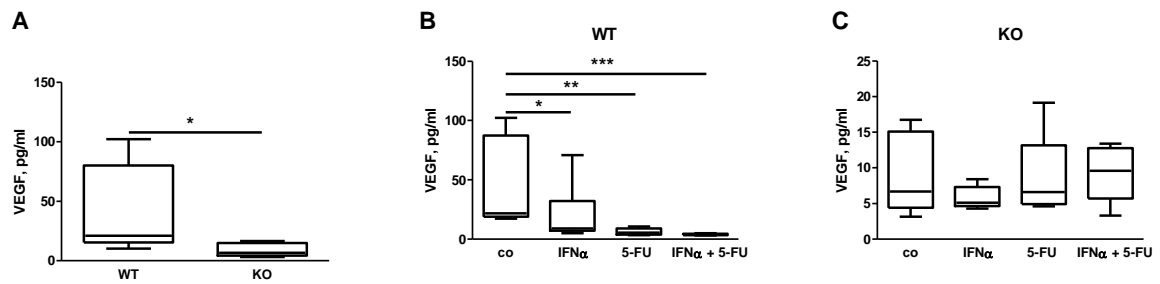


**Fig.3.3.5 Quantification of VEGF in serum samples of WT and B7-H1 KO mice with and without treatment (co).**

Mice were treated on Day 5, 7 and 9 after Panc02 implantation with IFN $\alpha$ , 5-FU or the combination of IFN $\alpha$ +5-FU. Four weeks after the surgery, blood was collected prior to killing of the mice. After clotting and centrifugation, the serum was processed by Luminex approach. The amount of VEGF was measured and analyzed using Bio-Plex Manager 4.0. Data from four independent experiments are presented as box plots with SEM ((splens: n = 9 for co, and n = 6 for IFN $\alpha$ ; 5-FU; IFN $\alpha$ +5-FU; tumors: n = 7 for co, n = 4-6 for IFN $\alpha$ ; 5-FU; IFN $\alpha$ +5-FU); \*p<0.05, \*\*p<0.01, \*\*\*p<0.001; control group vs. treatment groups; T-test (A) and one-way (B,C) ANOVA)

Taken together, in this experiment series where we analyzed *in vivo* cytokine production, we observed a significant difference in the cytokine production of IL-1 $\beta$  and VEGF between WT and B7-H1 KO tumor-bearing mice, with lower concentrations of both cytokines in the B7-H1 KO mice.

### **3.4 Role of B7-H1 expression on the functional phenotype of MDSC and on the sensitivity of splenocytes to MDSC mediated suppression**

#### **3.4.1 Effect of B7-H1 expression on the functional phenotype of MDSC**

In this first phase of this experiment series, we examined whether the presence of B7-H1 molecule has an effect on the functional phenotype of MDSC. To achieve this, we isolated MDSC from tumors of WT and B7-H1 KO mice using the MACS procedure and analyzed them with the help of flow cytometry. Their functional status was determined by assessing the iNOS and Arginase production from total MDSC as well as from their two subsets, granulocytic and monocytic MDSC.

The gating strategy for myeloid derived suppressor cells (MDSC) is shown in Fig.3.4.1.1. The FACS data (dot-plot, histogram) represent one typical result out of three independent experiments.

# Results

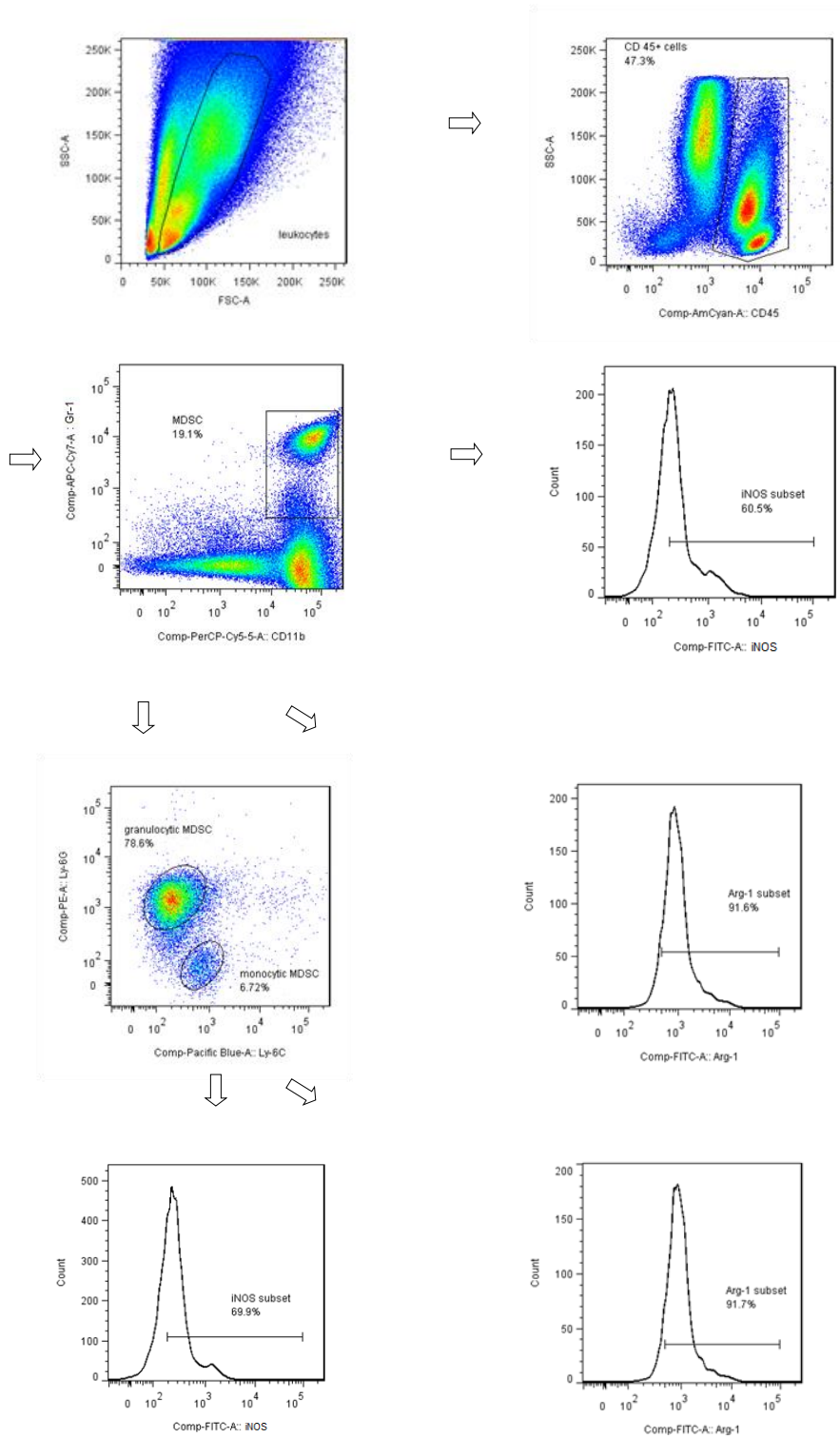


**Fig.3.4.1. 1 Gating strategy for MDSC in tumors of untreated tumor-bearing WT and B7-H1 KO mice using flow cytometry.**

Leukocytes were gated using FSC/SSC dot plot. Afterwards, we gated on CD45<sup>+</sup> cells and further on the cell population of Gr-1<sup>+</sup>CD11b<sup>+</sup> MDSC was marked. Then the two subsets of MDSC, granulocytic and monocytic MDSC were gated according to the expression of Ly-6G and Ly-6C. For the functional status, the iNOS<sup>+</sup> and Arginase<sup>+</sup> subsets were determined from all MDSC as well as from both subsets using histograms. All positive gates were set according to FMO controls.

First we determined the frequency of MDSC out of all leukocytes. A significantly lower percentage of MDSC was observed in tumors of B7-H1 KO mice compared to tumors of WT mice (Fig.3.4.1.2).

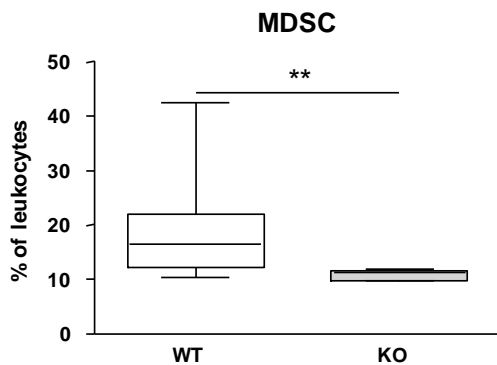


**Fig.3.4.1. 2 Quantification of MDSC in tumors of untreated tumor-bearing WT and B7-H1 KO mice.**

Four weeks after Panc02 implantation, the mice were killed and their organs were eviscerated. Single-cell suspensions of tumors were stained with specific antibodies. The frequency of MDSC was analyzed by flow cytometry. Data from three independent experiments are presented as box plots with SEM (( n = 15 for WT, and n = 5 for KO);\*\*p<0.01; T-test)

Next, we looked at the percentages of iNOS<sup>+</sup> cells out of total MDSC in WT and B7-H1 KO tumor-bearing mice. As one can see in Fig.3.4.1.3, no significant change in frequencies of iNOS<sup>+</sup> MDSC was seen between WT and B7-H1 KO tumor-bearing

mice. The iNOS MFI from MDSC showed no significant change in values between both the WT and B7-H1 KO mice.

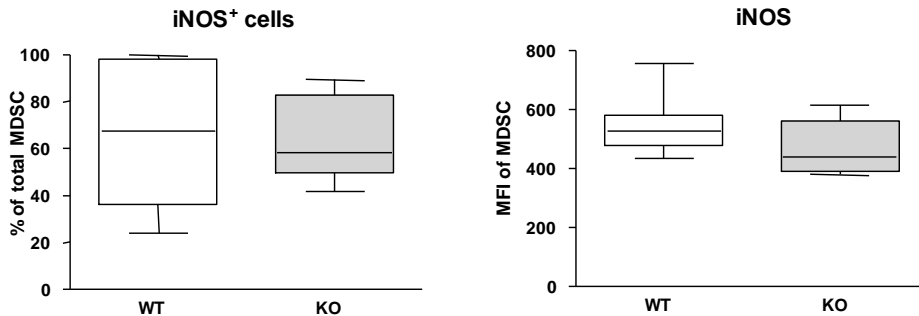


**Fig.3.4.1.3 Quantification of iNOS<sup>+</sup> cells of the total MDSC in tumors of untreated tumor-bearing WT and B7-H1 KO mice.**

Four weeks after Panc02 implantation, the mice were killed and their organs were eviscerated. Single-cell suspensions of tumors were stained with specific antibodies. The frequency of iNOS<sup>+</sup> cells, together with the MFI for iNOS, was analyzed by flow cytometry. Data from three independent experiments are presented as box plots with SEM (n = 15 for WT, and n = 5 for KO; T-test)

The analysis of WT tumors revealed no significant difference in the percentages of Arg<sup>+</sup> MDSC out of total MDSC as compared to those from B7-H1 KO tumors. When analyzing the MFI of Arg, no significant changes in values were detected between the samples of WT compared to samples of B7-H1 KO tumor-bearing mice (Fig.3.4.1.4).

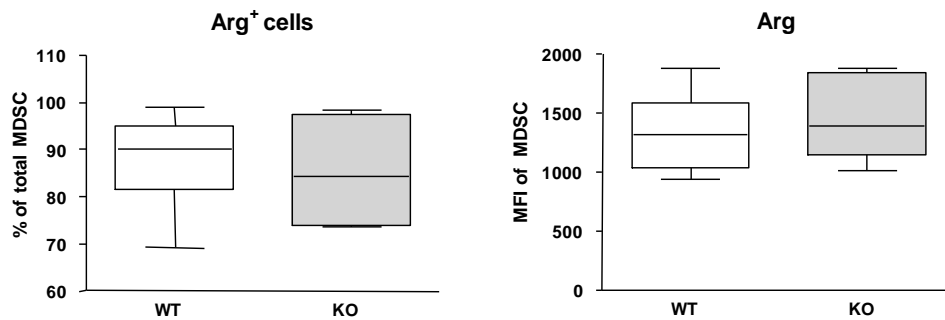


**Fig.3.4.1. 4 Quantification of Arg<sup>+</sup> cells of total MDSC in tumors of untreated tumor-bearing WT and B7-H1 KO mice.**

Four weeks after Panc02 implantation, the mice were killed and their organs were eviscerated. Single-cell suspensions of tumors were stained with specific antibodies. The frequency of Arg<sup>+</sup> cells, together with the MFI for Arg, was analyzed by flow cytometry. Data from three independent experiments are presented as box plots with SEM (n = 15 for WT, and n = 5 for KO; *T*-test)

Furthermore, we analyzed the granulocytic (gMDSC) and monocytic (mMDSC) subsets of MDSC. Significantly lower percentages of gMDSC out of the total Gr-1<sup>+</sup> CD11b<sup>+</sup> population were seen in B7-H1 KO tumors compared to tumors of WT mice. For the mMDSC out of the total MDSC, a tendency towards higher frequencies was determined in B7-H1 KO mice compared to WT mice (Fig.3.4.1.5).

## Results

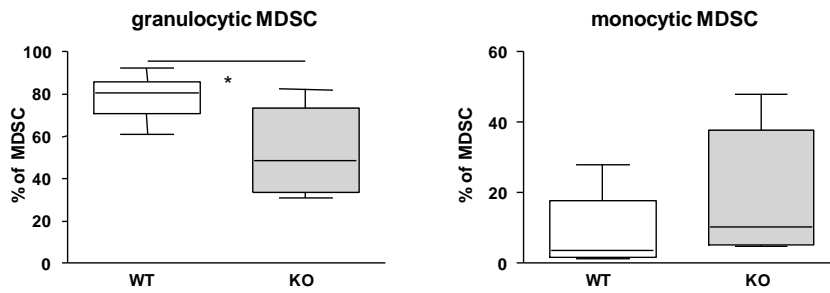


**Fig.3.4.1. 5 Quantification of granuloctytic and monocytic MDSC out of the total MDSC in tumors of untreated tumor-bearing WT and B7-H1 KO mice.**

Four weeks after Panc02 implantation, the mice were killed and their organs were eviscerated. Single-cell suspensions of tumors were stained with specific antibodies. The frequencies of granuloctytic and monocytic MDSC were analyzed by flow cytometry. Data from three independent experiments are presented as box plots with SEM (( n = 15 for WT, and n = 5 for KO);\*p<0.05; T-test )

Afterwards, we measured the frequencies of iNOS<sup>+</sup> and Arg<sup>+</sup> cells out of gMDSC. The analysis of iNOS<sup>+</sup> cells showed a clear tendency towards lower percentages for iNOS<sup>+</sup> gMDSC in tumors of B7-H1 KO mice compared to WT tumors. The MFI of iNOS from gMDSC showed no significant difference between WT and B7-H1 KO tumor-bearing mice. For the Arg production, no significant difference was determined between WT and B7-H1 KO mice. The MFI of Arg on gMDSC revealed no significant difference between both the WT and B7-H1 KO tumor-bearing mice (Fig.3.4.1.6).

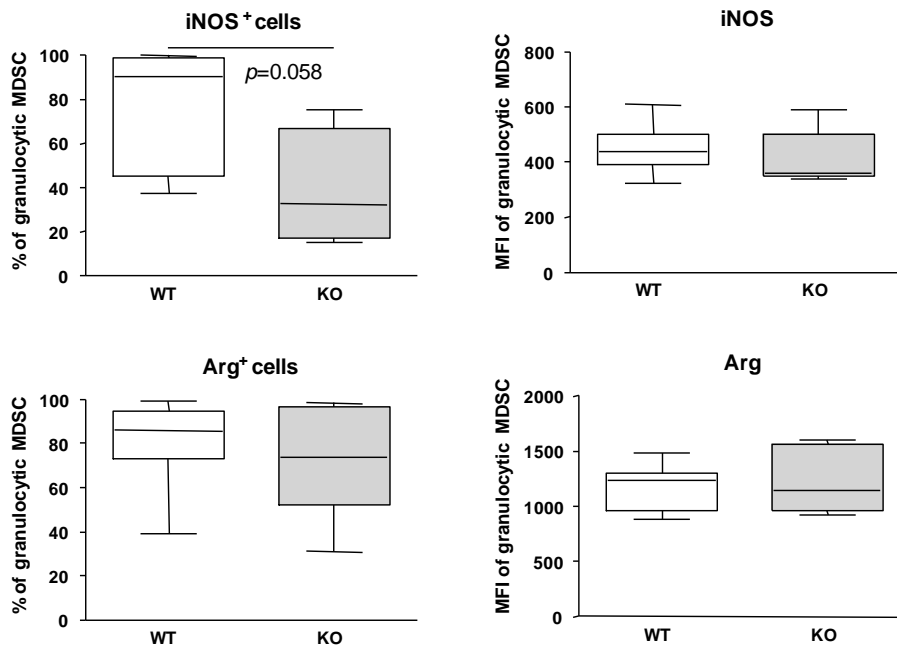


**Fig.3.4.1. 6 Quantification of iNOS<sup>+</sup> and Arg<sup>+</sup> cells out of granulocytic MDSC in tumors of untreated tumor-bearing WT and B7-H1 KO mice.**

Four weeks after Panc02 implantation, the mice were killed and their organs were eviscerated. Single-cell suspensions of tumors were stained with specific antibodies. The frequencies of iNOS<sup>+</sup> and Arg<sup>+</sup> cells, together with the MFI for iNOS and Arg, were analyzed by flow cytometry. Data from three independent experiments are presented as box plots with SEM (n = 15 for WT, and n = 5 for KO; T-test)

In B7-H1KO mice, the ratio of iNOS<sup>+</sup> cells within the mMDSC population was significantly lower compared to the WT mice. Beyond that, the iNOS MFI of mMDSC was significantly lower in B7-H1 KO mice compared to WT mice (Fig.3.4.1.7).

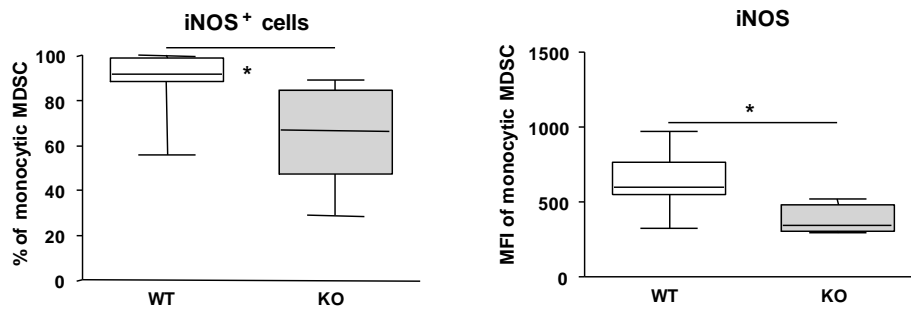


**Fig.3.4.1. 7 Quantification of iNOS<sup>+</sup> cells out of monocytic MDSC in tumors of untreated tumor bearing WT and KO mice.**

Four weeks after Panc02 implantation, the mice were killed and their organs were eviscerated. Single-cell suspensions of tumors were stained with specific antibodies. The frequency of iNOS<sup>+</sup> cells, together with the MFI for iNOS, was analyzed by flow cytometry. Data from three independent experiments are presented as box plots with SEM ((n = 15 for WT, and n = 5 for KO); \*p<0.05; T-test)

Taken together, this phase of the experiment series revealed a lower frequency of MDSC in B7-H1 KO tumor-bearing mice compared to WT mice. Furthermore, we detected a shift in the distribution of MDSC subsets, with lower ratios of gMDSC in B7-H1 KO tumor-bearing mice compared to WT mice. Concerning the functional status of MDSC, we observed a decrease in iNOS<sup>+</sup> MDSC of B7-H1 KO compared to the WT tumor-bearing mice.

### **3.4.2 Effect of B7-H1 expression on the sensitivity of splenocytes to MDSC mediated suppression**

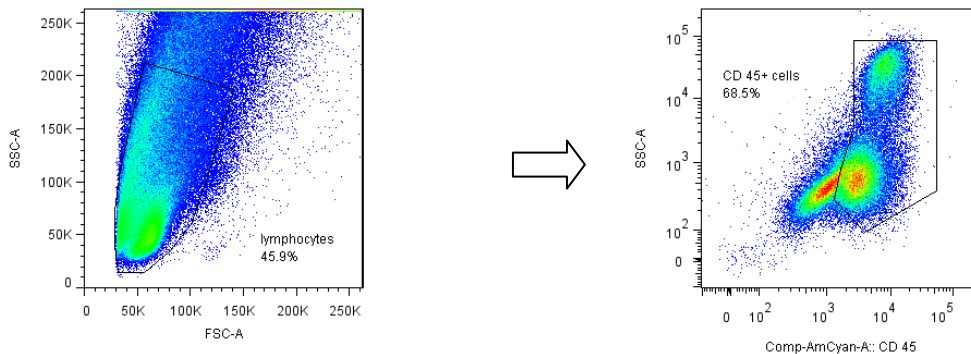
In this second part of this experiment series, we examined whether the presence of B7-H1 makes splenocytes from tumor-bearing mice more sensitive to MDSC mediated suppression. For this experiment, we cocultured the MACS isolated MDSC from tumors of WT mice with CFSE labeled splenocytes from WT and B7-H1KO tumor-bearing mice.

## Results

---

The experiment was performed in the presence/absence of CD3/CD28 activation. After 72 hours of incubation, we harvested the cells and analyzed them using flow cytometry. With the help of the CFSE labeling, we determined the proliferation status of the CD4<sup>+</sup>/CD8<sup>+</sup> T cell populations within splenocytes, and analyzed the inhibitory effect of MDSC on proliferated CD4<sup>+</sup>/CD8<sup>+</sup> T cells of WT and B7-H1 KO tumor-bearing mice.

The gating strategy for CD4<sup>+</sup> and CD8<sup>+</sup> T cells is shown in Fig.3.4.2.1. Here the intracellular panel was used because of the better CFSE performance. The FACS data (dot-plot, histogram) represent one typical result out of three independent experiments.



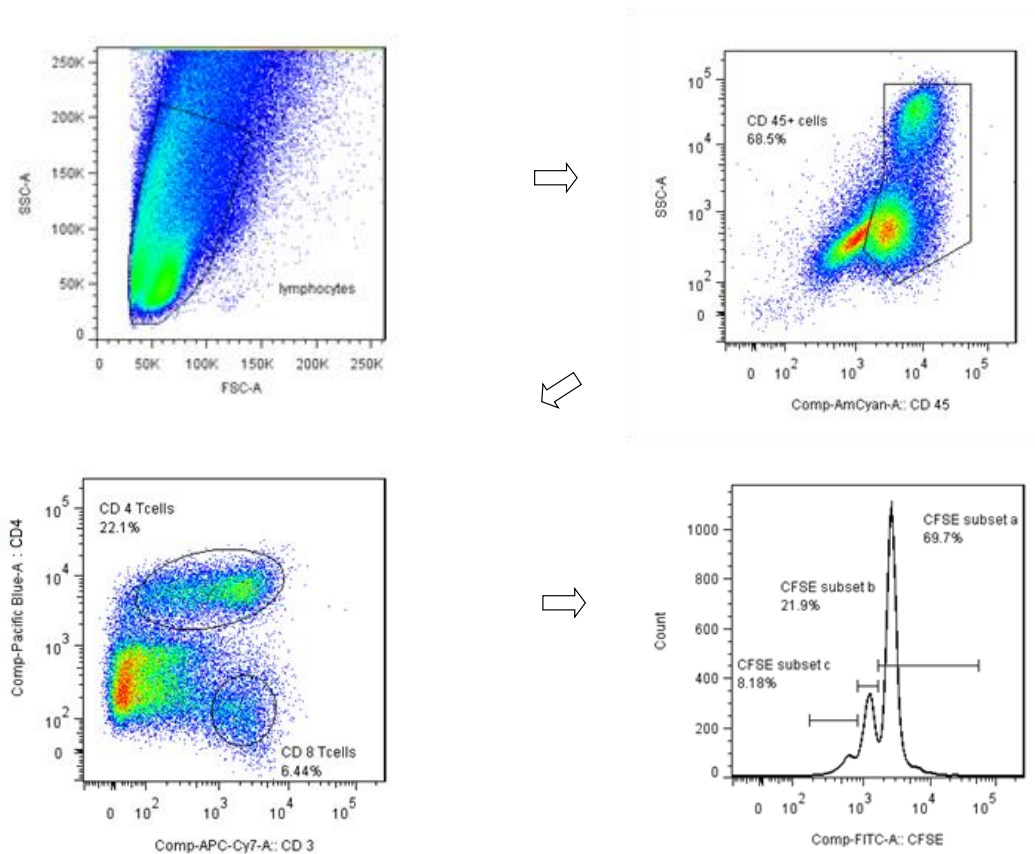


**Fig.3.4.2. 1 Gating strategy for CD4<sup>+</sup>/CD8<sup>+</sup> T cells in cocultures of MDSC and CFSE labeled splenocytes using flow cytometry.**

All activated and non-activated lymphocytes were gated using FSC/SSC dot plot. Furthermore, the CD45<sup>+</sup> cells were gated, and out of those we determined the CD4<sup>+</sup>/CD8<sup>+</sup> T cells. The proliferation status of CD4<sup>+</sup>/CD8<sup>+</sup> T cell population was determined and analyzed by the intensity of CFSE staining.

First, we determined the percentages of proliferated CD4<sup>+</sup> T cells out of all CD4<sup>+</sup> T cells and compared those between the cells of WT and B7-H1 KO mice. As expected, without prior cell activation no proliferation was seen; neither in WT nor in B7-H1 KO spleens. After activation, significantly higher ratios of proliferated CD4<sup>+</sup> T cells were seen in both the WT and B7-H1 KO mice (Fig.3.4.2.2 B,C). Moreover, a significant difference was seen between WT and B7-H1 KO mice, with lower percentages of proliferated CD4<sup>+</sup> T cells measured in B7-H1 KO mice compared to WT mice (Fig.3.4.2.2 A).

## Results

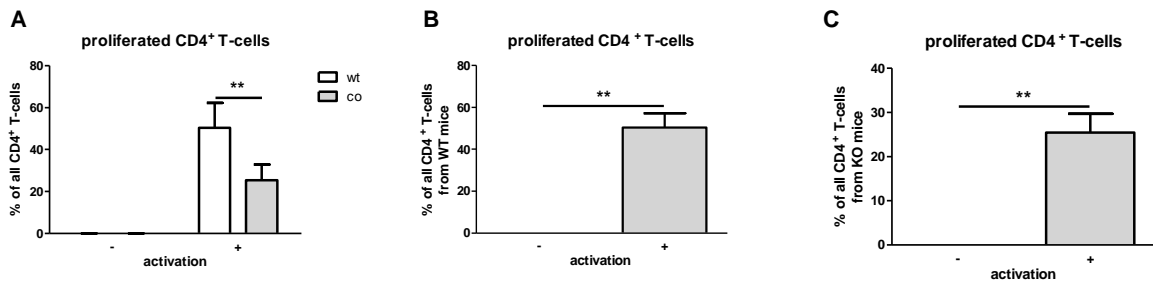


**Fig.3.4.2. 2 Quantification of proliferated CD4<sup>+</sup> T cells out of WT and B7-H1 KO splenocytes in culture.**

Four weeks after Panc02 implantation, the mice were killed and their organs eviscerated. Freshly isolated splenocytes were labeled with CFSE and cultured in the presence/ absence of CD3/CD28 antibody for 72 hours. Afterwards, the cells were stained with fluorescence labeled specific antibodies and analyzed by flow cytometry. Data from three independent experiments are presented as column bar graphs with SEM ((n = 15 for WT, and n = 5 for KO);\*\*p<0.01; two-way ANOVA (A) and T-test (B,C))

After we examined the activation and proliferation status of CD4<sup>+</sup> T cells, we analyzed whether MDSC from WT tumors could inhibit this proliferation, and if the splenocytes from WT and B7-H1 KO mice have different sensitivities to the MDSC mediated suppression. For this, we added WT MDSC to the activated splenocytes from either WT or B7-H1 KO mice. As one can see in Fig.3.4.2.3 B, a significant inhibition of proliferated CD4<sup>+</sup> T cells in the WT spleens was achieved after adding MDSC to the culture. In cultures of splenocytes from B7-H1 KO mice, also a clear tendency towards inhibition of proliferated CD4<sup>+</sup> T cells was measured after WT MDSCs were added (Fig.3.4.2.3 C). In Fig.3.4.2.3 A, the comparison between WT and B7-H1KO cultures is shown. The significant difference in the frequency of proliferated CD4<sup>+</sup> T cells between WT and B7-H1 KO splenocytes can be seen. After adding inhibitory MDSC to proliferated CD4<sup>+</sup> T cells, no significant difference in the percentage of inhibited cells was observed between cultures of WT and B7-H1 KO splenocytes (Fig.3.4.2.3 A).

## Results

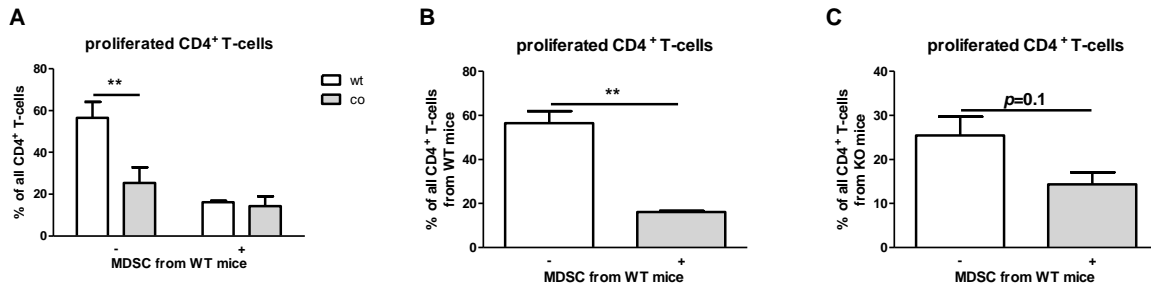


**Fig.3.4.2. 3 Effect of MDSC on proliferated CD4<sup>+</sup> T cells out of WT and B7-H1 KO splenocytes in coculture.**

Four weeks after Panc02 implantation, the mice were killed and their organs eviscerated. Freshly isolated splenocytes were labeled with CFSE and cultured in the presence/absence of CD3/CD28 antibody. WT MDSC were added to the culture. After 72 hours, the cells were stained with fluorescence labeled specific antibodies and the inhibitory effect of MDSC on proliferated CD4<sup>+</sup> T cells was analyzed by flow cytometry. Data from three independent experiments are presented as column bar graphs with SEM ((n = 15 for WT, and n = 5 for KO);\*\*p<0.01; two-way ANOVA (A) and T-test (B,C))

Afterwards, we analyzed the CD8<sup>+</sup> T cell population. Without activation with a CD3/CD28 antibody, no proliferation of CD8<sup>+</sup> T cells occurred. After activation, in cultures from both WT and B7-H1 KO mice, a significant increase in proliferated CD8<sup>+</sup> T cells out of all CD8<sup>+</sup> T cells was determined (Fig.3.4.2.4 B,C). As we compared WT and B7-H1 KO cultures to each other, no significant difference in the frequency of proliferated CD8<sup>+</sup> T cells was seen between WT and B7-H1 KO mice (Fig.3.4.2.4 A).

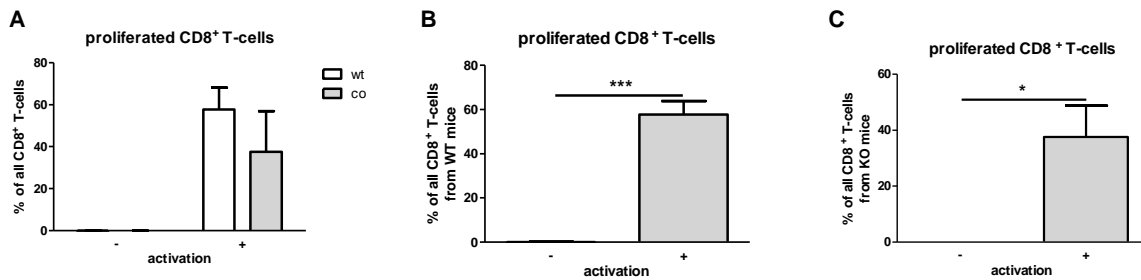


**Fig.3.4.2. 4 Quantification of proliferated CD8<sup>+</sup> T cells out of WT and B7-H1 KO splenocytes in culture.**

Four weeks after Panc02 implantation, the mice were killed and their organs eviscerated. Freshly isolated splenocytes were labeled with CFSE and cultured in the presence/ absence of CD3/CD28 antibody for 72 hours. Afterwards, the cells were stained with fluorescence labeled specific antibodies and analyzed by flow cytometry. Data from three independent experiments are presented as column bar graphs with SEM (n = 15 for WT, and n = 5 for KO); \*p<0.05, \*\*\*p<0.001; two-way ANOVA (A) and T-test (B,C)

After adding MDSC from the WT tumors to the activated cultures, a significant inhibition of proliferated CD8<sup>+</sup> T cells was observed in cultures of WT splenocytes (Fig.3.4.2.5 B). In the samples of B7-H1KO splenocytes, a tendency towards an inhibition of proliferated CD8<sup>+</sup> T cells was seen after adding MDSC from WT tumors to the cultures (Fig.3.4.2.5 C). For the percentages of proliferated CD8<sup>+</sup> T cells out of all CD8<sup>+</sup> T cells, a significant difference was found between splenocytes of WT and B7-H1KO mice, with lower proliferation in samples of B7-H1 KO mice. After adding inhibitory MDSC to proliferated CD8<sup>+</sup> T cells, no significant difference in the frequency of inhibited cells was observed between cultures of WT and B7-H1 KO splenocytes (Fig.3.4.2.5 A).

## Results

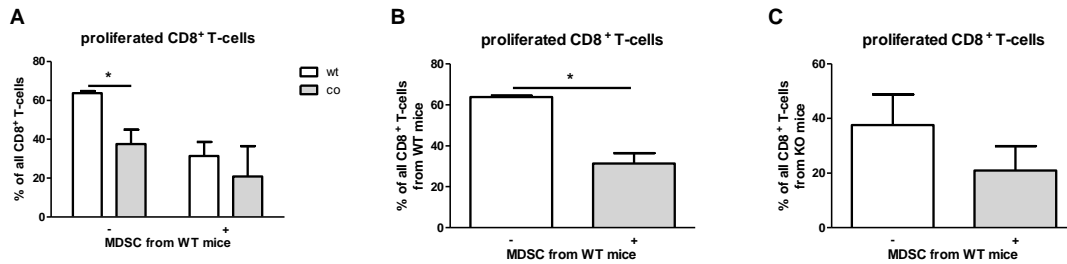


**Fig.3.4.2. Effect of MDSC on proliferated CD8<sup>+</sup> T cells out of WT and B7-H1 KO splenocytes in coculture.**

Four weeks after Panc02 implantation, the mice were killed and their organs eviscerated. Freshly isolated splenocytes were labeled with CFSE and cultured in the presence/absence of CD3/CD28 antibody. WT MDSC were added to the culture. After 72 hours, the cells were stained with fluorescence labeled specific antibodies and the inhibitory effect of MDSC on proliferated CD8<sup>+</sup> T cells was analyzed by flow cytometry. Data from three independent experiments are presented as column bar graphs with SEM ((n = 15 for WT, and n = 5 for KO); \*\*p<0.01; two-way ANOVA (A) and T-test (B,C))

Summarizing our results from this part of the experiment series, we observed that proliferation occurred after activation of CD4<sup>+</sup>/CD8<sup>+</sup> T cells from tumor-bearing mice. Furthermore, lower frequencies of proliferated CD4<sup>+</sup>/CD8<sup>+</sup> T cells were found in splenocytes of B7-H1 KO compared to WT mice. The inhibitory effect of WT MDSC on proliferated CD4<sup>+</sup>/CD8<sup>+</sup> T cells was seen in cultures of WT mice and B7-H1 KO tumor bearing mice.

### **3.5 Effects of B7-H1 presence on cytokines production in *in vitro* cocultures of WT/ B7-H1 KO splenocytes and WT MDSC**

In this experiment, we investigated the *in vitro* effect of a B7-H1 presence on cytokine production in cocultures of splenocytes from WT and B7-H1 KO tumor-bearing mice and WT MDSC (suppression assay). The MACS isolated MDSC from tumors of WT mice were cultivated with CFSE labeled splenocytes from WT and B7-H1 KO mice as in 3.4. The experiment was performed in the presence/ absence of CD3/CD28 activation. After 72 hours of incubation we collected the medium supernatants and analyzed those for the presence of IFN $\gamma$ , IL-1 $\beta$ , IL-2, IL-6, IL-10, VEGF and TGF- $\beta$  using Luminex approach. We compared the cytokine production of WT and B7-H1 KO splenocytes in the presence/ absence of CD3/CD28 activation. Moreover, we investigated the difference in cytokines production between WT and B7-H1 KO proliferated cells after their inhibition with MDSC.

First, we analyzed the cytokine IFN $\gamma$ . In WT samples, a significantly higher concentration of IFN $\gamma$  was found after activation of the cells with CD3/CD28 antibody (Fig.3.5.1 B). Also in the group of B7-H1 KO, a significant increase in IFN $\gamma$  concentration was found after activation of splenocytes (Fig.3.5.1 C). By comparing WT to B7-H1KO groups, one can see a significantly higher value of IFN $\gamma$  concentration in B7-H1 KO compared to WT for both the activated and non-activated splenocytes (Fig.3.5.1 A).

Next, we looked at the change in cytokine concentration after adding inhibitory MDSC to the activated samples. In samples containing WT MDSC, we saw a tendency to lower concentrations of IFN $\gamma$  compared to activated samples without WT MDSC in both groups of WT and B7-H1 KO splenocytes (Fig.3.5.1 E,F). In Fig.3.5.1 D, the comparison of IFN $\gamma$  concentration between cultures of WT and B7-H1 KO mice is

## Results

shown. No significant difference in the concentration of IFN $\gamma$  was determined when we compared activated WT and B7-H1 KO samples to each other. After adding inhibitory MDSC to activated cultures, no significant difference in the IFN $\gamma$  concentration was observed between cultures of WT and B7-H1 KO splenocytes (Fig.3.5.1 D).

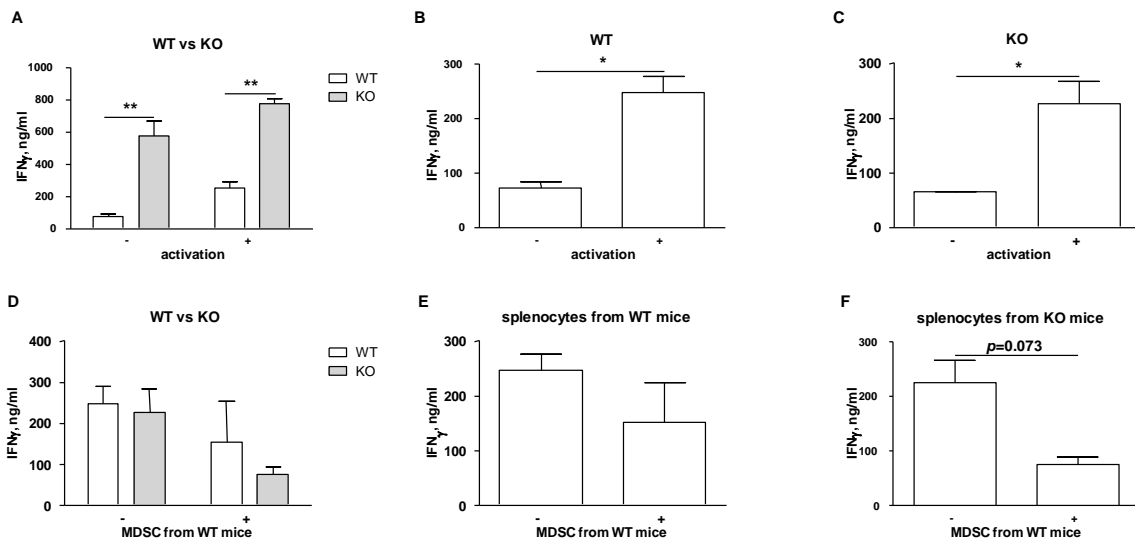


**Fig.3.5.1 Quantification of IFN $\gamma$  in supernatants from cocultures of WT or B7-H1 KO splenocytes (+/- activation) with and without MDSC from WT tumors.**

After 72 hours, the medium supernatant of the cocultures of CFSE labeled splenocytes and MDSC was collected and processed by Luminex approach. The concentration of IFN $\gamma$  was measured and analyzed using Bio-Plex Manager 4.0. Data are presented as column bar graphs with SEM (n =2-3; \*p<0.05, \*\*p<0.01; two-way ANOVA (A,D) and T-test (B,C,E,F))

For the cytokine IL-1 $\beta$ , no significant difference in concentrations was observed between samples with or without activation in the WT group (Fig.3.5.2 B). In B7-H1 KO, a tendency towards a higher IL-1 $\beta$  concentration was found in samples after activation with CD3/CD28 antibody compared to the ones without activation (Fig.3.5.2 C). Analyzing the IL-1 $\beta$  concentration of WT and B7-H1 KO in comparison, no significant difference was seen between WT and B7-H1 KO in both the activated and non-activated samples (Fig.3.5.2 A).

## Results

In the presence of inhibitory MDSC, no significant difference in IL-1 $\beta$  concentration was seen, neither in the WT group nor in the B7-H1 KO group, compared to samples without MDSC (Fig.3.5.2 E,F). In the analysis of WT and B7-H1KO groups in comparison, one sees in Fig.3.5.2 D no significant difference in the concentration of IL-1 $\beta$  in samples without MDSC. After adding inhibitory MDSC to activated cultures, no significant difference in the IFN $\gamma$  concentration was observed between cultures of WT and B7-H1 KO splenocytes (Fig.3.5.2 D).

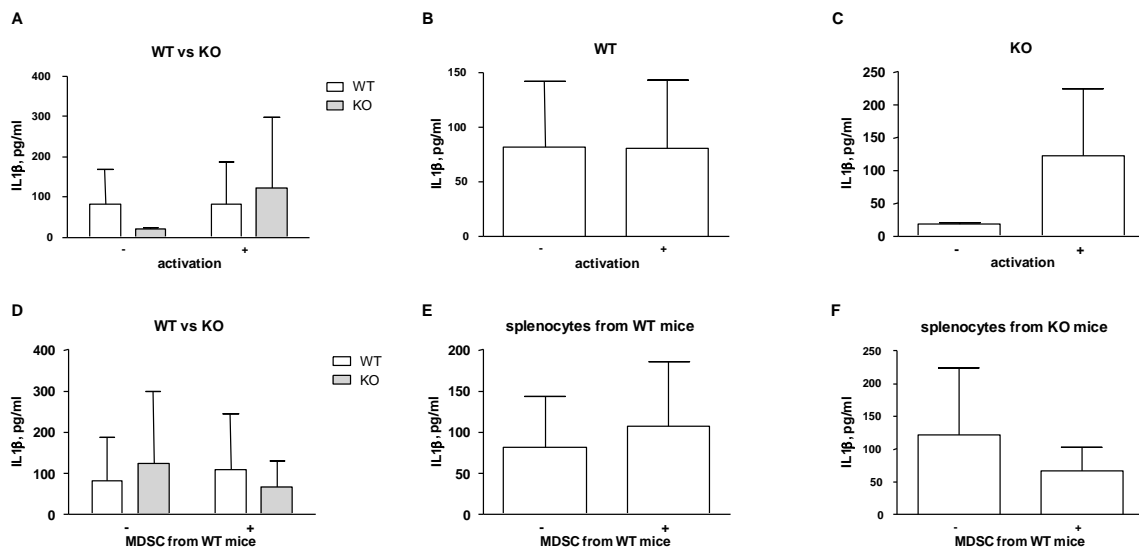


**Fig.3.5. 2 Quantification of IL-1 $\beta$  in supernatants from cocultures of WT or B7-H1 KO splenocytes (+/- activation) with and without MDSC from WT tumors.**

After 72 hours, the medium supernatant of the cocultures of CFSE labeled splenocytes and MDSC was collected and processed by Luminex approach. The concentration of IL-1 $\beta$  was measured and analyzed using Bio-Plex Manager 4.0. Data are presented as column bar graphs with SEM (n =2-3; two-way ANOVA (A,D) and *T*-test (B,C,E,F))

Next, we determined the changes in IL-2 concentration. When looking at WT and B7-H1 KO groups separately, significantly higher concentrations of IL-2 were found after activation with CD3/CD28 antibody in both the WT and B7-H1 KO groups (Fig.3.5.3 B,C). Between WT and B7-H1 KO in comparison, no significant difference in IL-2 concentration was seen in activated or non-activated samples (Fig.3.5.3 A).

## Results

After the coculture of MDSC with activated splenocytes, no change in the concentration of IL-2 was measured compared to cultures without MDSC; neither in WT nor in B7-H1 KO groups (Fig.3.5.3 E,F). As we compared WT and B7-H1 KO to each other, we have seen again no significant difference in IL-2 concentration in activated cultures between WT and B7-H1 KO. After adding WT MDSC to activated cultures, no significant difference in the IL-2 concentration was seen between cultures of WT and B7-H1 KO splenocytes (Fig.3.5.3 D).

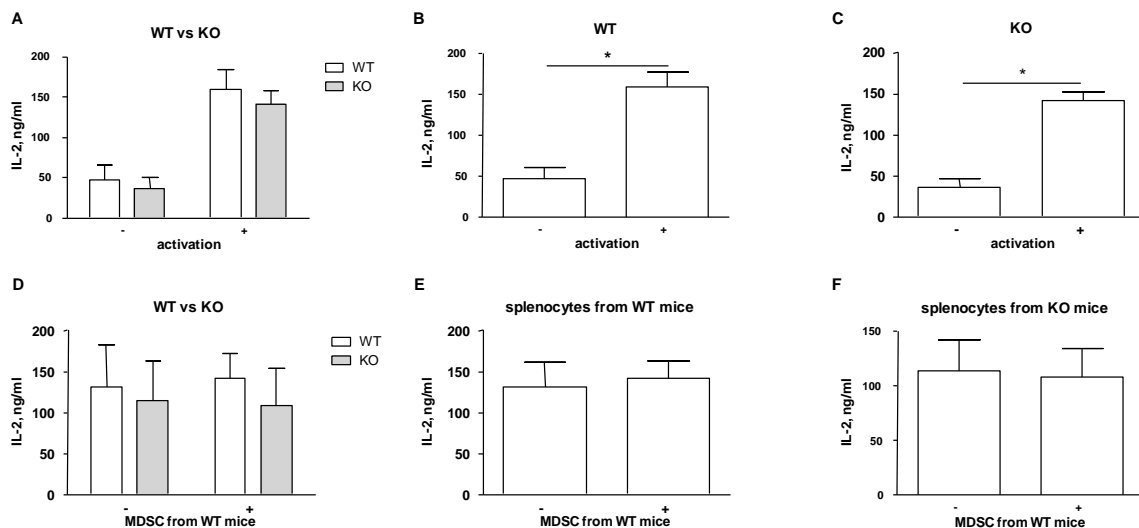


**Fig.3.5. 3 Quantification of IL-2 in supernatants from cocultures of WT or B7-H1 KO splenocytes (+/- activation) with and without MDSC from WT tumors.**

After 72 hours, the medium supernatant of the cocultures of CFSE labeled splenocytes and MDSC was collected and processed by Luminex approach. The concentration of IL-2 was measured and analyzed using Bio-Plex Manager 4.0. Data are presented as column bar graphs with SEM (n =2-3; \*p<0.05, \*\*p<0.01; two-way ANOVA (A,D) and T-test (B,C,E,F))

The analysis of the cytokine IL-6 is shown in the Fig.3.5.4. In the WT group, a tendency towards higher concentrations was found in the presence of CD3/CD28 activating antibody (Fig.3.5.4 B). In the B7-H1 KO group, a significant increase in IL-6 concentration was found after activation compared to non-activated samples (Fig.3.5.4 C). In WT non-activated cultures compared to B7-H1 KO, no significant

difference was registered. However, after activation, in cultures of B7-H1 KO splenocytes, significantly lower concentrations of IL-6 were measured compared to cultures of WT splenocytes (Fig.3.5.4 A).

In the inhibitory presence of MDSC, the tendency towards higher concentrations of IL-6 was seen in WT, as well as B7-H1 KO groups, compared to samples without MDSC presence (Fig.3.5.4 E,F). In Fig.3.5.4 D, the comparison of IL-6 concentration between cultures of WT and B7-H1 KO mice is shown. No significant difference in the concentration of IL-6 was determined when we compared activated WT and B7-H1 KO samples to each other. After adding inhibitory MDSC to activated cultures, a tendency towards lower IL-6 concentration was observed in cultures of B7-H1 KO compared to WT splenocytes (Fig.3.5.4 D).

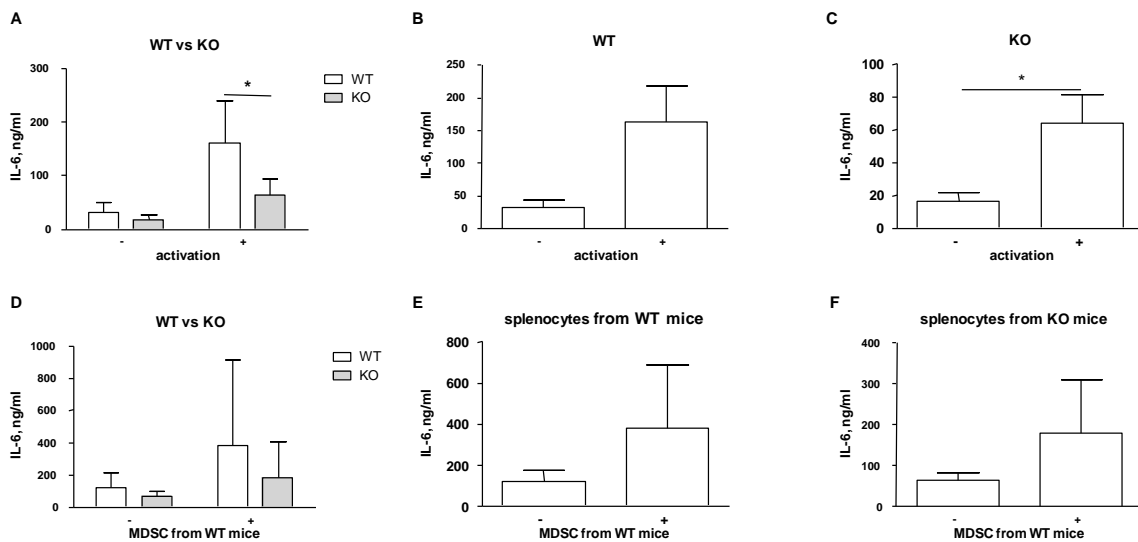


**Fig.3.5. 4 Quantification of IL-6 supernatants from cocultures of WT or B7-H1 KO splenocytes (+/- activation) with and without MDSC from WT tumors.**

After 72 hours, the medium supernatant of the cocultures of CFSE labeled splenocytes and MDSC was collected and processed by Luminex approach. The concentration of IL-6 was measured and analyzed using Bio-Plex Manager 4.0. Data are presented as column bar graphs with SEM (n =2-3; \*p<0.05, \*\*p<0.01; two-way ANOVA (A,D) and T-test (B,C,E,F))

The comparison of activated and non-activated cultures showed no significant change in IL-10 concentrations in the WT group (Fig.3.5.5 B). In the group of B7-H1 KO cells, a tendency towards higher IL-10 concentration was found after activation of splenocytes with CD3/CD28 antibody compared to non-activated samples (Fig.3.5.5 C). The WT and B7-H1 KO non-activated cultures in comparison, showed no significant difference. However, in the activated cultures, a tendency towards higher IL-10 concentration was seen in the group of B7-H1 KO cells compared to the group of WT cells (Fig.3.5.5 A).

After we added MDSC to activated WT cultures, the concentration of IL-10 was significantly higher compared to samples without MDSC (Fig.3.5.5 E). In B7-H1 KO cultures, no significant difference in IL-10 concentration between cultures with or without MDSC was determined (Fig.3.5.5 F). As we compared WT and B7-H1 KO to each other, first we again observed a tendency towards higher IL-10 concentration in activated cultures of B7-H1 KO compared to WT. After adding WT MDSC to activated cultures, the tendency towards lower IL-10 concentration was seen in cultures of B7-H1 KO compared to WT splenocytes (Fig.3.5.5 D).

## Results

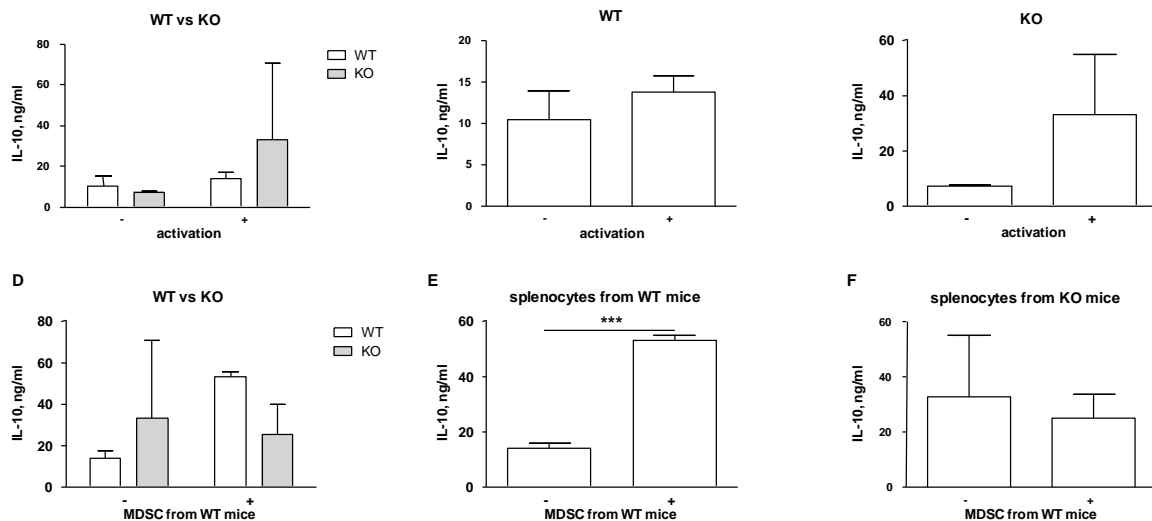


**Fig.3.5. 5 Quantification of IL-10 in supernatants from cocultures of WT or B7-H1 KO splenocytes (+/- activation) with and without MDSC from WT tumors.**

After 72 hours, the medium supernatant of the cocultures of CFSE labeled splenocytes and MDSC was collected and processed by Luminex approach. The concentration of IL-10 was measured and analyzed using Bio-Plex Manager 4.0. Data are presented as column bar graphs with SEM (n =2-3; \*p<0.05, \*\*p<0.01; two-way ANOVA (A,D) and T-test (B,C,E,F))

Next, we analyzed the concentrations of VEGF, which had already been associated with the presence of MDSC in a tumor milieu. In samples of WT mice, no significant difference in the concentration of VEGF was found between cultures of WT splenocytes with activation compared to cultures without activation (Fig.3.5.6 B). In the B7-H1 KO group, a tendency towards higher VEGF concentration was measured in the presence of CD3/CD28 activation compared to non-activated samples (Fig.3.5.6 C). The comparison between WT and B7-H1 KO showed no significant difference in the concentration of VEGF between WT and B7-H1 KO, neither in the activated nor in the non-activated cultures (Fig.3.5.6 A).

As one can see in Fig.3.5.6 E,F, significantly higher concentrations of VEGF were found in the presence of MDSC compared to cultures without inhibitory MDSC, in the cultures from both the WT and B7-H1 KO mice. Between WT and B7-H1 KO groups in comparison, no significant difference in VEGF concentration was seen between WT and B7-H1 KO in activated cultures without added MDSC. After adding inhibitory

## Results

MDSC to activated cultures, no significant difference in VEGF concentration was observed in cultures of WT compared to B7-H1 KO splenocytes (Fig.3.5.6 D).

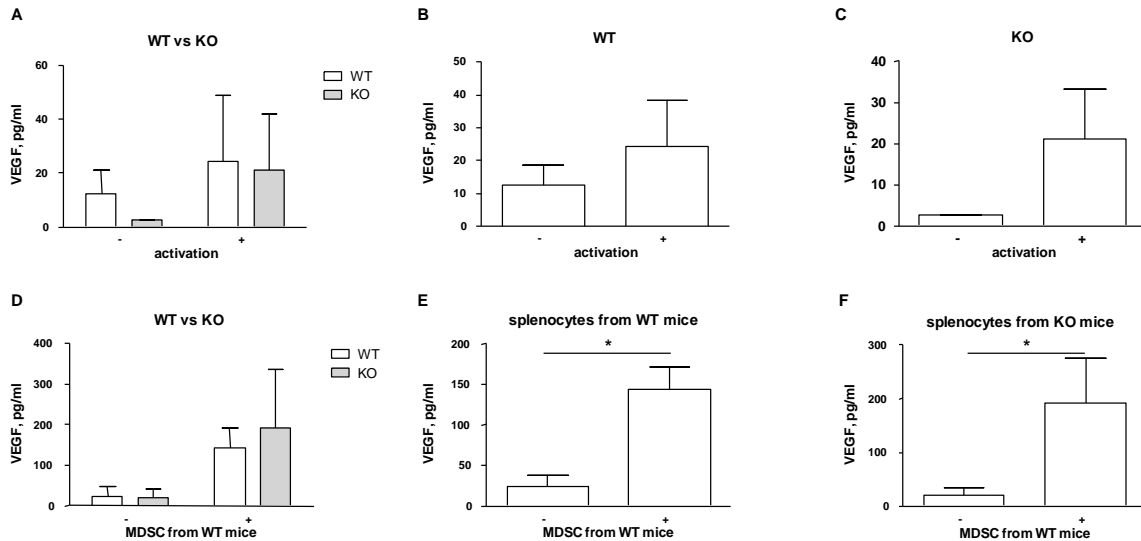


**Fig.3.5. 6 Quantification of VEGF in supernatants from cocultures of WT or B7-H1 KO splenocytes (+/- activation) with and without MDSC from WT tumors.**

After 72 hours, the medium supernatant of the cocultures of CFSE labeled splenocytes and MDSC was collected and processed by Luminex approach. The concentration of VEGF was measured and analyzed using Bio-Plex Manager 4.0. Data are presented as column bar graphs with SEM (n =2-3; \*p<0.05, \*\*p<0.01; two-way ANOVA (A,D) and T-test (B,C,E,F))

The last parameter we analyzed was TGF- $\beta$ . In both the WT and B7-H1 KO groups of mice, the activation of splenocytes with CD3/CD28 antibody did not induce a significant change in the concentration of TGF- $\beta$  compared to the concentration in non-activated cultures (Fig.3.5.7 B,C). Furthermore, the comparison between B7-H1 KO and WT cultures revealed no significant difference in the concentration of TGF- $\beta$ , neither before nor after activation (Fig.3.5.7 A).

In the presence of MDSC, in the WT samples a trend towards a higher concentration of TGF- $\beta$  was determined (Fig.3.5.7 E). In the B7-H1 KO samples, no significant difference in TGF- $\beta$  concentration was found between cultures with or without MDSC (Fig.3.5.7 F). In the analysis of WT and B7-H1KO groups in comparison, again one

## Results

can see in Fig.3.5.7 D no significant difference in the concentration of TGF- $\beta$  in samples without MDSC. After adding inhibitory MDSC to activated cultures, no significant difference in TGF- $\beta$  concentration was observed between cultures of WT and B7-H1 KO splenocytes (Fig.3.5.2 D).

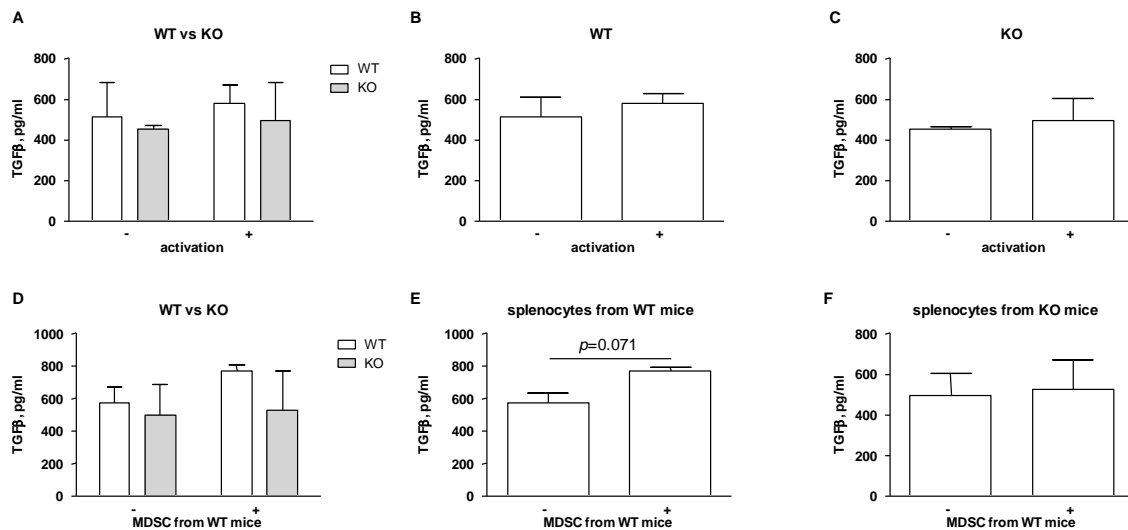


**Fig.3.5. 7 Quantification of TGF- $\beta$  in supernatants from cultures of WT or B7-H1 KO splenocytes (+/- activation) with and without MDSC from WT tumors.**

After 72 hours, the medium supernatant of the cocultures of CFSE labeled splenocytes and MDSC was collected and processed by Luminex approach. The concentration of TGF- $\beta$  was measured and analyzed using Bio-Plex Manager 4.0. Data are presented as column bar graphs with SEM (n =2-3; \* $p < 0.05$ , \*\* $p < 0.01$ ; two-way ANOVA (A,D) and *T*-test (B,C,E,F))

Taken together, the investigation of the cytokines revealed no significant difference between cultures of WT and B7-H1 KO splenocytes. Only in the analysis of VEGF concentration did we observe higher concentrations in the presence of WT MDSC in cocultures of both the WT and B7-H1 KO splenocytes.

### **3.6 Effects of chemo (5-FU) - and immunotherapy (IFN $\alpha$ ) on tumor volume and metastasis rate of WT and B7-H1 KO tumor-bearing mice**

The goal of this experiment series was to examine the differences in tumor volumes and metastasis rates between WT and B7-H1 KO tumor-bearing mice as well as in WT or B7-H1 KO mice separately between different treatments. For this purpose Panc02 cells were implanted and the mice received different treatments of IFN $\alpha$ , 5-FU or the combination of IFN $\alpha$ +5FU on Day 5, 7 and 9 post surgeries. Untreated mice were used as controls. After a period of four weeks the mice were killed, the tumors eviscerated and investigated. We also determined the peritoneal wall metastasis as well as metastasis of the colon and the liver.

First, we compared the number of WT and B7-H1 KO tumor-bearing mice that developed visible tumors after Panc02 cell implantation. Furthermore, the tumor volumes of untreated WT and B7-H1 KO control mice, as well as after treatment with IFN $\alpha$ , 5-FU or the combination of IFN $\alpha$ +5FU, were determined.

As one can see in Fig.3.6.1, a significantly lower number of untreated control B7-H1 KO mice developed visible tumors compared to the control WT mice. Analyzing the differences in tumor volume, tumors of untreated control B7-H1 KO mice were of a significantly smaller volume compared to tumors of the control WT mice.

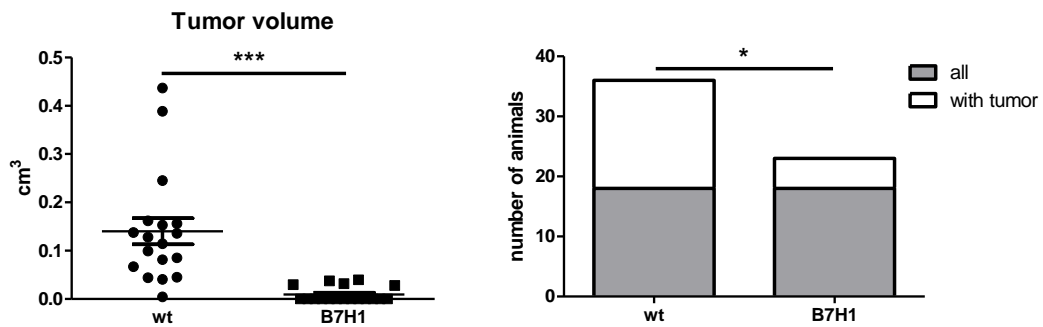


**Fig.3.6. 1 Difference in the rate of tumor development and tumor volume between WT and B7-H1 KO tumor-bearing mice.**

Four weeks after Panc02 implantation, the tumors were eviscerated, measured and the tumor rate and volume recorded and analyzed. Data from four independent experiments are presented as scatter plot or as stacked bars ((n = 9 for co, and n = 6 for IFN $\alpha$ ; 5-FU; IFN $\alpha$ +5-FU); \*p<0.05, \*\*\*p<0.001; T-test and  $\chi^2$ -test)

The comparison of tumor volume between WT and B7-H1 KO mice showed lower volumes in all four subgroups of B7-H1 KO mice compared to those groups of WT mice. Significantly lower volumes were found in the groups of 5-FU and IFN $\alpha$ +5-FU treatment compared to the untreated control group in WT tumor-bearing mice (Fig.3.6.2).

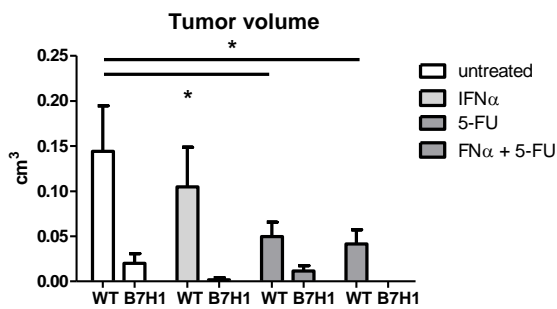


**Fig.3.6. 2** Difference in the tumor volume between WT and B7-H1 KO tumor-bearing mice with and without treatment.

Mice were treated on Day 5, 7 and 9 after Panc02 implantation with IFN $\alpha$ , 5-FU or the combination of IFN $\alpha$ +5-FU. Untreated mice were used as controls. Four weeks after Panc02 implantation, the tumors were eviscerated, measured and the tumor volume recorded and analyzed. Data from four independent experiments are presented as column bar graphs with SEM ((n = 9 for co, and n = 6 for IFN $\alpha$ ; 5-FU; IFN $\alpha$ +5-FU) \*p<0.05; two-way ANOVA)

A clear tendency towards lower tumor rates was found in B7-H1 KO mice compared to WT mice after IFN $\alpha$  treatment. Beyond that, the analysis showed that the tumor volume of IFN $\alpha$  treated mice was significantly lower in B7-H1 KO mice compared to WT mice (Fig.3.6.3).

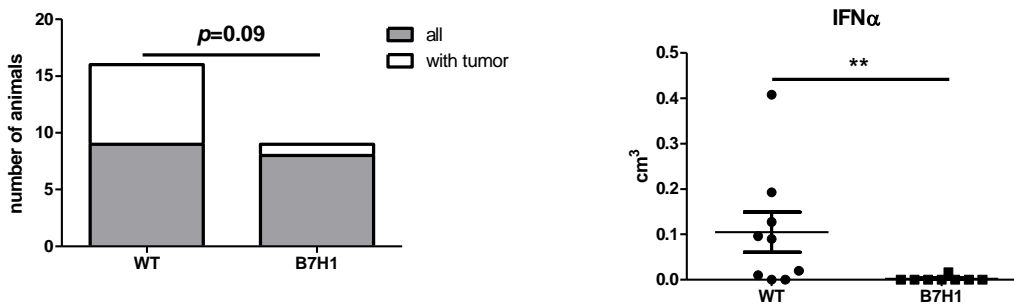


**Fig.3.6. 3** Difference in the rate of tumor development and tumor volume between WT and B7-H1 KO tumor-bearing mice receiving IFN $\alpha$  treatment.

Mice were treated on Day 5, 7 and 9 after Panc02 implantation with IFN $\alpha$ . Four weeks after Panc02 implantation, the tumors were eviscerated, measured and the tumor rate and volume recorded and analyzed. Data from four independent experiments are presented as scatter plot or as stacked bars ((n = 9 for co, and n = 6 for IFN $\alpha$ ; 5-FU; IFN $\alpha$ +5-FU); \*\*p<0.01; T-test and  $\chi^2$ -test)

In the groups of 5-FU treated WT and B7-H1 KO mice, no significant difference in the rate of visible tumor development was registered between WT and B7-H1 KO tumor-bearing mice. Instead, the tumor volume in 5-FU treated animals showed significantly lower volumes in the group of B7-H1 KO mice compared to WT mice (Fig.3.6.4).

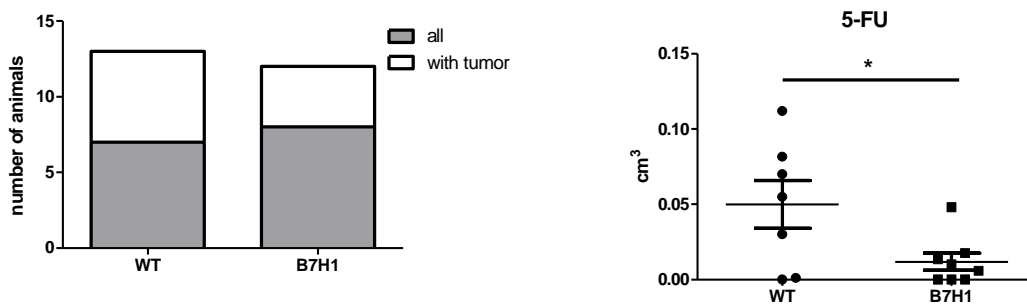


**Fig.3.6. 4 Difference in the rate of tumor development and tumor volume between WT and B7-H1 KO tumor-bearing mice receiving 5-FU treatment.**

nc02

implantation, the tumors were eviscerated, measured and the tumor rate and volume recorded and analyzed. Data from four independent experiments are presented as scatter plot or as stacked bars ((n = 9 for co, and n = 6 for IFN $\alpha$ ; 5-FU; IFN $\alpha$ +5-FU); \*p<0.05; T-test and  $\chi^2$ -test)

Comparing IFN $\alpha$ +5-FU treated WT to B7-H1 KO mice, the analysis of the tumor rate revealed significantly lower values in B7-H1 KO mice compared to WT mice. In the tumor volume of IFN $\alpha$ +5-FU treated animals, significantly lower volumes were determined for the group of B7-H1 KO mice compared to WT mice (Fig.3.6.5).

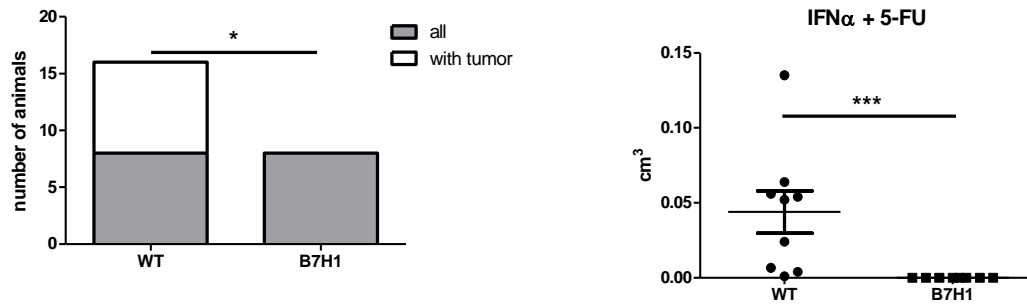


**Fig.3.6. 5 Difference in the rate of tumor development and tumor volume between WT and B7-H1 KO tumor-bearing mice receiving IFN $\alpha$ +5-FU treatment.**

Mice were treated on Day 5, 7 and 9 after Panc02 implantation with IFN $\alpha$ +5-FU. Four weeks after Panc02 implantation, the tumors were eviscerated, measured and the tumor rate and volume recorded and analyzed. Data from four independent experiments are presented as scatter plot or as stacked bars ((n = 9 for co, and n = 6 for IFN $\alpha$ ; 5-FU; IFN $\alpha$ +5-FU); \*p<0.05, \*\*\*p<0.001; T-test and  $\chi^2$ -test)

Afterwards, we looked at the metastasis rates in WT and B7-H1 KO tumor-bearing mice. A significant difference in the rate of peritoneal wall metastasis was seen between the untreated control WT and B7-H1 KO mice, with lower rates in B7-H1 KO mice (Fig.3.6.6 A). In the rate of colon metastasis, a significantly lower rate was found in the untreated control B7-H1 KO mice compared to WT mice (Fig.3.6.6 B). The comparison between untreated control WT and B7-H1 KO mice for liver metastasis showed a clear tendency towards lower rates in B7-H1 KO mice compared to WT mice (Fig.3.6.6 C).

Next, we compared the metastasis rates of peritoneal wall metastasis between WT and B7-H1 KO tumor-bearing mice who received treatment, either IFN $\alpha$ , 5-FU or the combination of IFN $\alpha$ +5-FU. The B7-H1 KO mice treated with IFN $\alpha$  developed significantly less often peritoneal wall metastasis compared to IFN $\alpha$ -treated WT mice (Fig.3.6.6 D). The rate of peritoneal wall metastasis in the groups of 5-FU treatment showed a tendency towards lower metastasis rates in B7-H1 KO mice compared to WT mice (Fig.3.6.6 E). In the IFN $\alpha$ +5FU treatment group, a tendency towards lower

## Results

metastasis rates was found in the B7-H1 KO mice compared to the WT mice (Fig.3.6.6 F).

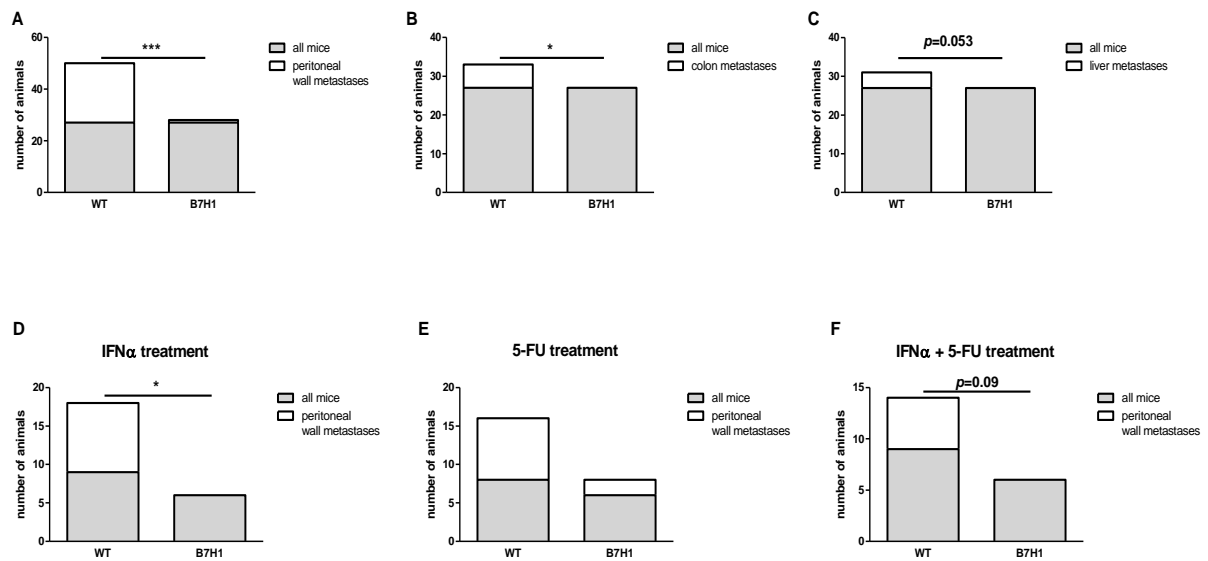


**Fig.3.6. 6 Difference in the metastasis rate between WT and B7-H1 KO tumor-bearing mice with and without treatment.**

Mice were treated on Day 5, 7 and 9 after Panc02 implantation with IFN $\alpha$ , 5-FU or the combination of IFN $\alpha$ +5-FU. Four weeks after Panc02 implantation, the mice were dissected and the colon, liver and peritoneal wall metastasis recorded and analyzed. Data from four independent experiments are presented as stacked bars ((n = 9 for co, and n = 6 for IFN $\alpha$ ; 5-FU; IFN $\alpha$ +5-FU); \*p<0.05, \*\*\*p<0.001;  $\chi^2$ -test)

This experiment series revealed a significant difference in the frequency of visible tumor development as well as in the tumor volume between the WT and B7-H1 KO tumor-bearing mice. We observed in the B7-H1 KO mice that both the frequency and the volume were significantly lower in the control as well as in all treatments compared to WT mice. Beyond that, the frequency of tumor metastasis was lower in all groups of B7-H1 KO mice compared to WT mice.

### **3.7 Effects of chemo (5-FU) - and immunotherapy (IFN $\alpha$ ) on the survival rate of WT and B7-H1 KO tumor-bearing mice**

We used WT and B7-H1 KO tumor-bearing mice to determine the effect of the B7-H1 regulatory molecule on the survival rate of WT and B7-H1 KO tumor-bearing mice. Beyond that, we examined the impact of our different treatments, compared to control, on the survival of tumor-bearing WT and B7-H1 KO mice. The WT and B7-H1 KO tumor-bearing mice were divided in different treatment groups, receiving either IFN $\alpha$ , 5-FU or the combination of IFN $\alpha$ +5-FU at Day 5, 7, and 9 after the surgery. Untreated mice were used as controls. Based on the experiment setting, mice that survived showing no cancer signs caused by tumor growth, were killed on Day 60 post op.

In the untreated control group, the median survival of WT mice was 35 days after the implantation of tumor cells. In the B7-H1 KO tumor-bearing mice who were missing the regulatory molecule B7-H1, the result was undefined because all B7-H1 KO mice were alive and showed no signs of cancer. This resulted in aborting the experiment on Day 60 post op. Therefore, the difference between WT and B7-H1 KO tumor-bearing mice was highly significant (Fig.3.7.1 A). In the therapy group of IFN $\alpha$ , a median survival of 42 days was determined for WT mice, whereas in the same group of B7-H1 KO mice, the result was again undefined. This was because all B7-H1 KO mice were alive and showed no signs of cancer, again resulting in aborting the experiment on Day 60 post op. Therefore, this result was highly significant (Fig.3.7.1 B). For the treatment group of 5-FU, a significant difference was seen between WT mice, with a median survival of 36 days compared to a median survival of 58.8 days in the 5-FU group of B7-H1 KO mice (Fig.3.7.1 C). The comparison between WT and B7-H1 KO tumor-bearing mice in the group of IFN $\alpha$ +5-FU, showed a significant difference between those mouse strains. In the WT mice, a median survival of 39

## Results

days was determined compared to an undefined parameter due to aborting the experiment on Day 60 post op for B7-H1 KO mice (Fig.3.7.1 D).

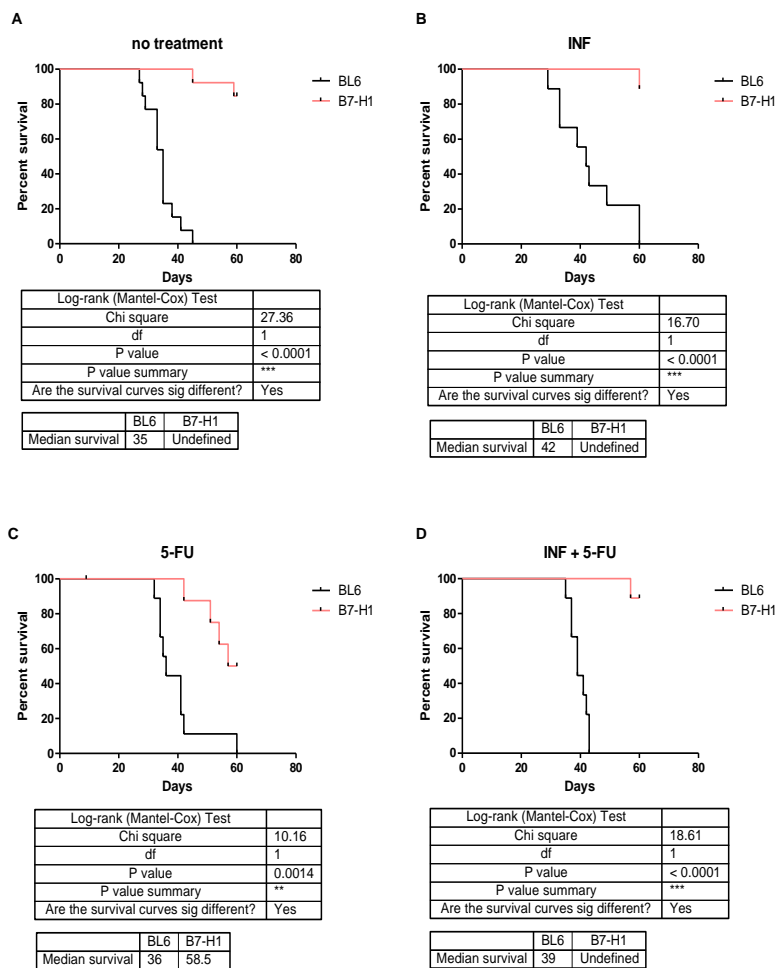


**Fig.3.7. 1 Difference in the survival rate between WT and B7-H1 KO tumor-bearing mice with and without treatment.**

Mice were treated on Day 5, 7 and 9 after Panc02 implantation with IFN $\alpha$ , 5-FU or the combination of IFN $\alpha$ +5-FU. Untreated mice were used as controls. The survival rate was recorded and analyzed. After Day 60, mice that survived were killed. Data from four independent experiments are presented as Kaplan-Meier curves ((n = 13 for co, and n = 9 for IFN $\alpha$ ; 5-FU; IFN $\alpha$ +5-FU); \*\*p<0.01, \*\*\*p<0.001; Log-rank test)

Afterwards, we analyzed the differences in survival rate between the control group and treatment groups of either WT or B7-H1 KO tumor-bearing mice. For the single therapies of WT mice, no statistical significance was seen between the treatments and the control. The highest median survival was found in the IFN $\alpha$  group at 42 days,

followed by the combination of IFN $\alpha$ +5-FU at 39 days and the 5-FU treatment at 36 days. The lowest value was determined for the control group with a median survival of 35 days. In the groups of B7-H1 KO mice, the median survival was analyzed as undefined for the control IFN $\alpha$  and IFN $\alpha$ +5-FU treatments, caused by aborting the experiment on Day 60 after the Panc02 implantation. In the 5-FU treated B7-H1 KO mice, the median survival was registered at Day 58.5 post op. Therefore, no significant difference was found between the control and treatment groups of B7-H1 KO mice (Fig.3.7.2).

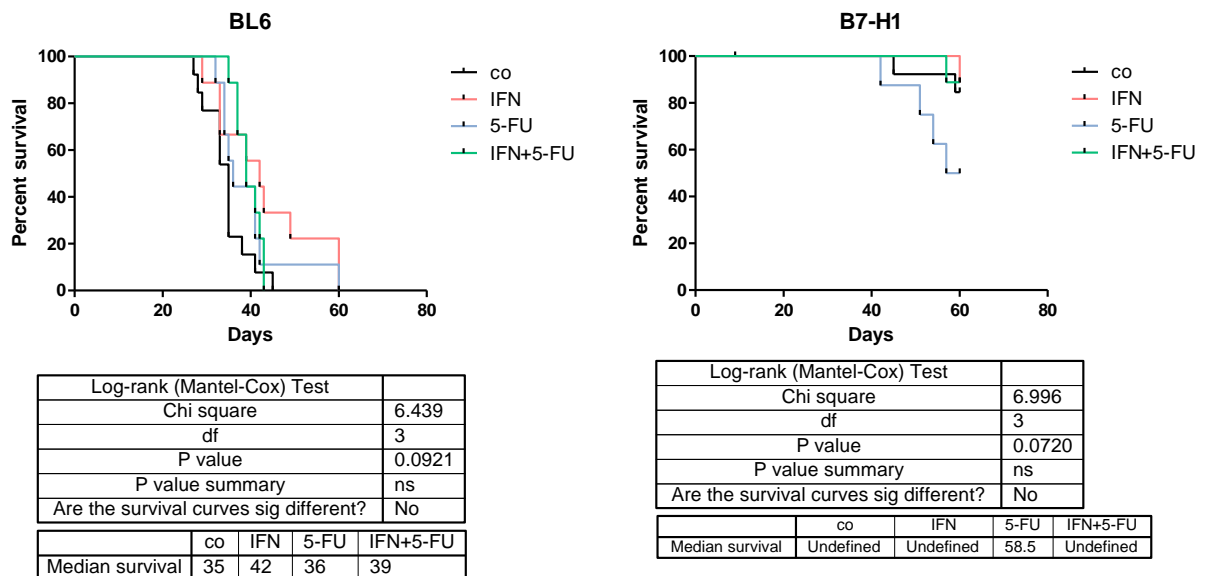


**Fig.3.7. 2** Difference in the survival rate between control groups (without treatment) and after treatment with IFN $\alpha$ , 5-FU or the combination of IFN $\alpha$ +5-FU of either WT or B7-H1 KO tumor-bearing mice.

Mice were treated on Day 5, 7 and 9 after Panc02 implantation with IFN $\alpha$ , 5-FU or the combination of IFN $\alpha$ +5-FU. Untreated mice were used as controls. The survival rate was recorded and analyzed. After Day 60, the mice that survived were killed. Data from four independent experiments are presented as Kaplan-Meier curves ((n = 13 for co, and n = 9 for IFN $\alpha$ ; 5-FU; IFN $\alpha$ +5-FU); Log-rank test)

Taken together, in this experiment series we were able to show that tumor-bearing B7-H1 KO mice that were lacking the regulatory molecule B7-H1, had a significantly higher survival rate compared to WT tumor-bearing mice, regardless the chosen

treatment. Whereas between the single treatment groups compared to the control of either WT or B7-H1 KO tumor-bearing mice, no significant difference was seen.

### 3.8 Analysis of the correlation between tumor volume and specific immune cell populations

After we analyzed several important cell populations involved in the anti-tumor immune response, we were also interested to see whether a relationship between the tumor volume and the frequency of specific immune cell populations can be found. Therefore, in this part of the experiment series we looked at the possible correlation between the analyzed tumor volume and specific cell populations, examined above phenotypically with FACS, using the Spearman correlation analysis. We could show that only for total MDSC, this correlation was of a statistical significance (Fig.3.2.6.1).

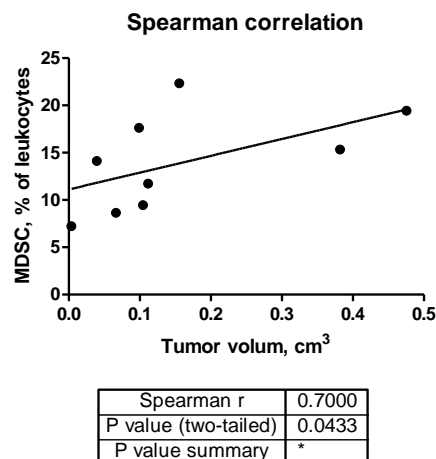


**Fig.3.8 1 Correlation between tumor volume and the percentage of MDSC out of leukocytes.**

The frequency of MDSC out of leukocytes was measured with flow cytometry, statistically analyzed and was set in correlation to the calculated tumor volume. Data from four independent experiments are presented as Spearman correlation ((tumors: n = 7 for co, n = 4-6 for IFN $\alpha$ ; 5-FU; IFN $\alpha$ +5-FU); \*p<0.05)

Since a correlation between the tumor volume and the frequencies of single cell populations was only seen for the suppressive cell population of MDSC, this result underscores the importance of MDSC for the establishment and development of tumors.

## 4. Discussion

Pancreatic cancer (PDAC) remains to this day a devastating disease with low chances of recovery, which are often caused by its late recognition, high metastasis rate and poor response to therapies such as radiation or chemotherapy. Therefore, the development of new therapies is more than ever before of great importance. New therapeutic approaches, for example immune therapy, offer more opportunities for the treatment of pancreatic cancer.

To make progress towards the goal of using immune therapy more effectively, a better understanding of the tumor immune response for PDAC is essential. Therefore, it is especially important to take a look at both the molecular as well as on the cellular level of immune regulation.

Tumors are able to escape the action of the immune system by different mechanisms, for example by reducing the expression of MHC molecules or by shedding antigens from the outer cell membrane [127, 128]. On the molecular level, the immunoinhibitory molecules B7-H1 and B7-DC are involved in the process of cellular and humoral immune regulation caused by the PD-1-PD-L pathway, and play a critical role in the tumor immune escape [110, 129]. In the anti-tumor immune response, both parts of the cellular level, the activation arm of the immune system ( $CD4^+/CD8^+$  T cells, DC) as well as the suppressive arm (MDSC, Treg), are important in understanding the detailed processes in pancreatic cancer. In this project, we analyzed the interplay between molecular and cellular processes in healthy mice to be able to better interpret our results later on in tumor-bearing mice.

One of the important activating cells for the action of the anti-tumor immune response are  $CD4^+/CD8^+$  T cells and their subsets. Dong et al. showed that in naïve B7-H1 KO mice, the absence of B7-H1 molecule increases the accumulation of  $CD8^+$  T cells in the liver [124]. Therefore, we analyzed them and their activation status in WT and B7-

H1 KO healthy as well as tumor-bearing mice. Determining the subsets of CD4<sup>+</sup>/CD8<sup>+</sup>T cells between spleens of WT and B7-H1 KO healthy mice, significantly higher ratios of CD8<sup>+</sup>/CD4<sup>+</sup> Tem and CD8<sup>+</sup>/CD4<sup>+</sup> Tcm were seen in splenocytes of B7-H1 KO compared to WT healthy mice and consequently less CD4<sup>+</sup>/CD8<sup>+</sup> Tnaive. Also in spleens of treated tumor-bearing B7-H1 KO mice, we found significantly higher frequencies of CD8<sup>+</sup> Teff and Tem as well as CD4<sup>+</sup> Tem and Tcm as compared to WT spleens. This leads us to the conclusion that in spleens of healthy, as well as tumor-bearing B7-H1 KO mice, the absence of B7-H1 molecule leads to higher ratios of CD4<sup>+</sup>/CD8<sup>+</sup> Tem and Tcm. This is in line with the fact that the molecule B7-H1 inhibits activated CD4/CD8 T cells [130]. This effect is important in the anti-tumor immune response. Generally, it was determined that CD8<sup>+</sup> T cell accumulation positively correlates with the survival of patients in cancers shown in pancreatic cancer and other tumors like colorectal cancer [131, 132]. Also, in human colorectal cancer patients, Pages, Berger et al. demonstrated that a high ratio of tumor infiltrating memory and effector memory T cells was associated with lower invasiveness of the tumor [133]. This leads us to the conclusion, that our result represents a general effect in tumors.

When we looked at the impact of chemo-and immunotherapy on the distribution of T cell subsets, we have seen significantly lower frequencies of CD4<sup>+</sup> Tem and significantly higher ratios of CD8<sup>+</sup> Tcm after applied IFN $\alpha$ +5-FU treatment in spleens of B7-H1 KO healthy mice. In spleens of tumor-bearing mice, we have also seen a trend towards lower frequencies of Teff and higher percentages of Tem and Tcm subsets after treatment with IFN $\alpha$ +5-FU. We observed in earlier experiments that the treatment with IFN $\alpha$  induced an increase in the number of effector memory CD8<sup>+</sup> T cells and in the CD8<sup>+</sup>/CD4<sup>+</sup> ratio in mice (Bazhin et al., unpublished data). It is widely known that chemotherapy not just kills tumor cells having a high rate of proliferation, it also rapidly affects dividing healthy cells like Teff. This could possibly explain the lower Teff frequencies observed by us.

The activation status of CD4<sup>+</sup>/CD8<sup>+</sup> T cells is also an important characteristic of these cells, and therefore, we also took a detailed look at the activation status of CD4<sup>+</sup>/CD8<sup>+</sup> T cells by analyzing the expression of CD69 early activation marker. In both experiment series, using either healthy or tumor-bearing WT and B7-H1 KO

mice, we saw no significant difference in CD69 expression between both mouse strains. This is in line with observations made in a leukemia tumor model by Salih, Wintterle et al., who did not find significant differences in CD69 expression of CD4<sup>+</sup>/CD8<sup>+</sup> T cells in the presence of the anti-B7-H1 antibody [134]. Considering the impact of chemo- and immunotherapy on the activation status, as expected after the applied IFN $\alpha$  and IFN $\alpha$ +5-FU therapy, a significant increase in the frequency of CD69<sup>+</sup> cells was determined in both healthy and tumor-bearing WT and B7-H1 KO mice. Actually, one would expect a higher CD69 expression in B7-H1 KO mice compared to WT mice, since this molecule is not inhibited in B7-H1 KO mice. A possible explanation for this is that B7-H1 KO mice lacking B7-H1 regulatory molecule from birth on, contrary to blocking B7-H1 molecule with antibodies in mice with an already developed and mature immune system. This is due to the fact that the immune system of B7-H1 KO mice tries to maintain the activating/suppressive balance by regulation.

Another important cell population of the activating arm of the immune cells are dendritic cells. DC are specialized in antigen presentation, which plays a key role in the initiation of primary immune responses. Several cytokines and prostaglandins are known to influence the maturation status of DC, for example TNF- $\alpha$ , IL-1 $\beta$ , IL-6 or PGE<sub>2</sub> [135]. Until today, it is not yet fully understood which role the molecule B7-H1 plays in this context, since it can also be expressed by the cell population of DC [136]. After maturation, DC stimulate antigen-specific T cells [137]. In spleens of healthy WT and B7-H1 KO mice, lower ratios of cDC were found after IFN $\alpha$  treatment. Furthermore, significantly lower percentages of cDC in spleens were determined after treatment of tumor-bearing B7-H1 KO mice with IFN $\alpha$  and IFN $\alpha$ +5-FU. For pDC, we found no meaningful differences. Analyzing the maturation status of cDC and pDC, only in spleens of WT tumor bearing mice did we find a decrease in the ratio of mature cDC after 5-FU and IFN $\alpha$ +5-FU treatment and a decrease in mature pDC ratio after IFN $\alpha$ +5-FU treatment. This is contrary to previous studies showing that IFN $\alpha$  enhanced the maturation of DCs [138]. One possible explanation for this can be the different experimental setting as well as that the approach of the other group was performed *in vitro* with human cells. We also analyzed the molecules CD80 and CD86 on mature cDC/pDC. Between spleens of WT and B7-H1 KO tumor-bearing

mice, comparable results were found. This is in line with observations made by Brandl, Ortler et al. who also observed comparable expressions of molecules like CD80, CD86 or B7-DC between WT and B7-H1 KO mice [139]. This allows us to assume that the presence/absence of the molecule B7-H1 has no decisive impact on the expression of those molecules. In spleens of B7-H1 KO tumor-bearing mice, IFN $\alpha$  and 5-FU treatment led to an increase in the ratio of CD80<sup>+</sup> mature cDC, and moreover, IFN $\alpha$  treatment also led to an increase in the percentage of CD86<sup>+</sup> mature cDC. This observation is supported by the data of *in vitro* studies where treatment of immature cDC with IFN $\alpha$  resulted in an upregulation of surface expression of molecules including CD80 and CD86 [140, 141]. This underscores the activating impact of IFN $\alpha$ , at least in B7-H1 KO tumor-bearing mice.

The molecular and cellular level of the immunosuppressive arms and the crosslinks between both of them is the other important aspect we need to consider to fully understand the tumor immunology of PDAC. Therefore, we analyzed the precise role the B7-H1 expression plays on cells of the immune system with the main focus on MDSC in the context of anti-tumor immunity in PDAC. Immunosuppressive MDSC (Gr-1<sup>+</sup>CD11b<sup>+</sup> compartment) are a heterogeneous group of cells that consists of immature myeloid cells from the bone marrow. In pathological situations such as sepsis, infectious disease or cancer, the differentiation into mature cells does not occur, resulting in the expansion of MDSC [95]. In our project, we were especially interested in Gr-1<sup>+</sup>CD11b<sup>+</sup> cells and their subsets in both a healthy and tumor condition, and additionally, how those cells are influenced by B7-H1 molecule expression. Beyond that, we compared the impact of chemo- and immunotherapy on this cell population. Even the absence of B7-H1 molecule on immune cells in B7-H1 KO mice showed such a large effect that we nearly had no visible tumors. Since we were especially interested in the interplay between MDSC and the B7-H1 molecule, we therefore used the tumors of B7-H1 KO mice to analyze this cell population in more detail. The linkage between MDSC and the regulatory molecule B7-H1 was already considered as an important aspect in the tumor immune mechanisms and was revealed by several scientists [99], but up to now, it has not been entirely examined and understood. We analyzed for the first time the connection between Gr-1<sup>+</sup> CD11b<sup>+</sup> cells and the molecule B7-H1, as well as the impact of chemo- and immune therapeutics in a healthy steady-state situation. The results revealed

significantly lower frequencies of Gr-1<sup>+</sup>CD11b<sup>+</sup> cells in B7-H1 KO splenocytes after treatment of the culture with 5-FU compared to those of WT healthy mice. This is in line with our earlier observations, examining the frequency of Gr-1<sup>+</sup> CD11b<sup>+</sup> cells in freshly splenocytes of healthy, untreated WT and B7-H1 KO mice (unpublished data). We found significantly lower ratios of Gr-1<sup>+</sup> CD11b<sup>+</sup> cells in B7-H1 KO compared to WT healthy mice. We can suggest that the molecule B7-H1 is at least one of the regulators that influences the Gr-1<sup>+</sup> CD11b<sup>+</sup> compartment. This is also supported by the results seen in tumor-bearing mice, where the analysis of MDSC population revealed lower frequencies of total MDSC in B7-H1 KO mice compared to WT mice. Additionally, the comparison between spleens of WT and B7-H1 KO tumor-bearing mice showed significantly lower ratios of MDSC in B7-H1 KO spleens compared to WT mice in all treatment groups and the control. This observation is in line with other observations made in ovarian cancer and ret melanoma models, showing a consistent functional interplay between the regulatory molecule B7-H1 and MDSC [142, 143]. So we can assume that it could represent a general effect on a various number of cancers. Based on the expression of the two epitopes of Gr-1, Ly-6G and Ly-6C, MDSC in mice can be divided in two subsets: granulocytic MDSC (CD11b<sup>+</sup>LY6G<sup>+</sup>LYC6<sup>low</sup>) and monocytic MDSC (CD11b<sup>+</sup>LY6G<sup>-</sup>LY6C<sup>high</sup>) [99]. Youn, Nagaraj et al. showed that in naïve mice, the ratio between gMDSC and mMDSC was 3:1. More often, the gMDSC subset was increased in tumor models, whereas the mMDSC subset was only increased in a few tumor models [99]. Beyond that, the ratio between gMDSC and mMDSC is much lower in the tumor site than in lymphoid organs [144]. In contrast, in our experiments we showed that in tumors of B7-H1 KO tumor-bearing mice, the ratio of gMDSC was decreased compared to WT tumor bearing mice. One possible explanation for our findings could be the tumor potential of Panc02 cells in B7-H1 KO mice, which seems to differentiate from the tumor potential in tumor models analyzed by Youn, Nagaraj et al. In spleens of B7-H1 KO mice treated with IFN $\alpha$ , we saw a shift in the MDSC subset towards a higher proportion of gMDSC and respectively lower frequencies of mMDSC. Examining the impact of chemo- and immunotherapy on MDSC, in WT tumors higher frequencies of total MDSC were seen after IFN $\alpha$ +5-FU treatment compared to the control group. Analyzing the impact of therapy on spleens of WT and B7-H1 KO tumor-bearing mice, we observed no significant differences in the frequencies of MDSC between

the groups of WT spleens. Instead, in B7-H1 KO spleens we observed higher ratios of MDSC in all treatment groups compared to the control, especially after we applied 5-FU and IFN $\alpha$ +5-FU treatments. These effects do not endorse the findings of Vincent, Mignot et al. who showed that a 5-FU treatment reduced the number of MDSC in the spleen and in the tumor bed of EL4 thymoma subcutaneous tumor-bearing mice [145]. This shows us that this is not a general effect of 5-FU treatment, but is rather specific and dependent upon factors like the tumor model and the chosen treatment regimen, which explains the contrary observation. Another aspect we have to consider is the phagocytic activity of MDSC, which can give a possible explanation for our observations [146]. The chemotherapeutic agent 5-FU kills cells, and those cell components phagocytosed by MDSC can possibly lead to an expansion of this cell population. The functionality of MDSC is of particular importance in the context of the suppressive capacity of this cell population.

A fact in cancer is that the activation of MDSC enhances their expression of arginase 1 (ARG1) and inducible nitric oxide synthase (iNOS), leading to augmentation of nitric oxide (NO) production [95]. In spleens of WT and B7-H1 KO tumor-bearing mice, we found no significant difference in the frequencies of iNOS<sup>+</sup> and Arg<sup>+</sup> MDSC. Instead, in tumors of untreated tumor-bearing WT and B7-H1 KO mice, significantly lower ratios of iNOS<sup>+</sup> gMDSC and mMDSC were determined in tumors of B7-H1 KO compared to WT tumor-bearing mice. This observation is supported by an ovarian cancer mouse model, where it was shown that the blockade of B7-H1 with antibodies resulted in an inhibition of the activity and expression of ARG I [147]. However, in addition to the data of Liu et al. we were the first who were able to show that also the production of iNOS is reduced in B7-H1 KO mice. This lets us conclude that B7-H1 KO mice not only have less MDSC frequencies, but also that those MDSC are not as functional in the production of NO-synthase. Especially interesting is that already the blockade of B7-H1 on immune cells (in B7-H1 KO mice) is sufficient enough to see an effect in the functional status of MDSC as compared to the blockade of both immune and tumor cells with antibodies, as investigated by Liu, Yu et al.

Several therapeutic agents have been described to influence the production of iNOS and arginase. Serafini, Meckel et al. examined the effect of a targeted therapy using phosphodiesterase-5 inhibitors, and found out that it can down-regulate ARG1 and

iNOS in murine MDSC, resulting in an increased spontaneous anti-tumor response [148]. However, another group examined the influence of IFN $\alpha$  on myeloid suppressor cells in a C26-colon carcinoma tumor model, and detected that IFN $\alpha$  therapy led to a more mature phenotype of MDSC with less immunosuppressive capacity, and furthermore, a trend towards lower ARG activity in MDSC of tumor-bearing mice [149]. In our experiments we found no influence from the applied chemo- and immunotherapy on the production of iNOS and ARG. A possible explanation for the varying results described above could be the different tumor model used by the other scientific groups, or the different applied therapeutic agents.

Another important aspect of antitumor response is the suppressive capacity of MDSC and the susceptibility of T cells to MDSC-mediated suppression. To analyze this, we performed the CFSE proliferation assay. As expected, proliferation of CD4<sup>+</sup> and CD8<sup>+</sup> T cells was seen after activation with CD3/CD28 activating antibody. In cultures of B7-H1 KO splenocytes, this activation was lower compared to cultures of WT splenocytes. Contrary to our results seen in B7-H1 KO mice, it was shown by Blank, Kuball et al. that anti B7-H1 antibody augmented the T cell expansion and proliferation [150]. This let us speculate that in B7-H1 KO mice, compensatory mechanisms try to keep the stimulatory/suppressive axis in balance resulting in a lower activation capacity of splenocytes. After we added WT MDSC to the cultures containing either WT or B7-H1 KO splenocytes, a significant suppression was seen in both WT and B7-H1 KO cultures. Between those, no obvious difference was determined. This shows the immunosuppressive capacity of MDSC on activating immune cells. It is also an interesting question if the absence of B7-H1 molecule on MDSC of B7-H1 KO mice could lead to certain effects. Unfortunately, we were technically not able to examine this aspect, but it would be interesting to investigate this point in the future.

The second cell population of the immunosuppressive arm we examined in our project are Treg. Since it was shown before that B7-H1 molecule plays an important role in the function of Treg [151-153], we also analyzed this cell population. In our *in vitro* experiment, we observed significantly higher percentages of Treg within splenocytes of healthy B7-H1 KO mice in the control as well as in all treatment groups compared to WT. This does not correlate with previous observations that B7-

H1 expression promotes a higher accumulation of Treg [152, 154, 155]. However, these results were obtained in a tumor model. In a healthy state, it is tempting to assume that the immune system of B7-H1 KO mice tries to keep the stimulatory/suppressive balance by increasing the number of Treg.

As we had already noted several differences between WT and B7-H1 KO healthy and tumor-bearing mice, we were also interested in whether the expression of the regulatory molecules B7-H1/B7-DC can also be influenced by the action of different cells as well as by therapeutic agents. The regulatory molecules B7-H1 and B7-DC are involved in the process of cellular and humoral immune regulation caused by the PD-1-PD-L pathway, and play a critical role in the tumor immune escape [110, 129]. So far, the expression of B7-H1 in tumors was described in various types of carcinoma, including pancreatic cancer [116, 120]. It is known that B7-H1 expression can act as both an activator on DC as well as a suppressor on MDSC. Therefore, in our experiments the difference in regulatory B7-H1 in WT and B7-DC molecule expression in B7-H1 KO was analyzed in healthy and tumor-bearing mice. Furthermore, we determined a possible impact of chemo- and immunotherapy on the expression of those regulatory molecules. In splenocytes of healthy WT and B7-H1 KO mice, for the cell population of mature cDC we found a significant increase in the frequency of B7-DC<sup>+</sup> cDC in B7-H1 KO mice after the treatment of cultures with IFN $\alpha$  and IFN $\alpha$ +5-FU. As we looked into our *in vivo* experiments at splenocytes of tumor bearing WT and B7-H1 KO mice, a significant decrease in B7-H1 MFI of total MDSC was found after treatment of WT mice with IFN $\alpha$ +5-FU. It was shown that the expression of cytokines can be influenced by B7-H1/B7-DC molecule. Therefore, we took a detailed look at this aspect. It was observed before that several cytokines are known to specifically induce up-regulation of B7-H1 molecule in DCs, for example IL-27 [122], IFN $\beta$  in multiple sclerosis patients [156] as well as IFN $\gamma$  in patients with pancreatic cancer [120] or chronic hepatitis b [157]. Also B7-DC expression was found to be inducible on DCs after stimulation with cytokines like IFN $\gamma$ , IL-4 or GM-CSF [158]. This is partially in line with our observations, that cytokines in our experimental setting IFN $\alpha$  can modulate the expression of immunosuppressive molecules like B7-H1/B7-DC as well as their intensity of expression per cell (MFI). To what extent 5-FU also has an impact on B7-H1/B7-DC expression needs to be investigated further.

This because 5-FU kills cells, and by inference, activates DC and MDSC and therefore possibly has an impact on B7-H1 molecule expression.

To furthermore compare WT and B7-H1 KO mice, we also examined the cytokine as well as growth factors produced by those two mouse strains in serum samples of tumor-bearing mice as well as in medium supernatants from the coculture of splenocytes and MDSC from the proliferation assay. Due to the anti-inflammatory effect and the impact of those cytokines on aspects like tumor volume, we analyzed those cytokines in detail.

In our work, lower VEGF concentrations were found in B7-H1 KO compared to WT tumor-bearing mice. This is not surprisingly since VEGF is a proangiogenic growth factor involved in the pathogenesis of many cancers [159, 160]. Folkman showed that the angiogenesis leads to the spread of tumor cells resulting in metastasis [161, 162]. Despite conflicting results, with no correlation to the outcome in pancreatic cancer patients [163, 164], in more than 90 percent of pancreatic cancer, overexpression of VEGF and its receptors was registered as correlating with larger tumor size, distant metastasis and poor prognosis [165-170]. In line with the above seen results, the determined lower VEGF concentrations observed in B7-H1 KO mice is advantageous and encourages our linkage between B7-H1 KO mice and smaller tumor volumes and longer survival rates discussed later on in more detail. Analyzing the impact of chemo- and immunotherapy on the VEGF serum concentration, in WT tumor-bearing mice, the highest concentration was found in the untreated control group and the lowest in the combined group receiving IFN $\alpha$ +5-FU treatment. Between the treatment groups and the control in B7-H1 KO tumor-bearing mice, we found no significant difference. Our results are partially in line with earlier observations made in human neuroendocrine tumors, that IFN $\alpha$  inhibits VEGF gene transcription [171]. Also others have noted before that therapeutics can have an impact on the VEGF concentration, for example Legros, Bourcier et al. showed that Imatinib mesylate decreases VEGF plasma concentration in patients suffering from myeloid leukemia [172]. This allows us to speculate that at least in WT mice, the combined applied therapy leads to a decrease in VEGF concentration, which has a positive impact on those animals.

Another important aspect we need to consider in the context of VEGF concentration is that on the one hand, this cytokine has an activating impact on MDSC, but on the

other hand, can also be produced by MDSC [173, 174]. To further pursue the question whether MDSCs also have an impact on the VEGF concentration, we therefore examined the change in VEGF concentration in medium supernatants with and without the presence of immunosuppressive WT MDSC. It was shown before that VEGF is one of the factors able to induce MDSC expansion [173] and beyond that, VEGF serum levels directly correlate with the frequency of MDSC in the blood and spleen (reviewed in [175, 176]). Since we observed in our experiment higher concentrations of VEGF in the presence of WT MDSC in both supernatants of cultures containing WT or B7-H1 KO splenocytes, this is in line with previous investigations. Taken together, a feedback between VEGF concentration, the immunosuppressive capacity of MDSC and B7-H1 molecule can be drawn and leads us to several main conclusions. First, B7-H1 KO tumor-bearing mice have an advantage over WT mice due to lower serum VEGF levels. Second, the positive effect of combined chemo- and immunotherapy in WT mice resulting in lower VEGF concentrations and therefore less pronounced tumor-cell spread and distant metastasis. Third, higher MDSC ratios lead to increased VEGF concentrations. Since we have discussed earlier that B7-H1 KO tumor-bearing mice have less MDSC, this is another aspect in the prerequisite for a lower metastasis rate and a longer survival.

IL-1 $\beta$  plays an important role in tumorigenesis and development. It is known that this cytokine expression is augmented in most human cancers and that high plasma IL-1 $\beta$  levels are associated with a worse prognosis (reviewed in [177]). Moreover, it is known that B7-H1 inhibits anti-cancer immune response by the interaction with its T lymphocyte ligand PD-1, resulting in the impairment of cytokine production [63, 178] and T lymphocyte anergy and apoptosis [112, 179-181]. Our results of the analysis of the examined cytokine IL-1 $\beta$  revealed significantly lower concentrations in serum samples of B7-H1 KO compared to WT tumor-bearing mice. The analysis of chemo- and immunotherapy impact revealed significantly higher IL-1 $\beta$  concentrations in serum samples of IFN $\alpha$  and IFN $\alpha$ +5-FU treated B7-H1 KO mice. It was shown by Xu, Yin et al. that IL-1 $\beta$  inhibition reduces tumor growth by limiting inflammation, and furthermore, by inducing the maturation of MDSC into M1 macrophages [177]. We showed that B7-H1 KO mice have lower IL-1 $\beta$  serum concentrations, and this result lets us assume that it is another factor resulting in lower MDSC ratios and lower tumor volume in B7-H1 KO mice that was observed by us.

IL-6 belongs to the pro-inflammatory cytokines and is linked to poor prognosis in different hematopoietic and solid tumors [182, 183]. We found no significant differences in IL-6 serum concentrations between WT and B7-H1 tumor-bearing mice. In samples of WT tumor-bearing mice, the treatment with IFN $\alpha$ +5-FU increased the cytokine production of IL-6, whereas in samples of B7-H1 KO tumor-bearing mice, a 5-FU treatment increased the concentration of IL-6. As it is known that IL-6 concentration is triggered by IL-1 $\beta$  cytokine in the tumor microenvironment [184], it is not surprising that in our experiment, both the concentration of IL-6 and IL-1 $\beta$  are increased in serum samples of tumor-bearing mice.

So far, we have discussed the changes and differences in systemic cytokine concentrations. As a next step, we also analyzed the medium supernatants of our cocultures containing activated/ non-activated splenocytes and immunosuppressive MDSC in detail. IFN $\gamma$  is a cytokine that promotes anti-tumor immunity and moreover has proinflammatory characteristics important to the action of T cells (reviewed in [185]). In our results, we have seen significantly higher IFN $\gamma$  concentrations after activation of splenocytes with CD3/CD28 in both mouse strains. The comparison of B7-H1 KO to WT samples showed significantly higher concentrations of IFN $\gamma$  in the supernatants of B7-H1 KO splenocytes. This is in line with data showing that the B7-H1 blockade with antibodies and induce a significant increase in IFN $\gamma$  concentration in a mouse pancreatic tumor model [186]. Furthermore, after adding WT MDSC to the culture, a tendency towards decreased IFN $\gamma$  concentrations was determined. With our results we were able to demonstrate a higher IFN $\gamma$  production in cultures of B7-H1 KO splenocytes, which can at least partially explain the higher anti-tumor immunity of B7-H1 KO mice resulting in lower tumor volumes and longer survival rates. Our data also revealed the immunosuppressive effect of MDSC, explaining the decrease in IFN $\gamma$  concentration. With our observations, we can suggest that B7-H1 molecule plays an important role for IFN $\gamma$  production.

Concerning IL-10, it is generally known that this cytokine has anti-inflammatory capacities. However, IL-10 cytokine is important for maintaining the IFN $\gamma$ /IL-10 balance in the organism. It was observed that the presence of B7-H1 molecules is associated with an increase in IL-10 cytokine production [63]. Our analysis of IL-10 cytokine concentration in medium supernatants showed however higher

concentrations of this cytokine after activation with CD3/CD28 antibody in samples of B7-H1 KO splenocytes compared to WT splenocytes. This could explain the higher concentration of IL-10 without an impact of the molecule B7-H1 on this result. Also in other diseases like infection with *Plasmodium vivax* malaria, significantly higher levels of both pro- (IFN- $\gamma$ ) and anti-inflammatory (IL-10) cytokines were observed [187], showing that parallel increases can be found in different pathological situations. Furthermore, after adding WT MDSC to the culture, in samples containing WT splenocytes a highly significant increase in IL-10 concentration was determined. Since we did not see an increase in IFN $\gamma$  concentration in the presence of MDSC, this would likely point out in this case that the IFN $\gamma$ /IL-10 balance plays no decisive role.

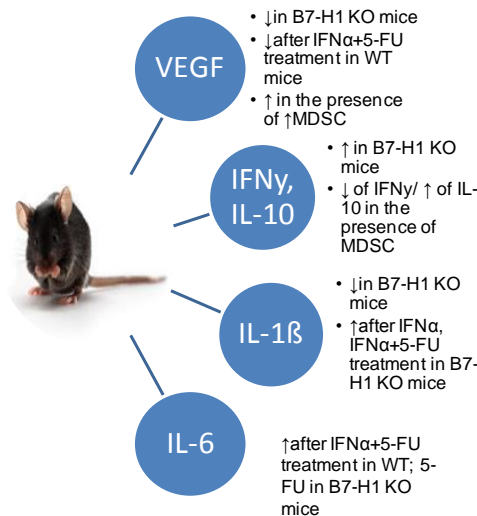


**Fig.4. 1 Differences in cytokine and growth factor concentration between WT and B7-H1 KO tumor-bearing mice with and without treatment**

From our data, one can see that such immunological players as discussed above, can probably be linked and influenced by each other. However, the most important aspect in pancreatic cancer patients is the clinical outcome. It was reported that B7-H1 expression on tumor cells correlates with an inferior clinical outcome in various solid human cancers like kidney [118], breast [188], ovarian [189], bladder [190], liver [191], and gastric [119] cancer. Previously, it was shown in PDAC patients that high B7-H1 expression is correlated to an unfavorable prognosis for these patients [116, 120]. In our survival experiment series, comparing WT and B7-H1 KO tumor-bearing mice in

an orthotopic Panc02 tumor model, we were able to show that B7-H1 KO tumor-bearing mice had a significantly higher survival rate compared to WT mice, regardless the chosen treatment. This is also consistent with observations made in colorectal cancer patients, where a longer survival was determined for patients with lower B7-H1 expression compared to those with a higher expression of this molecule [192]. This shows that a longer survival due to lower/no B7-H1 molecule expression is not specific for one cancer type, but is valid for various tumors in patients and mice and can be considered as a general effect.

The success of anti-tumor therapy is measured on a longer survival rate, and moreover, on parameters such as tumor size and distant metastasis rate. Therefore, we used an experiment series to examine the differences in tumor development, tumor volume and metastasis rates between our two mouse strains as well as between the different applied treatments. Significantly lower volumes of visible tumors were found in B7-H1 KO mice in the control group as well as in all treatment groups compared to WT mice. In a pancreatic tumor model, the blocking of either B7-H1 or B7-DC with antibodies revealed an efficient inhibition of tumor growth [186]. In a murine acute myeloid leukemia model, it was shown that mice lacking B7-H1 as well as mice treated with a B7-H1 blocking antibody, had a significantly lower tumor burden and survived longer [193]. Also in other cancers like melanoma, renal-cell and ovarian cancer, similar results, including tumor shrinkage, were observed after applying a B7-H1 blocking antibody [194]. Since we and others showed that the absence of B7-H1 molecule leads to lower tumor volumes in several tumor models, we assume that it is a general effect and independent of the tumor model as well as of the type of blockade by the B7-H1 molecule. Especially remarkable at this point is that blocking B7-H1 molecules on immune cells sufficiently reveals what an important role immune cells have in a cancer situation. Beyond that, as expected the impact of chemo- and immunotherapy can also influence the tumor volume. We demonstrated a significantly lower tumor volume in both mouse strains after treatment with 5-FU and the combination of IFN $\alpha$ +5-FU compared to the controls. This is supported by the data in a hematoma 22 tumor model, where a reduction of the tumor volume was seen in mice after 5-FU treatment [195]. This confirms our results that treatment of 5-Fu is able to reduce tumor volume in pancreatic cancer, but also in other cancers as

investigated by others. In addition, IFN $\alpha$  with its considered radio- and chemo sensitizing effect, is able to improve the impact of chemotherapy [55, 56].

By analyzing the metastasis rate of tumor-bearing mice, we observed lower rates of visible distant metastasis in B7-H1 KO compared to WT tumor-bearing mice. This observation was made for peritoneal wall metastasis as well as for the analysis of liver and colon metastasis. Also in patients with colorectal cancer, Song, Chen et al. reported a correlation between the overexpression of B7-H1 molecule and distant metastasis [192]. In other human cancers like Soft Tissue Sarcomas [196] and renal cell cancer [197], the B7-H1 expression in those patients was associated with distant metastasis and a poor prognosis. This confirms our hypothesis that the B7-H1 regulatory molecule plays a decisive role resulting in a poor prognosis for patients suffering from cancer, and that this effect is not specific for pancreatic cancer seems to be a general observation seen in tumor patients.

A following important question is whether a causal relationship between the tumor volume and different cells of the immune system can be drawn. To examine this, we analyzed possible correlations by evaluating the data from our different experiment series using Spearman correlation analysis. Only between the tumor volume and MDSC, was a significant correlation observed in the analysis. Previously, published data from animal studies also suggested a linear relationship between primary tumor size and MDSC [198]. Between other cell fractions like Treg, DC or T lymphocytes, and the tumor volume of tumor-bearing mice, no such connection was recognizable. This confirms once again the immunosuppressive capacity of MDSC in a tumor milieu and the important role of MDSC in the establishment and development of PDAC.

Summarizing the results of this project, the absence of the regulatory molecule B7-H1 seems to considerably influence tumor development and establishment, and furthermore, the survival rate in tumor-bearing B7-H1 KO mice. A number of different but related factors have to be taken into consideration. First, the decreased number of immunosuppressive MDSC in B7-H1 KO mice seems to have a major impact. Second, the higher frequency of especially CD8<sup>+</sup> T cell subsets like Tem and Tcm is associated with the absence of the B7-H1 molecule. Third, the lower serum concentration of the proangiogenic growth factor VEGF in tumor-bearing B7-H1

KO mice diminishes the tumor cell spread resulting in lower rates of distant metastases and a more favorable prognosis. Fourth, the higher IFN $\gamma$  and lower IL-1 $\beta$  level in B7-H1 KO mice compared to WT mice. But most important, the lower tumor volume and distant metastasis rates as well as the longer survival in B7-H1 KO mice compared to WT mice.

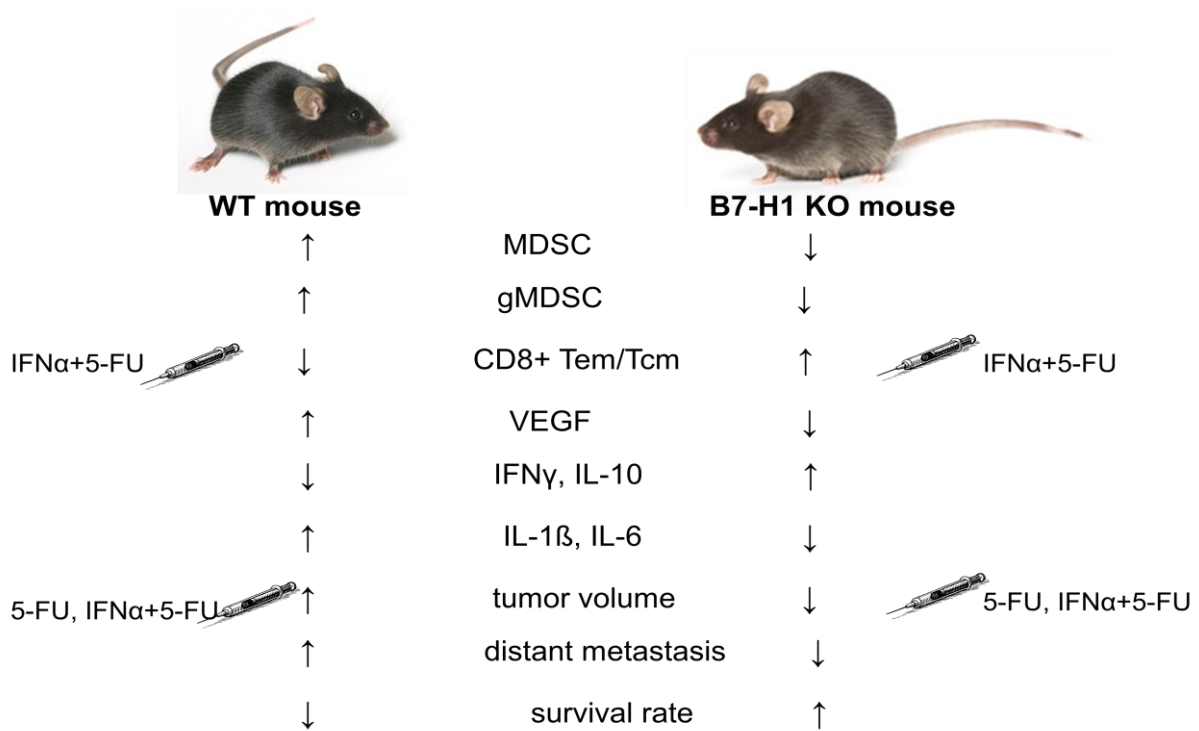


**Fig.4. 2 Summarized presentation of the most meaningful results**

## 5. Summary

PDAC remains today a devastating disease characterized by a poor prognosis and low survival rates in patients. This is primarily due to its late recognition, high metastasis rates and poor response to curative therapies such as chemotherapy or radiation. Immune therapy could provide promising opportunities for the treatment of PDAC. But first, it is important to analyze the immune system of PDAC patients, respectively mice. In this work, we analyzed the precise role of the B7-H1 expression on cells of the immune system, with the main focus on MDSC in the context of anti-tumor immunity in PDAC in both *in vitro* and *in vivo* experiments using WT and B7-H1 KO healthy and tumor-bearing mice. Higher ratios of CD4<sup>+</sup>/CD8<sup>+</sup> Tem and Tcm were seen in splenocytes of B7-H1 KO compared to WT healthy and tumor-bearing mice. The analysis of the MDSC population revealed lower frequencies of total MDSC in spleens of B7-H1 KO compared to spleens of WT tumor-bearing mice. After the 5-FU and IFN $\alpha$ +5-FU treatment, higher ratios of MDSC were seen in B7-H1 KO spleens. In tumors of B7-H1 KO mice, significantly lower ratios of MDSC and a decreased ratio of gMDSC were observed compared to that in WT tumor-bearing mice. Furthermore, significantly lower ratios of iNOS<sup>+</sup> gMDSC and mMDSC were determined in tumors of B7-H1 KO compared to untreated WT tumor-bearing mice. In splenocytes of tumor-bearing WT mice, a significant decrease in B7-H1 MFI of total MDSC was found after treatment with IFN $\alpha$ +5-FU. Lower VEGF concentrations were found in serum samples of B7-H1 KO compared to WT tumor-bearing mice, and higher concentrations were found in medium supernatants in the presence of WT MDSC. The analysis of IL-1 $\beta$  revealed significantly lower concentrations in serum samples of B7-H1 KO compared to WT tumor-bearing mice. For IFN $\gamma$ , significantly higher concentrations were found in medium supernatants containing B7-H1 KO splenocytes. In our survival experiment series, we demonstrated a significantly higher survival rate as well as a lower tumor frequency, tumor volume and distant metastasis rate in B7-H1 KO compared to WT mice, regardless the chosen treatment. Beyond that, a significantly lower tumor volume was determined after treatment of both mouse strains with 5-FU and IFN $\alpha$ +5-FU. In summary, through this work we characterized the immune system of WT and B7-H1 KO healthy and PDAC - bearing mice with a main focus on the molecule B7-H1 and MDSC, as well as the impact of chemo- and immune therapy.

## 6. Zusammenfassung

Charakteristisch für das Pankreasadenokarzinom (PDAC) sind eine schlechte Prognose und geringe Überlebensraten verursacht durch zu späte Diagnose, hohe Metastasierungsraten und geringes Ansprechen auf Chemotherapie oder Bestrahlung. Immuntherapie könnte einen neuen Therapieansatz des PDAC darstellen. Zunächst ist es wichtig, das Immunsystem betroffener Patienten/Mäuse genauer zu analysieren. In dieser Arbeit haben wir die Rolle der B7-H1 Expression auf Zellen des Immunsystems, besonders MDSC, im Zusammenhang mit der Anti-Tumor-Immunität im PDAC in *in vitro* und *in vivo* Experimenten an WT und B7-H1 KO gesunden und tumortragenden Mäusen untersucht. Einen höheren Anteil an CD4<sup>+</sup>/CD8<sup>+</sup> Tem und Tcm gab es in Splenozyten von gesunden und tumortragenden B7-H1 KO im Vergleich zu WT Mäusen. Niedrigere Prozentzahlen von MDSC wurden in Milzen von tumortragenden B7-H1 KO im Vergleich zu WT Mäusen gesehen. Nach 5-FU und IFN $\alpha$ +5-FU Behandlung stieg die Anzahl an MDSC in B7-H1 KO Milzen an. B7-H1 KO Tumoren wiesen signifikant niedrigere Anteile von MDSC und gMDSC auf als WT Tumoren. Die Zahl an iNOS<sup>+</sup> gMDSC und mMDSC war signifikant geringer in Tumoren unbehandelter B7-H1 KO als in WT Mäusen. Weiterhin wurde in Splenozyten tumortragender WT Mäuse ein signifikant geringerer B7-H1 MFI Wert von MDSC nach IFN $\alpha$ +5-FU Behandlung bestimmt. In Serumproben von B7-H1 KO tumortragenden Mäusen sind geringere VEGF Konzentrationen festgestellt worden und in Mediumüberständen waren sie höher in der Anwesenheit von MDSC. Die IL-1 $\beta$  Serumkonzentration waren signifikant niedriger in tumortragenden B7-H1 KO als in WT Mäusen. Zudem wurden signifikant höhere IFN $\gamma$  Konzentrationen in Mediumüberständen mit B7-H1 KO Splenozyten gemessen. Anhand unserer Survival-Experimente haben wir sowohl eine signifikant höhere Überlebensrate als auch niedrigere Tumorfrequenzen, Tumorumfänge und Metastasierungsraten in B7-H1 KO Mäusen gesehen im Vergleich zu WT, unabhängig von der Therapie. Zudem wurden in beiden Mausstämmen signifikant niedrigere Tumorumfänge nach 5-FU und IFN $\alpha$ +5-FU Behandlung bestimmt. Zusammenfassend haben wir in dieser Arbeit das Immunsystem von gesunden und PDAC tumortragenden WT und B7-H1 KO Mäusen, mit dem Schwerpunkt auf dem Molekül B7-H1 und MDSC sowie den Einfluss von Chemo- und Immuntherapie, untersucht.

### III. List of Literature

1. Ed by Standring, S., *Gray's Anatomy*. Vol. 40th edition. 2008: Churchill Livingstone.
2. Fricke-Richter, B.-. *Atlas der Anatomie des Hundes*. Vol. 8. Auflage. 2007: Schlütersche.
3. Despopoulos, S.-. *Taschenatlas der Physiologie*. Vol. 7. Auflage. 2007: Thieme.
4. Jemal, A., R. Siegel, E. Ward, Y. Hao, J. Xu and M.J. Thun, *Cancer statistics, 2009*. CA Cancer J Clin, 2009. 59(4): p. 225-49.
5. Chu, D., W. Kohlmann and D.G. Adler, *Identification and screening of individuals at increased risk for pancreatic cancer with emphasis on known environmental and genetic factors and hereditary syndromes*. JOP, 2010. 11(3): p. 203-12.
6. Kaur, S., M.J. Baine, M. Jain, A.R. Sasson and S.K. Batra, *Early diagnosis of pancreatic cancer: challenges and new developments*. Biomark Med, 2012. 6(5): p. 597-612.
7. Dahme E., W.E., *Grundriß der speziellen anatomischen Pathologie der Haustiere*. Vol. 6. Auflage. 2007: Enke.
8. Bonath, K.H., *Kleintierkrankheiten Chirurgie der Weichteile*. Vol. 2. Auflage. 2014: Ulmer.
9. Farrow, D.C. and S. Davis, *Risk of pancreatic cancer in relation to medical history and the use of tobacco, alcohol and coffee*. Int J Cancer, 1990. 45(5): p. 816-20.
10. Lowenfels, A.B. and P. Maisonneuve, *Epidemiology and prevention of pancreatic cancer*. Jpn J Clin Oncol, 2004. 34(5): p. 238-44.
11. Lowenfels, A.B., P. Maisonneuve, G. Cavallini, R.W. Ammann, P.G. Lankisch, J.R. Andersen, E.P. Dimagno, A. Andren-Sandberg and L. Domellof, *Pancreatitis and the risk of pancreatic cancer. International Pancreatitis Study Group*. N Engl J Med, 1993. 328(20): p. 1433-7.
12. Haddock, G. and D.C. Carter, *Aetiology of pancreatic cancer*. Br J Surg, 1990. 77(10): p. 1159-66.
13. Greenhalf, W., C. Grocock, M. Harcus and J. Neoptolemos, *Screening of high-risk families for pancreatic cancer*. Pancreatology, 2009. 9(3): p. 215-22.

## List of Literature

---

14. Lynch, H.T., T. Smyrk, S.E. Kern, R.H. Hruban, C.J. Lightdale, S.J. Lemon, J.F. Lynch, L.R. Fusaro, R.M. Fusaro and P. Ghadirian, *Familial pancreatic cancer: a review*. *Semin Oncol*, 1996. 23(2): p. 251-75.
15. Hruban, R.H., R.E. Wilentz and S.E. Kern, *Genetic progression in the pancreatic ducts*. *Am J Pathol*, 2000. 156(6): p. 1821-5.
16. Hruban, R.H., N.V. Adsay, J. Albores-Saavedra, C. Compton, E.S. Garrett, S.N. Goodman, S.E. Kern, D.S. Klimstra, G. Kloppel, D.S. Longnecker, J. Luttges and G.J. Offerhaus, *Pancreatic intraepithelial neoplasia: a new nomenclature and classification system for pancreatic duct lesions*. *Am J Surg Pathol*, 2001. 25(5): p. 579-86.
17. Goggins, M., R.H. Hruban and S.E. Kern, *BRCA2 is inactivated late in the development of pancreatic intraepithelial neoplasia: evidence and implications*. *Am J Pathol*, 2000. 156(5): p. 1767-71.
18. Wilentz, R.E., C.A. Iacobuzio-Donahue, P. Argani, D.M. McCarthy, J.L. Parsons, C.J. Yeo, S.E. Kern and R.H. Hruban, *Loss of expression of Dpc4 in pancreatic intraepithelial neoplasia: evidence that DPC4 inactivation occurs late in neoplastic progression*. *Cancer Res*, 2000. 60(7): p. 2002-6.
19. Shay, J.W., *Molecular pathogenesis of aging and cancer: are telomeres and telomerase the connection?* *J Clin Pathol*, 1997. 50(10): p. 799-800.
20. van Heek, N.T., A.K. Meeker, S.E. Kern, C.J. Yeo, K.D. Lillemoe, J.L. Cameron, G.J. Offerhaus, J.L. Hicks, R.E. Wilentz, M.G. Goggins, A.M. De Marzo, R.H. Hruban and A. Maitra, *Telomere shortening is nearly universal in pancreatic intraepithelial neoplasia*. *Am J Pathol*, 2002. 161(5): p. 1541-7.
21. Yachida, S., S. Jones, I. Bozic, T. Antal, R. Leary, B. Fu, M. Kamiyama, R.H. Hruban, J.R. Eshleman, M.A. Nowak, V.E. Velculescu, K.W. Kinzler, B. Vogelstein and C.A. Iacobuzio-Donahue, *Distant metastasis occurs late during the genetic evolution of pancreatic cancer*. *Nature*, 2010. 467(7319): p. 1114-7.
22. Krech, R.L. and D. Walsh, *Symptoms of pancreatic cancer*. *J Pain Symptom Manage*, 1991. 6(6): p. 360-7.
23. Norton, J.A., *Surgery- Basic Science and Clinical Evidence*. Vol. 2. Edition. 2008: Springer Verlag.
24. Gerok-Huber-Meinertz-Zeidler, *Die Innere Medizin*. Vol. 11. Auflage. 2007: Schattauer.
25. Bakkevold, K.E., B. Arnesjo and B. Kambestad, *Carcinoma of the pancreas and papilla of Vater: presenting symptoms, signs, and diagnosis related to stage and tumour site. A prospective multicentre trial in 472 patients*. *Norwegian Pancreatic Cancer Trial*. *Scand J Gastroenterol*, 1992. 27(4): p. 317-25.

## List of Literature

---

26. Wiersema, M.J., P. Vilmann, M. Giovannini, K.J. Chang and L.M. Wiersema, *Endosonography-guided fine-needle aspiration biopsy: diagnostic accuracy and complication assessment*. *Gastroenterology*, 1997. 112(4): p. 1087-95.
27. Bares, R., P. Klever, D. Hellwig, S. Hauptmann, J. Fass, U. Hambuechen, L. Zopp, B. Mueller, U. Buell and V. Schumpelick, *Pancreatic cancer detected by positron emission tomography with 18F-labelled deoxyglucose: method and first results*. *Nucl Med Commun*, 1993. 14(7): p. 596-601.
28. Kahaleh, M., A.J. Hernandez, J. Tokar, R.B. Adams, V.M. Shami and P. Yeaton, *Interventional EUS-guided cholangiography: evaluation of a technique in evolution*. *Gastrointest Endosc*, 2006. 64(1): p. 52-9.
29. Spillmann, T., H. Schnell-Kretschmer, M. Dick, K.A. Grondahl, T.C. Lenhard and S.K. Rust, *Endoscopic retrograde cholangio-pancreatography in dogs with chronic gastrointestinal problems*. *Vet Radiol Ultrasound*, 2005. 46(4): p. 293-9.
30. Berger, A.C., M. Garcia, Jr., J.P. Hoffman, W.F. Regine, R.A. Abrams, H. Safran, A. Konski, A.B. Benson, 3rd, J. MacDonald and C.G. Willett, *Postresection CA 19-9 predicts overall survival in patients with pancreatic cancer treated with adjuvant chemoradiation: a prospective validation by RTOG 9704*. *J Clin Oncol*, 2008. 26(36): p. 5918-22.
31. Freelove, R. and A.D. Walling, *Pancreatic cancer: diagnosis and management*. *Am Fam Physician*, 2006. 73(3): p. 485-92.
32. Gillen, S., T. Schuster, C. Meyer Zum Buschenfelde, H. Friess and J. Kleeff, *Preoperative/neoadjuvant therapy in pancreatic cancer: a systematic review and meta-analysis of response and resection percentages*. *PLoS Med*, 2010. 7(4): p. e1000267.
33. Carter, D.C., *Cancer of the pancreas*. *Gut*, 1990. 31(5): p. 494-6.
34. Sharma, C., K.M. Eltawil, P.D. Renfrew, M.J. Walsh and M. Molinari, *Advances in diagnosis, treatment and palliation of pancreatic carcinoma: 1990-2010*. *World J Gastroenterol*, 2011. 17(7): p. 867-97.
35. Neoptolemos, J.P., D.D. Stocken, H. Friess, C. Bassi, J.A. Dunn, H. Hickey, H. Beger, L. Fernandez-Cruz, C. Dervenis, F. Lacaine, M. Falconi, P. Pederzoli, A. Pap, D. Spooner, D.J. Kerr, M.W. Buchler and C. European Study Group for Pancreatic, *A randomized trial of chemoradiotherapy and chemotherapy after resection of pancreatic cancer*. *N Engl J Med*, 2004. 350(12): p. 1200-10.
36. Cameron, J.L., T.S. Riall, J. Coleman and K.A. Belcher, *One thousand consecutive pancreaticoduodenectomies*. *Ann Surg*, 2006. 244(1): p. 10-5.
37. Kennedy, E.P. and C.J. Yeo, *The case for routine use of adjuvant therapy in pancreatic cancer*. *J Surg Oncol*, 2007. 95(7): p. 597-603.

## List of Literature

---

38. Richter, A., M. Niedergethmann, J.W. Sturm, D. Lorenz, S. Post and M. Trede, *Long-term results of partial pancreaticoduodenectomy for ductal adenocarcinoma of the pancreatic head: 25-year experience*. World J Surg, 2003. 27(3): p. 324-9.
39. Lim, J.E., M.W. Chien and C.C. Earle, *Prognostic factors following curative resection for pancreatic adenocarcinoma: a population-based, linked database analysis of 396 patients*. Ann Surg, 2003. 237(1): p. 74-85.
40. Hishinuma, S., Y. Ogata, M. Tomikawa, I. Ozawa, K. Hirabayashi and S. Igarashi, *Patterns of recurrence after curative resection of pancreatic cancer, based on autopsy findings*. J Gastrointest Surg, 2006. 10(4): p. 511-8.
41. Guo, X.Z., Z.M. Cui and X. Liu, *Current developments, problems and solutions in the non-surgical treatment of pancreatic cancer*. World J Gastrointest Oncol, 2013. 5(2): p. 20-8.
42. Bouchard, M., R.A. Amos, T.M. Briere, S. Beddar and C.H. Crane, *Dose escalation with proton or photon radiation treatment for pancreatic cancer*. Radiother Oncol, 2009. 92(2): p. 238-43.
43. Hong, T.S., D.L. Craft, F. Carlsson and T.R. Bortfeld, *Multicriteria optimization in intensity-modulated radiation therapy treatment planning for locally advanced cancer of the pancreatic head*. Int J Radiat Oncol Biol Phys, 2008. 72(4): p. 1208-14.
44. Sultana, A., C. Tudur Smith, D. Cunningham, N. Starling, D. Tait, J.P. Neoptolemos and P. Ghaneh, *Systematic review, including meta-analyses, on the management of locally advanced pancreatic cancer using radiation/combined modality therapy*. Br J Cancer, 2007. 96(8): p. 1183-90.
45. Burris, H.A., 3rd, M.J. Moore, J. Andersen, M.R. Green, M.L. Rothenberg, M.R. Modiano, M.C. Cripps, R.K. Portenoy, A.M. Storniolo, P. Tarassoff, R. Nelson, F.A. Dorr, C.D. Stephens and D.D. Von Hoff, *Improvements in survival and clinical benefit with gemcitabine as first-line therapy for patients with advanced pancreas cancer: a randomized trial*. J Clin Oncol, 1997. 15(6): p. 2403-13.
46. Neoptolemos, J.P., J.A. Dunn, D.D. Stocken, J. Almond, K. Link, H. Beger, C. Bassi, M. Falconi, P. Pederzoli, C. Dervenis, L. Fernandez-Cruz, F. Lacaine, A. Pap, D. Spooner, D.J. Kerr, H. Friess, M.W. Buchler and C. European Study Group for Pancreatic, *Adjuvant chemoradiotherapy and chemotherapy in resectable pancreatic cancer: a randomised controlled trial*. Lancet, 2001. 358(9293): p. 1576-85.
47. Pliarchopoulou, K. and D. Pectasides, *Pancreatic cancer: current and future treatment strategies*. Cancer Treat Rev, 2009. 35(5): p. 431-6.
48. Conroy, T., F. Desseigne, M. Ychou, O. Bouche, R. Guimbaud, Y. Becouarn, A. Adenis, J.L. Raoul, S. Gourgou-Bourgade, C. de la Fouchardiere, J. Bennouna, J.B. Bachet, F. Khemissa-Akouz, D. Pere-Verge, C. Delbaldo, E. Assenat, B. Chauffert, P. Michel, C. Montoto-Grillot, M. Ducreux, U. Groupe Tumeurs Digestives of and P. Intergroup, *FOLFIRINOX versus gemcitabine for metastatic pancreatic cancer*. N Engl J Med, 2011. 364(19): p. 1817-25.

## List of Literature

---

49. [www.cancer.gov/2012](http://www.cancer.gov/2012).
50. Laheru, D. and E.M. Jaffee, *Immunotherapy for pancreatic cancer - science driving clinical progress*. Nat Rev Cancer, 2005. 5(6): p. 459-67.
51. Kirkwood, J., *Cancer immunotherapy: the interferon-alpha experience*. Semin Oncol, 2002. 29(3 Suppl 7): p. 18-26.
52. Belardelli, F., M. Ferrantini, E. Proietti and J.M. Kirkwood, *Interferon-alpha in tumor immunity and immunotherapy*. Cytokine Growth Factor Rev, 2002. 13(2): p. 119-34.
53. Gutterman, J.U., *Cytokine therapeutics: lessons from interferon alpha*. Proc Natl Acad Sci U S A, 1994. 91(4): p. 1198-205.
54. Iacopino, F., G. Ferrandina, G. Scambia, P. Benedetti-Panici, S. Mancuso and G. Sica, *Interferons inhibit EGF-stimulated cell growth and reduce EGF binding in human breast cancer cells*. Anticancer Res, 1996. 16(4A): p. 1919-24.
55. Ma, J.H., E. Patrut, J. Schmidt, H.P. Knaebel, M.W. Buchler and A. Marten, *Synergistic effects of interferon-alpha in combination with chemoradiation on human pancreatic adenocarcinoma*. World J Gastroenterol, 2005. 11(10): p. 1521-8.
56. Schmidt, J., E.M. Patrut, J. Ma, D. Jager, H.P. Knaebel, M.W. Buchler and A. Marten, *Immunomodulatory impact of interferon-alpha in combination with chemoradiation of pancreatic adenocarcinoma (CapRI)*. Cancer Immunol Immunother, 2006. 55(11): p. 1396-405.
57. Khallouf, H., A. Marten, S. Serba, V. Teichgraber, M.W. Buchler, D. Jager and J. Schmidt, *5-Fluorouracil and interferon-alpha immunochemotherapy enhances immunogenicity of murine pancreatic cancer through upregulation of NKG2D ligands and MHC class I*. J Immunother, 2012. 35(3): p. 245-53.
58. Zhu, Y., I. Tibensky, J. Schmidt, E. Ryschich and A. Marten, *Interferon-alpha enhances antitumor effect of chemotherapy in an orthotopic mouse model for pancreatic adenocarcinoma*. J Immunother, 2008. 31(7): p. 599-606.
59. Pfeffer, L.M., C.A. Dinarello, R.B. Herberman, B.R. Williams, E.C. Borden, R. Bordens, M.R. Walter, T.L. Nagabhushan, P.P. Trotta and S. Pestka, *Biological properties of recombinant alpha-interferons: 40th anniversary of the discovery of interferons*. Cancer Res, 1998. 58(12): p. 2489-99.
60. Marrack, P., J. Kappler and T. Mitchell, *Type I interferons keep activated T cells alive*. J Exp Med, 1999. 189(3): p. 521-30.
61. Matikainen, S., T. Sareneva, T. Ronni, A. Lehtonen, P.J. Koskinen and I. Julkunen, *Interferon-alpha activates multiple STAT proteins and upregulates proliferation-associated IL-2Ralpha, c-myc, and pim-1 genes in human T cells*. Blood, 1999. 93(6): p. 1980-91.

## List of Literature

---

62. Coyle, A.J. and J.C. Gutierrez-Ramos, *The expanding B7 superfamily: increasing complexity in costimulatory signals regulating T cell function*. Nat Immunol, 2001. 2(3): p. 203-9.
63. Dong, H., G. Zhu, K. Tamada and L. Chen, *B7-H1, a third member of the B7 family, co-stimulates T-cell proliferation and interleukin-10 secretion*. Nat Med, 1999. 5(12): p. 1365-9.
64. Murphy, K., *Janeway's Immunobiology*. Vol. 8. Edition. 2011: Taylor & Francis Ltd.
65. Romagnani, S., *Type 1 T helper and type 2 T helper cells: functions, regulation and role in protection and disease*. Int J Clin Lab Res, 1991. 21(2): p. 152-8.
66. Luckheeram, R.V., R. Zhou, A.D. Verma and B. Xia, *CD4(+)T cells: differentiation and functions*. Clin Dev Immunol, 2012. 2012: p. 925135.
67. Pipkin, M.E. and J. Lieberman, *Delivering the kiss of death: progress on understanding how perforin works*. Curr Opin Immunol, 2007. 19(3): p. 301-8.
68. Harty, J.T., A.R. Tinnereim and D.W. White, *CD8+ T cell effector mechanisms in resistance to infection*. Annu Rev Immunol, 2000. 18: p. 275-308.
69. Sallusto, F., J. Geginat and A. Lanzavecchia, *Central memory and effector memory T cell subsets: function, generation, and maintenance*. Annu Rev Immunol, 2004. 22: p. 745-63.
70. Sallusto, F., D. Lenig, R. Forster, M. Lipp and A. Lanzavecchia, *Two subsets of memory T lymphocytes with distinct homing potentials and effector functions*. Nature, 1999. 401(6754): p. 708-12.
71. Lenschow, D.J., T.L. Walunas and J.A. Bluestone, *CD28/B7 system of T cell costimulation*. Annu Rev Immunol, 1996. 14: p. 233-58.
72. Freeman, G.J., A.S. Freedman, J.M. Segil, G. Lee, J.F. Whitman and L.M. Nadler, *B7, a new member of the Ig superfamily with unique expression on activated and neoplastic B cells*. J Immunol, 1989. 143(8): p. 2714-22.
73. Liu, Y.J., *IPC: professional type 1 interferon-producing cells and plasmacytoid dendritic cell precursors*. Annu Rev Immunol, 2005. 23: p. 275-306.
74. O'Keeffe, M., H. Hochrein, D. Vremec, I. Caminschi, J.L. Miller, E.M. Anders, L. Wu, M.H. Lahoud, S. Henri, B. Scott, P. Hertzog, L. Tatarczuch and K. Shortman, *Mouse plasmacytoid cells: long-lived cells, heterogeneous in surface phenotype and function, that differentiate into CD8(+) dendritic cells only after microbial stimulus*. J Exp Med, 2002. 196(10): p. 1307-19.
75. Nakano, H., M. Yanagita and M.D. Gunn, *CD11c(+)B220(+)Gr-1(+) cells in mouse lymph nodes and spleen display characteristics of plasmacytoid dendritic cells*. J Exp Med, 2001. 194(8): p. 1171-8.

## List of Literature

---

76. Shevach, E.M., *CD4+ CD25+ suppressor T cells: more questions than answers*. Nat Rev Immunol, 2002. 2(6): p. 389-400.
77. Toda, A. and C.A. Piccirillo, *Development and function of naturally occurring CD4+CD25+ regulatory T cells*. J Leukoc Biol, 2006. 80(3): p. 458-70.
78. Sakaguchi, S., N. Sakaguchi, M. Asano, M. Itoh and M. Toda, *Immunologic self-tolerance maintained by activated T cells expressing IL-2 receptor alpha-chains (CD25). Breakdown of a single mechanism of self-tolerance causes various autoimmune diseases*. J Immunol, 1995. 155(3): p. 1151-64.
79. Ziegler, S.F., *FOXP3: of mice and men*. Annu Rev Immunol, 2006. 24: p. 209-26.
80. Roncador, G., P.J. Brown, L. Maestre, S. Hue, J.L. Martinez-Torrecuadrada, K.L. Ling, S. Pratap, C. Toms, B.C. Fox, V. Cerundolo, F. Powrie and A.H. Banham, *Analysis of FOXP3 protein expression in human CD4+CD25+ regulatory T cells at the single-cell level*. Eur J Immunol, 2005. 35(6): p. 1681-91.
81. Karakhanova, S., M. Munder, M. Schneider, M. Bonyhadi, A.D. Ho and M. Goerner, *Highly efficient expansion of human CD4+CD25+ regulatory T cells for cellular immunotherapy in patients with graft-versus-host disease*. J Immunother, 2006. 29(3): p. 336-49.
82. Roncarolo, M.G., S. Gregori, M. Battaglia, R. Bacchetta, K. Fleischhauer and M.K. Levings, *Interleukin-10-secreting type 1 regulatory T cells in rodents and humans*. Immunol Rev, 2006. 212: p. 28-50.
83. Cesana, G.C., G. DeRaffele, S. Cohen, D. Moroziewicz, J. Mitcham, J. Stoutenburg, K. Cheung, C. Hesdorffer, S. Kim-Schulze and H.L. Kaufman, *Characterization of CD4+CD25+ regulatory T cells in patients treated with high-dose interleukin-2 for metastatic melanoma or renal cell carcinoma*. J Clin Oncol, 2006. 24(7): p. 1169-77.
84. Lu, L.F. and A. Rudensky, *Molecular orchestration of differentiation and function of regulatory T cells*. Genes Dev, 2009. 23(11): p. 1270-82.
85. Shevach, E.M., *Mechanisms of foxp3+ T regulatory cell-mediated suppression*. Immunity, 2009. 30(5): p. 636-45.
86. Campbell, D.J. and M.A. Koch, *Phenotypical and functional specialization of FOXP3+ regulatory T cells*. Nat Rev Immunol, 2011. 11(2): p. 119-30.
87. Scheffold, A., K.M. Murphy and T. Hofer, *Competition for cytokines: T(reg) cells take all*. Nat Immunol, 2007. 8(12): p. 1285-7.

## List of Literature

---

88. Chen, W., W. Jin, N. Hardegen, K.J. Lei, L. Li, N. Marinos, G. McGrady and S.M. Wahl, *Conversion of peripheral CD4+CD25- naive T cells to CD4+CD25+ regulatory T cells by TGF-beta induction of transcription factor Foxp3*. J Exp Med, 2003. 198(12): p. 1875-86.
89. Vignali, D.A., L.W. Collison and C.J. Workman, *How regulatory T cells work*. Nat Rev Immunol, 2008. 8(7): p. 523-32.
90. Shevchenko, I., S. Karakhanova, S. Soltek, J. Link, J. Bayry, J. Werner, V. Umansky and A.V. Bazhin, *Low-dose gemcitabine depletes regulatory T cells and improves survival in the orthotopic Panc02 model of pancreatic cancer*. Int J Cancer, 2013. 133(1): p. 98-107.
91. Zou, W., *Immunosuppressive networks in the tumour environment and their therapeutic relevance*. Nat Rev Cancer, 2005. 5(4): p. 263-74.
92. Whiteside, T.L., *Immune responses to malignancies*. J Allergy Clin Immunol, 2010. 125(2 Suppl 2): p. S272-83.
93. Linehan, D.C. and P.S. Goedegebuure, *CD25+ CD4+ regulatory T-cells in cancer*. Immunol Res, 2005. 32(1-3): p. 155-68.
94. Moo-Young, T.A., J.W. Larson, B.A. Belt, M.C. Tan, W.G. Hawkins, T.J. Eberlein, P.S. Goedegebuure and D.C. Linehan, *Tumor-derived TGF-beta mediates conversion of CD4+Foxp3+ regulatory T cells in a murine model of pancreas cancer*. J Immunother, 2009. 32(1): p. 12-21.
95. Gabrilovich, D.I. and S. Nagaraj, *Myeloid-derived suppressor cells as regulators of the immune system*. Nat Rev Immunol, 2009. 9(3): p. 162-74.
96. Ochoa, A.C., A.H. Zea, C. Hernandez and P.C. Rodriguez, *Arginase, prostaglandins, and myeloid-derived suppressor cells in renal cell carcinoma*. Clin Cancer Res, 2007. 13(2 Pt 2): p. 721s-726s.
97. Almand, B., J.I. Clark, E. Nikitina, J. van Beynen, N.R. English, S.C. Knight, D.P. Carbone and D.I. Gabrilovich, *Increased production of immature myeloid cells in cancer patients: a mechanism of immunosuppression in cancer*. J Immunol, 2001. 166(1): p. 678-89.
98. Kusmartsev, S., Y. Nefedova, D. Yoder and D.I. Gabrilovich, *Antigen-specific inhibition of CD8+ T cell response by immature myeloid cells in cancer is mediated by reactive oxygen species*. J Immunol, 2004. 172(2): p. 989-99.
99. Youn, J.I., S. Nagaraj, M. Collazo and D.I. Gabrilovich, *Subsets of myeloid-derived suppressor cells in tumor-bearing mice*. J Immunol, 2008. 181(8): p. 5791-802.
100. Bronte, V., P. Serafini, A. Mazzoni, D.M. Segal and P. Zanovello, *L-arginine metabolism in myeloid cells controls T-lymphocyte functions*. Trends Immunol, 2003. 24(6): p. 302-6.

## List of Literature

---

101. Bronte, V., P. Serafini, C. De Santo, I. Marigo, V. Tosello, A. Mazzoni, D.M. Segal, C. Staib, M. Lowel, G. Sutter, M.P. Colombo and P. Zanovello, *IL-4-induced arginase 1 suppresses alloreactive T cells in tumor-bearing mice*. J Immunol, 2003. 170(1): p. 270-8.
102. Rodriguez, P.C., A.H. Zea, K.S. Culotta, J. Zabaleta, J.B. Ochoa and A.C. Ochoa, *Regulation of T cell receptor CD3zeta chain expression by L-arginine*. J Biol Chem, 2002. 277(24): p. 21123-9.
103. Rodriguez, P.C., D.G. Quiceno and A.C. Ochoa, *L-arginine availability regulates T-lymphocyte cell-cycle progression*. Blood, 2007. 109(4): p. 1568-73.
104. Schmielau, J. and O.J. Finn, *Activated granulocytes and granulocyte-derived hydrogen peroxide are the underlying mechanism of suppression of t-cell function in advanced cancer patients*. Cancer Res, 2001. 61(12): p. 4756-60.
105. Kusmartsev, S. and D.I. Gabrilovich, *Inhibition of myeloid cell differentiation in cancer: the role of reactive oxygen species*. J Leukoc Biol, 2003. 74(2): p. 186-96.
106. Corzo, C.A., M.J. Cotter, P. Cheng, F. Cheng, S. Kusmartsev, E. Sotomayor, T. Padhya, T.V. McCaffrey, J.C. McCaffrey and D.I. Gabrilovich, *Mechanism regulating reactive oxygen species in tumor-induced myeloid-derived suppressor cells*. J Immunol, 2009. 182(9): p. 5693-701.
107. Huang, B., P.Y. Pan, Q. Li, A.I. Sato, D.E. Levy, J. Bromberg, C.M. Divino and S.H. Chen, *Gr-1+CD115+ immature myeloid suppressor cells mediate the development of tumor-induced T regulatory cells and T-cell anergy in tumor-bearing host*. Cancer Res, 2006. 66(2): p. 1123-31.
108. Sherger, M., W. Kisseberth, C. London, S. Olivo-Marston and T.L. Papenfuss, *Identification of myeloid derived suppressor cells in the peripheral blood of tumor bearing dogs*. BMC Vet Res, 2012. 8: p. 209.
109. Goulart, M.R., G.E. Pluhar and J.R. Ohlfest, *Identification of myeloid derived suppressor cells in dogs with naturally occurring cancer*. PLoS One, 2012. 7(3): p. e33274.
110. Greenwald, R.J., G.J. Freeman and A.H. Sharpe, *The B7 family revisited*. Annu Rev Immunol, 2005. 23: p. 515-48.
111. Keir, M.E., S.C. Liang, I. Guleria, Y.E. Latchman, A. Qipo, L.A. Albacker, M. Koulmanda, G.J. Freeman, M.H. Sayegh and A.H. Sharpe, *Tissue expression of PD-L1 mediates peripheral T cell tolerance*. J Exp Med, 2006. 203(4): p. 883-95.
112. Dong, H., S.E. Strome, D.R. Salomao, H. Tamura, F. Hirano, D.B. Flies, P.C. Roche, J. Lu, G. Zhu, K. Tamada, V.A. Lennon, E. Celis and L. Chen, *Tumor-associated B7-H1 promotes T-cell apoptosis: a potential mechanism of immune evasion*. Nat Med, 2002. 8(8): p. 793-800.

## List of Literature

---

113. Amarnath, S., C.W. Mangus, J.C. Wang, F. Wei, A. He, V. Kapoor, J.E. Foley, P.R. Massey, T.C. Felizardo, J.L. Riley, B.L. Levine, C.H. June, J.A. Medin and D.H. Fowler, *The PDL1-PD1 axis converts human TH1 cells into regulatory T cells*. *Sci Transl Med*, 2011. 3(111): p. 111ra120.
114. Moore, K.W., R. de Waal Malefyt, R.L. Coffman and A. O'Garra, *Interleukin-10 and the interleukin-10 receptor*. *Annu Rev Immunol*, 2001. 19: p. 683-765.
115. Akdis, C.A. and K. Blaser, *Mechanisms of interleukin-10-mediated immune suppression*. *Immunology*, 2001. 103(2): p. 131-6.
116. Nomi, T., M. Sho, T. Akahori, K. Hamada, A. Kubo, H. Kanehiro, S. Nakamura, K. Enomoto, H. Yagita, M. Azuma and Y. Nakajima, *Clinical significance and therapeutic potential of the programmed death-1 ligand/programmed death-1 pathway in human pancreatic cancer*. *Clin Cancer Res*, 2007. 13(7): p. 2151-7.
117. Ohigashi, Y., M. Sho, Y. Yamada, Y. Tsurui, K. Hamada, N. Ikeda, T. Mizuno, R. Yoriki, H. Kashizuka, K. Yane, F. Tsushima, N. Otsuki, H. Yagita, M. Azuma and Y. Nakajima, *Clinical significance of programmed death-1 ligand-1 and programmed death-1 ligand-2 expression in human esophageal cancer*. *Clin Cancer Res*, 2005. 11(8): p. 2947-53.
118. Thompson, R.H., S.M. Kuntz, B.C. Leibovich, H. Dong, C.M. Lohse, W.S. Webster, S. Sengupta, I. Frank, A.S. Parker, H. Zincke, M.L. Blute, T.J. Sebo, J.C. Cheville and E.D. Kwon, *Tumor B7-H1 is associated with poor prognosis in renal cell carcinoma patients with long-term follow-up*. *Cancer Res*, 2006. 66(7): p. 3381-5.
119. Wu, C., Y. Zhu, J. Jiang, J. Zhao, X.G. Zhang and N. Xu, *Immunohistochemical localization of programmed death-1 ligand-1 (PD-L1) in gastric carcinoma and its clinical significance*. *Acta Histochem*, 2006. 108(1): p. 19-24.
120. Loos, M., N.A. Giese, J. Kleeff, T. Giese, M.M. Gaida, F. Bergmann, M. Laschinger, W.B. M and H. Friess, *Clinical significance and regulation of the costimulatory molecule B7-H1 in pancreatic cancer*. *Cancer Lett*, 2008. 268(1): p. 98-109.
121. Chen, X.L., S.X. Yuan, C. Chen, Y.X. Mao, G. Xu and X.Y. Wang, *[Expression of B7-H1 protein in human pancreatic carcinoma tissues and its clinical significance]*. *Ai Zheng*, 2009. 28(12): p. 1328-32.
122. Karakhanova, S., T. Bedke, A.H. Enk and K. Mahnke, *IL-27 renders DC immunosuppressive by induction of B7-H1*. *J Leukoc Biol*, 2011. 89(6): p. 837-45.
123. Karakhanova, S., S. Meisel, S. Ring, K. Mahnke and A.H. Enk, *ERK/p38 MAP-kinases and PI3K are involved in the differential regulation of B7-H1 expression in DC subsets*. *Eur J Immunol*, 2010. 40(1): p. 254-66.

## List of Literature

---

124. Dong, H., G. Zhu, K. Tamada, D.B. Flies, J.M. van Deursen and L. Chen, *B7-H1 determines accumulation and deletion of intrahepatic CD8(+) T lymphocytes*. *Immunity*, 2004. 20(3): p. 327-36.
125. Corbett, T.H., B.J. Roberts, W.R. Leopold, J.C. Peckham, L.J. Wilkoff, D.P. Griswold, Jr. and F.M. Schabel, Jr., *Induction and chemotherapeutic response of two transplantable ductal adenocarcinomas of the pancreas in C57BL/6 mice*. *Cancer Res*, 1984. 44(2): p. 717-26.
126. Yang, Y., S. Karakhanova, S. Soltek, J. Werner, P.P. Philippov and A.V. Bazhin, *In vivo immunoregulatory properties of the novel mitochondria-targeted antioxidant SkQ1*. *Mol Immunol*, 2012. 52(1): p. 19-29.
127. Law, S.K., *Antigen shedding and metastasis of tumour cells*. *Clin Exp Immunol*, 1991. 85(1): p. 1-2.
128. Muller, L., R. Kiessling, R.C. Rees and G. Pawelec, *Escape mechanisms in tumor immunity: an update*. *J Environ Pathol Toxicol Oncol*, 2002. 21(4): p. 277-330.
129. Okazaki, T. and T. Honjo, *The PD-1-PD-L pathway in immunological tolerance*. *Trends Immunol*, 2006. 27(4): p. 195-201.
130. Freeman, G.J., A.J. Long, Y. Iwai, K. Bourque, T. Chernova, H. Nishimura, L.J. Fitz, N. Malenkovich, T. Okazaki, M.C. Byrne, H.F. Horton, L. Fouser, L. Carter, V. Ling, M.R. Bowman, B.M. Carreno, M. Collins, C.R. Wood and T. Honjo, *Engagement of the PD-1 immunoinhibitory receptor by a novel B7 family member leads to negative regulation of lymphocyte activation*. *J Exp Med*, 2000. 192(7): p. 1027-34.
131. Galon, J., A. Costes, F. Sanchez-Cabo, A. Kirilovsky, B. Mlecnik, C. Lagorce-Pages, M. Tosolini, M. Camus, A. Berger, P. Wind, F. Zinzindohoue, P. Bruneval, P.H. Cugnenc, Z. Trajanoski, W.H. Fridman and F. Pages, *Type, density, and location of immune cells within human colorectal tumors predict clinical outcome*. *Science*, 2006. 313(5795): p. 1960-4.
132. Ene-Obong, A., A.J. Clear, J. Watt, J. Wang, R. Fatah, J.C. Riches, J.F. Marshall, J. Chin-Aleong, C. Chelala, J.G. Gribben, A.G. Ramsay and H.M. Kocher, *Activated pancreatic stellate cells sequester CD8+ T cells to reduce their infiltration of the juxtatumoral compartment of pancreatic ductal adenocarcinoma*. *Gastroenterology*, 2013. 145(5): p. 1121-32.
133. Pages, F., A. Berger, M. Camus, F. Sanchez-Cabo, A. Costes, R. Molidor, B. Mlecnik, A. Kirilovsky, M. Nilsson, D. Damotte, T. Meatchi, P. Bruneval, P.H. Cugnenc, Z. Trajanoski, W.H. Fridman and J. Galon, *Effector memory T cells, early metastasis, and survival in colorectal cancer*. *N Engl J Med*, 2005. 353(25): p. 2654-66.
134. Salih, H.R., S. Wintterle, M. Krusch, A. Kroner, Y.H. Huang, L. Chen and H. Wiendl, *The role of leukemia-derived B7-H1 (PD-L1) in tumor-T-cell interactions in humans*. *Exp Hematol*, 2006. 34(7): p. 888-94.

## List of Literature

---

135. Jonuleit, H., U. Kuhn, G. Muller, K. Steinbrink, L. Paragnik, E. Schmitt, J. Knop and A.H. Enk, *Pro-inflammatory cytokines and prostaglandins induce maturation of potent immunostimulatory dendritic cells under fetal calf serum-free conditions*. Eur J Immunol, 1997. 27(12): p. 3135-42.
136. Keir, M.E., L.M. Francisco and A.H. Sharpe, *PD-1 and its ligands in T-cell immunity*. Curr Opin Immunol, 2007. 19(3): p. 309-14.
137. Banchereau, J. and R.M. Steinman, *Dendritic cells and the control of immunity*. Nature, 1998. 392(6673): p. 245-52.
138. Nguyen-Pham, T.N., M.S. Lim, T.A. Nguyen, Y.K. Lee, C.J. Jin, H.J. Lee, C.Y. Hong, J.S. Ahn, D.H. Yang, Y.K. Kim, I.J. Chung, B.C. Park, H.J. Kim and J.J. Lee, *Type I and II interferons enhance dendritic cell maturation and migration capacity by regulating CD38 and CD74 that have synergistic effects with TLR agonists*. Cell Mol Immunol, 2011. 8(4): p. 341-7.
139. Brandl, C., S. Ortler, T. Herrmann, S. Cardell, M.B. Lutz and H. Wiendl, *B7-H1-deficiency enhances the potential of tolerogenic dendritic cells by activating CD1d-restricted type II NKT cells*. PLoS One, 2010. 5(5): p. e10800.
140. Gallucci, S., M. Lolkema and P. Matzinger, *Natural adjuvants: endogenous activators of dendritic cells*. Nat Med, 1999. 5(11): p. 1249-55.
141. Ito, T., R. Amakawa, M. Inaba, S. Ikehara, K. Inaba and S. Fukuhara, *Differential regulation of human blood dendritic cell subsets by IFNs*. J Immunol, 2001. 166(5): p. 2961-9.
142. Fujimura, T., S. Ring, V. Umansky, K. Mahnke and A.H. Enk, *Regulatory T cells stimulate B7-H1 expression in myeloid-derived suppressor cells in ret melanomas*. J Invest Dermatol, 2012. 132(4): p. 1239-46.
143. Liu, Y., B. Zeng, Z. Zhang, Y. Zhang and R. Yang, *B7-H1 on myeloid-derived suppressor cells in immune suppression by a mouse model of ovarian cancer*. Clin Immunol, 2008. 129(3): p. 471-81.
144. Youn, J.I. and D.I. Gabrilovich, *The biology of myeloid-derived suppressor cells: the blessing and the curse of morphological and functional heterogeneity*. Eur J Immunol, 2010. 40(11): p. 2969-75.
145. Vincent, J., G. Mignot, F. Chalmin, S. Ladoire, M. Bruchard, A. Chevriaux, F. Martin, L. Apetoh, C. Rebe and F. Ghiringhelli, *5-Fluorouracil selectively kills tumor-associated myeloid-derived suppressor cells resulting in enhanced T cell-dependent antitumor immunity*. Cancer Res, 2010. 70(8): p. 3052-61.
146. Youn, J.I., M. Collazo, I.N. Shalova, S.K. Biswas and D.I. Gabrilovich, *Characterization of the nature of granulocytic myeloid-derived suppressor cells in tumor-bearing mice*. J Leukoc Biol, 2012. 91(1): p. 167-81.

## List of Literature

---

147. Liu, Y., Y. Yu, S. Yang, B. Zeng, Z. Zhang, G. Jiao, Y. Zhang, L. Cai and R. Yang, *Regulation of arginase I activity and expression by both PD-1 and CTLA-4 on the myeloid-derived suppressor cells*. Cancer Immunol Immunother, 2009. 58(5): p. 687-97.
148. Serafini, P., K. Meckel, M. Kelso, K. Noonan, J. Califano, W. Koch, L. Dolcetti, V. Bronte and I. Borrello, *Phosphodiesterase-5 inhibition augments endogenous antitumor immunity by reducing myeloid-derived suppressor cell function*. J Exp Med, 2006. 203(12): p. 2691-702.
149. Bauer, H., *Der Effekt einer durch Toll-like-Rezeptor-Liganden induzierten Interferon-alpha-Produktion auf myeloide Suppressorzellen*. 2014, LMU München.
150. Blank, C., J. Kuball, S. Voelkl, H. Wiendl, B. Becker, B. Walter, O. Majdic, T.F. Gajewski, M. Theobald, R. Andreesen and A. Mackensen, *Blockade of PD-L1 (B7-H1) augments human tumor-specific T cell responses in vitro*. Int J Cancer, 2006. 119(2): p. 317-27.
151. Kitazawa, Y., M. Fujino, Q. Wang, H. Kimura, M. Azuma, M. Kubo, R. Abe and X.K. Li, *Involvement of the programmed death-1/programmed death-1 ligand pathway in CD4+CD25+ regulatory T-cell activity to suppress alloimmune responses*. Transplantation, 2007. 83(6): p. 774-82.
152. Francisco, L.M., V.H. Salinas, K.E. Brown, V.K. Vanguri, G.J. Freeman, V.K. Kuchroo and A.H. Sharpe, *PD-L1 regulates the development, maintenance, and function of induced regulatory T cells*. J Exp Med, 2009. 206(13): p. 3015-29.
153. Zhou, Q., M.E. Munger, S.L. Highfill, J. Tolar, B.J. Weigel, M. Riddle, A.H. Sharpe, D.A. Vallera, M. Azuma, B.L. Levine, C.H. June, W.J. Murphy, D.H. Munn and B.R. Blazar, *Program death-1 signaling and regulatory T cells collaborate to resist the function of adoptively transferred cytotoxic T lymphocytes in advanced acute myeloid leukemia*. Blood, 2010. 116(14): p. 2484-93.
154. Wang, L., K. Pino-Lagos, V.C. de Vries, I. Guleria, M.H. Sayegh and R.J. Noelle, *Programmed death 1 ligand signaling regulates the generation of adaptive Foxp3+CD4+ regulatory T cells*. Proc Natl Acad Sci U S A, 2008. 105(27): p. 9331-6.
155. Hua, D., J. Sun, Y. Mao, L.J. Chen, Y.Y. Wu and X.G. Zhang, *B7-H1 expression is associated with expansion of regulatory T cells in colorectal carcinoma*. World J Gastroenterol, 2012. 18(9): p. 971-8.
156. Schreiner, B., M. Mitsdoerffer, B.C. Kieseier, L. Chen, H.P. Hartung, M. Weller and H. Wiendl, *Interferon-beta enhances monocyte and dendritic cell expression of B7-H1 (PD-L1), a strong inhibitor of autologous T-cell activation: relevance for the immune modulatory effect in multiple sclerosis*. J Neuroimmunol, 2004. 155(1-2): p. 172-82.
157. Chen, L., Z. Zhang, W. Chen, Z. Zhang, Y. Li, M. Shi, J. Zhang, L. Chen, S. Wang and F.S. Wang, *B7-H1 up-regulation on myeloid dendritic cells significantly suppresses T cell immune function in patients with chronic hepatitis B*. J Immunol, 2007. 178(10): p. 6634-41.

## List of Literature

---

158. Loke, P. and J.P. Allison, *PD-L1 and PD-L2 are differentially regulated by Th1 and Th2 cells*. Proc Natl Acad Sci U S A, 2003. 100(9): p. 5336-41.
159. Ferrara, N., *Vascular endothelial growth factor and the regulation of angiogenesis*. Recent Prog Horm Res, 2000. 55: p. 15-35; discussion 35-6.
160. Ferrara, N. and T. Davis-Smyth, *The biology of vascular endothelial growth factor*. Endocr Rev, 1997. 18(1): p. 4-25.
161. Folkman, J., *Angiogenesis*. Annu Rev Med, 2006. 57: p. 1-18.
162. Folkman, J., *Role of angiogenesis in tumor growth and metastasis*. Semin Oncol, 2002. 29(6 Suppl 16): p. 15-8.
163. Ellis, L.M., Y. Takahashi, C.J. Fenoglio, K.R. Cleary, C.D. Bucana and D.B. Evans, *Vessel counts and vascular endothelial growth factor expression in pancreatic adenocarcinoma*. Eur J Cancer, 1998. 34(3): p. 337-40.
164. Fujimoto, K., R. Hosotani, M. Wada, J.U. Lee, T. Koshiba, Y. Miyamoto, S. Tsuji, S. Nakajima, R. Doi and M. Imamura, *Expression of two angiogenic factors, vascular endothelial growth factor and platelet-derived endothelial cell growth factor in human pancreatic cancer, and its relationship to angiogenesis*. Eur J Cancer, 1998. 34(9): p. 1439-47.
165. Itakura, J., T. Ishiwata, H. Friess, H. Fujii, Y. Matsumoto, M.W. Buchler and M. Korc, *Enhanced expression of vascular endothelial growth factor in human pancreatic cancer correlates with local disease progression*. Clin Cancer Res, 1997. 3(8): p. 1309-16.
166. Luo, J., P. Guo, K. Matsuda, N. Truong, A. Lee, C. Chun, S.Y. Cheng and M. Korc, *Pancreatic cancer cell-derived vascular endothelial growth factor is biologically active in vitro and enhances tumorigenicity in vivo*. Int J Cancer, 2001. 92(3): p. 361-9.
167. Kuwahara, K., T. Sasaki, Y. Kuwada, M. Murakami, S. Yamasaki and K. Chayama, *Expressions of angiogenic factors in pancreatic ductal carcinoma: a correlative study with clinicopathologic parameters and patient survival*. Pancreas, 2003. 26(4): p. 344-9.
168. Karayiannakis, A.J., H. Bolanaki, K.N. Syrigos, B. Asimakopoulos, A. Polychronidis, S. Anagnostoulis and C. Simopoulos, *Serum vascular endothelial growth factor levels in pancreatic cancer patients correlate with advanced and metastatic disease and poor prognosis*. Cancer Lett, 2003. 194(1): p. 119-24.
169. Seo, Y., H. Baba, T. Fukuda, M. Takashima and K. Sugimachi, *High expression of vascular endothelial growth factor is associated with liver metastasis and a poor prognosis for patients with ductal pancreatic adenocarcinoma*. Cancer, 2000. 88(10): p. 2239-45.

## List of Literature

---

170. Talar-Wojnarowska, R., A. Gasiorowska, M. Olakowski, A. Lekstan, P. Lampe, B. Smolarz, H. Romanowicz-Makowska, A. Kulig and E. Malecka-Panas, *Vascular endothelial growth factor (VEGF) genotype and serum concentration in patients with pancreatic adenocarcinoma and chronic pancreatitis*. J Physiol Pharmacol, 2010. 61(6): p. 711-6.
171. von Marschall, Z., A. Scholz, T. Cramer, G. Schafer, M. Schirner, K. Oberg, B. Wiedenmann, M. Hocker and S. Rosewicz, *Effects of interferon alpha on vascular endothelial growth factor gene transcription and tumor angiogenesis*. J Natl Cancer Inst, 2003. 95(6): p. 437-48.
172. Legros, L., C. Bourcier, A. Jacquel, F.X. Mahon, J.P. Cassuto, P. Auberger and G. Pages, *Imatinib mesylate (STI571) decreases the vascular endothelial growth factor plasma concentration in patients with chronic myeloid leukemia*. Blood, 2004. 104(2): p. 495-501.
173. Gabrilovich, D., T. Ishida, T. Oyama, S. Ran, V. Kravtsov, S. Nadaf and D.P. Carbone, *Vascular endothelial growth factor inhibits the development of dendritic cells and dramatically affects the differentiation of multiple hematopoietic lineages in vivo*. Blood, 1998. 92(11): p. 4150-66.
174. Murdoch, C., M. Muthana, S.B. Coffelt and C.E. Lewis, *The role of myeloid cells in the promotion of tumour angiogenesis*. Nat Rev Cancer, 2008. 8(8): p. 618-31.
175. Ohm, J.E. and D.P. Carbone, *VEGF as a mediator of tumor-associated immunodeficiency*. Immunol Res, 2001. 23(2-3): p. 263-72.
176. Rodriguez, P.C. and A.C. Ochoa, *Arginine regulation by myeloid derived suppressor cells and tolerance in cancer: mechanisms and therapeutic perspectives*. Immunol Rev, 2008. 222: p. 180-91.
177. Xu, J., Z. Yin, S. Cao, W. Gao, L. Liu, Y. Yin, P. Liu and Y. Shu, *Systematic review and meta-analysis on the association between IL-1B polymorphisms and cancer risk*. PLoS One, 2013. 8(5): p. e63654.
178. Keir, M.E., M.J. Butte, G.J. Freeman and A.H. Sharpe, *PD-1 and its ligands in tolerance and immunity*. Annu Rev Immunol, 2008. 26: p. 677-704.
179. Selenko-Gebauer, N., O. Majdic, A. Szekeres, G. Hofler, E. Guthann, U. Korthauer, G. Zlabinger, P. Steinberger, W.F. Pickl, H. Stockinger, W. Knapp and J. Stockl, *B7-H1 (programmed death-1 ligand) on dendritic cells is involved in the induction and maintenance of T cell anergy*. J Immunol, 2003. 170(7): p. 3637-44.
180. Iwai, Y., M. Ishida, Y. Tanaka, T. Okazaki, T. Honjo and N. Minato, *Involvement of PD-L1 on tumor cells in the escape from host immune system and tumor immunotherapy by PD-L1 blockade*. Proc Natl Acad Sci U S A, 2002. 99(19): p. 12293-7.
181. Blank, C., I. Brown, A.C. Peterson, M. Spiotto, Y. Iwai, T. Honjo and T.F. Gajewski, *PD-L1/B7H-1 inhibits the effector phase of tumor rejection by T cell receptor (TCR) transgenic CD8+ T cells*. Cancer Res, 2004. 64(3): p. 1140-5.

## List of Literature

---

182. Fayad, L., M.J. Keating, J.M. Reuben, S. O'Brien, B.N. Lee, S. Lerner and R. Kurzrock, *Interleukin-6 and interleukin-10 levels in chronic lymphocytic leukemia: correlation with phenotypic characteristics and outcome*. Blood, 2001. 97(1): p. 256-63.
183. Blay, J.Y., S. Negrier, V. Combaret, S. Attali, E. Goillot, Y. Merrouche, A. Mercatello, A. Ravault, J.M. Tourani, J.F. Moskvotchenko and et al., *Serum level of interleukin 6 as a prognosis factor in metastatic renal cell carcinoma*. Cancer Res, 1992. 52(12): p. 3317-22.
184. Lust, J.A., M.Q. Lacy, S.R. Zeldenrust, A. Dispenzieri, M.A. Gertz, T.E. Witzig, S. Kumar, S.R. Hayman, S.J. Russell, F.K. Buadi, S.M. Geyer, M.E. Campbell, R.A. Kyle, S.V. Rajkumar, P.R. Greipp, M.P. Kline, Y. Xiong, L.L. Moon-Tasson and K.A. Donovan, *Induction of a chronic disease state in patients with smoldering or indolent multiple myeloma by targeting interleukin 1{beta}-induced interleukin 6 production and the myeloma proliferative component*. Mayo Clin Proc, 2009. 84(2): p. 114-22.
185. Bekisz, J., Y. Sato, C. Johnson, S.R. Husain, R.K. Puri and K.C. Zoon, *Immunomodulatory effects of interferons in malignancies*. J Interferon Cytokine Res, 2013. 33(4): p. 154-61.
186. Okudaira, K., R. Hokari, Y. Tsuzuki, Y. Okada, S. Komoto, C. Watanabe, C. Kurihara, A. Kawaguchi, S. Nagao, M. Azuma, H. Yagita and S. Miura, *Blockade of B7-H1 or B7-DC induces an anti-tumor effect in a mouse pancreatic cancer model*. Int J Oncol, 2009. 35(4): p. 741-9.
187. Medina, T.S., S.P. Costa, M.D. Oliveira, A.M. Ventura, J.M. Souza, T.F. Gomes, A.C. Vallinoto, M.M. Pova, J.S. Silva and M.G. Cunha, *Increased interleukin-10 and interferon-gamma levels in Plasmodium vivax malaria suggest a reciprocal regulation which is not altered by IL-10 gene promoter polymorphism*. Malar J, 2011. 10: p. 264.
188. Ghebeh, H., S. Mohammed, A. Al-Omar, A. Qattan, C. Lehe, G. Al-Qudaihi, N. Elkum, M. Alshabanah, S. Bin Amer, A. Tulbah, D. Ajarim, T. Al-Tweigeri and S. Dermime, *The B7-H1 (PD-L1) T lymphocyte-inhibitory molecule is expressed in breast cancer patients with infiltrating ductal carcinoma: correlation with important high-risk prognostic factors*. Neoplasia, 2006. 8(3): p. 190-8.
189. Hamanishi, J., M. Mandai, M. Iwasaki, T. Okazaki, Y. Tanaka, K. Yamaguchi, T. Higuchi, H. Yagi, K. Takakura, N. Minato, T. Honjo and S. Fujii, *Programmed cell death 1 ligand 1 and tumor-infiltrating CD8+ T lymphocytes are prognostic factors of human ovarian cancer*. Proc Natl Acad Sci U S A, 2007. 104(9): p. 3360-5.
190. Inman, B.A., T.J. Sebo, X. Frigola, H. Dong, E.J. Bergstralh, I. Frank, Y. Fradet, L. Lacombe and E.D. Kwon, *PD-L1 (B7-H1) expression by urothelial carcinoma of the bladder and BCG-induced granulomata: associations with localized stage progression*. Cancer, 2007. 109(8): p. 1499-505.
191. Zeng, Z., F. Shi, L. Zhou, M.N. Zhang, Y. Chen, X.J. Chang, Y.Y. Lu, W.L. Bai, J.H. Qu, C.P. Wang, H. Wang, M. Lou, F.S. Wang, J.Y. Lv and Y.P. Yang, *Upregulation of circulating PD-L1/PD-1 is*

## List of Literature

---

*associated with poor post-cryoablation prognosis in patients with HBV-related hepatocellular carcinoma.* PLoS One, 2011. 6(9): p. e23621.

192. Song, M., D. Chen, B. Lu, C. Wang, J. Zhang, L. Huang, X. Wang, C.L. Timmons, J. Hu, B. Liu, X. Wu, L. Wang, J. Wang and H. Liu, *PTEN loss increases PD-L1 protein expression and affects the correlation between PD-L1 expression and clinical parameters in colorectal cancer.* PLoS One, 2013. 8(6): p. e65821.

193. Zhang, L., T.F. Gajewski and J. Kline, *PD-1/PD-L1 interactions inhibit antitumor immune responses in a murine acute myeloid leukemia model.* Blood, 2009. 114(8): p. 1545-52.

194. Brahmer, J.R., S.S. Tykodi, L.Q. Chow, W.J. Hwu, S.L. Topalian, P. Hwu, C.G. Drake, L.H. Camacho, J. Kauh, K. Odunsi, H.C. Pitot, O. Hamid, S. Bhatia, R. Martins, K. Eaton, S. Chen, T.M. Salay, S. Alaparthi, J.F. Grosso, A.J. Korman, S.M. Parker, S. Agrawal, S.M. Goldberg, D.M. Pardoll, A. Gupta and J.M. Wigginton, *Safety and activity of anti-PD-L1 antibody in patients with advanced cancer.* N Engl J Med, 2012. 366(26): p. 2455-65.

195. Cao, Z., Z. Zhang, Z. Huang, R. Wang, A. Yang, L. Liao and J. Du, *Antitumor and immunomodulatory effects of low-dose 5-FU on hepatoma 22 tumor-bearing mice.* Oncol Lett, 2014. 7(4): p. 1260-1264.

196. Kim, J.R., Y.J. Moon, K.S. Kwon, J.S. Bae, S. Wagle, K.M. Kim, H.S. Park, H. Lee, W.S. Moon, M.J. Chung, M.J. Kang and K.Y. Jang, *Tumor infiltrating PD1-positive lymphocytes and the expression of PD-L1 predict poor prognosis of soft tissue sarcomas.* PLoS One, 2013. 8(12): p. e82870.

197. Thompson, R.H., H. Dong and E.D. Kwon, *Implications of B7-H1 expression in clear cell carcinoma of the kidney for prognostication and therapy.* Clin Cancer Res, 2007. 13(2 Pt 2): p. 709s-715s.

198. Melani, C., C. Chiodoni, G. Forni and M.P. Colombo, *Myeloid cell expansion elicited by the progression of spontaneous mammary carcinomas in c-erbB-2 transgenic BALB/c mice suppresses immune reactivity.* Blood, 2003. 102(6): p. 2138-45.

## IV. List of Figures

Fig.2.2.3. 1 Photos of blood sample collection, dissection and measuring of organs ..41

Fig.3.1.1. 1 Quantification of lymphocytes from WT and B7-H1 KO mice in control groups (without treatment, co) and after the treatment of splenocytes in *in vitro* cultures with IFN $\alpha$ , 5-FU and IFN $\alpha$ +5-FU.....50

Fig.3.1.1. 2 Gating strategy for CD4<sup>+</sup>/CD8<sup>+</sup> T cells in splenocytes using flow cytometry. ....52

Fig.3.1.1. 3 Quantification of CD4<sup>+</sup>T cells from WT and B7-H1 KO mice in control groups (without treatment, co) and after the treatment of splenocytes in *in vitro* cultures with IFN $\alpha$ , 5-FU and IFN $\alpha$ +5-FU.....53

Fig.3.1.1. 4 Quantification of CD69 expression on CD4<sup>+</sup>T cells from WT and B7-H1 KO mice in control groups (without treatment, co) and after the treatment of splenocytes in *in vitro* cultures with IFN $\alpha$ , 5-FU and IFN $\alpha$ +5-FU. ....54

Fig.3.1.1. 5 Quantification of naïve CD4<sup>+</sup>T cells from WT and B7-H1 KO mice in control groups (without treatment, co) and after the treatment of splenocytes in *in vitro* cultures with IFN $\alpha$ , 5-FU and IFN $\alpha$ +5-FU. ....55

Fig.3.1.1. 6 Quantification of effector CD4<sup>+</sup>T cells from WT and B7-H1 KO mice in control groups (without treatment, co) and after the treatment of splenocytes in *in vitro* cultures with IFN $\alpha$ , 5-FU and IFN $\alpha$ +5-FU. ....56

Fig.3.1.1. 7 Quantification of CD69 expression on effector CD4<sup>+</sup>T cells from WT and B7-H1 KO mice in control groups (without treatment, co) and after the treatment of splenocytes in *in vitro* cultures with IFN $\alpha$ , 5-FU and IFN $\alpha$ +5-FU. ....57

Fig.3.1.1. 8 Quantification of effector memory CD4<sup>+</sup>T cells from WT and B7-H1 KO mice in control groups (without treatment, co) and after the treatment of splenocytes in *in vitro* cultures with IFN $\alpha$ , 5-FU and IFN $\alpha$ +5-FU.....58

Fig.3.1.1. 9 Quantification of CD69 expression on effector memory CD4<sup>+</sup>T cells from WT and B7-H1 KO mice in control groups (without treatment, co) and after the

## List of Figures

---

treatment of splenocytes in <i>in vitro</i> cultures with IFN $\alpha$ , 5-FU and IFN $\alpha$ +5-FU. .....	59
Fig.3.1.1. 10 Quantification of central memory CD4 <sup>+</sup> T cells from WT and B7-H1 KO mice in control groups (without treatment, co) and after the treatment of splenocytes in <i>in vitro</i> cultures with IFN $\alpha$ , 5-FU and IFN $\alpha$ +5-FU. ....	60
Fig.3.1.1. 11 Quantification of CD69 expression on central memory CD4 <sup>+</sup> T cells from WT and B7-H1 KO mice in control groups (without treatment, co) and after the treatment of splenocytes in <i>in vitro</i> cultures with IFN $\alpha$ , 5-FU and IFN $\alpha$ +5-FU. .....	61
Fig.3.1.1. 12 Quantification of CD8 <sup>+</sup> T cells from WT and B7-H1 KO mice in control groups (without treatment, co) and after the treatment of splenocytes in <i>in vitro</i> cultures with IFN $\alpha$ , 5-FU and IFN $\alpha$ +5-FU. ....	62
Fig.3.1.1. 13 Quantification of CD69 expression on CD8 <sup>+</sup> T cells from WT and B7-H1 KO mice in control groups (without treatment, co) and after the treatment of splenocytes in <i>in vitro</i> cultures with IFN $\alpha$ , 5-FU and IFN $\alpha$ +5-FU. ....	63
Fig.3.1.1. 14 Quantification of naïve CD8 <sup>+</sup> T cells from WT and B7-H1 KO mice in control groups (without treatment, co) and after the treatment of splenocytes in <i>in vitro</i> cultures with IFN $\alpha$ , 5-FU and IFN $\alpha$ +5-FU. ....	64
Fig.3.1.1. 15 Quantification of effector CD8 <sup>+</sup> T cells from WT and B7-H1 KO mice in control groups (without treatment, co) and after the treatment of splenocytes in <i>in vitro</i> cultures with IFN $\alpha$ , 5-FU and IFN $\alpha$ +5-FU. ....	65
Fig.3.1.1. 16 Quantification of CD69 expression on effector CD8 <sup>+</sup> T cells from WT and B7-H1 KO mice in control groups (without treatment, co) and after the treatment of splenocytes in <i>in vitro</i> cultures with IFN $\alpha$ , 5-FU and IFN $\alpha$ +5-FU. .....	66
Fig.3.1.1. 17 Quantification of effector memory CD8 <sup>+</sup> T cells from WT and B7-H1 KO mice in control groups (without treatment, co) and after the treatment of splenocytes in <i>in vitro</i> cultures with IFN $\alpha$ , 5-FU and IFN $\alpha$ +5-FU. ....	67
Fig.3.1.1. 18 Quantification of CD69 expression on effector memory CD8 <sup>+</sup> T cells from WT and B7-H1 KO mice in control groups (without treatment, co) and after the treatment of splenocytes in <i>in vitro</i> cultures with IFN $\alpha$ , 5-FU and IFN $\alpha$ +5-FU. .....	68

## List of Figures

---

Fig.3.1.1. 19 Quantification of central memory CD8 <sup>+</sup> T cells from WT and B7-H1 KO mice in control groups (without treatment, co) and after the treatment of splenocytes in <i>in vitro</i> cultures with IFN $\alpha$ , 5-FU and IFN $\alpha$ +5-FU. ....	69
Fig.3.1.1. 20 Quantification of CD69 expression on central memory CD8 <sup>+</sup> T cells from WT and B7-H1 KO mice in control groups (without treatment, co) and after the treatment of splenocytes in <i>in vitro</i> cultures with IFN $\alpha$ , 5-FU and IFN $\alpha$ +5-FU. ....	70
Fig.3.1.2. 1 Gating strategy for regulatory T cells and Tcon in splenocytes using flow cytometry. ....	71
Fig.3.1.2. 2 Quantification of Treg from WT and B7-H1 KO mice in control groups (without treatment, co) and after the treatment of splenocytes in <i>in vitro</i> cultures with IFN $\alpha$ , 5-FU and IFN $\alpha$ +5-FU.....	72
Fig.3.1.2. 3 Quantification of Tcon from WT and B7-H1 KO mice in control groups (without treatment, co) and after the treatment of splenocytes in <i>in vitro</i> cultures with IFN $\alpha$ , 5-FU and IFN $\alpha$ +5-FU.....	73
Fig.3.1.2. 4 Quantification of activated Tcon from WT and B7-H1 KO mice in control groups (without treatment, co) and after the treatment of splenocytes in <i>in vitro</i> cultures with IFN $\alpha$ , 5-FU and IFN $\alpha$ +5-FU.....	73
Fig.3.1.3. 1 Gating strategy for dendritic cells in splenocytes using flow cytometry. ...	76
Fig.3.1.3. 2 Quantification of cDC and pDC from WT and B7-H1 KO mice in control groups (without treatment, co) and after the treatment of splenocytes in <i>in vitro</i> cultures with IFN $\alpha$ , 5-FU and IFN $\alpha$ +5-FU.....	77
Fig.3.1.3. 3 Quantification of mature cDC and pDC from WT and B7-H1 KO mice in control groups (without treatment, co) and after the treatment of splenocytes in <i>in vitro</i> cultures with IFN $\alpha$ , 5-FU and IFN $\alpha$ +5-FU. ....	78
Fig.3.1.3. 4 Quantification of CD80 expression on mature cDC from WT and B7-H1 KO mice in control groups (without treatment, co) and after the treatment of splenocytes in <i>in vitro</i> cultures with IFN $\alpha$ , 5-FU and IFN $\alpha$ +5-FU. ....	79
Fig.3.1.3. 5 Quantification of CD86 expression on mature cDC from WT and B7-H1 KO mice in control groups (without treatment, co) and after the treatment of splenocytes in <i>in vitro</i> cultures with IFN $\alpha$ , 5-FU and IFN $\alpha$ +5-FU. ....	80

## List of Figures

---

Fig.3.1.3. 6 Quantification of CD80 expression on mature pDC from WT and B7-H1 KO mice in control groups (without treatment, co) and after the treatment of splenocytes in <i>in vitro</i> cultures with IFN $\alpha$ , 5-FU and IFN $\alpha$ +5-FU. ....	81
Fig.3.1.3. 7 Quantification of CD86 expression on mature pDC from WT and B7-H1 KO mice in control groups (without treatment, co) and after the treatment of splenocytes in <i>in vitro</i> cultures with IFN $\alpha$ , 5-FU and IFN $\alpha$ +5-FU. ....	83
Fig.3.1.3. 8 Quantification of B7-H1/B7-DC expression on mature cDC from WT and B7-H1 KO mice in control groups (without treatment, co) and after the treatment of splenocytes in <i>in vitro</i> cultures with IFN $\alpha$ , 5-FU and IFN $\alpha$ +5-FU. ....	84
Fig.3.1.3. 9 Quantification of B7-H1/B7-DC expression on mature pDC from WT and B7-H1 KO mice in control groups (without treatment, co) and after the treatment of splenocytes in <i>in vitro</i> cultures with IFN $\alpha$ , 5-FU and IFN $\alpha$ +5-FU. ....	85
Fig.3.1.4. 1 Gating strategy for Gr-1 <sup>+</sup> CD11b <sup>+</sup> cell population in splenocytes using flow cytometry. ....	87
Fig.3.1.4. 2 Quantification of Gr-1 <sup>+</sup> CD11b <sup>+</sup> cells from WT and B7-H1 KO mice in control groups (without treatment, co) and after the treatment of splenocytes in <i>in vitro</i> cultures with IFN $\alpha$ , 5-FU and IFN $\alpha$ +5-FU. ....	88
Fig.3.1.4. 3 Quantification of B7-H1/B7-DC MFI of Gr-1 <sup>+</sup> CD11b <sup>+</sup> cells from WT and B7-H1 KO mice in control groups (without treatment, co) and after the treatment of splenocytes in <i>in vitro</i> cultures with IFN $\alpha$ , 5-FU and IFN $\alpha$ +5-FU. ....	89
Fig.3.2.1.1 Gating strategy for CD4 <sup>+</sup> /CD8 <sup>+</sup> T cells in spleens and tumors using flow cytometry. ....	92
Fig.3.2.1.2 Quantification of CD8 <sup>+</sup> T cells in spleens and tumors from tumor bearing WT and B7-H1 KO mice with and without treatment (co). ....	93
Fig.3.2.1.3 Quantification of CD69 expression on CD8 <sup>+</sup> T cells in spleens and tumors from tumor-bearing WT and B7-H1 KO mice with and without treatment (co). ....	94
Fig.3.2.1.4 Quantification of naïve CD8 <sup>+</sup> T cells in spleens and tumors from tumor-bearing WT and B7-H1 KO mice with and without treatment (co). ....	95

## List of Figures

---

Fig.3.2.1.5 Quantification of effector CD8 <sup>+</sup> T cells in spleens and tumors from tumor-bearing WT and B7-H1 KO mice with and without treatment (co). .....	96
Fig.3.2.1.6 Quantification of CD69 expression on effector CD8 <sup>+</sup> T cells in spleens and tumors from tumor-bearing WT and B7-H1 KO mice with and without treatment (co). .....	97
Fig.3.2.1.7 Quantification of effector memory CD8 <sup>+</sup> T cells in spleens and tumors from tumor-bearing WT and B7-H1 KO mice with and without treatment (co). .....	98
Fig.3.2.1.8 Quantification of CD69 expression on effector memory CD8 <sup>+</sup> T cells in spleens and tumors from tumor-bearing WT and B7-H1 KO mice with and without treatment (co). .....	100
Fig.3.2.1.9 Quantification of central memory CD8 <sup>+</sup> T cells in spleens and tumors from tumor-bearing WT and B7-H1 KO mice with and without treatment (co). .....	101
Fig.3.2.1.10 Quantification of CD69 expression on central memory CD8 <sup>+</sup> T cells in spleens and tumors from tumor-bearing WT and B7-H1 KO mice with and without treatment (co). .....	102
Fig.3.2.1.11 Quantification of CD4 <sup>+</sup> T cells in spleens and tumors from tumor-bearing WT and B7-H1 KO mice with and without treatment (co). .....	103
Fig.3.2.1.12 Quantification of CD69 expression on CD4 <sup>+</sup> T cells in spleens and tumors from tumor-bearing WT and B7-H1 KO mice with and without treatment (co). .....	104
Fig.3.2.1.13 Quantification of naïve CD4 <sup>+</sup> T cells in spleens and tumors from tumor-bearing WT and B7-H1 KO mice with and without treatment (co). .....	105
Fig.3.2.1.14 Quantification of effector CD4 <sup>+</sup> T cells in spleens and tumors from tumor-bearing WT and B7-H1 KO mice with and without treatment (co). .....	106
Fig.3.2.1.15 Quantification of CD69 expression on effector CD4 <sup>+</sup> T cells in spleens and tumors from tumor-bearing WT and B7-H1 KO mice with and without treatment (co). .....	107
Fig.3.2.1.16 Quantification of effector memory CD4 <sup>+</sup> T cells in spleens and tumors from tumor-bearing WT and B7-H1 KO mice with and without treatment (co). .....	108
Fig.3.2.1.17 Quantification of CD69 expression on effector memory CD4 <sup>+</sup> T cells in spleens and tumors from tumor-bearing WT and B7-H1 KO mice with and without treatment (co). .....	109

## List of Figures

---

Fig.3.2.1.18 Quantification of central memory CD4 <sup>+</sup> T cells in spleens and tumors from tumor-bearing WT and B7-H1 KO mice with and without treatment (co). ....	110
Fig.3.2.1.19 Quantification of CD69 expression on central memory CD4 <sup>+</sup> T cells in spleens and tumors from tumor-bearing WT and B7-H1 KO mice with and without treatment (co). .....	111
Fig.3.2.2. 1 Gatingstrategy for Myeloid derived suppressor cells (MDSC) in spleens and tumors from tumor-bearing WT and B7-H1 KO mice using flow cytometry. ....	114
Fig.3.2.2. 2 Quantification of MDSC in spleens and tumors from tumor-bearing WT and B7-H1 KO mice with and without treatment (co).....	115
Fig.3.2.2. 3 Quantification of gMDSC in spleens and tumors from tumor-bearing WT and B7-H1 KO mice with and without treatment (co).....	116
Fig.3.2.2. 4 Quantification of mMDSC in spleens and tumors from tumor-bearing WT and B7-H1 KO mice with and without treatment (co).....	117
Fig.3.2.2. 5 Quantification of iNOS expression of MDSC in spleens and tumors from tumor-bearing WT and B7-H1 KO mice with and without treatment (co). ....	118
Fig.3.2.2. 6 Quantification of iNOS expression of gMDSC in spleens and tumors from tumor-bearing WT and B7-H1 KO mice with and without treatment (co). ....	120
Fig.3.2.2. 7 Quantificationof iNOS expression of mMDSC in spleens and tumors from tumor-bearing WT and B7-H1 KO mice with and without treatment (co). ....	121
Fig.3.2.2. 8 Quantification of Arg expression of MDSC in spleens and tumors from tumor-bearing WT and B7-H1 KO mice with and without treatment (co). ....	123
Fig.3.2.2. 9 Quantification of Arg expression of gMDSC in spleens and tumors from tumor-bearing WT and B7-H1 KO mice with and without treatment (co). ....	124
Fig.3.2.3. 1 Quantification of B7-H1 expression on MDSC in spleens and tumors from tumor-bearing WT mice with and without treatment (co). ....	125
Fig.3.2.3. 2 Quantification of B7-H1 expression on gMDSC in spleens and tumors from tumor-bearing WT mice with and without treatment (co). ....	126
Fig.3.2.3. 3 Quantification of B7-H1 expression on mMDSC in spleens and tumors from tumor-bearing WT mice with and without treatment (co). ....	127

## List of Figures

---

Fig.3.2.3. 4 Quantification of B7-DC expression on MDSC, gMDSC and mMDSC in spleens from tumor-bearing B7-H1 KO mice with and without treatment (co). .....	128
Fig.3.2.4. 1 Gating strategy for regulatory T cells in spleens and tumors using flow cytometry. ....	131
Fig.3.2.4. 2 Quantification of Treg in spleens and tumors from tumor-bearing WT and B7-H1 KO mice with and without treatment (co).....	132
Fig.3.2.4. 3 Quantification of Tcon in spleens and tumors from tumor-bearing WT and B7-H1 KO mice with and without treatment (co).....	133
Fig.3.2.4. 4 Quantification of activated Tcon in spleens and tumors from tumor-bearing WT and B7-H1 KO mice with and without treatment (co). ....	134
Fig.3.2.5. 1 Gating strategy for dendritic cells in spleens and tumors using flow cytometry. ....	137
Fig.3.2.5. 2 Quantification of cDC and their maturation status in spleens and tumors from tumor-bearing WT and B7-H1 KO mice with and without treatment (co). .....	139
Fig.3.2.5. 3 Quantification of CD80 expression on mature cDC in spleens and tumors from tumor-bearing WT and B7-H1 KO mice with and without treatment (co). .....	140
Fig.3.2.5. 4 Quantification of CD86 expression on mature cDC in spleens and tumors from tumor-bearing WT and B7-H1 KO mice with and without treatment (co). .....	142
Fig.3.2.5. 5 Quantification of B7-H1/B7-DC expression on cDC in spleens and tumors from tumor-bearing WT and B7-H1 KO mice with and without treatment (co). .....	143
Fig.3.2.5. 6 Quantification of pDC and their maturation status in spleens and tumors from tumor-bearing WT and B7-H1 KO mice with and without treatment (co). .....	144
Fig.3.2.5. 7 Quantification of CD80 expression on mature pDC in spleens and tumors from tumor-bearing WT and B7-H1 KO mice with and without treatment (co). .....	146

## List of Figures

---

Fig.3.2.5. 8 Quantification of CD86 expression on mature pDC in spleens and tumors from tumor-bearing WT and B7-H1 KO mice with and without treatment (co). .....	147
Fig.3.2.5. 9 Quantification of B7-H1/B7-DC expression of pDC in spleens and tumors of tumor-bearing WT and B7-H1 KO mice with and without treatment (co). .	148
Fig.3.3. 1 Quantification of TGF- $\beta$ in serum samples of WT and B7-H1 KO tumor-bearing mice with and without treatment (co).....	150
Fig.3.3. 2 Quantification of IL-1 $\beta$ in serum samples of WT and B7-H1 KO mice with and without treatment (co). .....	151
Fig.3.3. 3 Quantification of IL-2 in serum samples of WT and B7-H1 KO mice with and without treatment (co). .....	152
Fig.3.3. 4 Quantification of IL-6 in serum samples of WT and B7-H1 KO mice with and without treatment (co). .....	153
Fig.3.3. 5 Quantification of VEGF in serum samples of WT and B7-H1 KO mice with and without treatment (co). .....	154
Fig.3.4.1. 1 Gating strategy for MDSC in tumors of untreated tumor-bearing WT and B7-H1 KO mice using flow cytometry. ....	157
Fig.3.4.1. 2 Quantification of MDSC in tumors of untreated tumor-bearing WT and B7-H1 KO mice. ....	157
Fig.3.4.1. 3 Quantification of iNOS <sup>+</sup> cells of the total MDSC in tumors of untreated tumor-bearing WT and B7-H1 KO mice.....	158
Fig.3.4.1. 4 Quantification of Arg <sup>+</sup> cells of total MDSC in tumors of untreated tumor-bearing WT and B7-H1 KO mice.....	159
Fig.3.4.1. 5 Quantification of granulocytic and monocytic MDSC out of the total MDSC in tumors of untreated tumor-bearing WT and B7-H1 KO mice. ....	160
Fig.3.4.1. 6 Quantification of iNOS <sup>+</sup> and Arg <sup>+</sup> cells out of granulocytic MDSC in tumors of untreated tumor-bearing WT and B7-H1 KO mice.....	161
Fig.3.4.1. 7 Quantification of iNOS <sup>+</sup> cells out of monocytic MDSC in tumors of untreated tumor bearing WT and KO mice.....	162
Fig.3.4.2. 1 Gating strategy for CD4 <sup>+</sup> /CD8 <sup>+</sup> T cells in cocultures of MDSC and CFSE labeled splenocytes using flow cytometry. ....	164

## List of Figures

---

Fig.3.4.2. 2 Quantification of proliferated CD4 <sup>+</sup> T cells out of WT and B7-H1 KO splenocytes in culture. ....	165
Fig.3.4.2. 3 Effect of MDSC on proliferated CD4 <sup>+</sup> T cells out of WT and B7-H1 KO splenocytes in coculture.....	166
Fig.3.4.2. 4 Quantification of proliferated CD8 <sup>+</sup> T cells out of WT and B7-H1 KO splenocytes in culture. ....	167
Fig.3.4.2. 5Effect of MDSC on proliferated CD8 <sup>+</sup> T cells out of WT and B7-H1 KO splenocytes in coculture.....	168
Fig.3.5. 1Quantification of IFN $\gamma$ in supernatants from cocultures of WT or B7-H1 KO splenocytes (+/- activation) with and without MDSC from WT tumors. ....	170
Fig.3.5. 2 Quantification of IL-1 $\beta$ in supernatants from cocultures of WT or B7-H1 KO splenocytes (+/- activation) with and without MDSC from WT tumors. ....	171
Fig.3.5. 3 Quantification of IL-2 in supernatants from cocultures of WT or B7-H1 KO splenocytes (+/- activation) with and without MDSC from WT tumors. ....	172
Fig.3.5. 4 Quantification of IL-6 supernatants from cocultures of WT or B7-H1 KO splenocytes (+/- activation) with and without MDSC from WT tumors. ....	173
Fig.3.5. 5 Quantification of IL-10 in supernatants from cocultures of WT or B7-H1 KO splenocytes (+/- activation) with and without MDSC from WT tumors. ....	175
Fig.3.5. 6 Quantification of VEGF in supernatants from cocultures of WT or B7-H1 KO splenocytes (+/- activation) with and without MDSC from WT tumors. ....	176
Fig.3.5. 7 Quantification of TGF- $\beta$ in supernatants from cultures of WT or B7-H1 KO splenocytes (+/- activation) with and without MDSC from WT tumors. ....	177
Fig.3.6. 1 Difference in the rate of tumor development and tumor volume between WT and B7-H1 KO tumor-bearing mice. ....	179
Fig.3.6. 2 Difference in the tumor volume between WT and B7-H1 KO tumor-bearing mice with and without treatment. ....	180
Fig.3.6. 3 Difference in the rate of tumor development and tumor volume between WT and B7-H1 KO tumor-bearing mice receiving IFN $\alpha$ treatment. ....	180
Fig.3.6. 4 Difference in the rate of tumor development and tumor volume between WT and B7-H1 KO tumor-bearing mice receiving 5-FU treatment. ....	181
Fig.3.6. 5 Difference in the rate of tumor development and tumor volume between WT and B7-H1 KO tumor-bearing mice receiving IFN $\alpha$ +5-FU treatment. ....	182

## List of Figures

---

Fig.3.6. 6 Difference in the metastasis rate between WT and B7-H1 KO tumor-bearing mice with and without treatment.....	183
Fig.3.7. 1 Difference in the survival rate between WT and B7-H1 KO tumor-bearing mice with and without treatment.....	185
Fig.3.7. 2 Difference in the survival rate between control groups (without treatment) and after treatment with IFN $\alpha$ , 5-FU or the combination of IFN $\alpha$ +5-FU of either WT or B7-H1 KO tumor-bearing mice. ....	186
Fig.3.8 1 Correlation between tumor volume and the percentage of MDSC out of leukocytes.....	188
Fig.4. 1 Differences in cytokine and growth factor concentration between WT and B7-H1 KO tumor-bearing mice with and without treatment.....	201
Fig.4. 2 Summarized presentation of the most meaningful results .....	204

## V. List of Tables

Tab.2.1.3. 2 Pharmaceutical products.....	33
Tab.2.1.4. 2 Anti-mouse antibodies for flow cytometry.....	35
Tab.2.1.5 2 Laboratory Equipment.....	36
Tab.2.1.6. 2 Laboratory consumables.....	37
Tab.2.1.7. 2 Laboratory solutions.....	37
Tab.2.1.9. 2 Softwares.....	39

## **VI. Acknowledgement**

Herrn Prof. Dr. Reto Neiger vom Klinikum Veterinärmedizin in Gießen danke ich für die Übernahme der Betreuung am Fachbereich.

Herrn Prof. Dr. Eberhard Burkhardt danke ich für die aufschlussreiche und engagierte Kritik im Vorfeld der Disputation.

Insbesondere danke ich meinen Betreuern in Heidelberg, Herrn Prof Dr. Alexandr V. Bazhin und Frau Dr. Svetlana Karakhanova für die engagierte und großzügige Unterstützung.

Den Mitarbeiter/-innen im Labor, Markus Herbst, Tina Maxelon und Inna Schwarting für die offene Aufnahme ins Team, das freundschaftliche Arbeitsklima, das geduldige Anlernen der Methoden und die Unterstützung bei meinen Experimenten. Herrn Dr. Yuhui Yang, Robert Ose und Ivan Shevchenko danke ich für die Einarbeitung ins Thema und für die nette Zusammenarbeit. Den Mitdoktoranden/-innen Andreas Mathes, Moritz Heinrich, Jasmin Fritz, Caroline Maier, Ramona Brecht und Henriette Bunge danke ich für die tolle Zeit im Labor und die gegenseitige Unterstützung bei unseren Experimenten. Ihr alle habt für mich die Zeit im Institut in Heidelberg zu einer ganz Besonderen gemacht.

Herrn Dave Hannu aus Verden danke ich für die Durchsicht des Manuskriptes.

Am meisten danke ich meinem Mann Ezzedine, meinen Eltern und meinen Brüdern für ihre Liebe und die jahrelange Unterstützung und Hilfe, ohne die das Studium der Tiermedizin und diese Doktorarbeit nicht möglich gewesen wären.



*édition scientifique*  
**VVB LAUFERSWEILER VERLAG**

VVB LAUFERSWEILER VERLAG  
STAUFBENBERGRING 15  
D-35396 GIESSEN

Tel: 0641-5599888 Fax: -5599890  
redaktion@doktorverlag.de  
www.doktorverlag.de

ISBN: 978-3-8359-6352-8



9 17 8 3 8 3 5 19 6 3 5 2 8